The University Of Sheffield.

The Role of Adrenomedullin Signalling in Pancreatic Cancer

By

Kamilla Janina Anna Bigos

A thesis submitted in partial fulfilment of the requirements for the degree of Doctor of Philosophy

The University of Sheffield

Faculty of Medicine, Dentistry and Health

Department of Oncology and Metabolism

Submission date

September 2021

Acknowledgements

I would like to begin by thanking my supervisors' Dr Gareth Richards and Professor Tim Skerry for seeing potential in me that I didn't see in myself. Your endless support throughout my PhD and your approachable nature has not only enabled me to complete my thesis, but also allowed me to believe in myself that little bit more. Thank you for supporting me when I doubted myself and encouraging me to see the potential in myself.

I would also like to thank and acknowledge all the members of my lab group and within the department, old and new, who have been nothing but supportive throughout this journey. I have always felt like there has been someone to make me laugh or provide a shoulder to cry on. I would like to personally thank Dr Ameera Jailani who has been both an amazing friend, support and guide over the past 4 years. She has been an absolute inspiration to me with her efforts to go above and beyond to support me and other scientists within the department. I would also like to thank Dr Paris Avgoustou who has also been an incredible friend and support throughout my PhD. Feeling like I could approach him at any time for help and guidance. There really are not enough words to describe how grateful I am for the both of you, your kindness and the laughter we have shared is something I will never forget.

I also began this journey with Dr Ewan Lilley and Dr Joe Holmes who were incredibly supportive, especially in moments of self-doubt and made me laugh a lot. Part of my journey was also made complete by placement students, Lucy Dascombe and Megan Poxon who were a refreshing addition to the lab. They fully embraced me for who I am and have become amazing friends. I would also like to personally thank Lucy for putting up with me as her placement supervisor and supporting me through endless western blots and in situ hybridisation optimisation that didn't always work. I am so excited for you to start your journey as a PhD student. Dr Karan Shah also deserves a special thanks, you have helped me whenever I have needed guidance and support. You have also been a massive source of fun and entertainment throughout my PhD which was much needed to power through the

more stressful times. You have all fully embraced me for who I am and made me feel comfortable confiding in each and every one of you. This has really made helped me gain confidence throughout my PhD.

I would like to thank the Wellcome trust and the University of Sheffield for funding my PhD, enabling me to embark on this journey and contribute to important research. Being given an opportunity to develop as a scientist has made me grow an enormous amount in confidence and made me believe in myself more than I ever have. It has not been an easy journey, but this opportunity has made me for the first time feel proud of myself. I couldn't have done this without both the funders and my incredible lab group.

Lastly, I would like to thank my friends and family who have been there for me before my PhD began and continued supporting me throughout. I would like to thank my Mama and Tata who have continuously inspired me to work hard and persevere when faced with challenges. Naprawd*ę was* docieniam i wszytko co zrobiliście dla mnie, zawsze będe wdzięczna, kocham was mocno. My sister/second Mama, Klaudia, deserves a special thanks for inspiring me to pursue a career in science. She has always supported me from a young age, her kindness and willingness to help others has always made me want to be the best person I can be. I don't think either of us thought I would have managed to write a whole thesis without asking for any grammatical support but I DID IT!

There are just a few more special people I would like to mention. I would like to thank Nikki and Georgia who have laughed and cried with me for the past 4 years, I couldn't have asked for more supportive and understanding friends. The laughter and joy you both fill me with is indescribable. Thank you to Claire, Poppy and Joe, you have also all been through this crazy ride with me and have continuously made me laugh and feel supported. I could honestly keep listing the people who I feel have had an impact on these past 4 years but this would end up being a thesis in itself. It's time to stop the typing now, submit my thesis, breathe and just say one final big THANK YOU!

Statement of Attribution

cAMP assays shown in Figure 3. were completed by **Dr Ameera Jailani** and published in her thesis (March 2019).

In vivo subcutaneous and orthoptic experiments (Chapter 6, Section 6.2.1 and 6.2.2) were conducted together with **Dr Paris Avgoustou** and **Dr Ameera Jailani**. They aided in the orthotopic implantation of cells into the pancreas and suturing of wounds. They also trained me to become competent in subcutaneous injection of D-Luciferin into flank of the mouse.

Ki67 immunostaining on tumour sections collected from the orthotopic *in vivo* experiments were completed together with **Edward Church**, a Sheffield Hallam placement student working with our laboratory group.

Abstract

Pancreatic cancer (PaCa) is the 4th most common cause of cancer related death and incidence rates are increasing. Understanding how PaCa develops is important for earlier detection and better treatment outcomes. ADM is a peptide hormone associated with many cancers. It has physiological and pathological roles regulated through receptor complexes composed of CLR and RAMPs. RAMPs alter the selectivity of receptor, the AM1 receptor (CLR and RAMP-2) is associated with physiological roles (regulating blood pressure), the AM2 receptor (CLR and RAMP-3) is associated with pathological roles. The AM2 receptor has been shown to regulate tumour growth and survival, angiogenesis, immunosuppression and epithelial-to-mesenchymal transition.

The aim of this study was the elucidate the role of ADM in PaCa. The results showed that in a panel of seven PaCa cell lines, ADM, CLR and RAMPs were expressed at both mRNA and protein level. Therefore, inducible CFPAC-1 ADM KDs, CFPAC-1 RAMP-3 KDs and scrshRNA controls were developed and used for *in vitro* and *in vivo* experiments. *In vitro,* viability and apoptosis assays showed that both KD and control cells responded to gemcitabine treatment but not to 5-fluorouracil. *In vivo,* both orthotopic and subcutaneous models showed no significant difference in tumour weight or volume between different groups (CFPAC-1 ADM KD, scrshRNA and wild-type cells). There were no significant differences between the percentage of immune cells in different groups. Furthermore, immunohistochemistry showed no significant differences in the number of Ki67 positive cells. Analysis of α-SMA and endomucin needed further work.

Overall, the results demonstrate that ADM and its receptor components are expressed in PaCa cell lines. However, further elucidation of the exact role of ADM in tumour development is needed with more focus on the tumour stroma. Focus on pancreatic stellate cells (α-SMA) shows promise in the field of PaCa.

Table of Contents

Acknowledgements i

Statement of Attribution iii

Abstract iv

List of figures xii

List of Tables xvi

List of Abbreviation xviii

1.0 INTRODUCTION 1

1.1 Pancreatic cancer (PaCa) 2

1.1.1 Pancreatic cancer incidence and diagnosis 2

1.1.2 Pancreas function 3

1.1.3 Pancreatic cancer types 6

1.1.4 Risk Factors for PaCa 11

1.1.5 Diagnosis and symptoms 14

1.1.6 Current treatments 18

1.2 Adrenomedullin (ADM) and its physiological roles 21

1.2.1 ADM synthesis 22

1.2.2 Adrenomedullin receptors 23

1.2.3 Signalling pathways 26

1.2.4 Physiological roles of ADM and its expression in different organs 28

1.3 Adrenomedullin and Cancer 35

1.3.1 Proliferation 36

1.3.2 Apoptosis 38

1.3.3 Angiogenesis 40

1.3.4 Invasion/Migration 47

1.3.5 Immune evasion 51

1.3.6 Adrenomedullin and desmoplasia 56

1.4 Conclusion 57

1.5 Hypothesis 57

1.6 Aims and objectives 57

CHAPTER 2: GENERAL METHODS 59

2.0 Materials and methods 60

2.1 Cell culture 60

2.2 Endpoint PCR 63

2.3 Quantitative Real-Time PCR (QPCR) 68

2.4 Western blotting 71

2.8 Statistical analysis 75

CHAPTER 3: PaCa CELL LINE CHARACTERISATION 77

3.1 Introduction 78

3.1.1 ADM and its receptors in PaCa 78

3.1.2 ADM and its receptors in other cancers 81

3.1.3 Hypothesis 83

3.1.4 Aims and objectives 84

3.2 Methods 85

3.2.1 Cell culture 85
3.2.2 Endpoint PCR 85
3.2.3 QPCR 85
3.2.4 Western blot 86
3.2.5 cAMP assays 86
3.3 Results 90
3.3.1 PaCa Cell morphology 90
3.3.2 mRNA expression of ADM/CLR/RAMPs 93
3.3.3 Protein expression of RAMPs 103
3.3.4 Stimulation of PaCa cells with calcitonin superfamily 105
3.4 Discussion 108
3.4.1 PaCa cell line morphology 108
3.4.2 PaCa cell lines express ADM and its receptor components 110
3.3.3 PaCa cell lines are stimulated by ADM, CGRP and IMD to produce cAMP 114
3.5 Conclusion 116
CHAPTER 4: KNOCKDOWN CHARACTERISATION AND VALIDATION 117
4.1 Introduction 118
4.1.1 ADM knockdown studies 118
4.1.2 RAMP-3 knockdown studies 120
4.1.3 Aims and Objectives 121
4.2 Methods 122
4.2.1 Transduction of ADM/RAMP-3 with SMARTvector inducible lentiviral shRNA 122

4.2.2 GFP cell sort of CFPAC-1 ADM/RAMP-3 knockdowns 127

4.2.3 ADM knockdown validation by QPCR 128

4.2.4 Lentiviral transduction of ADM knockdown cells and ScrshRNA cells with firefly luciferase (Luc-RFP) 129

4.2.5 CFPAC-1 ADM KD, RAMP-3 KD, scrshRNA and WT viability assay 130

4.3 Results 132

4.3.1 Knockdown validation 132

4.3.2 Lentiviral transduction of KD cells with firefly luciferase (Luc-RFP) 141

4.4 Discussion 143

4.4.1 CFPAC-1 ADM knockdowns are validated, whilst RAMP-3 knockdowns need further validation 143

4.4.2 CFPAC-1 ADM KD and CFPAC-1 RAMP-3 KD reduce cell viability compared to CFPAC-1 WT cells 147

4.5 Conclusion 149

CHAPTER 5: EFFECTS OF ADM AND RAMP-3 KNOCKDOWNS ON PROLIFERATION AND APOPTOSIS 150

5.1 Introduction 151

5.1.1 The use of gemcitabine and 5-FU in PaCa treatment 151

5.1.2 ADM and proliferation of cancer cells 152

5.1.3 The role of ADM in regulating apoptosis in cancer and resistance to chemotherapy 154

5.1.4 Hypothesis 156

5.1.5 Aim and Objectives 156

5.2 Methods 158

5.2.1 Gemicitabine and 5-FU Viability assay 158

5.2.2 Gemicitabine and 5-FU Apoptosis assay 158

5.3 Results 161

5.3.1 Effect of gemcitabine on viability and apoptosis of KD cells 161

5.3.2 Effect of 5-FU on viability and apoptosis of KD cells 165

5.4 Discussion 169

5.4.1 CFPAC-1 KD cells respond to gemcitabine resulting in a decrease in PaCa proliferation 169

5.4.2 Viability assays show that CFPAC-1 KD cells are resistant to 5-FU treatment 172

5.4.3 CFPAC-1 KD cells are sensitive to gemcitabine which induces apoptosis 173

5.4.4 CFPAC-1 KD cells are resistant to 5-FU treatment and do not induce apoptosis 175

5.5 Conclusion 179

CHAPTER 6: EFFECT OF ADM KD ON THE PaCa MICROENVIRONMENT 182

6.1 Introduction 183

6.1.2 Pancreatic stellate cells (PSCs) role in desmoplasia 183

6.1.2 The extracellular matrix (ECM) in PaCa progression 188

6.1.3 Immune cells 190

6.1.4 Endothelial cells and angiogenesis 192

6.1.5 Neuronal cells 194

6.1.6 Summary 195

6.1.7 Hypothesis 196

6.1.8 Aims and objectives 196

6.2 Methods 198

6.2.1 In vivo orthotopic model 198

6.2.2 In vivo subcutaneous model 206

6.3 Results 209

6.3.1 Comparison of orthotopic tumour weight and luminescence of CFPAC-1 ADM KDs and scrshRNA 209

6.3.2 Comparison of CFPAC-1 ADM KD and CFPAC-1 scrshRNA tumour luminescence determined by IVIS 212

6.3.3 Orthotopic model interim and endpoint organ weights 214

6.3.4 CFPAC-1 ADM KD and CFPAC-1 scrshRNA immune analysis 217

6.3.5 Comparison of CFPAC-1 ADM KD and scrshRNA histology and Ki67 proliferating cells 220

6.3.6 *In vivo* differences in tumour volume and weight following between CFPAC-1 ADM KDs, CFPAC-1 scrshRNA and CFPAC-1 WT cells (subcutaneous) 226

6.3.7 *In vivo* analysis of organ weights of CFPAC-1 ADM KD compared to CFPAC-1 scrshRNA and CFPAC-1 WT cells 229

6.4 Discussion 231

6.4.1 CFPAC-1 ADM KDs, scrshRNA and WT cell effect on tumour growth and proliferation 231

6.4.2 CFPAC-1 ADM KD and CFPAC-1 scrshRNA effects on organs 237

6.4.3 CFPAC-1 ADM KDs and CFPAC-1 scrshRNA effects on immune cells 239

6.4.4 Conclusion 244

CHAPTER 7: GENERAL DISCUSSION 246

7.1 General discussion 247

7.1.1 Characterisation 249

7.1.2 Knockdown development and validation 251

7.1.3 Viability and apoptosis 252

7.1.4 In vivo 255

7.1.5 Future work 262

7.1.6 Conclusion 265

APPENDIX 267

References 270

List of Figures

Figure 1.1 Projected cancer deaths by 2035. 3

Figure 1.2 The structure of the pancreas. 4

Figure 1.3 Acinar-to-ductal metaplasia progressing from premalignant PanINs to malignant PDAC. . 9

Figure 1.4 Adrenomedullin (ADM) synthesis. 23

Figure 1.5 Adrenomedullin receptor.. 24

Figure 1.6 Adrenomedullin pathways. 28

Figure 1.7 mRNA and protein expression of ADM in different tissues and blood. 32

Figure 1.8 mRNA and protein expression of CLR in different tissues and blood. 33

Figure 1.9 mRNA expression of RAMP-1 (A), RAMP-2 (B) and RAMP-3 (C) in different tissues and blood. 34

Figure 1.10 ADM role in the extrinsic apoptosis pathway. 40

Figure 1.11 ADM role in angiogenesis. 44

Figure 1.12 ADM role in invasion and migration.. 51

Figure 2.1 Phase image of CFPAC-1 cell line at 70% confluency used for both in vitro and in vivo experiments.. 62

Figure 2.2 Norgen HighRanger 1kb DNA ladder 67

Figure 2.3 Example of sequencing data. 68

Figure 2.4 QPCR amplification plot for AM in PaCa cell lines 71

Figure 2.5 Normalized BCA assay standard curve 73

Figure 3.1 Principles of the LANCE cAMP assay 87

Figure 3.2 Phase-contrast images of a panel of seven pancreatic cell lines from American Type Culture Collection (ATCC). 92

Figure 3.3 RAMP-1 endpoint PCR. 94

Figure 3.4 RAMP-1 sequencing data from CFPAC-1 PaCa RNA sample. 95

Figure 3.5 RAMP-2 endpoint PCR.. 96

Figure 3.6 RAMP-2 sequencing. 96

Figure 3.7 RAMP-3 endpoint PCR. 97

Figure 3.8 RAMP-3 sequencing. 98

Figure 3.9 ADM endpoint PCR. 99

Figure 3.10 ADM sequencing. 100

Figure 3.11 CLR endpoint PCR. 101

Figure 3.12 CLR sequencing. 102

Figure 3.13 RAMP-1 protein expression determined by western blotting. 104

Figure 3.14 RAMP-2 protein expression determined by western blotting. 105

Figure 3.15 RAMP-3 protein expression determined by western blotting. 105

Figure 3.16 Effect of calcitonin peptides (ADM, CGRP, IMD) on cAMP production of seven PaCa cell lines.. 106

Figure 4.1 Dharmacon SMARTvector Inducible Lentiviral shRNA vector structure 123

Figure 4.2 ADM sequence from NCBI GenBank. SMARTvector inducible lentiviral shRNA sequences for ADM are highlighted. 125

Figure 4.3 RAMP-3 sequence from NCBI GenBank. SMARTvector inducible lentiviral shRNA sequences for RAMP-3 are highlighted. 126

Figure 4.4 Firefly Luciferase vector adapted from the Amsbio manual. 129

Figure 4.5 Principles of the RealTime Glo™ MT Viability assay. 130

Figure 4.6 Day 1 and Day 7 CFPAC-1 ADM inducible lentiviral shRNA KD induction. 133

Figure 4.7 CFPAC-1 ADM KD doxycycline (dox) induction over seven days. 134

Figure 4.8 Day 1 and Day 7 CFPAC-1 RAMP-3 inducible lentiviral shRNA KD induction. 135

Figure 4.9 CFPAC-1 RAMP-3 knockdown doxycycline (dox) induction over seven days.. 136

Figure 4.10 Day 1 and Day 7 CFPAC-1 inducible scrambled shRNA (scrshRNA) control doxycycline induction. 137

Figure 4.11 CFPAC-1 scrshRNA doxycycline (dox) induction over seven days.. 138

Figure 4.12 Expression of ADM in CFPAC-1 ADM KD relative to CFPAC-1 scrshRNA determined by QPCR.. 139

Figure 4.13 CFPAC-1 ADM KD, RAMP-3 KD, scrshRNA and WT percentage viability relative to baseline read.. 140

Figure 4.14 Luminescence of CFPAC-1 ADM KD and CFPAC-1 scrshRNA controls transduced with Luc-RFP.. 141

Figure 4.15 Luciferase expression in CFPAC-1 ADM KD-LucRFP and CFPAC-1 scrshRNA-LucRFP cells imaged before in vivo orthotopic experiment following addition of D-luciferin substrate.. 142

Figure 5.1 Schematic diagram of the Caspase 3/7 assay.. 159

Figure 5.2 Effect of different doses of gemcitabine on percentage viability determined over 3 days. 162

Figure 5.3 Day 3 gemcitabine viability dose response of CFPAC-1 ADM KD, CFPAC-1 RAMP-3 KD, CFPAC-1 scrshRNA, CFPAC-1 WT cells..... 163

Figure 5.4 Effect of different doses of gemcitabine on apoptosis of KD cells. 164

Figure 5.5 Effect of different doses of 5-FU on % viability over 3 days. 165

Figure 5.6 Day 3 5-FU % viability dose response of CFPAC-1 ADM KD, CFPAC-1 RAMP-3 KD, CFPAC-1 scrshRNA, CFPAC-1 WT cells. 166

Figure 5.7 Effect of different doses of 5-FU on apoptosis of KD cells. 168

Figure 6.1 The role of activated PSCs in the crosstalk with PaCa tumour cells**.**. 185

Figure 6.2 Orthotopic in vivo schematic. 200

Figure 6.3 Bioluminescent quantification of pancreatic tumours. 201

Figure 6.4 Bioluminescence of (A) Primary pancreatic tumour and spleen, (B) organs (C) and empty body measured by IVIS to check for metastasis from primary tumour site. 202

Figure 6.5 Ki67 tumour section annotation on QuPath..... 204

Figure 6.6 QuPath positive cell detection parameters. 205

Figure 6.7 Analysis of Ki67 positive cells using QuPath.. 206

Figure 6.8 Day 17 and Day 45 tumour weights following orthotopic injection of CFPAC-1 ADM KDs or CFPAC-1 scrshRNA into 5-6 week old BALB/C female mice.. 211

Figure 6.9 CFPAC-1 ADM KD and CFPAC-1 scrshRNA tumour luminescence following orthotopic injection of cells into the pancreas determined by IVIS.. 213

Figure 6.10 CFPAC-1 ADM KDs and CFPAC-1 scrshRNA day 17 and 45 organ weights following orthotopic injection of cells into pancreas. 215

Figure 6.11 A graph to show proportion of mice with potential stomach metastases in CFPAC-1 ADM KD and CFPAC-1 scrshRNA groups. 216

Figure 6.12 CFPAC-1 scrshRNA day 45 no DOX and DOX on/off/on organ IVIS luminescence.. 217

Figure 6.13 Day 17 and day 45 CFPAC-1 ADM KD and CFPAC-1 scrshRNA whole blood immune analysis.. 219

Figure 6.14 Day 17 and Day 45 CFPAC-1 scrshRNA and CFPAC-1 ADM KD doxycycline induced IVIS images and H&E stains. 222

Figure 6.15 Day 17 and day 45 CFPAC-1 scrshRNA and CFPAC-1 ADM KD dox on/off/on IVIS images and H&E stains.. 223

Figure 6.16 Day 17 and day 45 CFPAC-1 scrshRNA and CFPAC-1 ADM KD no dox IVIS images and H&E stains.. 224

Figure 6.17 Ki67 positive percentage cells in CFPAC-1 ADM KDs and CFPAC-1 scrshRNA. 226

Figure 6.18 Subcutaneous tumour volume (mm^3) and weight (mg) of CFPAC-1 ADM KDs, CFPAC-1 scrshRNA and CFPAC-1 WT cells either induced with doxycycline (dox) or untreated (no dox)..... 228

Figure 6.19 Subcutaneous organ weights in CFPAC-1 ADM KDs, scrshRNA and WT cells following induction of KD with doxycycline (dox) or no doxycycline treatment (no dox). 230

Figure 8.1 Example H&E stomach histology collected at day 45 from CFPAC-1 scrshRNA no dox group. 269

List of Tables

Table 1.1 Endocrine cells that form the islet of Langerhans 5

Table 1.2 Types of premalignant and malignant exocrine tumours 8

Table 1.3 Types of endocrine tumour 10

Table 1.4 Diagnostic tests used for pancreatic cancer 16

Table 1.5 TNM staging for pancreatic cancer 17

Table 1.6 One year survival predictions based on stage of cancer, TNM and location 17

Table 1.7 Therapies available for PaCa patients at different stages of cancer 20

Table 1.8 Mechanism of action of different chemotherapies 20

Table 1.9 GPCR superfamily classes 24

Table 1.10 RAMP and CLR/CTR receptor complexes showing the rank of ligand potencies 26

Table 2.1 Characteristics of cell lines purchased from ATCC including organism, gender, age, histology, tumour source, mutation and mycoplasma status 60

Table 2.2 Cell lines, optimal growth media and supplements 61

Table 2.3 Volume of reagents used with different flask sizes in culture 61

Table 2.4 List of reagent volumes required for ReliaPrep™ Cell MiniPrep System 63

Table 2.5 Reliaprep™ MiniPrep System DNAse I mix recipe 64

Table 2.6 Absorbance ratios for RNA purity 64

Table 2.7 List of volumes and reagents required for cDNA synthesis 65

Table 2.8 Reaction components for endpoint PCR per reaction for endpoint PCR per reaction for ADM, RAMP-1, RAMP-2 and CLR 65

Table 2.9 Reaction components for RAMP-3 endpoint PCR 66

Table 2.10 Primer sequences, product size, annealing temperatures and cycle number 66

Table 2.11 NanoScript 2 reverse transcription annealing step……69

Table 2.12 Precision NanoScript 2 reverse transcription extension mix……69

Table 2.13 Mastermix for QPCR reaction……70

Table 2.14 Primer sequences for ADM designed by PrimerDesign with double dye hydrolysis probe and FAM reporter……70

Table 2.15 Dilutions prepared to make a standard curve for BCA assay……73

Table 2.16 Primary antibody dilutions and blocks……75

Table 2.17 Secondary antibody dilutions……75

Table 3.1 Summary of ADM and its receptor component expression. Expression was measured as mRNA and protein by western blot or immunostaining……83

Table 3.2 Stimulation buffer recipe for cAMP assays……88

Table 3.3 Half-log serial dilution of calcitonin family peptides for cAMP assay……88

Table 3.4 Half-log serial dilutions of forskolin for cAMP assay……89

Table 3.5 ADM and RAMP-1 mRNA expression in seven PaCa cell lines detected by quantitative real-time polymerase chain reaction (QPCR)……103

Table 4.1 SMARTvector inducible lentiviral shRNA clone ID for ADM, RAMP-3 and scrambled control……124

Table 4.2 A list of the samples that were RNA extracted to validate the knockdown of CFPAC-1 cells……128

Table 6.1 Doxycycline water regime……199

Table 6.2 The subcutaneous *in vivo* experiment was split into 6 groups according to cell type and KD cells were induced by doxycycline……207

List of Abbreviations

5-FU- 5-fluorouracil

ACTB- beta actin

ADM- adrenomedullin

ADM KD- adrenomedullin knockdown

ADM_{22-52}- adrenomedullin fragment antagonist

ADMR- adrenomedullin receptor

Akt- protein kinase B

AMY- amylin

ANOVA- Analysis of variance

AP-1- activator protein 1

ATCC- American Type Culture Collection

Bcl-2- B cell lymphoma-2

bFGF- basic fibroblast growth factor

BMDCs- Bone marrow derived-dendritic cells

BMDMs- bone marrow derived macrophages

BSA- bovine serum albumin

cAMP- cyclic adenosine monophosphate

CFPAC-1 ADM KD- CFPAC-1 pancreatic cell line transduced with inducible lentiviral adrenomedullin shRNA to produce a knockdown

CFPAC-1 ADM KD-LucRFP- CFPAC-1 adrenomedullin knockdowns transduced with adenovirus encoding firefly luciferase with RFP tag

CFPAC-1 LucRFP- CFPAC-1 wild-type cells transduced with adenovirus encoding firefly luciferase with RFP tag

CFPAC-1- pancreatic cancer cell line

CFPAC-1 scrshRNA-LucRFP- CFPAC-1 transduced with adenovirus encoding firefly luciferase with RFP tag

CFPAC-1 scrshRNA- CFPAC-1 pancreatic cell line transduced with inducible lentiviral scrambled shRNA to produce control

CFPAC-1 WT- CFPAC-1 wild-type cells

CGRP- Calcitonin-gene related peptide

CLR- calcitonin receptor-like receptor

CT- Computed Tomography

CTR- Calcitonin receptor

DAB- 3,3'-Diaminobenzidine

DMEM- Dulbecco's modified Eagle medium

DMSO- dimethyl sulfoxide

DTT- dithiothreitol

ECM- extracellular matrix

EDTA- Ethylenediamine tetraacetic acid

EMT- epithelial-to-mesenchymal transition

ERK- extracellular signal-regulated kinase

ESPAC- European Study Group for Pancreatic Cancer

FACS- Fluorescent-activated cell sorter

FAK- focal adhesion kinase

FGF- fibroblast growth factor

FOLFIRINOX- folinic acid (leucovorin), 5-fluorouracil, irinotecan, oxaplatin

GFP- green fluorescent protein

GPCR- G protein-coupled receptor

H&E- Haematoxylin and Eosin staining

HBSS- Hank's buffered saline solution

HIF-1- Hypoxia Inducible Factor

HUVEC- Human umbilical venous endothelial cell

IBMX- Isobutylmethylxanthine

ICAM-1- Intracellular cell adhesion molecule 1

IHC- Immunohistochemistry

IL1β- interleukin 1 beta

IMD- intermedin

IPMN- intraepithelial neoplasia

IVIS- *In Vivo* Imaging System

JNK- c-Jun N-terminal kinase

KD- knockdown

LB- Laemmli buffer

MAPK- mitogen activated protein kinase

MCNs- mucinous cystic neoplasms

MDSCs- Myeloid Derived Suppressor Cells

MMC- myelomonocytic cells

MMPs- Matrix metalloproteinases

MOI- multiplicity of infection

MRI- Magnetic Resonance Imaging

MTT assay- is a colorimetric assay used to measure metabolic cell activity

NFκB- nuclear factor κB

NHDF- normal human dermal fibroblasts

ns- not significant

OS- overall survival

PaCa- Pancreatic Cancer

PAMP- Pro adrenomedullin

PanIN- pancreatic intraepithelial neoplasia

PBS- phosphate buffered saline

PDAC- Pancreatic ductal adenocarcinoma

PDGF- Platelet derived growth factor

PDPN- podoplanin

PET- Positron Emission Tomography

PSCs- Pancreatic stellate cells; also known as CAFs (cancer associated fibroblasts) or myofibroblast like cells

QPCR- quantitative polymerase chain reaction

rADM- recombinant ADM

RAMP- Receptor Activity Modifying Protein

RFP- red fluorescent protein

ROI- region of interest

RPMI- Roswell Park Memorial Institute

SDS- sodium dodecyl sulfate

SEER- Surveillance, Epidemiology and End Results Program

shRNA- small hairpin RNA

TAM- Tumour associated macrophages

TBE- Tris borate EDTA

TBS- Tris-buffered saline

TE- Tris-EDTA

TGF-β- Transforming growth factor beta

TGS- Tris/Glycine/SDS

TIMPs- Tissue inhibitors of metalloproteinases

TNFα- Tumour necrosis factor alpha

TNM staging- T= Tumour, N= nodes, M= metastasis, this is used to stage cancer

Tregs- T regulatory Cells

VCAM-1- Vascular cell adhesion molecule 1

VEGF- Vascular endothelial growth factor

VSMCs- vascular smooth muscle cells

αAM- anti-ADM antibody

αAMR- anti-ADM receptor antibody

α-SMA- alpha smooth muscle actin

1.0 INTRODUCTION

1.1 Pancreatic cancer

1.1.1 Pancreatic cancer incidence and diagnosis

Pancreatic cancer (PaCa) is now the 17th most common cancer in Europe and the 10th most common cancer in the UK (2017) due to an increasingly ageing population in more developed countries. It is the 4th most common cause of cancer-related deaths, accounting for 6% of cancer deaths (Ferlay et al., 2018) and out of all cancer types, it has the lowest 5 year survival rate of 8% (Siegel, Miller, & Jemal, 2018). In the UK between 1993-2017, the incidence rates of PaCa cases increased by 17%. Furthermore, Rahib *et al* (2014) have predicted that by 2035 PaCa will become the second most common cause of cancer-related death. These predictions are based on demographic changes and average annual percentage changes (AAPC) in death rates (Figure 1.1). With the same number of deaths each year as the number of patients diagnosed with PaCa and the previously described predictions, there is increasing pressure to find improved methods of diagnosis and treatment (Ferlay et al., 2018).

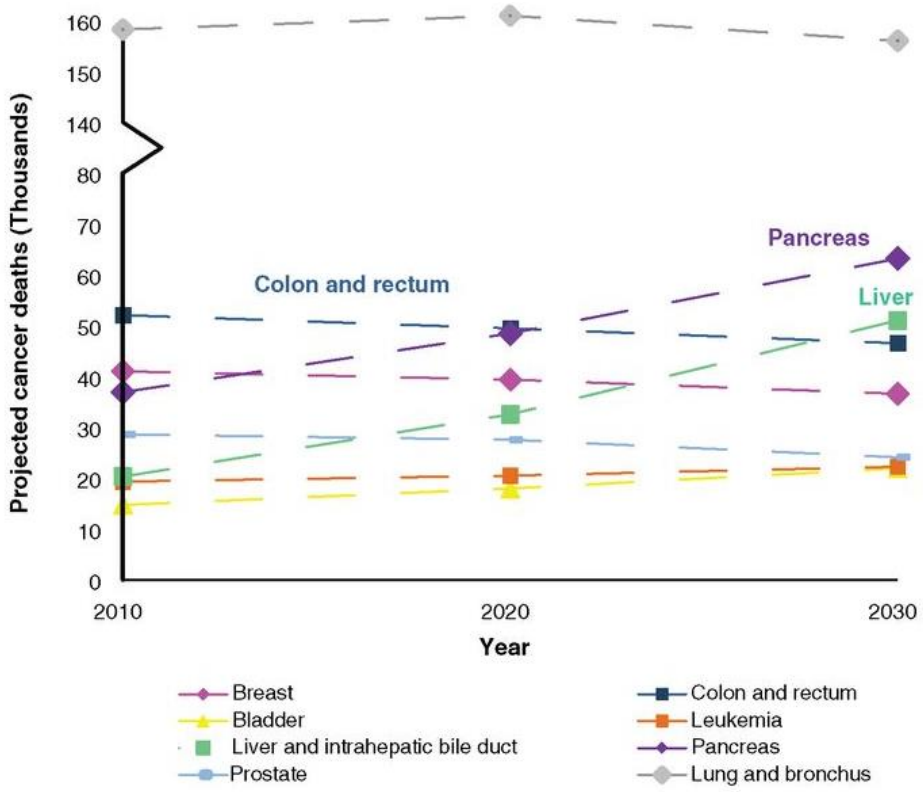

Figure 1.1 Projected cancer deaths by 2030 based on data collected in the United States. Rahib *et al* (2014) used demographic changes and average annual percentage change (AAPC) in death rates to predict deaths in cancers. The data shows that by 2030, PaCa is predicted to become the second most common cause of cancer related death.

1.1.2 Pancreas function

To understand the symptoms of PaCa and the prognosis associated with tumours in different parts of the pancreas, it is important to understand its structure and function. It is a relatively quiescent organ that has both exocrine and endocrine functions (Figure 1.2). It plays an important role in digestion of food and regulation of blood sugar. Dysfunction in the pancreas can lead to diseases including diabetes, pancreatitis and PaCa.

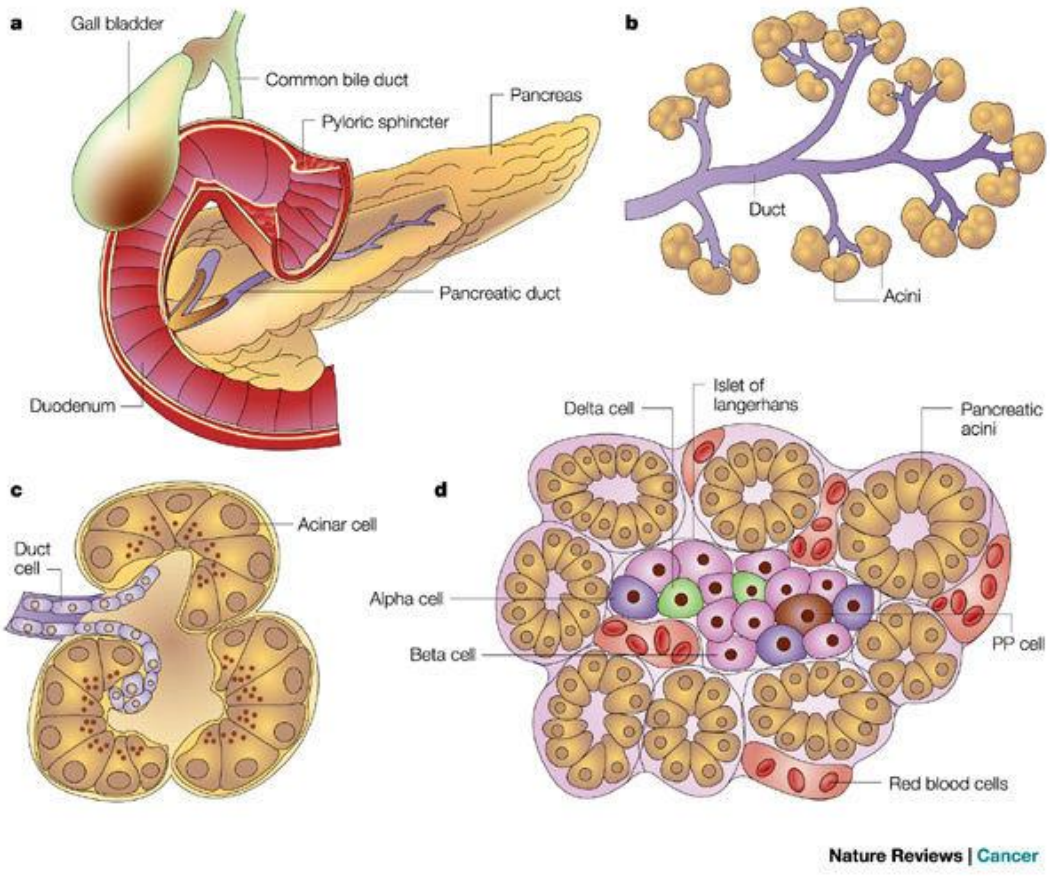

Figure 1.2 The structure of the pancreas. **(A)** The pancreas has two main roles; digestion of food and regulation of blood glucose. It contains a main pancreatic duct that releases digestive enzymes from other ducts into the duodenum together with bile from the common bile duct. This connection forms the Ampulla of Vater which is located at the top of duodenum and aids in the digestion of food (exocrine function). **(B)** Exocrine pancreas composed of acinar and duct cells. Acinar cells contain digestive enzymes and constitute the bulk of pancreatic tissue. Ducts add mucous and bicarbonate to the enzyme mix that is released into the duodenum **(C)** The structure of the acinar cells stemming off the pancreatic duct. **(D)** The Islet of Langerhans (forming the endocrine portion) embedded within exocrine tissue containing a group of 4 main cell types; alpha cells, beta cells, delta cells and pancreatic polypeptide cells. These all release hormones directly into the bloodstream to regulate blood glucose levels (alpha and beta cells) and modulate the secretion of other pancreatic cell types (delta and pancreatic polypeptide cells (Copyright 2002 with permission from Nature Reviews, Bardeesy & DePinho, 2002)

1.1.2.1 Exocrine function

The main exocrine function of the pancreas is to aid in the digestion of food. When food enters the stomach, enzymes are released from the system of pancreatic ducts which drain into the main pancreatic duct (Figure 1.2). This joins the common bile duct to form the Ampulla of Vater located in the first portion of the duodenum. The digestive enzymes from the pancreas combined with the bile are released into the duodenum to digest fat, carbohydrates and protein. PaCa often blocks both ducts causing malabsorption and jaundice.

1.1.2.2 Endocrine function

The endocrine part of the pancreas is composed of the Islet of Langerhans, these are composed of 4 different cell types that release hormones directly into the bloodstream (Table 1.1). Insulin and glucagon are the main hormones released.

Table 1.1 Endocrine cells that form the islet of Langerhans

Cell type	Function
Alpha Cells	These are glucagon secreting cells and account for approximately 20% of cells within an islet. Low blood glucose levels stimulate the release of this hormone.
Beta Cells	These cells release insulin and account for approximately 75% of islet cells. When blood glucose levels are elevated, insulin is released to bring levels back to normal.
Delta Cells	These cells make up 10% of an islet and release the hormone somatostatin. This inhibits the release of glucagon, insulin and pancreatic polypeptide.
Pancreatic polypeptide (PP) cells	These are mainly located in the head of the pancreas and it has been suggested that its main role is in regulating satiety. It can also inhibit pancreatic polypeptide secretions.

1.1.3 Pancreatic cancer types

Pancreatic tumours can be divided into exocrine tumours (non-pancreatic hormone secreting cells) (section 1.1.2.1) or endocrine tumours (pancreatic hormone secreting) (section 1.1.2.2) with pancreatic ductal adenocarcinoma (PDAC) being the most common subtype belonging to the exocrine tumour family. The location of tumours in the pancreas is important as it can affect the prognosis of patients; 65% of tumours are in the head, 15% are in the body/tail of the pancreas, whilst the remainder diffusely involve the gland (Figure 1.2) (Artinyan et al., 2008; Dreyer et al., 2018). Tomasello *et al* (2019) found that long term prognosis of pancreatic head cancer is better than body/tail PaCa. Patients with pancreatic head cancers present with symptoms sooner due to biliary obstruction. This causes abdominal pain, jaundice, dark urine, and light coloured stools. Earlier diagnosis means that patients are more likely to be offered tumour resection and therefore, have a better prognosis. Body/tail tumours of the pancreas are commonly associated with non-specific symptoms including unexplained weight loss and pain. Biliary obstruction is less likely in body/tail PaCa due to tumour location and therefore symptoms including jaundice are less likely to be present. Jaundice is a more visible symptom as it causes yellowing of the skin which makes it easier for doctors to locate the root cause of the problem faster (De La Cruz et al., 2014; Tomasello et al., 2019).

1.1.2.1 Exocrine tumours

The physiological role of the exocrine pancreas is to release digestive enzymes into the pancreatic ducts and into the duodenum (Section 1.1.2.1) (Pan & Wright, 2011)**.** Disruption of this system often leads to weight loss, anorexia, jaundice and abdominal pain which patients commonly present with (Porta et al., 2005). Exocrine PaCa has a worse prognosis due to the lack of specific symptoms. The majority of exocrine tumours (95%) are PDACs and are distinguished by the cell type and location (Table 1.2).

In some cases premalignant lesions including pancreatic intraepithelial neoplasms (PanINs) (Figure 1.3) and intraepithelial neoplasias (IPMNs) develop before primary PaCa tumours establish (Table 1.2).

These are more commonly located in the head of the pancreas. PanINs are flat or papillary lesions located in interlobular pancreatic ducts, they have columnar to cuboidal cells with varying amounts of mucin (Hruban et al., 2001; Zamboni et al., 2013). They often develop in a process called acinar-to-ductal metaplasia (Figure 1.3), acinar cells transdifferentiate into more epithelial/ductal like phenotypes when exposed to environmental changes including tissue damage, inflammation or stress (e.g. hypoxia). During the transition from acinar cells to a more ductal phenotype, the acinar cells gain more progenitor cell like characteristics. This activates proto-oncogenes including *KRAS* that transforms the cells to PanINs (Friedlander et al., 2009; Orth et al., 2019). Following acinar-to-ductal metaplasia and the development of PanINs, *TP53* and *SMAD4* mutations transform the tumour into a malignant phenotype (PDAC) (Figure 1.3). These mutations can often drive PDAC to metastasise (Chen et al., 2014; Morton et al., 2010; Orth et al., 2019). PDAC is frequently located in the head of the pancreas and is an epithelial tumour with ductal cells (Table 1.2).

IPMNs are cystic pancreatic lesions and tumours of the duct epithelium. IPMNs are histologically subdivided by their origin and whether lesions involve main ducts or branch ducts. The subtypes are; intestinal main duct IPMN, pancreatobiliary main duct IPMN, gastric branch duct IPMN and oncocytic main duct IPMN. Each IPMN is characterised by cell types, intestinal IPMNs have columnar cells with elongated nuclei, pancreatobiliary IPMNs are characterised branched papillae and high grade intraepithelial neoplasms. Oncocytic IPMNs have a branched papillary structure and eosinophilic cytoplasm mixed with goblet cells and mucin producing cells (Distler et al., 2013; Hruban et al., 2001; Zamboni et al., 2013). Mucinous cystic neoplasms (MCNs) are also premalignant lesions and are found exclusively in the body and tail of pancreas in middle aged women. The structure of these tumours include tall mucin-secreting cells and dense cellular ovarian-type stroma (Crippa et al., 2008).

There also other rare types of malignant lesions that include, pancreatic squamous cell carcinoma (SCC) which is equally distributed between the head, tail and body of the pancreas and is composed of squamous cells (Simone et al., 2013). Another rare subtype of PaCa is pancreatic adenosquamous

carincoma, accounting for 1-4% of cases. This is typically found in the body/tail of the pancreas and is composed of both squamous and glandular cells (Boyd et al., 2012). Ampullary cancers are located in the ampulla of Vater which is a small opening where the pancreatic and bile ducts connect to the small intestine (Perysinakis, Margaris, & Kouraklis, 2014) (Table 1.2).

Table 1.2 Types of premalignant and malignant exocrine tumours

Type	Description	Location	Incidence	Symptoms	References
Premalignant lesions					
Pancreatic intraepithelial neoplasms (PanINs)	- Non-invasive precursors lesions - Flat or papillary lesions in pancreatic ducts - Transition from intraepithelial to invasive pancreatic neoplasias (Figure 1.2)	Head or body of the pancreas	Most common precursor to PDAC	Abdominal pain, jaundice, dyspepsia, weight loss, nausea and vomiting	(Distler et al., 2014; Hackeng et al., 2016; Zamboni et al., 2013; Andea, Sarkar, & Adsay, 2003; Yu et al., 2018)
Intraductal papillary mucinous neoplasms (IPMN)	- Cystic pancreatic tumours of the duct epithelium - Papillary epithelial proliferation and mucin production lead to dilatation of ducts - 1/3 of cases are associated with invasive carcinoma of the tubular and colloid type	Pancreatic head (often not invasive)	Less than 10% of all pancreatic neoplasms	Abdominal pain, back pain, weight loss, appetite loss and jaundice	(Distler et al., 2014; Chanjuan & Hruban, 2012; Adsay et al., 2004; Andea et al., 2003; Mimura et al., 2010)
Mucinous cystic neoplasms (MCNs)	- Often detected incidentally - Common in women - 5-year survival is almost 100% - Pancreas resection offered in 60% of cases	Head and body of the pancreas	Least common out of premalignant lesions	Asymptomatic	(Distler et al., 2014; Crippa et al., 2008; Valsangkar et al., 2012; Yamao et al., 2011)
Malignant lesions					
Pancreatic ductal adenocarcinoma (PDAC)	- Poor prognosis with 5-year survival of 3-5%.	Mainly head of the pancreas	95% of all pancreatic tumours	Weakness, loss of appetite, weight loss, abdominal pain,	(Hackeng et al., 2016; Fatima, 2010;

	-PanINs are the most frequent precursors to PDAC.	in ductal cells.		bile in urine, cholestasis	Pancreatic Cancer UK, 2018; Porta et al., 2005)
Squamous cell carcinoma	- Squamous epithelium structure - Poor prognosis (patients not sensitive to chemo- or radio-therapy - Surgical resection increases median survival of 7 months.	Head, tail or body	Primary rare malignancy accounting for 0.5-2% of cases.	Indistinguishable symptoms from PDAC	(Abedi et al., 2017; Zhang et al., 2018;Al-Shehri, Silverman, & King, 2008; (Meng-dan Xu et al, 2017; Zhang et al., 2018)
Adenosquamous	- Combination of ductal adenocarcinoma and squamous cell carcinoma cells. - Poor median survival of 6 months.	Head of the pancreas	Rare PaCa accounting for 1-4% of cases	Indistinguishable symptoms from PDAC	(Fang et al., 2017; Boyd et al., 2012)
Ampullary cancer	- Develops in the Ampulla de Vater which blocks the bile duct - 5-year overall survival is 40-45%	Head of pancreas	Rare cancer accounting for 6-8% of pancreatic head tumours	Biliary obstructive symptoms including jaundice	(Perysinakis et al., 2014; Sommerville et al., 2009)

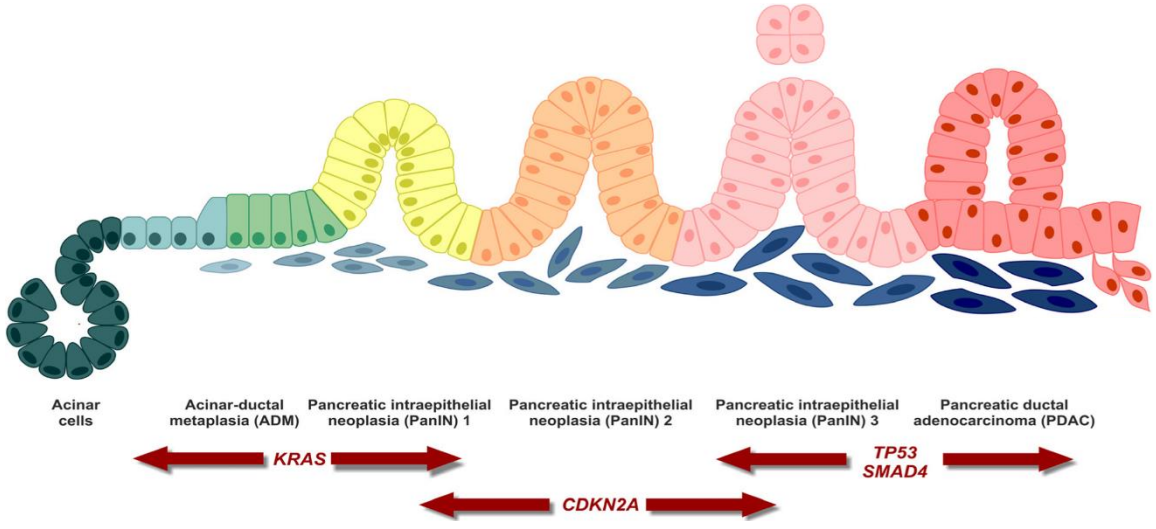

Figure 1.3 Acinar-to-ductal metaplasia progressing from premalignant PanINs to malignant PDAC. Genetic mutations drive the neoplastic changes from KRAS mutations in early stages of PDAC

development to TP53 and SMAD4 mutations in late stages which leads to invasive PDAC. Figure adapted with permission from Springer Nature (Orth *et al*.,2019) ©2019.

1.1.3.2 Endocrine tumours

Neuroendocrine tumours are less common than exocrine tumours, accounting for approximately 5% of PaCa cases (Table 1.3) (Rawla, Sunkara, & Gaduputi, 2019). The endocrine function of the pancreas is to release hormones including amylin, insulin and glucagon into the bloodstream (section 1.1.2.2) therefore patients often present with diabetes (Aggarwal et al., 2012; Bardeesy & DePinho, 2002). Patients with endocrine tumours have a much better prognosis than those with exocrine disease (Rawla et al., 2019) with a 1 year survival rate of 72.8% and an overall 5 year survival rate of 54% which increases to 93% if the tumour remains localised to the pancreas (American Cancer Society, 2021; Man, Wu, Shen, & Zhu, 2018). Meanwhile, PDAC patients have a 1 year survival rate of 18% which drops to 4% at 5 years (Cancer Research UK, 2017).

Table 1.3 Types of endocrine tumour

Type	Description	Location	Incidence	Symptoms	References
Gastrinomas (or Zollinger Ellison syndrome)	- Develop in neuroendocrine cells that produce gastrin - Time between presentation and diagnosis is often after 5 years - 50-60% of cases are malignant at the time of diagnosis	Pancreatic head or duodenum	Rare	Peptic ulcers develop	(Jensen et al., 2007; Roy et al., 2000; Muniraj et al., 2013)
Insulinomas	Predominantly benign, with less than 10% becoming malignant	Islet cells	-1-2% of cases -Most common pancreatic neuroendocrine neoplasm	Hypoglycaemia from overproduction of insulin	(Cancer Research, 2017a; Muniraj et al., 2013)
Somatostatinomas	Secrete large amounts of somatostatin,	-Common in the head of	Rare (1 in 40 million)	Characterised by the onset of diabetes,	(Cancer Research, 2019;

	controlling the release of other hormones within the pancreas	the pancreas -70% of tumours become malignant		cholelithiases, and diarrhoea	Muniraj et al., 2013; Williamson, et al., 2011)
VIPomas	-Increases release vasoactive intestinal peptide (VIP). VIP controls salt, water and sugar levels in the GI tract	-Develops in islets -40-70% of tumours become malignant	Rare (1 in 10 million)	Characterised by diarrhoea, hyperkalaemia and dehydration	(Cancer Research, 2019; Muniraj et al., 2013)
Glucagonomas	-Excess production of glucagon which is important in raising blood sugar levels	-Islet cells --50-80% of tumours become malignant	Rare (2 in 100 million)	Common symptoms include a rash, glucose intolerance and weight loss	(Muniraj et al., 2013; Cancer Research, 2019)
Non-functioning	-Slow growing tumours -Non-functioning as they do not secrete hormones -More than 60% are malignant.	Head of the pancreas	1-2% of all pancreatic tumours	-Often asymptomatic before significant tumour burden -Diagnosed when scans are completed for other indications	(Small et al., 2015 ;Cloyd & Poultsides, 2015; Akerstrom & Hellman, 2007)

1.1.4 Risk Factors for Pancreatic Cancer

PaCa is becoming increasingly common with the success in treating other cancers, and is predicted to become the second most common cause of cancer-related death by 2035 (Rahib et al., 2014). However, there are clear risk factors that increase incidence in subgroups of the population, such as age (Ferlay et al., 2018), obesity (Gonzalez, Sweetland, & Spencer, 2003; Larsson, Orsini, & Wolk, 2007), smoking (Howes et al., 2004; Lynch et al., 2009) and chronic pancreatitis (Howes et al., 2004).

Approximately 20% of PaCa cases are related to smoking, Yuan *et al* (2017) found that there is a 40% increased risk of death in patients who smoke. However, they also showed that stopping smoking

prior to diagnosis has no impact on patient survival. Furthermore, a meta-analysis study showed that there is a 75% increased risk of developing PaCa compared to non-smoker based on estimates across 4 continents which persists 10 years after smoking cessation (Iodice et al., 2008). Additionally, there is evidence for the mechanism by which smoking increases PaCa incidence as exposure to nicotine increased phosphorylation of c-Met (a mesenchymal-epithelial transition factor) which in turn increased growth and metastases of PaCa. Hermann *et al* (2014) compared mice with *K-Ras* mutations that were nicotine-treated to those without nicotine exposure, showing that the mice treated with nicotine developed PanIN and PDAC lesions. Furthermore, they demonstrated that the nicotine acetylcholine receptor modulates proliferation and apoptosis of PaCa cells.

With a rising number of the population becoming obese, increasing attention has been drawn to the association between cancer and obesity. Li *et al* (2009) showed that overweight people between the ages of 14-39 years and obese individuals between the age 20-49 years showed increased risk of PaCa regardless of their diabetic status. Individuals who were obese at a later age (between 20-49) had an earlier onset of PaCa by 2-6 years with a median diagnosis of 59 years, compared to 61 years and 64 years in overweight and normal weight individuals respectively. Furthermore, there is a larger association between men with a high BMI and PaCa. However, individuals who became obese at 40, did not appear to increase their likelihood of developing PaCa. Dawson *et al* (2013) used a $Kras^{G12D}$ mouse model to show that a high calorie/high fat diet can induce pancreatic inflammation and neoplasia in the presence of the *Kras* mutation. These results demonstrate that there are links between obesity and increased risk of PaCa, particularly if obesity is onset from a young age.

Additionally, a common side effect of obesity is the development of type II diabetes and this has been associated with increased risk of developing pancreatic malignancies. Ben *et al* (2011) ran a meta-analysis study on diabetes and PaCa risk, showing a 2-fold increase in risk of developing PaCa. 20-30% of patients with PaCa develop diabetes 2-4 years before diagnosis. However, it is also common for patients to develop type IIIc diabetes as a result of their PaCa diagnosis. Yuan *et al* (2015) showed that

patients with long-term diabetes had decreased survival, whilst in patients with short-term diabetes survival was not affected. In these cases, surgical resection often resolves the diabetes. Long term diabetes may decrease survival as hyperglycaemia has been shown to have a direct impact on cancer cell proliferation, migration and apoptosis (Ryu, Park, & Scherer, 2014).

With an increasingly ageing populating, there has been a rise in the number of cases of various diseases. In the UK between 2015 and 2017, 47% of new cases of PaCa were in people over the age of 75. There is a steep rise in cases between the ages of 50-54 however, the highest rates occur at 85-89 (Cancer Research UK, 2017). In literature there is a lot of speculation about the suitability of elderly patients to undergo pancreatic resection (Whipple procedure). Generally older patients have a higher ECOG status and American Society of Anaesthesiology scores (ASA) which may deem them unfit to undergo surgery. Therefore, the increasing death rates in PaCa may be attributed to the ageing population and their lack of suitability for surgery. Melis *et al* (2012) analysed the outcome of Whipple's procedure in PaCa patients below the age of 80 and above the age of 80. They found that patients over 80, had a worse ECOG status and higher ASA score, longer post-operative hospital stay and higher overall morbidity. In another study comparing the effects of Whipple's procedure between younger patients (<70) and older patients (>70), older patients had a higher risk of developing a morbidity. Pre-operative co-morbidities (diabetes, pulmonary issues, cardiac diseases and neurological issues) were also more common in older patients and they were also shown to have a higher ASA score. Overall, elderly patients had higher mortality than younger patients. The percentage of older patients in this study (37.4%) was lower than younger patients which may indicate that elderly patients may have pre-operative co-morbidities that cause death prior to consideration of surgical resection (Haigh, Bilimoria, & DiFronzo, 2011).

Family history is also a risk factor but to what degree is yet to be determined. A family history of ovarian, breast or colorectal cancer has been associated with increased risk of PaCa in some studies. *BRCA2* mutations have been found in approximately 6% of pancreatic patients with a family history

(Couch et al., 2007). Jacobs *et al* (2010) pooled analysis concludes that family history is associated with a moderately increased risk of developing PaCa, this may be from inherited genetic mutations or a previous history of other cancers including, prostate. In conclusion, the risk of developing PaCa can be increased by multiple factors including a history of smoking, obesity, diabetes, ageing population and family history. Better understanding of early markers of PaCa and understanding the risk factors associated with PaCa could help reduce the poor survival rates associated with the disease.

1.1.5 Diagnosis and symptoms

PaCa is difficult to diagnose as it begins with non-specific symptoms which include abdominal and back pain, nausea and subsequently weight loss caused by malabsorption. These symptoms are not exclusive to PaCa making early diagnosis difficult. The late diagnosis means that only 10-20% of tumours are resectable and therefore poor prognosis is prevalent within the disease (Kommalapati et al., 2018).

There is debate within literature over tumour location and poorer prognosis. Dreyer *et al* (2018) suggest that tumours in the head of the pancreas are associated with a better outcome which is mirrored by Artinyan *et al* (2008). It is suggested that this may be as patients with tumours in the head of the pancreas present with earlier symptoms including jaundice and are therefore diagnosed sooner. This means tumour resection is more likely to be available and result in a better outcome. However, body/tail tumours present with weight loss and pain at more advanced stages (including metastasis) which often means resectability is not an option. In contrast to Dreyer *et al* (2018) and Artinyan *et al* (2008), Winer *et al* (2019) found that although tumours at the head of the pancreas are detected earlier and have a higher chance of being resected, they are often not responsive to adjuvant therapy. Therefore, overall survival is worse in these patients. These data highlight the importance of recognising both the symptoms associated with PaCa for earlier diagnosis and the location of PaCa tumours. Recognising and understanding the significance of tumour location could be important so that patients can receive the most suitable treatment resulting in a better outcome.

Comorbidities such as diabetes often occur from the loss of β-islet cell function (Aggarwal et al., 2012), and in later stages jaundice may arise caused by blockage to the bile duct (Huggett & Pereira, 2011; Mateos and Conlon. 2016). Abdominal and back pain often present in patients from enlargement of the pancreas at the head or tail of the tumour which presses on other organs. The cancer often spreads to pancreatic nerves causing the associated "back" pain which is caused by referred pain from the pancreas (Okusaka et al., 2001). Nausea and vomiting commonly occur when the cancer spreads to the far end of the stomach causing a partial blockage, making it difficult for food to leave the stomach. Gallbladder and liver enlargement can be symptoms of PaCa. Gallbladder enlargement is caused by blockage of the bile duct, resulting in a build-up of bile in the gallbladder and jaundice. Liver enlargement is caused by spread of the cancer to the liver, this happens in approximately 50% of cases and results in poorer patient outcome (Smeenk et al., 2005).

Blood clots can also occur is PaCa patients, this is particularly prevalent in patients with metastasis (3.3-fold increased risk compared to patients with localised PaCa), in patients receiving chemotherapy (4.8-fold increase within 3 months of discontinuing treatment) or in post-operative patients (4.5-fold increase 30 days post-operatively compared to surgical patients without cancer) (Blom, Osanto, & Rosendaal, 2005; Campello et al., 2019). In conclusion, these data highlight the difficulty in being able to recognise specific symptoms relating to PaCa. This often leads to misdiagnosis or late stage diagnosis resulting in poorer prognosis.

Methods of diagnosing patients depends on the symptoms presented and how clear the diagnosis is from initial scans (Table 1.4). CT and MRI scans are the most commonly used diagnostic and staging tools pre-operatively (Zhang et al., 2012). Blood tests measuring tumour marker CA-19 are also performed alongside scans as an easy, relatively non-invasive test that can aid in diagnosis of the patients. Other scans and tests listed in Table 1.4 are used to gain additional information after initial diagnosis. Some individuals are offered CT scans as part of PaCa surveillance, including individuals with hereditary pancreatitis and PRSS1 mutations. People with BRCA1/2, PALB2, CDKN2A mutations, first

degree relatives with PaCa and individuals with Peutz-Jeghers syndrome (a predisposition to cancers of the abdominal organs and viscera) are also offered surveillance (NICE, 2018).

Table 1.4 Diagnostic tests used for pancreatic cancer

Diagnostic test	Criteria	References
CT scan	This is the initial scan used on patients. It is commonly used in individuals that present with obstructive jaundice, pancreatic abnormalities with no jaundice and cysts.	(NICE, 2018; Pancreatic Cancer, 2018)
MRI/magnetic resonance cholangiopancreatopgraphy (MRCP)	Obstructive jaundice, pancreatic abnormalities and no jaundice and cysts. MRCP is used to look at blockages in the bile duct by scanning the bile duct, liver, gallbladder and pancreas.	(NICE, 2018)
Positron- Emission tomography (PET) scan	Obstructive jaundice and pancreatic abnormalities.	(NICE, 2018)
Endoscopic ultrasound (EUS)	If diagnosis is not clear from scans, this can be used to take a biopsy.	(NICE, 2018)
Endoscopic retrograde cholangiopancreatography (ERCP)	This is usually carried out when other imaging tools do not show pancreatic lesions and/or if the patient has jaundice. It can also be used if there is a blockage to the bile duct to insert a stent.	(NICE, 2018)
Endoscopic ultrasound fine needle aspiration	This is generally used with pancreatic cysts if more information is needed on the likelihood of malignancy. This provides a cytological sample but can also be used with a carcinoembryonic antigen (CEA) assay.	(NICE, 2018; Pancreatic Cancer, 2018)
Blood tests	Blood tests can be used to look at blood counts, liver and kidney function, how severe jaundice is and CA19-9 levels. CA19-9 tumour marker is not always present in higher levels in PaCa patients. Furthermore, other cancers and conditions can increase levels so it is not specific to PaCa	(Pancreatic Cancer, 2018; NICE, 2018)

Following the described scans and tests (Table 1.4), the stage of the cancer can be diagnosed to determine the appropriate treatment (Table 1.5 to Table 1.7) (Section 1.1.6). The stage is determined using the TNM staging system which looks at size of the tumour, whether it has spread to lymph nodes and whether it has metastasised. The outcome patients have is largely dependent on the stage the cancer is diagnosed and whether they are suitable for surgery (Table 1.7).

Table 1.5 TNM staging for pancreatic cancer (Amin et al., 2017; Sobin, Gospodarowicz, & Wittekind, 2009)

T (tumour)	
T1A	Tumour is < 0.5cm in any direction
T1B	Tumour is > 0.5cm but < 1cm in any direction
T1C	Tumour is > 1cm but < 2cm in any direction
T2	Tumour is > 2cm but < 4cm in any direction
T3	Tumour is > 4cm
T4	Tumour has grown outside of pancreas into large blood vessel
N (nodes)	
N0	No lymph nodes containing cancer
N1	1-3 lymph nodes that contain cancer cells
N2	Cancer involves more than 4 lymph nodes
M(Metastasis)	
M0	Cancer has not spread to distant organs
M1	Can has spread to distant organs

Table 1.6 One year survival predictions based on stage of cancer, TNM and location (Bilimoria et al., 2007.; Edge et al., 2015; Pancreatic Cancer, 2018)

				Surgery		**No surgery**	
Stage	**TNM**	**Location**	**Size**	**1 year survival**	**% cases diagnosed**	**1 year survival**	**% cases diagnosed**
1A	T1,NO,MO	Completely in the pancreas	<2 cm	71.3%	8.8%	29.2%	4.4%
1B	T2, NO, MO		2-4 cm	67.3%	11.0%	26.0%	5.4%
2A	T3, NO, MO	Spread to surrounding tissues but not involving lymph nodes	>4cm	60.7%	17.9%	25.0%	10.1%
2B	T1-3, N1, MO	Spread to surrounding tissue, involving lymph nodes	Any size	52.7%	36.4%	26.9%	11.8%
3	T4, NX, MO	Locally advanced. Spread to stomach, spleen, large bowel or		44.5%	13.2%	27.0%	13.0%

		blood vessels near pancreas					
4	TX, NX, M1	Advanced/metastatic-spread to other parts of the body including lungs, liver and peritoneum		19.2%	12.7%	8.3%	55.2%

1.1.6 Current treatments

The current treatment options available for PaCa patients depends on the stage of cancer (Table 1.7), for example, chemotherapy with more adverse effects is not recommended for later stage patients. Neoadjuvant therapy, surgical resection and adjuvant therapy are offered to patients' dependent on the severity of the disease. Surgery is shown to significantly improve patient outcome however, this is only available to a small number of patients (10-20%) due to late diagnosis. Therefore, early detection can make a significant difference to patient outcome.

Takahashi *et al* (2018) analysed PaCa patient samples from stage I to IV and showed that the size of a tumour can determine median overall survival (OS). Tumours >2cm compared to tumours <2cm showed a poorer median OS of 20.5 months compared to 30.6 months respectively. Hsu *et al* (2018) compared 5 year survival in patients with stage I, IIA and IIB PaCa with tumours of <2.5cm and >2.5cm showing a 5 year survival of 17.5% and 6.0% respectively. This suggests that the size of a tumour has an impact on patient survival. The type of treatment offered to tumours >2cm also impacts survival. Surgery performed on these tumours frequently results in an R1 tumour resection (macroscopic removal of tumour but microscopic margins of positive tumour).

Furthermore, surgery alone results in an median OS of 21.3 months but neoadjuvant chemotherapy or neoadjuvant radiotherapy increases median OS to 22.9 months and 25.8 months respectively, indicating a positive effect of therapy prior to surgery (Takahashi et al., 2018). Van Tienhoven *et al* (2018) compared PDAC patients with Stage I and II cancer. They showed that patients who have immediate surgery followed by adjuvant therapy had a lower median OS (13.5 months) compared to patients with pre-operative chemoradiotherapy, surgery followed by adjuvant therapy (median OS

17.1 months). Patients receiving neoadjuvant therapy had a 65% chance of an R0 resection (macroscopic removal of tumour) compared to 31% in adjuvant therapy alone. Tummers *et al* (2019) have shown that median OS is effected by the type of resection achieved (patients had stage I-IV). Median OS increased from 15 months to 22 months when patients had an R0 resection.

Chakraborty & Singh (2013) compared outcomes of patients without vascular invasion (Stage I, IIA and IIB) who had surgery to remove the tumour to those that didn't. The results highlighted that surgery can significantly improve survival in these patients and showed that those who had surgery had a median OS of 18 months and without surgery has an median OS of 7 months. However, these experiments did not consider patients who may have had neoadjuvant therapy which could have increased overall survival further.

Neoptolemos *et al* (2010) compared patients (Stage I-IVa) treated with gemcitabine (the standard PaCa treatment since the early 1990s) or fluorouracil (5-FU) with folinic acid (Table 1.8) in an ESPAC-3 trial. Gemcitabine increased survival by 23.6 months compared to 23 months with the 5-FU/folinic acid combination. This suggests there is no significant difference between the two treatments however, 5-FU did cause more adverse effects. Von Hoff *et al* (2017) compared treatment with gemcitabine in combination with nab-paclitaxel to gemcitabine alone in advanced stage patients, survival increased by 35% in the first year of treatment in the combination therapy group compared to 9% in patients treated with gemcitabine alone. Although this combination therapy is less toxic than FOLFIRNOX, OS was lower at 6.7 months compared to 8.5 months with FOLFIRNOX.

Conroy *et al* (2011) compared gemcitabine therapy to a modified FOLFIRINOX (FOLFIRINOX without bolus 5-FU). The modified FOLFORINOX significantly improved median OS to 54.4 months compared to 35 months in gemcitabine. However, the modified FOLFIRINOX did result in a higher percentage of patients suffering with grade 3/4 adverse effects (75.9% vs 52.9%). These results suggest that chemotherapy has to be carefully considered as most patients diagnosed with PaCa are elderly and therefore may be less tolerant of the adverse effects despite the suggested improved survival in

patients. These studies demonstrate the need for treatment that not only improves patient survival but also has fewer adverse effects.

Table 1.7 Therapies available for PaCa patients at different stages of cancer (Cancer Research UK., 2017; Cancer Research UK., 2019; NICE, 2018; El Kamar, Grossbard, & Kozuch, 2003; Werner et al., 2013)

Stage	Treatment options
Stage I and II	Surgery is an option as tumours are resectable. Post-operative chemotherapy is given once patient has recovered. Treatment options include: - Gemcitabine and capecitabine - Gemcitabine and nab-paclitaxel - Gemcitabine alone if not well enough after surgery - FOLFIRINOX
Stage III	30% of patients present at this stage. Surgery can be offered but with no curative purpose, simply for symptomatic relief so obstructive jaundice and gastric outlet obstruction using a stent or bypass surgery. Stage I and II chemotherapies available.
Stage IV (metastatic)	50% of patients present at this stage. Chemotherapy is not curative, it is used to shrink tumour and relieve symptoms associated with the advanced disease. Surgery is also available to relieve symptoms. 1st line options- FOLFIRINOX or if patients are fit (*EGOG 0-1) Gemcitabine with nab-paclitaxel for people unable to tolerate FOLFIRINOX 2nd line options- oxaliplatin-based chemotherapy if not used in first line therapy Gemcitabine alone if patient is deemed unfit.

**ECOG (Eastern Cooperative Oncology Group)- this determines patients level of functionality to determine their suitability for treatment.*

Table 1.8 Mechanism of action of different chemotherapies

Chemotherapeutic agent	Mechanism of action	Reference
Gemcitabine	It is a deoxycytidine analogue that incorporates into DNA which prevents DNA synthesis and causes cell death.	(Plunkett et al., 1995)
Capecitabine	This is pro-drug metabolised to 5-fluorouracil (5-FU) which is a thymidylate synthase inhibitor which inhibits thymidine	(Miwa et al., 1998)

	monophosphate production. This is the active form of thymidine which is required for DNA synthesis.	
Nab-paclitaxel (or abraxane)	A mitotic inhibitor that inhibits microtubule reorganisation and therefore causes cell death.	(Yardley, 2013) (Manfredi & Horwitz, 1984)
FOLFIRINOX	This is a combination chemotherapy. **FOL-** this is folinic acid which enhances the effects of 5-FU **F-** this is 5-FU which incorporates in to the DNA molecule and inhibits DNA synthesis. **IRIN-** this is irinotecan which is a topoisomerase inhibitor which prevents DNA from uncoiling and duplicating **OX-** oxaloplatin is a platinum based anti-neoplastic agent that inhibits DNA repair and/or DNA synthesis.	(Moran & Keyomars, 1987)- get better reference for FOL (Santi, McHenry, & Sommer, 1974) (Hsiang & Liu, 1988) (Arango et al., 2004) (Faivrea, Chan, Salinas, Woynarowska, & Woynarowski, 2003)

1.2 Adrenomedullin (ADM) and its physiological roles

As previously described, PaCa is often diagnosed too late due to non-specific symptoms. However, individuals with hereditary pancreatitis, germline mutations or new-onset diabetes may be offered tests to monitor if there are any changes that indicate the development of PaCa. There are currently no blood tests specific to PaCa or that can be used as early indicators of PaCa developing (Pereira et al., 2020). There is evidence showing that ADM is elevated in serum in patients with PaCa (Francesco et al., 2016; Keleg et al., 2007) and this could potentially be significant as it could be used as part of PaCa diagnosis. However, elevated ADM levels are not specific to PaCa as there is evidence for increased levels in other cancers and diseases including sepsis. Therefore, measuring ADM in serum could be a supplementary aid in the diagnosis of PaCa but not as an exclusive method of diagnosis.

ADM is a 52-amino acid peptide encoded by *adm*, it was originally isolated by Kitamura *et al* (1993) from an adrenal medulla pheochromocytoma. It functions as a circulating hormone and local paracrine

mediator that has both physiological and pathological roles. It belongs to the calcitonin superfamily which includes amylin, CGRP, calcitonin and ADM (Schönauer, Els-Heindl, & Beck-Sickinger, 2017). These have similar structural homology with a 6 amino acid ring formed by a disulphide bond between residues 16 and 21 (Ishimitsu, Kojima, et al., 1994)

1.2.1 ADM synthesis

In humans, ADM is encoded by a gene on chromosome 11 and consists of 4 exons and 3 introns (Ishimitsu, Kojima, et al., 1994). Its precursor, preproADM (185 amino acids) is cleaved at the N-terminal signalling peptide (21 amino acids) to make proADM (184 amino acids). Pro-ADM goes through a second cleavage to produce pro-ADM N-terminal 20 peptide (PAMP), mid-regional pro ADM, adrenotensin and glycine extended 53 amino acid peptide (Figure 1.4) (Gumusel et al., 1995; Kazuo Kitamura et al., 1998, 1993). The glycated form of ADM is inactive (accounts for 85% of ADM) and undergoes an enzymatic reaction to produce the mature 52 amino acid ADM by amidation (15% of ADM) (Meeran et al., 1997). It is mainly synthesised and secreted by endothelial cells (ECs) and vascular endothelial smooth muscle cells (VSMCs) that express ADM receptors. This suggests that ADM has an autocrine/paracrine function in vasculature (Sugo et al., 1994; Sugo et al., 1994). The circulating ADM half-life is 22 minutes and it is rapidly degraded by N-terminus proteases (Meeran et al., 1997).

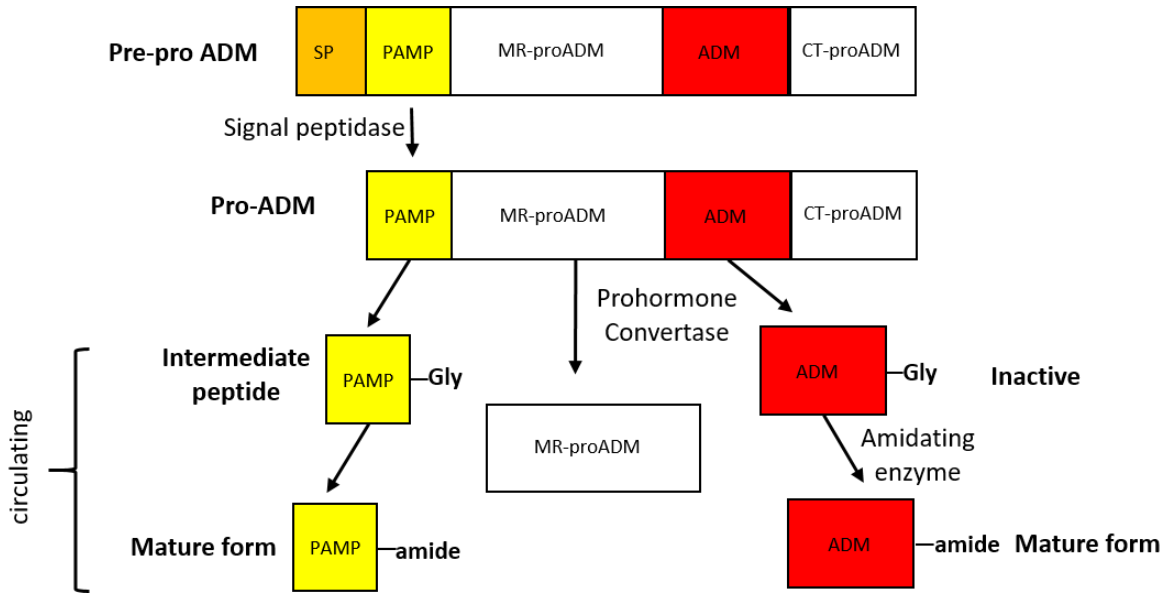

Pre-pro ADM: pre-pro adrenomedullin; PAMP: proadrenomedullin NH_2 terminal 20 peptide; MR-proADM: midregional proadrenomedullin; ADM: adrenomedullin; CT-proADM: C-terminally glycine extended adrenomedullin

Figure 1.4 Adrenomedullin (ADM) synthesis. Prepro-ADM is cleaved at the N terminal signalling peptide and produces Pro-ADM. Pro-ADM undergoes a second cleavage to produce, PAMP, MR-proADM, ADM and CT-proADM. PAMP is activated following an enzymatic reaction with an amidating enzyme to produce mature PAMP. ADM is activated by an enzymatic reaction where it is cleaved at the C-terminal to produce 52 amino acid, ADM. Figure adapted with permission from Oxford University press (Weber et al., 2017) ©2019

1.2.2 Adrenomedullin receptors

ADM primarily mediates its effects through a Family of B G-Protein coupled receptor (GPCR) that forms a complex with a receptor activity-modifying protein (RAMP) (Figure 1.5). This is discussed in further detail below.

1.2.2.1 G-Protein Coupled Receptors

GPCRs are the largest family of cell surface receptors and account for 40% of drug targets. They are 7 transmembrane (7-TM) receptors that form either homo- or hetero- dimers. They regulate intracellular signalling cascades in response to hormones, ions, photons, odorants and other stimuli.

Each has an alpha-helical segment which is separated by alternating intra/extracellular loops. GPCRs can be split into 6 different superfamily classes (Table 1.9).

Table 1.9 GPCR superfamily classes

Class	Receptor family	Examples
A	Rhodopsin like	Rhodopsin/Histamine
B	Secretin	CTR/CLR/GLP/PTH
C	Glutamate	$GABA_B$/GPRC6A
D	Fungal pheromone	Mating factors
E	cAMP receptors	Serpentine
F	Frizzled	Frizzled and smoothened receptors

CTR: calcitonin receptor; CLR: calcitonin receptor-like receptor; GLP: glucagon like peptide receptor; PTH: parathyroid hormone receptor; cAMP: cyclic adenosine monophosphate; $GABA_B$: gamma-aminobutyric acid class B; GPRC6A: G protein-coupled receptor family C, group 6, member A

GPCRs are composed of 3 regions; the N terminal extracellular loop for ligand binding, the 7-TM middle segment and the intracellular C terminal. Ligand binding at the N terminus causes a conformational change in the receptor and activates the C terminal triggering a downstream signalling cascade (Section 1.2.3). ADM receptors are heterodimeric complexes made of a family B GPCR, the calcitonin-like receptor (CLR), which pairs with a single transmembrane RAMPs (Figure 1.5).

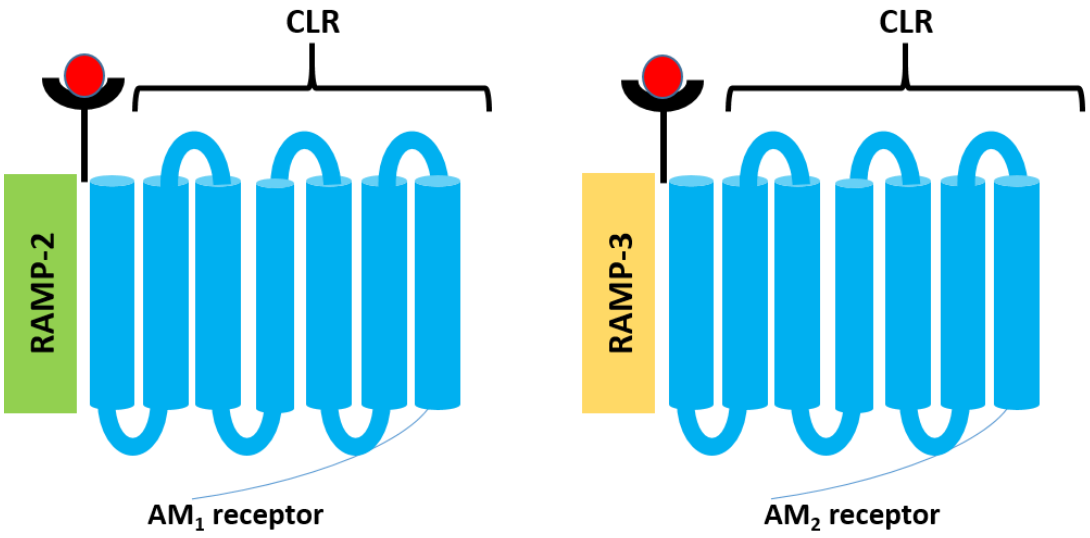

Figure 1.5 Adrenomedullin receptor. ADM (red) can bind to one of two receptors composed of a 7 transmembrane GPCR, calcitonin like receptor (CLR) (in blue) and a receptor activity-modifying protein

(RAMP). Different RAMPs form different receptors; RAMP-2/CLR complexes generate the AM_1 receptor (green) and RAMP-3/CLR make the AM_2 receptor (yellow). These have different physiological roles involving the regulation of blood pressure and promoting tumorigenesis.

1.2.2.2 Calcitonin receptor-like receptor (CLR)

CLR is a 7-TM complex that makes up part of the ADM receptor. It has a molecular weight of approximately 70 kDa and shares 55% sequence homology with calcitonin receptor (CTR). However, unlike CTR, CLR can only reach the cell surface with RAMP trafficking. RAMP-1 traffics CLR to the surface by terminal glycosylation (McLatchie et al., 1998) and RAMP-2 and RAMP-3 cause core glycosylation of CLR (Foord et al., 1999). Once CLR and RAMP are at the cell surface, the appropriate ligand can bind and activate downstream cell signalling (McLatchie et al., 1998).

1.2.2.3 Receptor activity modifying proteins

RAMPs are a small family of intrinsic proteins with only 3 members in humans named RAMP-1, RAMP-2 and RAMP-3. These proteins share only 30% sequence homology. They have a single transmembrane spanning domain with an extracellular N terminal domain (90-100 amino acids) and a short intracellular C terminal domain (approximately 9 amino acids). The short C terminus has two basic residues which act as an endoplasmic retention signal. RAMP-1 is not glycosylated whilst RAMP-2 and RAMP-3 have two glycosylation sites. When RAMPs and CLR come together they override the endoplasmic retention signal at the C terminus and translocate the receptor complex from the endoplasmic reticulum to the plasma membrane. It is proposed that RAMPs aid in the trafficking of CLR to the cell surface (Steiner et al., 2002; McLatchie et al., 1998). . However, Flahaut, Rossier, & Firsov (2002) suggest only the RAMP-1/CRLR complex require dimerization to be trafficked to the plasma membrane. RAMP-2 and RAMP-3 contain N-glycosylated sites, only require N-glycan for their transport to the cell surface and therefore heterodimer assembly is not required for CLR cell surface expression. RAMPs also have a role in altering selectivity of a receptor for particular ligands (Table 1.10) (McLatchie et al., 1998).

RAMPs interact with many different receptor types including the oestrogen receptor GPR30, PTH_1 and PTH_2 receptors and the calcium sensing receptor (Bouschet, Martin, & Henley, 2012; Christopoulos et al., 2003; Christopoulos et al., 1999; Lenhart et al., 2013; Serafin et al., 2020). However, CTR and CLR interactions with RAMPs are specifically associated with ADM ligand binding. The potency of ADM, CGRP, intermedin (IMD) and amylin for the different receptors alters dependent on which RAMP interacts with either CLR or CTR (Table 1.10) (Hay, Poyner, & Sexton, 2006; Riveiro et al., 2021). RAMPs are essential for the trafficking of CLR to the cell surface and therefore crucial for ADM and CGRP receptor activity.

Table 1.10 RAMP and CLR/CTR receptor complexes showing the rank of ligand potencies

Receptor	Ligand	Ligand potency
RAMP-1 + CLR (CGRP)	CGRP	CGRP > IMD > ADM > AMY
RAMP-2 + CLR (AM1r)	ADM	ADM > IMD > CGRP> AMY
RAMP-3 + CLR (AM2r)	ADM	ADM > IMD > CGRP > AMY
RAMP-1 + CTR (AMY1)	AMY	AMY ≥ CGRP > IMD > CT > ADM
RAMP-2 +CTR (AMY2)	AMY	AMY
RAMP-3 + CTR (AMY3)	AMY	AMY > CGRP > AM

CGRP: calcitonin gene-related peptide; ADM: adrenomedullin; AMY: amylin; CLR: calcitonin receptor-like receptor; CTR: calcitonin receptor; CT: calcitonin; IMD: intermedin; RAMP: receptor activity modifying protein

1.2.3 Signalling pathways

ADM mediates its actions through three main signalling pathways which include cAMP, Akt and mitogen activate protein kinase (MAPK). Binding of the ADM ligand to AM1 receptor or AM2 receptor causes a conformational change that activates the intracellular C terminus. One pathway activated is the cAMP pathway which initiates either Gαs, Gαi or Gαq signalling. The Gαs pathway is an activating pathway, binding of ADM to the RAMP/CLR receptor induces the dissociation of the α-unit from the αβγ-complex on the N terminal. The α-subunit will bind to adenylyl cyclase which generates cAMP.

cAMP converts inactive protein kinase A (PKA) to active PKA and induces a downstream signal (Blom et al., 2012; Sassone-Corsi, 2012)

The cAMP pathway associated with ADM is important in regulating vascular and muscle cells. In many cell types, ADM and CGRP receptors are coupled with G_s proteins which activates adenylate cyclase and therefore intracellular levels of cAMP. In bovine aortic endothelial cells and vascular smooth muscle cells (VSMCs), accumulation of cAMP causes an increase in calcium efflux leading to relaxation of vascular cells (Shimekake et al., 1995). In prostate cancer, cAMP has been shown to increase cancer cell proliferation and invasion (Berenguer-Daize et al., 2013) (Figure 1.6).

The PI_3K/Akt pathway is also regulated by ADM and is often activated in vascular endothelial cells. It has been shown to have roles in regulating vasodilation, apoptosis proliferation and migration (Nishimatsu et al., 2001; Okumura et al., 2004). In hepatocellular carcinoma this pathway is induced following an increase in ADM expression in hypoxic conditions which promotes cancer cell proliferation (Park et al., 2008) (Figure 1.6).

The activation of the MAPK/ERK pathway has roles in regulating cell death, increasing proliferation and invasion of cancer cells and inducing angiogenesis in cancer. ADM also induces this pathway to protect malignant cells from hypoxia induced cell death by the upregulation of Bcl-2 (Wu et al, 2015). In prostate and lung cancer, ADM has been shown to induce the MAPK pathway to increase proliferation and invasion of these cells (Berenguer-Daizé et al., 2013; Greillier & Tounsi, 2015). The diversity of this pathway expands to inducing angiogenesis, where Kim *et al* (2003) showed that ADM induces angiogenesis in endothelial cells through the AKT/ERK 1/2 focal adhesion pathway. Furthermore, Chen *et al* (2015) show that ADM induced VEGF expression in ovarian cells via the JNK/Activator protein 1 pathway (AP-1) (Figure 1.6).

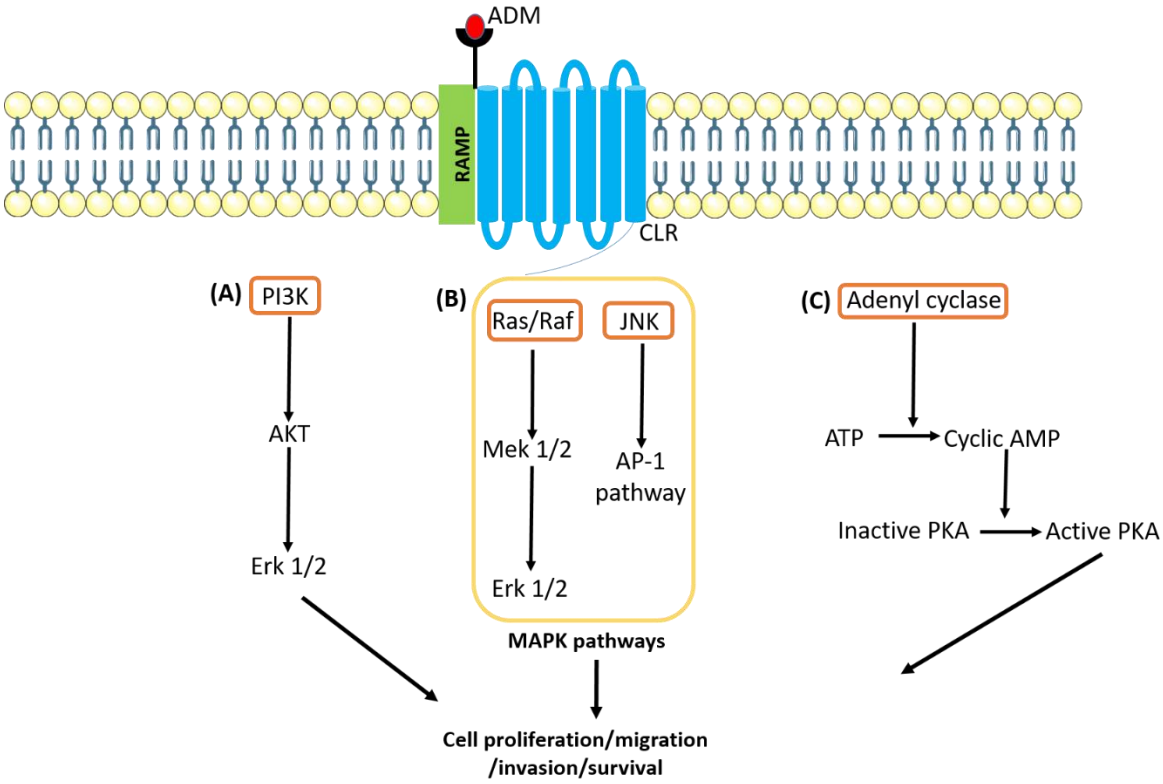

Figure 1.6 Adrenomedullin pathways. ADM induces its effects through 3 main pathways which include; PI3K, MAPK and cAMP. **(A)** ADM mediates the PI3K pathway in hypoxic conditions and induces cancer cell proliferation. **(B)** ADM activates the MAPK pathway and increases the proliferation and invasion of cancer cells and protects malignant cells from hypoxia induced apoptosis by upregulating Bcl-2. Angiogenesis can also be induced by this pathway through the JNK/AP-1 pathway. **(C)** cAMP contributes to increased proliferation and invasion of cancer cells by activating PKA.

ADM: adrenomedullin; PI3K: phosphoinositide 3 kinase; AP-1: activator protein 1, PKA; protein kinase A

1.2.4 Physiological roles of ADM and its expression in different organs

ADM RNA and protein is distributed in normal tissues, the highest level of ADM expression is found in the placenta and adipose tissue (Figure 1.7). At protein level there is similar distribution of ADM across many organs including the pancreas, female tissues, kidney, GI tract (specifically the stomach), bone marrow and immune organs. Figure 1.8 shows mRNA and protein expression of CLR and its

distribution. The highest RNA and protein levels is in the lungs. Protein expression is also high in the female tissue, skin, bone marrow and lymphoid tissues. RNA expression is relatively low in all the organs except the lungs. RAMP-1 RNA expression varies between organs as shown by Figure 1.9. RAMP-1 has the highest RNA expression female reproductive organs followed by smooth muscle and brain tissue according to analysis by the human protein atlas (HPA). RAMP-2 RNA is distributed amongst all organs with the highest RNA expression in the lungs, female reproductive organs, smooth muscle and adipose tissue respectively. Whilst RAMP-3 has the highest RNA expression in the lungs, thyroid and lymph nodes. These data obtained from HPA show the diversity in RNA and protein expression of ADM and its receptor components across many different organs. It shows the importance of ADM in regulating the functions of the human body and how alterations in ADM expression may impair the function of these organs and change ADM effects from physiological to pathological. Previous studies have shown that RAMP-2 is more abundantly expressed and has an important physiological role however, in pathological conditions where ADM levels elevate in plasma for example, in pregnancy, sepsis or heart failure, RAMP-3 expression becomes more prominent (Sonia Martínez-Herrero & Martínez, 2013).

The first discovered physiological role of ADM was in vasodilation leading to reduced peripheral resistance and therefore hypotension. Blood pressure is regulated by ADM in the kidneys, brain and vessels (Kitamura et al., 1993). In the cardiovascular system, ADM lowers blood pressure by decreasing peripheral vascular resistance. Other physiological systems regulated by ADM include the gastrointestinal, reproductive and immune system. ADM also has pathological roles, it has been shown to induce multiple cancer-promoting effects. These include stimulating tumour growth via proliferation of cells, promoting angiogenesis, inducing metastasis and evading the immune system (Section 1.3). Recently more attention has been drawn to the interactions with ADM and the pancreatic cancer stroma and the potential therapeutic implications. However, as ADM has an important role physiologically in the kidneys, heart and pancreas, it also means that dysregulation of this system can induce diseases including renal failure, hypertension and diabetes.

1.2.4.1 Physiological role of ADM in the pancreas

In the pancreas, ADM is located in the endocrine portion of the organ. Immunocytochemistry, immunofluorescence and molecular studies have shown that ADM and its receptor components (CLR and RAMPs) are present in the β- islet cells of the pancreas. Therefore, it has been suggested that ADM has a role in regulation of insulin secretion and may explain why some patients develop new-onset diabetes when they are diagnosed with PaCa (Martinez et al., 2000). It has been reported that ADM is secreted from pancreatic polypeptide cells into the bloodstream and is transported to β cells. ADM binding induces a cAMP signal which inhibits insulin secretion resulting in an increase in glucose (Zudaire, Martínez, & Cuttitta, 2001; Martinez et al., 2000). This is further supported by Martinez *et al* (1996) who added ADM dose dependently to rat islets and at a concentration of 1 μM, insulin secretion was inhibited by 78%. Another potential role of ADM, is control the secretion of amylase as it has been proposed that ADM inhibits amylase secretion in rat pancreatic acini. Tsuchida *et al* (1999) identified a dose dependent inhibition of amylase secretion in rat acini suggesting that ADM may also have an exocrine role.

1.2.4.2 Physiological role of ADM in the reproductive system

Within the reproductive system, ADM has been shown to have an important role throughout pregnancy. ADM knockouts in mice resulted in embryo lethality (Dackor et al., 2007), suggesting that ADM is important in foetal development (Shindo et al., 2001). Suppression of ADM results in a shortage of placental vascularisation, malformation of the basement membrane in the aorta and cervical arteries, detachment of endothelial cells from the basement structure and oedema (Ichikawa-Shindo et al., 2008; Li et al., 2006). Minegishi et al (1999) show a progressive increase in ADM plasma concentration from the non-pregnant follicular phase through to the third trimester, increasing from 6.4 fmol/ml to 21.5 fmol/ml respectively. They also showed that ADM is expressed at mRNA level in the placenta and may have a role in trophoblast development, providing nutrients to the embryo.

RAMP-2 knockouts result in embryo lethality midgestation (Ichikawa-Shindo et al., 2008) however, RAMP-3 knockout mice have been shown to survive until old age (Dackor et al., 2007).

1.2.4.3 Physiological role of ADM in the kidneys

In the kidneys, immunostaining has shown expression of ADM in the collecting ducts, distal convoluted tubes, vessels, glomerular mesangial cells, endothelial cells and podocytes. Furthermore, ADM mRNA expression has been shown in the glomerulus, distal tubules, medullary collecting duct cells (Asada et al., 1999; Hino et al., 2005; Jougasaki et al., 1995; Nishikimi, 2007). CLR, RAMP-2 and RAMP-3 were also shown to be expressed in rat renal cortex and medulla (Yoshihara et al., 2001). These data suggest that ADM and its receptors play a role in regulation of renal haemodynamics, glomerular filtration and sodium homeostasis (Cockcroft et al., 1997; Ishiyama et al., 1993; Kitamura et al., 1993; Passaglia et al., 2014).

1.2.4.4 Physiological role of ADM in the GI tract

Within the GI tract, positive ADM staining has been shown to be located in enterochromaffin-like chief cells of the gastric fundus, glandular epithelia and gastrin containing cells of the pyloric mucosa and in neuroendocrine cells. ADM was identified as being localised near blood vessels in the neuroendocrine cells. ADM mRNA has been detected in non-endocrine cells of the basal half of the mucosa (Fukuda et al., 1999; Kitani et al., 1999; Sakata et al., 1998; Tajima et al., 1999). Rossowski, Jiang, & Coy (1997) have shown that the role of ADM within the GI tract may be in the regulation of gastric acid secretion. They showed that ADM is a potent inhibitor of gastric acid secretion (Hirsch et al., 2003; Rossowski et al., 1997). As previously discussed, ADM has a major role in regulating vasculature including angiogenesis and the regulation of blood pressure, Salomone *et al* (2003) have shown that ADM is also found in the mucosal layer of the stomach and regulates blood supply to the gastrointestinal region to prevent gastric ulcers forming. There has also been a suggested link between the regulation of gastric emptying by ADM produced in the brain (S. Martínez-Herrero & Martínez, 2016).

These data combined show the extent of ADMs impact under normal physiological conditions. This would be an important consideration if therapies were developed against ADM for PaCa treatment, as it would be important to ensure the described physiological effects of ADM would not be effected by treatment.

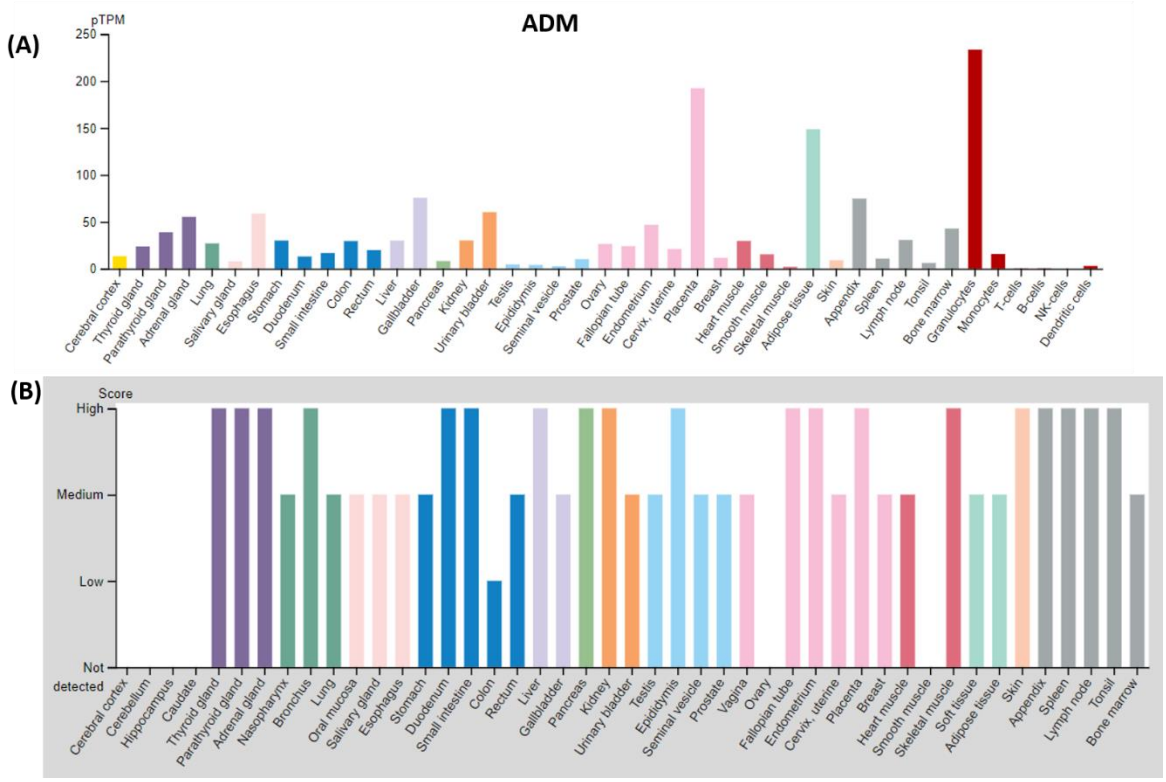

Figure 1.7 mRNA and protein expression of ADM in different tissues and blood. (A) ADM RNA expression shown as mean protein transcript per million (pTPM), which corresponds to the mean values of individual samples for each tissue. Data obtained from HPA RNA-seq analysis which is used to estimate the transcript abundance in different cells, tissues and blood samples. (B) ADM protein expression in different tissues is scored as not detected, low, medium or high expression. https://v18.proteinatlas.org/ENSG00000148926-ADM/tissue

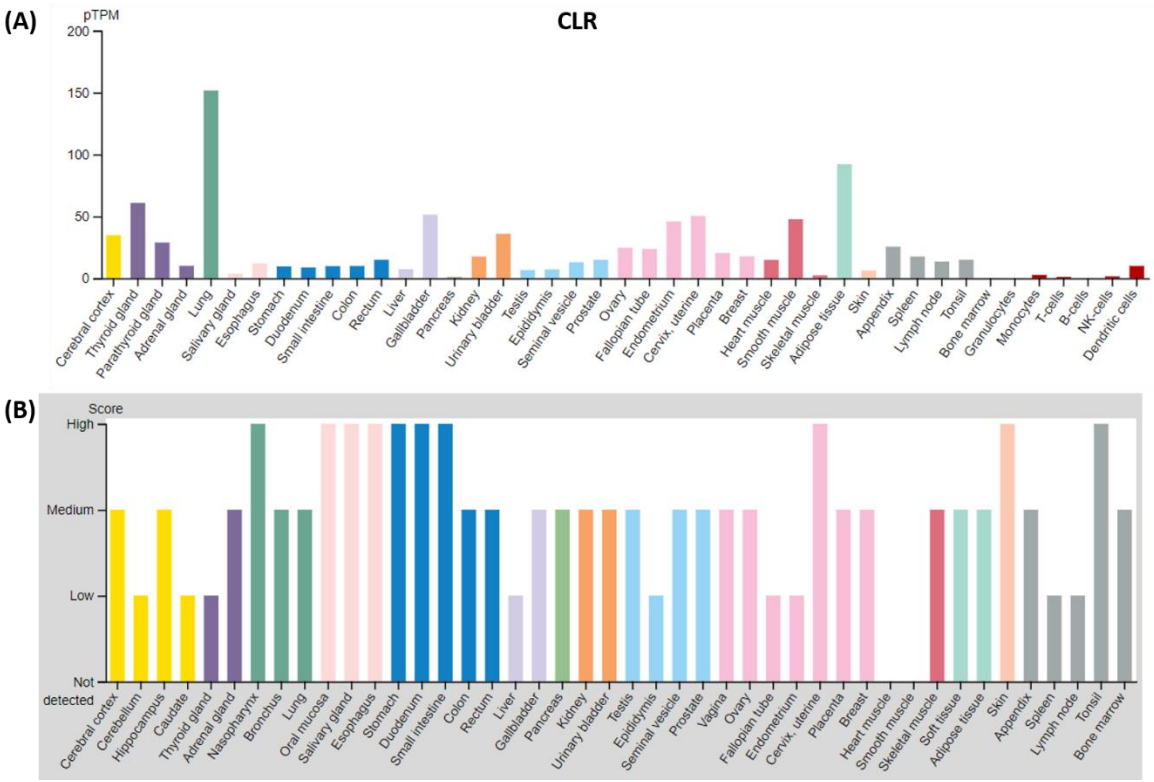

Figure 1.8 mRNA and protein expression of CLR in different tissues and blood. (A) CLR RNA expression, shown as mean protein transcript per million (pTPM), which correspond to mean values of individual samples for each tissue. Data obtained from HPA RNA-seq analysis which is used to estimate the transcript abundance in different cells, tissues and blood samples. (B) CLR protein expression of different tissues is scored as not detected, low, medium or high expression https://www.proteinatlas.org/ENSG00000064989-CALCRL/tissue

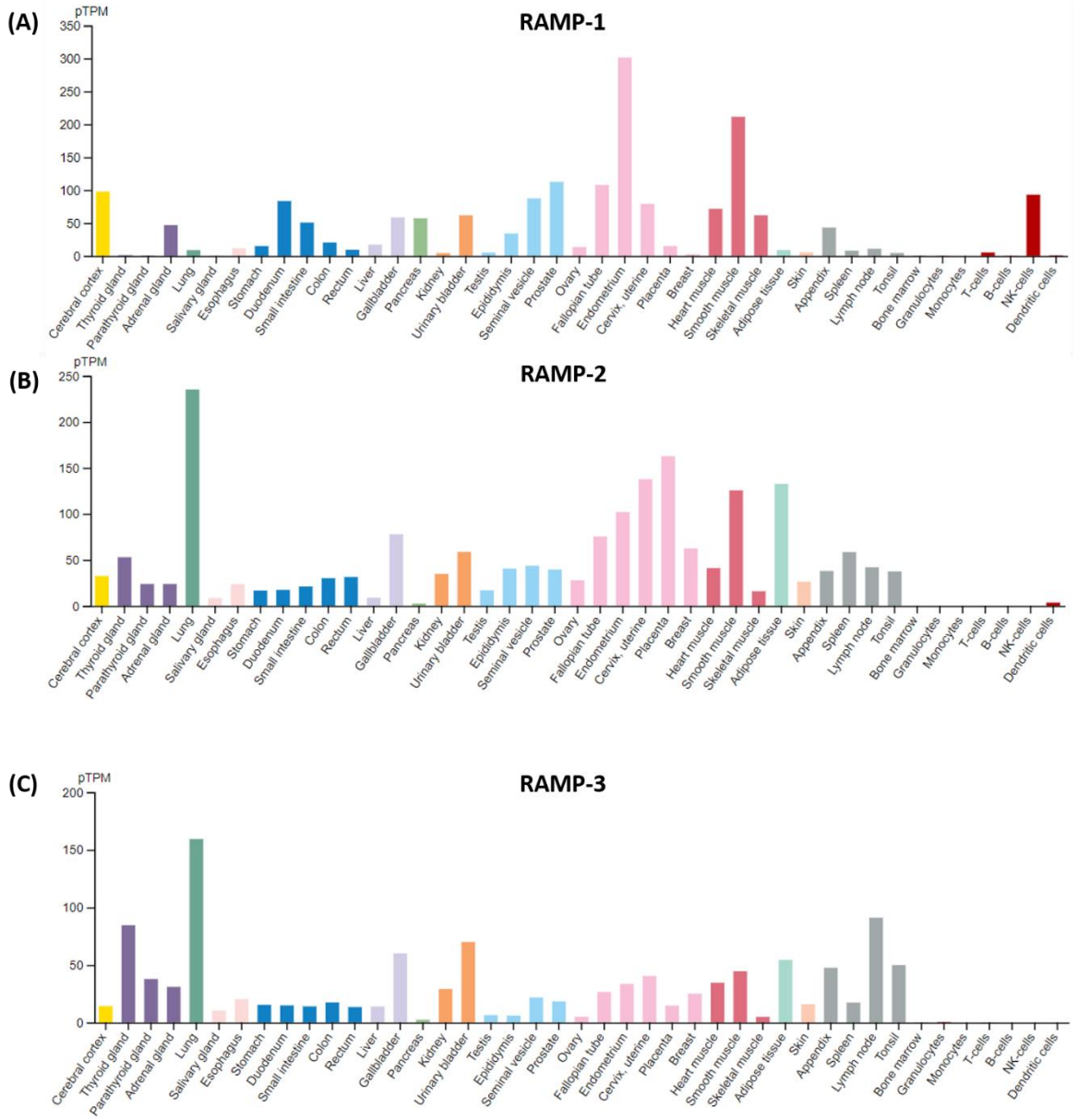

Figure 1.9 mRNA expression of RAMP-1 (A), RAMP-2 (B) and RAMP-3 (C) in different tissues and blood. RAMP RNA expression is shown as mean protein transcript per million (pTPM), which corresponds to mean values of individual samples for each tissue. Data obtained from HPA RNA-seq analysis which is used to estimate the transcript abundance in different cells, tissues and blood samples https://v18.proteinatlas.org/ENSG00000132329-RAMP1/tissue https://www.proteinatlas.org/ENSG00000131477-RAMP2/tissuehttps://www.proteinatlas.org/ENSG00000122679-RAMP3/tissue

1.2.5 Role of Proadrenomedullin N-terminal peptide (PAMP)

PAMP is a biologically active molecule produced as a result of proteolytic cleavage of pro-ADM as shown in Figure 1.4. It has been identified in plasma, adrenal medulla, the right atrium, kidneys and brain. The receptor PAMP binds to has been suggested to be MrgX2, unlike ADM which has been shown to induce its effect through the AM1 and AM2 receptors (Meyrath et al., 2021).

Physiologically, PAMP has been shown to exert hypotensive activity in rats and cats. In human disease, elevated plasma levels of PAMP has been associated with hypertension, renal failure and congestive heart failure (Mahata et al., 1998). More recently, PAMP has been shown to act as an antimicrobial peptide and as an endogenous ligand to chemokine receptor, ACKR3. ACKR3 has been shown to have roles in regulating embryogenesis, hematopoeisis, neuronal migration, angiogenesis and cardiac development (Ajish, Yang, Kumar, & Yub, 2020; Meyrath et al., 2021).

1.3 Adrenomedullin and Cancer

The tumour microenvironment is diverse and hosts multiple different cell types and conditions that promote cancer cell survival. ADM plays a vital role in the communication between these different cell types. It is secreted by both cancer cells and tumour stromal cells including macrophages, pericytes, fibroblasts and endothelial cells. This extensive network is connected by the expression and secretion of ADM in these different cell types. Therefore, ADM is associated with multiple hallmarks of cancer including inducing proliferation, inducing angiogenesis, evading apoptosis and immune evasion.

In PaCa, the formation of dense fibrous scar tissue (desmoplasia) plays a key role in current therapies being largely unsuccessful due to the hypoxic hypovascular environment that develops. Therefore, understanding the role of ADM in the development of scar tissue and its interactions with different stromal tissue cells, could provide a novel therapeutic target. In this section, the role of ADM in promoting different pro-tumorigenic effects is discussed and provides understanding of why ADM may play a role in the development of PaCa.

1.3.1 Proliferation

In a normal tissue, proliferation of cells is tightly regulated by the production and release of growth promoting signals however, in cancer this often becomes dysregulated. Studies looking at the effects of ADM on proliferative behaviour of cancer cells have shown both stimulatory and inhibitory effects.

In Capan-1, COLO-357 and Panc-1 PaCa cell lines, ADM was observed to have both stimulatory and inhibitory effects on proliferation. Addition of recombinant bioactive ADM to the cell lines at a concentration of 1 nM resulted in increased proliferation of the cancer cells (Keleg et al., 2007). Another study showed ADM blocked TGF-β growth inhibition and therefore promoted the proliferation of the cells (Kleeff & Korc, 1998). Whilst higher concentrations of the recombinant ADM (100-1000 nM) decreased the proliferation of the cells (Keleg et al., 2007). Kleeff & Korc (1998) observed that TGF-1β inhibited growth of COLO-357 cells in a dose and time dependent manner through the phosphorylation of Smad 2/3. These results suggest that ADM induces proliferation in Paca cells, potentially by inhibiting TGF-β. However, higher concentrations of recombinant ADM appeared to inhibit cell proliferation.

In prostate cancer, Berenguer *et al* (2008) showed a significant increase in LNCaP prostate cancer (PCa) tumour growth when injected intra-peritoneally or intra-tumorally with ADM. Berenguer-Daizé *et al* (2013) also showed that ADM has growth promoting effects *in vitro* by treating DU145 PCa cells with different doses of ADM and showed a dose dependent increase in proliferation using MTT assays. Furthermore, Berenguer-Daizé *et al* (2013) showed that PC-3 and DU145 PCa cells treated with an anti-ADM antibody (αAM), showed a dose dependent decrease in cell proliferation. This suggests that ADM plays a role in the proliferation of cancer cell growth. Treatment of DU145 xenografts *in vivo* with αAM also resulted in decreased tumour growth. It was suggested that ADM mediated cell proliferation is through the cAMP/CRAF/MEK/ERK pathways.

However, Abasolo *et al* (2004) showed contrasting results, suggesting ADM has inhibitory effects on cancer cell proliferation. Proliferation assays demonstrated that ADM overexpression resulted in

inhibition of cell proliferation in PC-3 and LNCaP cells however, not in DU145 cells. Furthermore, *in vivo*, PC-3 tumours overexpressing ADM showed decreased tumour volume. An important consideration in the *in vivo* study may be that the cells were injected subcutaneously. An orthotopic experiment may have been a better alternative as the cells would have been in a more representative tumour microenvironment. In conclusion, these results show contrasting results however, both studies carried out different methods of determining ADM effect on proliferation.

Abasolo *et al* (2004) also looked at ADM receptor expression in prostate cancer, showing mRNA expression of the RAMP-2/CRLR receptor using endpoint PCR and northern blot analysis. Berenguer-Daizé *et al* (2013) also analysed RAMP-3 expression and showed the expression of ADM, CLR, RAMP-2 and RAMP-3 in prostate cancer sections, tumour xenografts and at mRNA level. These results may explain why Abasolo *et al* (2004) saw a decrease in cell proliferation whereas Berenguer-Daizé *et al* (2013) saw an increase in cell proliferation. These data may indicate that the proliferative effects of ADM are specifically induced by the RAMP-3/CLR complex.

In breast cancer cell lines, T47D and MCF7, overexpression of ADM under stressful conditions including serum deprivation or exposure to TNF-α resulted in a survival advantage for the cells. Ras, Raf, PKC, MAPKp49 expression increased together with cell proliferation when ADM was overexpressed in these cell lines. These data suggest that ADM promotes oncogenic signal transduction (Martínez et al., 2002).

Ouafik *et al* (2002) demonstrated that ADM has growth promoting effects in U87 glioblastoma cells. *In vitro* blockage of ADM using αAM resulted in decreased growth of cells. In *vivo,* U87 cells injected subcutaneously were treated with αAM and showed a 70% decrease in tumour growth. The mechanism by which ADM induces proliferation in these cells was suggested by Ouafik, Berenguer-Daizé, & Berthois (2009) to be JNK/c-Jun/AP-1 pathway which increases cyclin D1 levels. This pathway was also described by Zhang *et al* (2009) in an ovarian cancer cell line, CAOV3. They proposed that

AP1 binds to the ADM promoter and on induction of ADM through the basic fibroblast growth factor (bFGF), the JNK-AP-1 pathway is induced which promotes proliferation.

Nouguerède *et al* (2013) treated HT-29 colorectal cancer cells with synthetic ADM and showed an increase in proliferation of cancer cells. *In vivo* treatment of HT-29 tumour xenografts with αAM resulted in supressed tumour growth. Deville *et al* (2009) also showed ADM to induce proliferation in clear cell renal carcinoma cells, BIZ and 786-0. Both these studies treated cells with anti-CLR, anti-RAMP-2 and anti-RAMP-3 antibodies which all showed a decrease in basal proliferation suggesting that ADM induces its proliferative effects through these receptors.

Overall, the collective data show that ADM has a direct role in inducing proliferation of cancer cells, including in PaCa. ADM induces these effects through the MAPK pathways; ERK and JNK-AP-1 (Figure 1.6). These data provide the first evidence that ADM plays an important role in pro-tumorigenic effects through the RAMP-2/-3 and CLR receptors.

1.3.2 Apoptosis

Resisting cell death is another hallmark of cancer that promotes cancer cell survival. This mechanism regulates the cell life cycle and ADM has a role in regulating the transcription factors that are important for this process. BxPC-3, Panc-1 and MPanc-96 PaCa cells treated with ADM antagonist (ADM_{22-52}) showed reduced basal NFκB activity compared to untreated cells expressing ADM. NFκB function is to inhibit apoptosis (Figure 1.10) therefore, the ADM_{22-52} inhibiting its activity suggests ADM has a direct role in controlling the transcription of this molecule and therefore apoptosis in PaCa (Ramachandran et al., 2007).

Martinez *et al* (2002) overexpressed ADM in T47D and MCF7 breast cancer cells under serum starved conditions showing a reduction in apoptosis and a decrease in caspase-8, Bax and Bid proteins (Figure 1.10). This result was mimicked by Abasolo, Montuenga, & Calvo (2006) with serum starved ADM overexpressing PC-3 cells. Treating the overexpressing PC-3 cells with etoposide (chemotherapy) prevented the usual pro-apoptotic action and increased the Bcl-2/Bax ratio. The role of Bcl-2 is to

prevent apoptosis by binding to Bax which is a pro-apoptotic molecule. Ishikawa endometrial cancer cells overexpressing ADM under hypoxic conditions also showed increased resistance to apoptosis and an increase in Bcl-2 (Oehler *et al.* 2001) (Figure 1.10). In contrast, Oehler *et al* (2001) silenced the expression of ADM using shRNA in ovarian cells, HO8910. This resulted in decreased expression of Bcl-2 and therefore increased apoptosis. The interaction between ADM and Bcl-2 has been demonstrated by Li *et al* (2003) revealing ADM and Bcl-2 are immunolocalised in the cytoplasm of invasive cervical squamous carcinoma. However, ADM and Bcl-2 were not immunolocalised in the cytoplasm of normal cervical epithelium and carcinoma intraepithelial neoplasias (Li *et al,* 2003). These results suggest a relationship between ADM, Bcl-2 and inhibition of apoptosis in cancer cells specifically and normal tissue.

ADM knockdown (ADM KD) studies in bladder and colon cancer correlated with an increase in apoptosis with reduced levels of ADM. Liu *et al* (2013) developed ADM KD T24 urothelial cells and showed increased apoptosis in the KD cells, compared to non-transfected cells when stained for annexin-V. In ADM KD colon tumour xenografts, Wang *et al* (2014) showed increased caspase-3 staining of tissues and a reduction in tumour size. Furthermore, Deville *et al* (2009) showed a clear relationship between ADM and caspase-3 in clear cell renal carcinoma epithelial cells, showing higher ADM expression levels correlated with decreased caspase-3 activity (Figure 1.10). These results demonstrate that decreasing ADM expression increases apoptosis and caspase-3 activity.

In colorectal HT-29 mouse xenografts treated with αAM, there was an increase in apoptosis. The apoptotic index (% of apoptotic cells/bodies per all tumour cells) was measured using MAb F7-26 antibody and showed a 2-3 fold higher number of apoptotic cells in αAM treated cells than controls (Nouguerède et al., 2013). In conclusion, ADM plays a role in the regulation of apoptosis by interacting with molecules from the apoptotic pathway including NFκb, Bcl-2, caspase-8 and caspase-3 (Figure 1.10). The results demonstrate the role of ADM in promoting cancer cell survival.

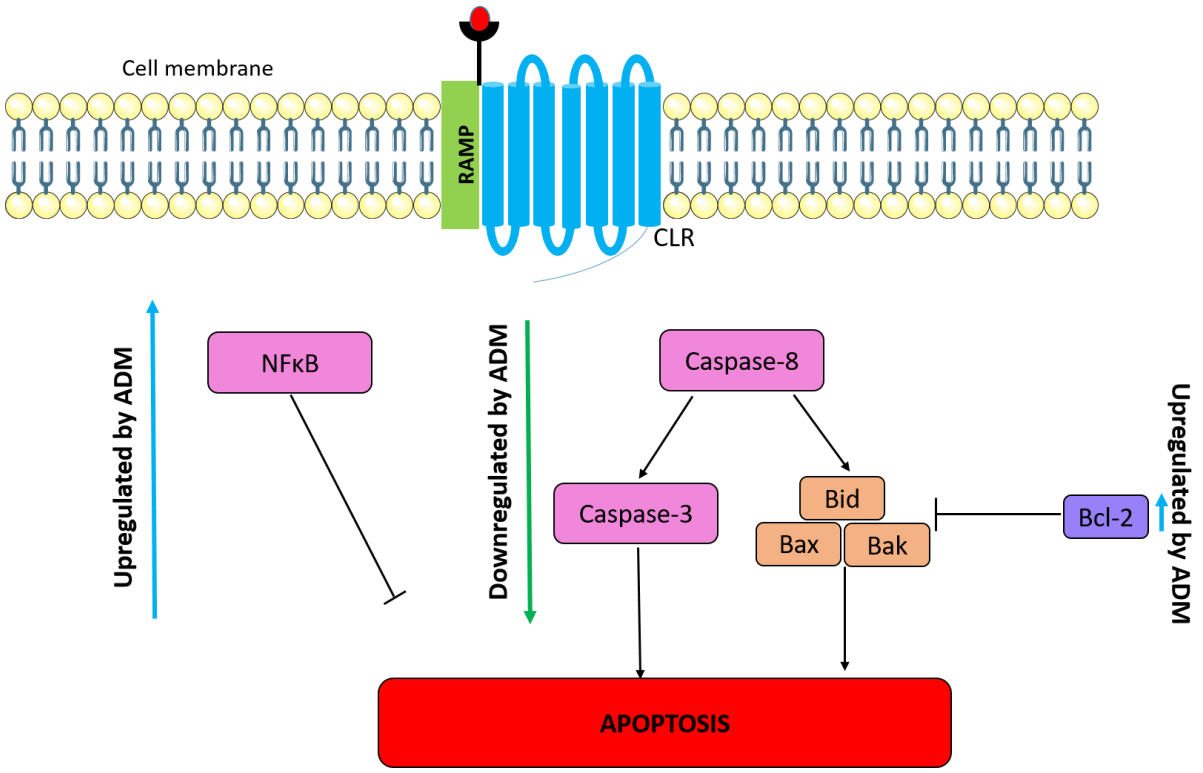

Figure 1.10 ADM role in the extrinsic apoptosis pathway. ADM downregulates of caspase-8 and caspase-3 which decreases Bid/Bax/Bak expression and inhibits apoptosis. ADM upregulates Bcl-2 and NFκB which also inhibits apoptosis. Figure adapted with copyright permission from Macmillan Publisher Ltd ©2011, Olsson & Zhivotovsky (2011)

1.3.3 Angiogenesis

Angiogenesis is a key component of a tumour microenvironment as it provides a source of oxygen and nutrients for tumours grow. In a study by Ishikawa *et al* (2003), treatment of PaCa cells with ADM_{22-52} antagonist decreased growth of tumours *in vivo.* Immunohistochemistry analysis of these tumours showed significantly smaller blood vessels in tumours treated with the antagonist.

Iimuro *et al* (2004) looked at the effects ADM had on inducing angiogenesis comparing heterozygous sarcoma 180 ADM knockout mice to wild-type (WT) mice. Both groups were injected with either ADM or ADM_{22-52} (competitive antagonist). WT mice treated with ADM showed an increase in tumour weight and capillary density within and around the tumour. Whilst mice treated with the antagonist showed reduced tumour growth and capillary density similar to the ADM knockouts. Glioblastoma

tumours injected subcutaneously *in vivo* by Ouafik *et al* (2002) also showed less vascularisation in tumours treated with αAM antibody compared to controls. Whilst, Oehler *et al* (2002) showed significantly increased vascular density in endometrial tumours overexpressing ADM. These results were also shown in other studies by Tsuchiya *et al* (2010), Berenguer-Daizé *et al* (2013) and Berenguer *et al* (2008) in DU145 and LNCaP prostate cancer cells and renal cell carcinoma (RCC) respectively. They treated tumour xenografts with either ADM or ADM_{22-52}. Interestingly, Tsuchiya *et al* (2010) showed that treating normal endothelial cells with ADM or the antagonist had no effect on angiogenesis. These results suggest that ADM has a role in directly altering vascular density in cancer specifically and therefore it promotes tumour growth.

The study by Iimuro *et al* (2004) also investigated angiogenesis and its pathways using co-culturing experiments. Endothelial cells co-cultured with fibroblasts showed an increase in capillary formation when treated with ADM and VEGF combined. ADM alone did not increase capillary formation, whilst VEGF alone did which suggests ADM enhances the effects of VEGF. Proliferation of HUVECs was also greater with a combination of ADM and VEGF. Furthermore, culturing endothelial cells with ADM showed a time and dose dependent increase in VEGF. Similarly, ADM minimally activated the Akt pathway alone however, ADM in combination with VEGF showed a time and dose dependent increase in Akt activation. This suggests that ADM induces angiogenesis by increasing VEGF-induced Akt activation (Figure 1.11).

Chen *et al* (2015) also looked at the association between ADM and VEGF in HO-8910 epithelial ovarian cancer cells. They also found that ADM enhanced VEGF expression in a dose and time dependent manner. Furthermore, JNK expression was also increased when ADM was added to the cancer cells. Adding a JNK inhibitor to the cells stopped ADM induced VEGF expression suggesting that the JNK/AP-1 pathway is activated by ADM and induces downstream angiogenesis (Figure 1.11). Treating co-cultured endothelial cells with HO-8910 cells with ADM also increased endothelial cell tube formation through ADM induction of VEGF via the JNK/AP-1 pathway.

Fernandez-Sauze *et al* (2004) also investigated the role of ADM in inducing angiogenesis and whether ADM and VEGF work synergistically to induce this process. *In vitro* they showed that synthetic ADM peptide induced HUVEC differentiation in matrigel similar to Kaafarani *et al* (2009) who showed this *in vivo.* The study showed HUVEC media treated with ADM over a period of 3 hours did not show an increase in VEGF secretion. They also investigated whether ADM-induced capillary tube formation is effected when VEGF neutralising antibody is added, finding that it does not reduce ADM induced capillary like tube formation but does eliminate VEGF-induced morphologic differentiation. These results were based on HUVEC cells alone, co-cultures with cancer cells may suggest a more synergistic relationship between ADM and VEGF as cancer cells form a network between these molecules and can trigger multiple pathways shown by studies completed by Keleg *et al* (2007) and Chen *et al* (2015).

Kaafarani *et al* (2009) injected matrigel plugs into mice either alone, with VEGF and bFGF or with ADM peptide. The results showed an increase in cellularity in both the VEGF/bFGF and ADM peptide matrigel plugs. The most significant increase in cellularity was in the ADM peptide treated plugs. A further experiment treating ADM matrigel plugs with different doses of anti-ADM receptor antibodies (αAMr) showed a dose dependent decrease in cellularity of the plugs. This study illustrates that ADM activates angiogenesis via the RAMP/CLR receptors.

Fernandez-Sauze *et al* (2004) showed that ADM induces HUVEC invasion and migration in a dose dependent manner. Migration increased by 97% when ADM was used as a chemoattractant. They also wanted to determine the receptors through which ADM mediates angiogenesis therefore, anti-CLR/anti-RAMP-2/anti-RAMP-3 antibodies were added to HUVEC cells. HUVEC cells were seeded in the upper compartment of a Boyden chamber and ADM, ADM/bFGF or bFGF alone were used as chemo-attractants. The most significant results showed that HUVEC cells treated with the αAMr antibodies showed the biggest reduction in HUVEC cell migration. Anti-RAMP-3 showed the largest reduction in migration. These data suggest that ADM induced both endothelial cell migration and that the chemotactic signalling is mediated via the CRLR/RAMP-2 and CRLR-RAMP-3 receptors.

Kocemba *et al* (2013) showed that ADM mediates its pro-angiogenic actions in non-solid tumours as well. They showed that in multiple myeloma cells (MM) ADM is highly expressed and secreted. They also demonstrated that the levels of ADM expression correlated with disease progression and molecular subtype. MM cells overexpressing ADM enhanced proliferation and angiogenesis of HUVEC cells. To show these effects were induced by ADM, HUVEC cells with treated with small molecule ADM antagonists which showed complete inhibition of proliferation and angiogenesis of HUVEC cells. To determine whether endogenous ADM induces these same effects, conditioned media from L363 MM cells that produced high levels of ADM under normoxic conditions was added to HUVECs. This promoted both angiogenic activity and induced proliferation of HUVEC cells. Adding the antagonists reduced endothelial mesh formation. These data also show that overexpression of ADM plays a role in angiogenesis.

Chen *et al* (2011) looked at the interaction between tumour associated macrophage (TAMs) ADM secretion and induction of angiogenesis. Immunofluorescent analysis showed that TAMs expressed ADM in human melanoma. Furthermore, co-culturing the cells resulted in increased ADM expression compared to TAMs and melanoma cells cultured alone. Secretion of ADM from TAMs treated with tumour cell conditioned media was much higher than tumour cells treated with TAM conditioned media. This suggests that TAMs increase ADM secretion. The role of ADM secretion and TAMs in inducing angiogenesis was examined by co-culturing TAM conditioned media with endothelial cells. This resulted in enhanced endothelial cells migration and tubule formation. Addition of a neutralising ADM antibody or ADM_{22-52} attenuated the effects of TAM induced angiogenesis *in vitro.* These results demonstrate how ADM is largely involved in the crosstalk between cells within the tumour microenvironment. These data specifically demonstrate the crosstalk between TAMs, ADM secretion and the induction of angiogenesis.

ADM has also been shown to interact with cancer associated fibroblasts (CAFs) and induce angiogenesis. CAFs play a large role in stromal development in PaCa and have been suggested to

contribute to the formation of desmoplasia and induction of angiogenesis. Benyahia *et al* (2017) looked at the role of CAFs in MCF-7 invasive breast carcinoma cells showing CAFs expression of ADM, AM1 receptor and AM2 receptor by immunostaining. *In vivo,* mice were injected with matrigel plugs containing CAFs independent of tumour cells which revealed in a significant increase in neovascularisation compared to normal human dermal fibroblast cells or without fibroblasts. Treatment of mice with αAMr resulted in a clear decrease in angiogenesis compared with control IgG treatment. Furthermore, histological examination revealed disruption to the tumour vasculature with depletion of vascular endothelial cells. Again, these results highlight they key role of ADM in the crosstalk between different cells that make up the tumour environment and induce pro-tumorigenic pathways including angiogenesis.

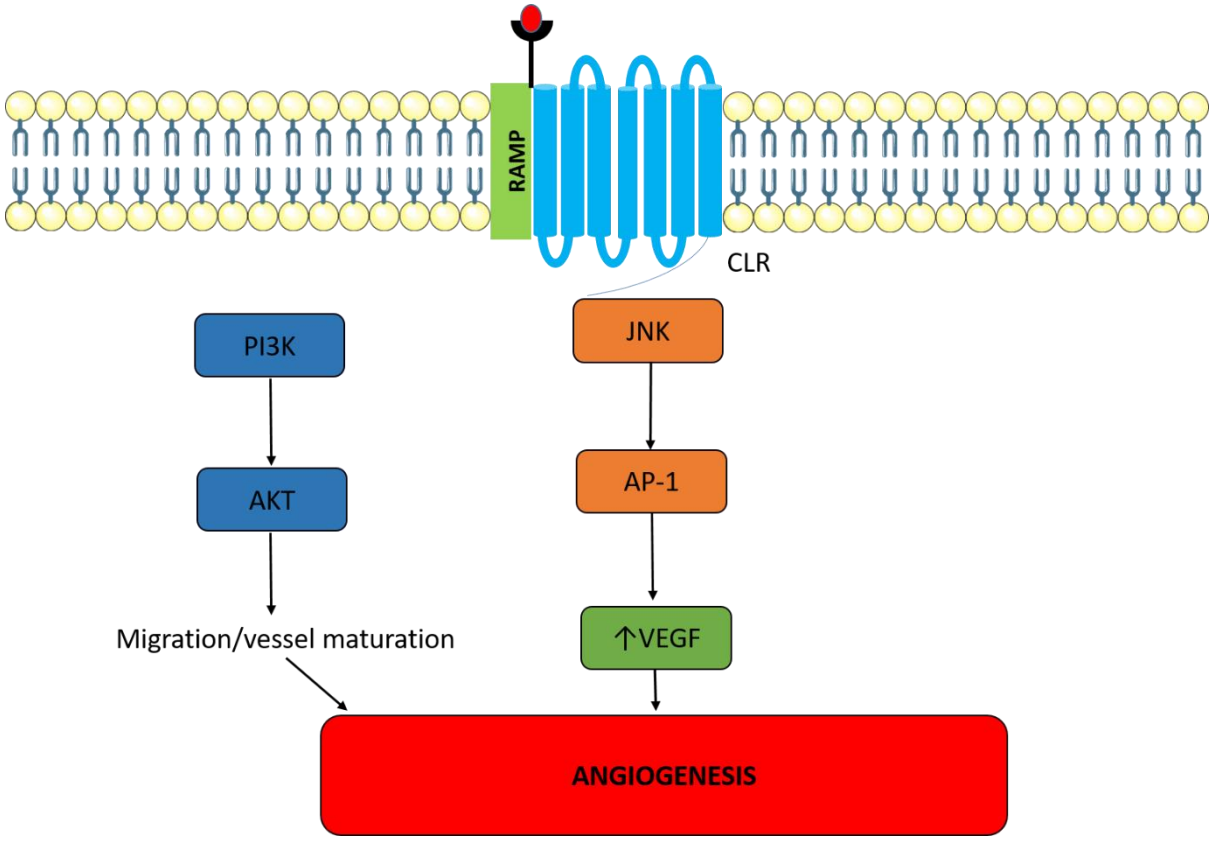

Figure 1.11 ADM role in angiogenesis. ADM increases VEGF levels through the JNK/AP-1 pathway which can directly induce angiogenesis or activate the PI3K/Akt pathway. PI3K activates AKT which induction migration and maturation of vessels resulting in angiogenesis

Another common feature of the tumour microenvironment is hypoxia, ADM is upregulated in hypoxic conditions which induces angiogenesis. Hypoxia is a state that occurs when cell growth exceeds oxygen supply to the capillary bed. Regions of hypoxia are detected by a transcription factor, hypoxia inducible factor 1 (HIF-1). HIF-1 is a heterodimer composed of HIF-1α and HIF-1β, the HIF-1α molecule has an oxygen degradation domain that is cleaved under normoxic conditions (Garayoa *et al*. 2000).

Keleg *et al* (2007) suggest that ADM may mediate its actions through VEGF in hypoxic conditions. PaCa cell line supernatant was treated with recombinant ADM (rADM) and secreted VEGF was measured. 3 out of 5 cells lines showed that ADM was strongly induced by hypoxia which increased invasiveness of the PaCa cell lines. Addition of recombinant ADM to the cell lines showed an increase in VEGF secretion of 65.2%, 43.4% and 14.3% in 3 out of 5 cell lines. These data suggest that ADM is upregulated under hypoxic conditions and induces VEGF expression therefore may have a role in inducing angiogenesis. However, 2 out of 5 cell lines did not show the same response, indicating that in some cell lines the effects of ADM may be direct, whilst in the unresponsive cancer cell lines the effects of ADM may be indirect.

Kocemba *et al* (2013) investigated the relationship between hypoxia and ADM expression. In two MM cell lines, there was an increase in ADM expression of both mRNA and protein (1.6-fold and 3.6-fold increase) expression when the cell lines were exposed to hypoxia. Additionally, the increased ADM secretion induced by hypoxia resulted in a 2-fold increase in HUVEC cell proliferation which was inhibited by normoxic conditions. These data demonstrate that ADM expression is clearly increased under hypoxic conditions and plays a role in inducing angiogenesis.

Fujita *et al* (2002) also showed an increase in ADM mRNA expression in 3 RCC cell lines in a time dependent manner when exposed to hypoxic conditions. They also showed an increase in VEGF expression in a time dependent manner but to a lesser degree. However, there were no changes in HIF-1 expression. They did show that there was a positive correlation between ADM mRNA expression

and microvessel count. The study concluded that ADM plays a crucial role in tumorigenesis by promoting angiogenesis through tumour generated VEGF in hypoxic conditions.

Uemura *et al* (2011) suggested ADM may be a good marker to determine the prognosis of colorectal cancer patients. They showed that patients with liver metastasis expressed high levels of ADM. Furthermore, the probability of disease-free survival was higher in patients expressing lower levels of ADM compared to higher levels from microarray analysis. They also investigated the relationship between ADM, HIF and VEGF expression showing a positive correlation between HIF-1 and ADM expression and VEGF and ADM expression. These data combined suggest that ADM expression could be a useful marker for patients with a higher risk of metastases and relapse in patients with colorectal cancer who have undergone curative resection. The higher risk associated with high ADM expression can be correlated with the increase expression of HIF-1 and VEGF, suggesting that ADM may promote angiogenesis. This study states that ADM and VEGF work synergistically and that ADM is a hypoxia induced gene.

A positive correlation between ADM expression and VEGF expression under hypoxic conditions was also show by Yao *et al* (2019) in osteosarcoma cells. The amount of ADM and VEGF expression in the cells increased in a time dependent manner, showing the highest mRNA and protein expression levels after 24 hours of hypoxia. To demonstrate ADM and VEGF have a direct relationship, MG-63 ADM KD cells were injected into nude mice showing that decreased ADM levels were associated with decreased tumour volumes and CD31 marker (vascular endothelial marker) compared to scrambled controls and PBS controls. Analysis of total protein from tumour tissue showed a significant reduction in VEGF expression in ADM KD mice, compared to control groups. These results show a direct relationship between ADM expression and VEGF and suggest that they work synergistically to induce angiogenesis and aid in tumour growth.

Zhang *et al* (2017) showed that ADM upregulated HIF-1α and VEGF in CAOV3 epithelial ovarian cancer cells overexpressing ADM, compared to ADM knockout cells that inhibited their expression. ADM also

promoted HUVEC proliferation, migration and tube formation. The study concluded that ADM is an upstream molecule of of HIF-1α/VEGF in this CAOV3 and promotes angiogenesis through HIF-1α and VEGF.

Overall, these results show the vast amount of data associating ADM with angiogenesis. The results highlight the diversity of ADM in communicating with multiple cell types (endothelial cells, TAMs and CAFs) molecules (HIF-1 and VEGF) and pathways (Akt-activation and JNK/AP-1) that all interact to induce angiogenesis and promote tumour survival. It has been shown that these pathways and molecules are induced through the CRLR/RAMP-2 and CRLR-RAMP-3 receptors, suggesting that these could be important in tumorigenesis and targets for future therapy targets in PaCa and other cancers.

1.3.4 Invasion/Migration

Invasion and migration are common hallmarks of cancer that lead to metastasis. Metastasis occurs when neoplastic tumour cells migrate into the lymphatic and blood vessels and invade distant organs. PaCa is often diagnosed once the tumour has metastasised, Dai *et al* (2020) investigated the receptors and molecules associated with this metastasis in PaCa. They found that activation of the ADM/RAMP-2 system by recombinant ADM and inhibition of the ADM/RAMP-3 system in PAN02 cells *in vivo* resulted in decreased metastasis. This suggests that the ADM/RAMP-3 system could be one of the main drivers of tumour metastasis in PaCa and could be used as a potential therapeutic target.

The above described *in vivo* model was developed after investigating the effects of tamoxifen induced RAMP-2 vascular endothelial cell specific knockouts and RAMP-3 knockouts in PAN02 cells. They found that PAN02 RAMP-2 endothelial knockouts injected into the spleen supressed tumour growth at site of injection and in metastatic liver however, there was increased liver metastasis compared to control. Masson trichrome staining showed an increase in fibrosis in RAMP-2 endothelial knockouts and increased expression of α-SMA and podoplanin (PDPN), which are both used as markers for CAFs and associated with increasing metastatic potential of tumours. However, in RAMP-3 knockouts there was decreased incidence of liver metastasis which was verified by decreased fibrosis and α-SMA/PDPN

expression in the tumour periphery. These results support that RAMP-3 plays a larger role in metastasis however, a limitation to this study is that the RAMP-2 knockouts were endothelial cell specific due to embryo lethality following full knockout. This means the conditions compared were not exactly the same as RAMP-3 knockouts were not endothelial cell specific. It also highlights that RAMP-3/CLR would be a more suitable therapeutic target.

The study described also showed that RAMP-3 knockouts decreased α-SMA/PDPN expression, which means the number of CAFs within the tumour site were lower in knockouts. CAFs play an important role in the development of tumour metastasis as they interact with many cells that make up the tumour microenvironment. They regulate growth, survival and invasiveness of cancer cells, as well as angiogenesis by the secretion of growth factors. Therefore, Dai *et al* (2020) compared RAMP-3 knockout CAF/PAN02 to RAMP-3 expressing CAF/PAN02 in both a subcutaneous model and orthotopic spleen model. The subcutaneous model showed that tumour weight, α-SMA, PDPN and Ki67 expression decreased in RAMP-3 knockout CAF/PAN02 mice compared to the overexpressing model. The orthotopic model showed lower incidence of metastasis in the RAMP-3 knockout CAF/PAN02 mice compared to RAMP-3 expressing CAF/PAN02 and PAN02 cells alone.

The potential for RAMP-3 as a metastatic driver was further supported by *in vitro* co-cultures showing less vimentin expression in PAN02 cells treated with conditioned media from RAMP-3 knockout CAFs compared to PAN02 treated with RAMP-3 expressing CAF conditioned media which showed very high vimentin expression. Vimentin is a mesenchymal marker and this data suggests that ADM may induce the epithelial-mesenchymal transition via the CRLR/RAMP-3 receptor to help promote metastases. Zhou *et al* (2015) transduced ADM into HuCCT1 and showed a downregulation of E-cadherin and ZO-1 and upregulation of N-cadherin, vimentin and mesenchymal transcription factors (ZEB 1 AND ZEB2). Whilst ADM KD resulted in the reversal of EMT. The study showed that ADM induces EMT specifically through ZEB1 which is a transcription factor associated with the regulation of EMT in epithelial cells. In conclusion, these data suggest that depletion of RAMP-3 in CAFS supresses tumour metastases and

growth and therefore, RAMP-3 plays a key role in tumorigenesis. Furthermore, ADM plays a key role in EMT potentially through the CRLR/RAMP-3 receptor.

Nouguerède *et al* (2013) also tried to correlate ADM receptor expression and lymph node and distant metastasis. They showed a correlation between increased ADM, RAMP-2, RAMP-3 and CLR expression and increased lymph node and distant metastasis in colorectal cancer tissues. Whilst, Siclari *et al* (2014) showed that overexpression of ADM in MDA-MB-231 breast cancer cells *in vivo* caused increased bone metastasis. This lead to poorer survival in overexpressing mice as the onset of metastasis was faster. These results support evidence that ADM plays a key role in driving metastasis in cancer.

Many studies have investigated the role of ADM in increasing invasiveness of cancer cells. Nouguerède *et al* (2013) showed a dose dependent increase in colorectal HT-29 cell invasion in response to increasing ADM concentration compared to controls. This has also been demonstrated in other cancers including liver, prostate, pancreatic, bladder, brain and colorectal cancers (Berenguer-Daizé et al., 2013; Deville et al., 2009; Keleg et al., 2007; Lim et al., 2014; Ramachandran et al., 2009; Wang et al., 2014; Zhou et al., 2015). These studies all used ADM as a chemoattractant and measured the amount of invasiveness compared to controls. Some of the studies treated cells with either αAM, ADM antagonists or ADM knockout cells which inhibited the invasiveness of the cells (Berenguer-Daizé et al., 2013; Chen et al., 2012; Keleg et al., 2007; Ramachandran et al., 2007). These results demonstrate that ADM has a direct effect on invasiveness in multiple cancers and could potentially be associated with increasing the invasiveness of PaCa.

ADM has been shown to increase migration in renal, ovarian and brain cancers. Deville *et al* (2009) showed a dose dependent increase in migration in BIZ and 786-O renal cancer cells treated with ADM. Deng *et al* (2012) investigated the mechanism by which ADM increases migration in HO8910 ovarian cancer cells by measuring levels of integrin α5β1, induced phosphorylation of FAK (focal adhesion kinase) and paxillin. They treated ovarian cells with ADM for 12 hours and showed an increase in the

aforementioned molecules. These molecules are part of the pathway that promotes invasion and migration by activating scaffold proteins including paxillin. Inhibiting integrin α5β1 using an antibody effectively downregulated the effects of ADM on migration but also inhibited phosphorylation of FAK and paxillin. Oulidi *et al* (2013) also showed an increase ADM was associated with increased adhesion, migration and invasion through phosphorylation of FAK, integrin β1 and activation of TRPV2 translocation to plasma membrane. Increased integrin levels resulted in binding and induction of fibronectin and increased invasion and metastasis in bladder cancer. Knocking out TRPV2 in prostate and bladder cancer cells, resulted in inhibition of ADM stimulatory effects on increasing fibronectin, migration and invasion. These data once again demonstrate the versatility of ADM in that it interacts with a number of molecules, all resulting in an increase in both invasion and migration.

ADMs role in inducing migration was shown by Lim *et al* (2014) in astroglioma cells. They suggest that oncostatin-M (OSM), a cytokine part of the interleukin-6 family induces STAT-3 phosphorylation and nuclear translocation which increases DNA binding of STAT-3 to ADM promoter and increases ADM mRNA and secretion. The downstream effect of the ADM was increased migration of astrioglioma cell migration in a dose dependent manner.

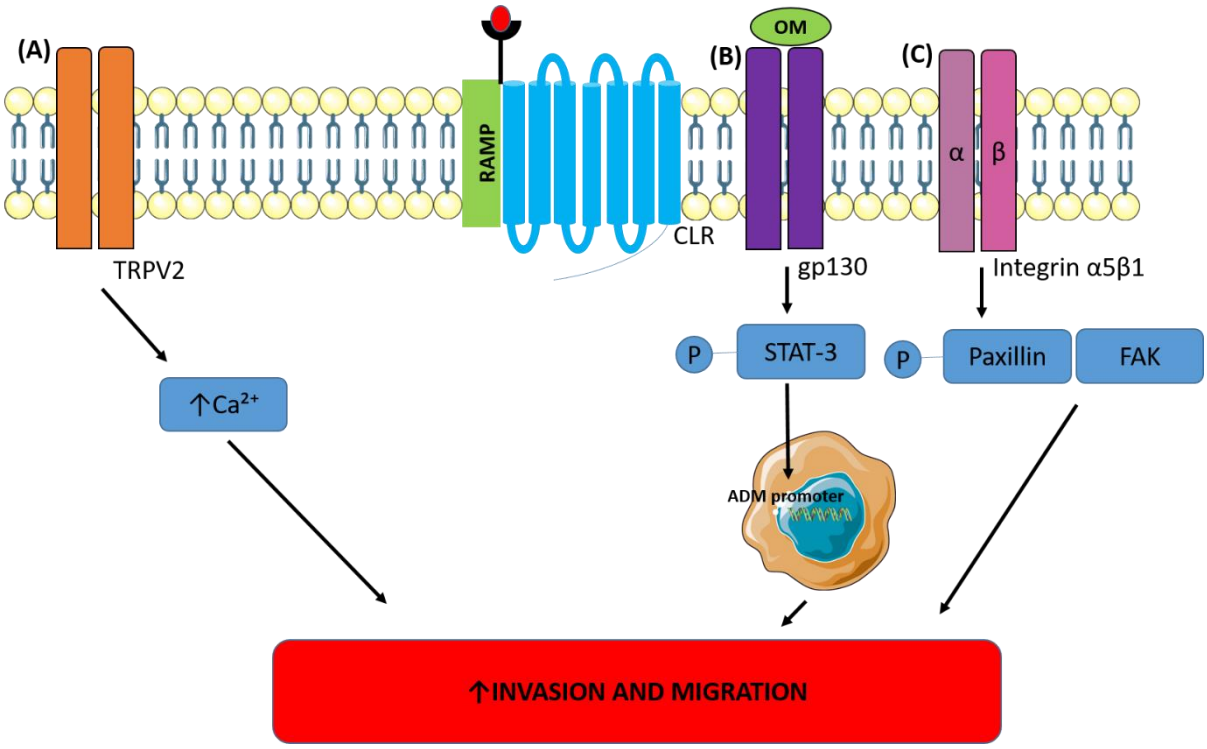

Figure 1.12 ADM role in invasion and migration. (A) Increasing levels of ADM cause the translocation of TRPV2 which increases calcium levels causes a downstream increase of invasion and migration of cancer cells. (B) Oncostatin M (OM) phosphorylates STAT-3 which binds to the ADM promoter and induces invasion and migration in cancer cells. (C) Integrin α5β1 phosphorylates FAK/Paxillin which increases invasion and migration.

In conclusion, ADM has a clear role in inducing invasion and migration of cancer cells which has been demonstrated extensively in PaCa (Figure 1.12). Moreover, this has been shown to be specific to the RAMP-3/CLR receptor. The diversity of ADM and its receptor in interacting with different molecules and cells has been evidenced again. The results show that ADM directly interacts with CAFs and that RAMP-3 knockouts in these cells results in decreased metastasis of PaCa. Furthermore, ADM has downstream effects on a number of pathways (integrin α5β1, FAK, paxillin, TRPV2, oncostatin-M and STAT-3) that induce invasion, migration and adhesion of cancer cells. These results could explain why PaCa is so difficult to treat as ADM interacts with a complex network of pathways which all contribute to a more aggressive cancer phenotype.

1.3.5 Immune evasion

Cancer cells have multiple mechanisms that aid in cancer survival and growth which includes evading the immune system. Xu *et al* (2016) have shown that infiltration of myelomonocytic cells (MMC) into the stroma is a hallmark of PDAC and associated with poor prognosis. MMC cells are multipotent cells that can differentiate into blood monocytes, macrophages or dendritic cells. Tumour infiltrating MMC cells mainly differentiate into macrophages or myeloid derived suppressor cells in the tumour microenvironment. In this study, high ADM expression in PaCa tumour tissues positively correlated with the density of CD11b+ (MMC cells). ADM and its receptor components (GPR182, CRLR, RAMP-2, RAMP-3) were also shown to be expressed on MMC cells. These data show that the ADM may induce MMC cells effects through the CRLR/RAMP-2/-3 receptors.

Xu *et al* (2016) showed ADM stimulates invasion and migration of MMC cells in a dose dependent manner. This effect was inhibited by adding either ADM_{22-52} or CLR antibody to the MMC cells. Matrigel plugs also displayed an increased recruitment of MMC cells following ADM treatment. To determine the mechanism by which migration and invasion of MMC cells is induced, inhibitors of MAPK, PI3K/Akt and eNOS were used. Treatment of MMC cells with these inhibitors reduced ADM induced invasion and migration suggesting that the aforementioned signalling pathways are downstream of ADM.

More cell-cell adhesion, trans-endothelial migration and cell-ECM adhesion of MMC cells was determined with higher expression levels of ADM which correlated with increased expression of VCAM-1 and ICAM-1 (adhesion molecules). Additionally, MS1 (mouse pancreatic islet endothelial cells) treated with conditioned media from PANC-1 tumour cells showed increased expression of VCAM-1 and ICAM-1 and MMC cell adhesion to MS1 cells which was reversed with ADM_{22-52} treatment (Xu et al., 2016).

ADM also induces myeloid cells (macrophages and tumour derived suppressor cells) to express pro-tumour phenotypes. Bone marrow derived macrophages (BMDMs) treated with ADM showed a 2-fold increase in CD206+ (M2 marker) by flow cytometry. Flow cytometry showed treatment of BMDMs with PANC-1 conditioned media showed a significant increase in the % of CD206+ cells. Therefore, ADM secreted from PaCa tumour cells polarises macrophages into a pro-tumour phenotype.

In vivo, overexpressing ADM in SW1990 cells (SW1190-ADM) resulted in increased CB11b+ MMC cell recruitment and angiogenesis compared to SW1990-vector control. The MMC cells were located close to blood vessels and attached to endothelial cells in the SW1990-ADM overexpressing cells. Treatment of SW1990-ADM cells with ADM antagonist resulted in decreased tumour growth, CD11b+ MMC cells and tumour angiogenesis. To determine the cause of inhibited tumour growth and angiogenesis, clodronate liposomes, which deplete CD11b+ MMC cells, were administered to both SW1990-ADM and SW1990-vector. This showed a significant decrease in macrophages, tumour growth and angiogenesis in SW1990-ADM mice. Therefore, MMC cells within tumours and ADM work together to

promote a pro-tumour environment and as a consequence, result in poorer disease free survival in patients with higher ADM levels.

Pang *et al* (2013) found that tumour derived ADM from ovarian cancer cell line HO8910 caused polarisation of macrophages to M2 phenotype. Macrophage polarisation is used to describe the conversion of macrophages from the M1 phenotype (anti-tumorigenesis) to the M2 phenotype (pro-tumorigenesis). This normally happens in response to changes in microenvironment signals. It has been suggested that cancer cells drive macrophages to change from M1 to M2 phenotype. CD206 is a marker of the M2 phenotype and co-culturing H08910 with macrophages showed a significant increase in its expression. Whilst HO8910 ADM KDs or ADM_{22-52} treated cells co-cultured with macrophages showed a significant decrease in ADM expression. These data show that tumour derived ADM induces macrophage polarisation to produce a pro-tumour environment. This same pattern was reflected with Arg-1 expression, Arg-1 is a marker of M2 macrophages and co-culturing HO8910 cells with macrophages resulted in increased Arg-1 expression in macrophages.

The study also shows that M2 polarised macrophages induce migration of HO8910 via RhoA. This was shown by inhibiting RhoA with C3 exoenzyme which not only resulted in decreased migration of cancer cells in co-culture with macrophages but also decreased stress fibre formation and cytoskeleton rearrangement of HO8910. Stress fibre formation and cytoskeleton rearrangement play a role in the migration of cancer cells, remodelling of the cytoskeleton provides a mechanical force for cell migration. Furthermore, ADM_{22-52} antagonist inhibited migratory effects of HO8910 in co-culture suggesting ADM signals through RhoA.

Chen *et al* (2011) also showed a significant increase in CD206 and Arg-1 when B16/F10 melanoma cells or ADM were co-cultured with 264.7 macrophages. They suggested macrophage polarisation is driven by ADM as ADM is co-localised with CLR and its receptor components (RAMP-2/RAMP-3) in RAW 264.7 macrophage cells. However, B16/F10 melanoma cells only express CLR therefore, they concluded that ADM works in an autocrine loop on TAMs. Furthermore, treatment of macrophages with B16/F10

conditioned media showed a significant increase in ADM secretion and expression of its receptor components in macrophages after 24 hours compared to B16/F10 cells treated with macrophage conditioned media. Therefore, this data shows that tumour cells enhance the autocrine effect on TAMS. *In vivo,* the effect of ADM receptor antagonists was assessed in B16/F10 and A375 melanoma tumour cells. ADM receptor antagonists significantly inhibited tumour growth and decreased expression of ADM in tumour tissue. Further analysis of tumour tissue showed a significant decrease the % of M2 phenotype macrophages. Together these results show an autocrine effect of ADM that drives macrophage polarisation and contributes to melanoma development.

Kubo *et al* (1998) demonstrated ADM ability to supress secretion of TNF-α and IL-6 under LPS stimulation in RAW 264.7 and mouse peritoneal macrophages to enhance immune evasion *in vitro*. In Swiss 3T3 fibroblast cells, ADM was also shown to inhibit TNF-α and IL1β. The mechanism through which ADM inhibits TNF-α was suggested to be the cAMP protein kinase A pathway as inhibiting ADM and cAMP protein kinase A rapidly restored TNF levels (Isumi et al., 1999). These results demonstrate ADM ability to interact with different molecules to help evade the immune system and aid in cancer survival.

Zudaire *et al* (2006) showed that in human lung and breast cancer tumours, confocal microscopy detected ADM producing mast cells within the tumour infiltrates. Mast cells are a type of granulocyte that form part of the immune system. Normally they respond to inflammation and allergic reactions but in cancer, it has been suggested that they can secrete pro-angiogenic factors, growth factors and pro- and anti- inflammatory mediators. MTT assays with co-cultures of A549 lung cancer cells treated with conditioned media from HMC-1 mast cells with either scrambled siRNA (HMC-Scr) or ADM siRNA (HMC-AM knockdown) showed faster proliferation of A549 cells in the presence of HMC-Scr conditioned media. These results suggest that ADM from mast cells is involved in the crosstalk with tumour cells to induce cancer cell proliferation. Furthermore, they showed that ADM induces pro-angiogenic effects in mast cells by increasing mast cell mRNA expression of VEGF, monocyte

chemotactic protein-1 and bFGF. This was also shown *in vivo* where HMC-1 cells with or without ADM neutralising antibody were injected into mice using a directed *in vivo* angiogenesis assay. Neovascularisation was seen in mice without the neutralising antibody and angiogenesis was inhibited in the presence of the neutralising antibody. The results suggest that mast cell driven angiogenesis is modulated by mast cell released ADM. In conclusion, ADM, mast cells and tumour cells interact with each other to induce pro-tumorigenic conditions including increased proliferation of cancer cells and induction of angiogenesis.

Lv *et al* (2018) showed that ADM induces mast cell degranulation and that is correlates with increased ADM expression in gastric tumours compared to normal tissue. Furthermore, they showed that ADM induces mast cell degranulation. When mast cells were co-cultured with tumour tissue culture supernatant (TTCS), addition of ADM_{22-52} inhibited mast cell degranulation. Akt phosphorylation was also inhibited as a consequence. These data show that tumour derived ADM plays a crucial role in mast cell degranulation by activating the PI3K-AKT pathway in gastric cancer. The pathway through which this mast cell degranulation is induced was suggested by Lv *et al* (2018) showing that ADM induced degranulation through the PI3-Akt signalling pathway. This induced proliferation and inhibited apoptosis of gastric cancer cells.

In conclusion, these data show that ADM interacts with molecules that make up the immune system to induce tumorigenic effects. High ADM expression correlated with high MMC levels which have been shown to differentiate into macrophages. ADM has been shown to drive macrophage polarisation resulting in the M2 phenotype and increased tumour growth. Furthermore, a relationship between ADM and mast cells has been found, ADM derived from mast cells has been shown to drive both cancer cell proliferation and invasion. These data not only show the interaction of ADM with different immune cells but show the crossover between ADM and different cancer hallmarks. It shows the complexity of cancer and the networks ADM forms.

1.3.6 Adrenomedullin and desmoplasia

The tumour microenvironment is composed of a multitude of cells including endothelial cells, immune cells, neuronal cells and CAFs. In PaCa, the tumour microenvironment results in a dense stromal environment with intense scar tissue around the tumour, known as desmoplasia. It is suggested that desmoplasia is largely responsible for patients lack of response to current therapies as the dense fibrous scar tissue around the tumours, makes the tumour microenvironment hypoxic and avascular. CAFs have been shown to express ADM and its receptors in multiple cancers suggesting it has a key role in the development of the stromal microenvironment.

Bhardwaj *et al* (2016) looked at the association between myb, a proto-oncogene, and ADM expression in the development of pancreatic desmoplasia. Examining pancreatic tumour xenografts inoculated with myb-overexpressing cells, there was an increase in desmoplasia compared to myb-silenced PaCa cells. There was increased staining of collagen I, fibronectin which are both important in extracellular proteins and an increase in α-SMA. Overexpressing myb resulted in increased proliferation of pancreatic stellate cells (precursor to CAFs) and silencing myb decreased proliferation of pancreatic stellate cells. When myb was overexpressed, ADM and *SHH* was shown to be upregulated. It was found that myb has binding sites on both SHH and the ADM promoters. SHH and ADM have an enhanced effect on tumour growth in combination, as opposed to alone. When pancreatic stellate cells were co-cultured with overexpressing myb PaCa cells, there was a significant growth reduction in cancer cells with addition of ADM antagonist in combination with a SHH neutralising antibody.

These results demonstrate the limited research around desmoplasia and PaCa. However, it does highlight the need for further research in this field as understanding the molecules associated with desmoplasia and the mechanisms could be crucial to improving treatment of PaCa. Gathering more evidence for ADM role in the development of the dense fibrous scar tissue, could make ADM and its receptors a valuable target for future therapy to use in combination with current chemotherapies.

1.4 Conclusion

The described data shows the complex and vast role that ADM has in cancer and specifically, its links with PaCa. Data show more research of ADM role in other cancers and therefore, highlights a gap in research in PaCa as it is evident that ADM influences many cancer hallmarks. The difficulty in diagnosing and treating PaCa is largely responsible for the poor statistics around PaCa survival. The described data lead to the investigation of the role of ADM in the crosstalk between PaCa and the pancreatic stroma in this study. Understanding this could provide evidence needed to support ADM blockade as a valuable target for future PaCa treatment either alone or as a combination therapy.

1.5 Hypothesis

To develop a further understanding of the role of ADM and RAMP-3 in the development of PaCa, the following null hypotheses will be addressed:

1) PaCa cell lines do not express ADM and its receptor components therefore, ADM has no functional role in PaCa.
2) ADM and RAMP-3 have no involvement in the regulation of proliferation in PaCa cells
3) ADM and RAMP-3 have no role in regulating response to currently used chemotherapies, gemcitabine and 5-FU
4) ADM has no influence on tumour growth and metastases

1.6 Aims and objectives

To investigate these null hypotheses, the following aims and objectives will be addressed:

1) A panel of 7 PaCa cell lines will be characterised for both mRNA and protein expression of ADM and its receptor components (CLR, RAMP-1, RAMP-2 and RAMP-3).
2) ADM and RAMP-3 KDs will be developed in a PaCa cell line to investigate the effect this has on proliferation of cells *in vitro* compared to wild-type cells.

3) ADM and RAMP-3 KD cells will be compared to wild-type cells to assess whether proliferation and apoptosis of KD cells is altered in response to gemcitabine and 5-FU.
4) ADM KDs will be used in, *in vivo* orthotopic and subcutaneous models to determine whether tumour growth and metastases differ compared to controls.

CHAPTER 2: GENERAL METHODS

2.0 Materials and methods

All reagents and commercial sources are listed in the Appendix. More detailed explanations for protocols are provided in chapters 3 to 6.

2.1 Cell culture

PaCa cell lines were obtained from ATCC and characteristics are defined in Table 2. 1. Cell lines were cultured in conditions specified in Table 2.2 and incubated at 37°C with 5% CO_2. Passages of 45 and below were used in experiments. Flasks were washed twice with PBS and had media changed 3 times a week. Cells were maintained at a confluence of 70-80% which was monitored by microscopy (Figure 2.1).

Table 2. 1 Characteristics of cell lines purchased from ATCC including organism, gender, age, histology, tumour source, mutation and mycoplasma status. All culture phenotypes were consistent with literature and supplier (ATCC) images (Cai et al., 2013; Chen et al., 1982; Kopantzev et al., 2019; Procacci et al., 2018; Tan et al., 1986)

Cell line	Organism	Gender/Age	Histology	Tumour source	Mutations	Mycoplasma tested
AsPC-1	Human	Female, 62 years	Adenocarcinoma	Metastasis, ascites	CDKN2A, FBXW7. KRAS, MAP2K4, TP53	✓
BxPC-3	Human	Female, 61 years	Adenocarcinoma	Primary	CDKN2A, MAP2K4, SMAD4, TP53	✓
Capan-2	Human	Male, 56 years	Adenocarcinoma	Primary	KRAS	✓
CFPAC-1**	Human	Male, 26 years	Ductal Adenocarcinoma	Metastasis, liver	KRAS, SMAD4, TP53	✓
HPAF-II***	Human	Male, 44 years	Adenocarcinoma	Metastasis, ascites	CDKN2A, KRAS, TP53	✓
Panc 10.05	Human	Male, nd	Adenocarcinoma	Primary	KRAS, TP53	✓
SW1990	Human	Male, 56 years	Adenocarcinoma, stage II	Metastasis, spleen	CDKN2A, KRAS	✓

Nd- not defined

**patient also had cystic fibrosis, no links made between cystic fibrosis causing pancreatic cancer (Schoumacher et al., 1990)

*** patient had metastasis to liver, diaphragm and lymph nodes

2.1.1 Sub-culturing/Harvesting

To sub-culture or harvest cells, cells were washed twice in PBS and detached for 5-10 minutes using appropriate volume of TrpLE (Table 2.3). To confirm cell detachment cells were checked under the microscope. Once confirmed, the appropriate volume of PBS was added (Table 2.3) and cells were transferred to a 15mL falcon tube and centrifuged at 250xg for 5 minutes to get a pellet. The pellet was resuspended in warm media. For sub-culturing, the appropriate volume of cells was added into a new flask containing warm media. To set up a new experiment cells were counted as described in section 2.1.4 and diluted in an appropriate volume of media.

Table 2.2 Cell lines, optimal growth media and supplements

Cell type	Media
ASPC-1	RPMI 15% FCS (Gibco) + 1mM sodium pyruvate and 1% penicillin-streptomycin.
BXPC-3	RPMI 10% FCS (Gibco) + 1mM sodium pyruvate and 1% penicillin-streptomycin.
Capan-2	McCoy's 5a 10% FCS (Sigma) + 1% penicillin-streptomycin.
CFPAC-1	DMEM 10% FCS (Gibco) + 1% penicillin-streptomycin.
HPAF-II	RPMI 10% FCS (Gibco) + 1mM sodium pyruvate and 1% penicillin-streptomycin.
Panc 10.05	RPMI 15% FCS (Gibco) + 1mM sodium pyruvate and 1% penicillin-streptomycin.
SW1990	DMEM 10% FCS (Gibco) + 1% pencillin-streptomycin.

FCS- foetal calf serum

Table 2.3 Volume of reagents used with different flask sizes in cell culture

Flask	PBS wash	Media	TrypLE	PBS wash (after detachment)
T25	2 mL	5 mL	1 mL	1 mL
T75	10 mL	10 mL	2 mL	2 mL
T175	15 mL	25 mL	4 mL	4 mL

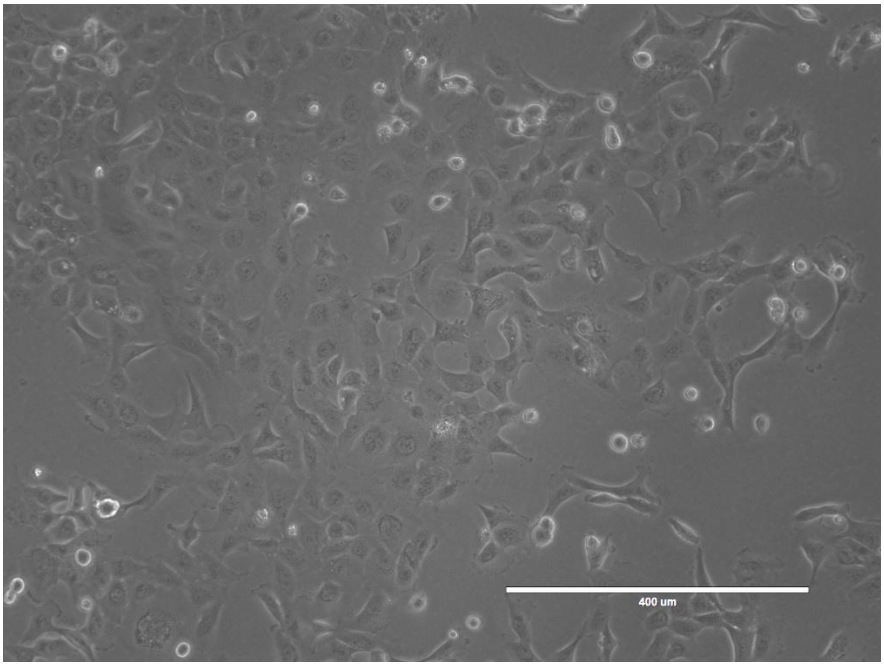

Figure 2.1 Phase image of CFPAC-1 cell line at 70% confluency used for both *in vitro* and *in vivo* experiments. Image was taken at 100x magnification.

2.1.2 Cell freezing

To avoid passaging cells too highly, cell stocks at lower passages (passages 5 to 15) were prepared and frozen. Cell suspensions were prepared as described in section 2.1.1 and counted (section 2.1.4) before centrifuging at 250 x g for 5 minutes. The pellets were resuspended in freezing media (optimal media containing 5% DMSO) and 1e6 cells/mL cells were transferred into cryo-tubes (1 mL each). Tubes were labelled with cell type, passage number and date of freezing. Cells were stored overnight in Mr Frosty ™ Freezing container at -80°C. For short term storage (up to a year), the cells were stored at -80°C, for longer term storage, the cells were stored in liquid nitrogen.

2.1.3 Cell thawing

To revive frozen cells, the cells were thawed at 37°C in a water bath and resuspended in 1 mL of warmed media. The resuspended cells were transferred into a 15 mL falcon and spun at 250 x g for 5 minutes. The cell pellet was resuspended into a 1mL of media and transferred into a T25 flask containing warmed media.

2.1.4 Cell counting

Trypan blue is used to differentiate between live and dead cells. Dead cells appear blue as they lose cell membrane integrity. 10 µL of cell suspension was added to 10 µL of trypan blue in a 0.5 mL centrifuge tube. Cell/Trypan blue suspensions were transferred into a counting slide and counted on the Thermo Fisher Countess II™ Automated cell counter.

2.2 Endpoint PCR

To determine whether the RAMPs, AM and CLR are expressed in the PaCa cell lines, endpoint PCR was used.

2.2.1 RNA extraction

RNA was extracted using the Promega Reliaprep™ Cell Miniprep System and performed at room temperature unless otherwise specified. The cells were prepared as described in section 2.1.1, counted as described in section 2.1.4 and spun at 300 x g for 5 minutes. The supernatant was discarded and the pellet was resuspended in 1mL ice cold PBS and spun at 300 x g for 5 minutes. Cells were then resuspended in appropriate volume BL +TG buffer and vortexed (Table 2.4).

Table 2.4 List of reagent volumes required for ReliaPrep™ Cell Miniprep System.

Cell count	BL + TG buffer (µL)	100% isopropanol (µL)	Water (µL)
$1x10^2$-$5x10^5$	100µL	35µL	15µL
$>5x10^5$-$2x10^6$	250µL	85µL	30µL
$>2x10^6$-$5x10^6$	500µL	170µL	50µL

The appropriate volume of Isopropanol was added to resuspended cell pellet and vortexed for 5 minutes (Table 2.4). ReliaPrep™ Minicolumns were placed in collection tubes and the cell lysate was transferred into the Minicolumn. This was centrifuged for 30 seconds at 14,000 x g and the liquid in the collection tube was discarded. 500µL of RNA wash solution was added to the Minicolumn and centrifuged at 14,000 x g for 30 seconds before the liquid in the collection tube was discarded. For

each sample, a DNAse I recipe mix was prepared (Table 2.5) and 30 µL was added to the Minicolumn and left for to incubate for 15 minutes at room temperature.

Table 2.5 ReliaPrep™ MiniPrep system DNAse I mix recipe

Reagent	Volume
Yellow core buffer	24.0 µL
0.09 M $MnCl_2$	3.0 µL
DNAse I enzyme	3.0 µL

After 15 minutes, 200 µL of column wash was added to the Minicolumn and spun at 14,000 x g for 15 seconds. 500 µL of RNA wash solution was added to the Minicolumn without discarding the liquid in the collection tube. This was spun at 14,000 x g for 30 seconds. The Minicolumn was transferred to a new collection tube and 300 µL of RNA wash solution was added and spun at 14,000 x g for 2 minutes. The Minicolumn was transferred into an elution tube before the appropriate volume of water was added (Table 2.4) and it was spun at 14,000 x g for 1 minute. The RNA collected in the elution tube was stored at -20°C until further use.

2.2.2 Quantification of RNA

To determine the concentration of RNA for cDNA synthesis and subsequent endpoint PCR and real-time PCR experiements, the Thermo Fisher NanoDrop™ 2000 was used. This determines the concentration of RNA at an optical density of 260nm. The optimal absorbance ratios for RNA are specified in Table 2.6.

Table 2.6 Absorbance ratios for RNA purity

Nucleic acid	260/280 ratio	260/230 ratio
RNA	2.0	2.0-2.2

2.2.3 cDNA synthesis

Following RNA extraction, cDNA was synthesised using the Thermo Fisher High Capacity RNA-to-cDNA™ kit. RNAase decontamination solution was used on all surfaces before the experiment to

minimise risk of contamination by ribonucleases. The RNA reaction mix was prepared in 0.2 mL PCR tubes using the reagents and volumes specified in Table 2.7. The final amount of RNA prepared was 1.0 µg. Following sample preparation, the samples were run at 37^{o}C for 60 minutes, 95^{o}C for 5 minutes and then were held at 4^{o}C using the Thermo Fisher Proflex™ PCR system. The samples were stored at -20^{o}C following preparation.

Table 2.7 List of volumes and reagents required for cDNA synthesis

Reagents	RT +ve (µL)	RT -ve (µL)
2X RT Buffer mix	10.0 µL	10.0µL
20X Enzyme mix	1.0 µL	-
RNA sample (1.0 µg)	Up to 9.0 µL	Up to 9.0 µL
Nuclease-free water	To make final volume 20.0 µL	To make final volume 20.0 µL
Total reaction volume	**20.0 µL**	**20.0 µL**

2.2.4 Endpoint PCR reaction

Endpoint PCR was carried out on prepared cDNA samples for 7 different PaCa cell lines using the Promega GoTaq® Hot Start Polymerase kit. The samples and reaction mix were prepared in a UV PCR cabinet to minimise risk of contamination. Before the reaction mix was prepared, pipette tips, pipettes, 0.2 mL PCR tubes and nuclease free water were placed under UV light for 30 minutes. The reagents were thawed on ice and vortexed before use. Reaction mixes were prepared in nuclease-free 0.2 mL reaction tubes as specified in Table 2.8 and Table 2.9. The reaction was run in the Thermo Fisher ProFlex™ using the general recommended temperatures and times; Denaturation was set to 95°C for 2 minutes, annealing temperatures and cycles were set according to the primer of interest (Table 2.10) and extension was at 72°C.

Table 2.8 Reaction components for endpoint PCR per reaction for ADM, RAMP-1, RAMP-2 and CLR

Reagents	Volume (µL)
5X green GoTaq® Flexibuffer	10.0 µL
$MgCl_2$ (25mM)	1.5 µL
F primer (10 µM)	1.0 µL
R primer (10 µM)	1.0 µL
dNTPs (10 mM)	1.0 µL
Polymerase (5u/µL)	0.25 µL

cDNA	1.0 µL
RNAase/DNAase free water	34.25 µL
Total volume	**50**.0 **µL**

Table 2.9 Reaction components for RAMP-3 endpoint PCR reaction

Reagents	Volume (µL)
5X green GoTaq® Flexibuffer	10.0 µL
$MgCl_2$ (25mM)	1.5 µL
F primer (10 µM)	5.0 µL
R primer (10 µM)	5.0 µL
dNTPs (10 mM)	1.0 µL
Polymerase (5u/µL)	0.25 µL
cDNA	1.0 µL
RNAase/DNAase free water	26.25 µL
Total volume	**50**.**0 µL**

Table 2.10 Primer sequences, product size, annealing temperature and cycle number

Target	Sequence	Size (BP)	Annealing temperature	Cycle number
ADM	F 5'- CTGATGTACCTGGGTTCGCT -3' R 5'- ATGTCCTGGGGCCGAATAAG -3'	197	54^0C	35
RAMP-1	F 5'-ATGCAGAGGTGGACAGGTTC-3' R 5'-GCCTACACAATGCCCTCAGT-3'	193	53^0C	35
RAMP-2	F 5'-CTGTCCTGAATCCCCACGAG-3' R 5'-CTCTCTGCCAAGGGATTGGG-3'	256	65^0C	35
RAMP-3	F 5'-AAGGTGGACGTCTGGAAGTG-3' R 5'-ATAACGATCAGCGGGATGAG-3'	227	56^0C	40
CLR	F 5'-CTTGGCTGGGGATTTCCACT-3' R 5'-CCTTCAGGTCGCCATGGAAT-3'	302	54.4^0C	35
GAPDH	F 5'-TTGTCAGCAATGCATCCTGC-3' R 5'-GCTTCACCACCTTCTTGATG-3'	354	56^0C	35

2.2.5 Gel electrophoresis

Gel electrophoresis used to visualise PCR products by size. PCR products were visualised on a 1.5% agarose gel. 1.5 g of agarose was added to 100 mL of Tris/Borate/EDTA (TBE) buffer and dissolved in the microwave. To visualise the PCR products, 5 µL of Ethidium bromide (2.5 µg) was added to the agarose gel. After the gel set (20 minutes), it was transferred into an electrophoresis gel chamber containing the 1X TBE buffer. 10 µL of Norgen HighRanger 1kb DNA ladder (Figure 2.2) was added into

the first well, followed by 10 µL of each sample including a water control. The gel was run for 45 minutes at 200V and visualised using the Gel Doc XR+ System.

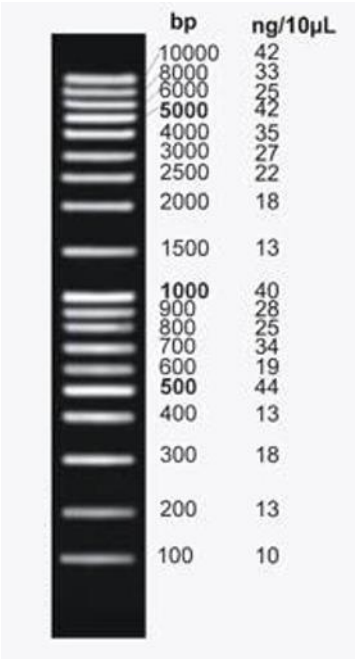

Figure 2.2. Norgen HighRanger 1kb DNA ladder

2.2.6 Sanger sequencing

To validate the endpoint PCR results, Sanger sequencing was used to confirm the correct targets were amplified (Figure 2.3). The PCR products were analysed by the University of Sheffield Core Genomic Facility using the BigDye™ Terminator v3.1 cycle sequencing kit and run on the Applied Biosystems 3730 DNA analyser (ThermoFischer, Paisley, UK). The results were viewed using FinchTV, an example of RAMP-3 sequencing data is shown in Figure 2.3 which was aligned using BLAST (Basic Local Alignment Search Tool, NCBI) to identify target sequence.

(A)

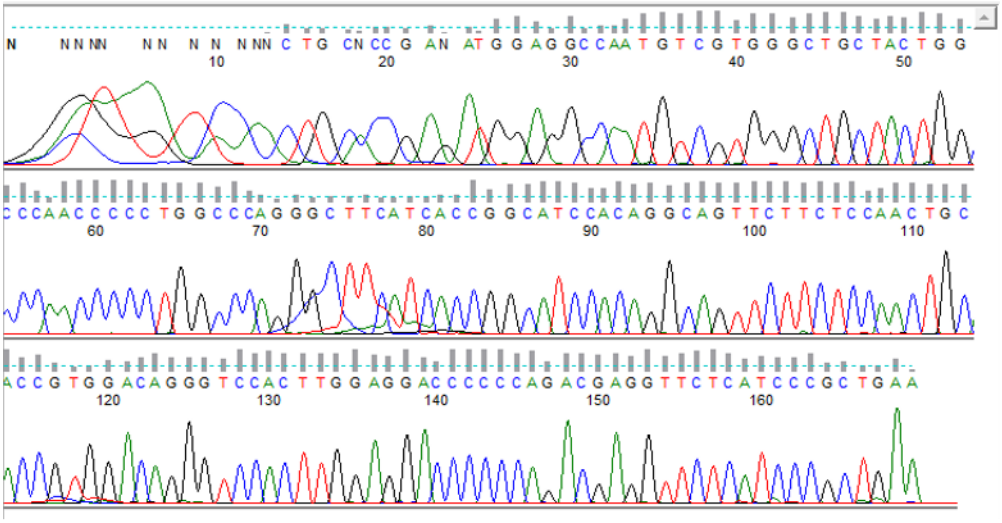

(B)

Homo sapiens receptor activity modifying protein 3 (RAMP3), mRNA

Sequence ID: NM_005856.3 **Length:** 1323 **Number of Matches:** 1

Range 1: 251 to 405 GenBank Graphics ▼ Next Match ▲ Prev

Score	Expect	Identities	Gaps	Strand
273 bits(302)	2e-69	153/155(99%)	0/155(0%)	Plus/Plus

```
Query  14   CTGCNCCGANATGGAGGCCAATGTCGTGGGCTGCTACTGGCCCAACCCCCTGGCCCAGGG  73
           |||| |||| ||||||||||||||||||||||||||||||||||||||||||||||||||
Sbjct  251  CTGCACCGAGATGGAGGCCAATGTCGTGGGCTGCTACTGGCCCAACCCCCTGGCCCAGGG  310

Query  74   CTTCATCACCGGCATCCACAGGCAGTTCTTCTCCAACTGCACCGTGGACAGGGTCCACTT  133
           ||||||||||||||||||||||||||||||||||||||||||||||||||||||||||||
Sbjct  311  CTTCATCACCGGCATCCACAGGCAGTTCTTCTCCAACTGCACCGTGGACAGGGTCCACTT  370

Query  134  GGAGGACCCCCCAGACGAGGTTCTCATCCCGCTGA  168
           |||||||||||||||||||||||||||||||||||
Sbjct  371  GGAGGACCCCCCAGACGAGGTTCTCATCCCGCTGA  405
```

Figure 2.3 Example of sequencing data. **(A)** RAMP-3 sequencing visualised on FinchTV software. **(B)** RAMP-3 NCBI Blast alignment of RAMP-3 sequencing data.

2.3 Quantitative Real-Time PCR (QPCR)

This is a method used to determine mRNA levels of ADM and RAMP-1 quantitatively.

2.3.1 cDNA synthesis

1.5 µg RNA was prepared using Primerdesign precision nanoScript2 reverse transcription kit. The reaction is split into two steps; annealing and extension. The annealing reaction mix was prepared in 0.2 mL nuclease-free PCR tubes as shown in Table 2.11 and was placed in the Thermo Fisher Proflex™ at 65^{o}C for 5 minutes and then immediately transferred onto ice.

Table 2.11 NanoScript 2 reverse transcription annealing step

Reagents	Volume (µL)
RNA template (1.5 µg)	x µL
RT primer (OligoDT)	1.0 µL
RNAase/DNAase free water	x µL
Total volume	**10 µL**

Following the annealing step, the extension mix was prepared as specified in Table 2.12 and 10 µL of the extension mix was added to 10 µL of the annealing mix. This was run at 42^{o}C for 20 minutes, 72^{o}C for 10 minutes and samples were held at 4^{o}C. Samples were stored at -20^{o}C.

Table 2.12 Precision nanoScript 2 reverse transcriptase extension mix

Reagents	RT +ve (µL)	RT -ve (µL)
NanoScript2 4X RT buffer	5.0 µL	5.0 µL
dNTP mix (10mM)	1.0 µL	1.0 µL
RNAase/DNAase free water	3.0 µL	4.0 µL
NanoScript2 enzyme	1.0 µL	-
Total volume	**10 µL**	**10 µL**

2.3.2 QPCR

QPCR was completed to quantify the levels of ADM and RAMP-1 in PaCa cell lines and for knockdown validation of ADM in CFPAC-1 cells. The Double-Dye hydrolysis geNorm 6 Gene kit was used to determine the appropriate housekeeping gene for the PaCa cell lines. ACTB (β-actin) was selected as the mRNA levels between cell lines were similar.

Primerdesign PrecisionPLUS mastermix with ROX was used for QPCR. ROX (rhodamine-X) is a reference dye used for normalisation of the fluorescent reporter signal, in this case. It allows for the correction of well-to-well variation from pipetting errors and fluorescent fluctuations. Primers were designed by PrimerDesign with a double-dye hydrolysis probe labelled with a 6-carboxyfluorescence (FAM) reporter. The hydrolysis probe used in this reaction was a Taqman style probe. The TaqMan probes works by releasing a fluorescent signal. During the QPCR reaction, in the denaturing step, the temperature is raised and the cDNA template is denatured. At this stage the TaqMan probe is

quenched. During the annealing phase, the temperature is lowered and the primers and probe bind to the specific target sequence. During the extension phase, the temperature is raised and the Taq DNA polymerase synthesises new strands of DNA using unlabelled primers and the template strand. When the polymerase reaches the TaqMan probe, its endogenous nuclease activity cleaves the probe and separates the fluorescent reporter dye FAM from the quencher. This results in a fluorescent signal, the amount of fluorescence released, equates to the amount of DNA template present in the PCR.

All QPCR equipment excluding the reagents were placed under UV light for 30 minutes. The cDNA synthesised was diluted to a concentration of 5 ng/µL in nuclease-free water to a total volume of 50 µL. 2.5 µL of the cDNA was loaded into a 384-well plate in triplicate, followed by 7.5 µL of PrimerDesign PrecisionPLUS MasterMix (Table 2.13) containing ADM primers (Table 2.14)

Table 2.13 Mastermix for QPCR reaction

Reagents	Volume (µL)
PrecisionPLUS QPCR Master Mix	5.0 µL
Primer/Probe	0.5 µL
RNAase/DNAase free water	2.0 µL
cDNA	2.5 µL
Total volume	**10.0 µL**

Table 2.14 Primer sequences for ADM designed by PrimerDesign with double dye hydrolysis probe and FAM reporter

Target	Sequence	Tm
ADM Forward	GCATGAAAGAGAAAGACTGATTACC	59°C
ADM Reverse	GCTGTTCGCATATCACCCATT	58°C

After loading the Thermo Scientific 384 well white plate with samples and mastermix, the plate was spun at 250 x g for 1 minute before running on the Applied Biosystems 7900 HT Fast Real-Time PCR. Each reaction was run for 40 cycles at 95°C for 2 minutes, 95°C for 10 seconds and 60°C for 1 minute. The data was analysed using the Sequence Detection System (SDS) v2.4 (Figure 2.4). Ct values

correlate to the number of cycles it takes for the fluorescent signal to cross the threshold. The Ct value is inversely related to the amount of starting DNA.

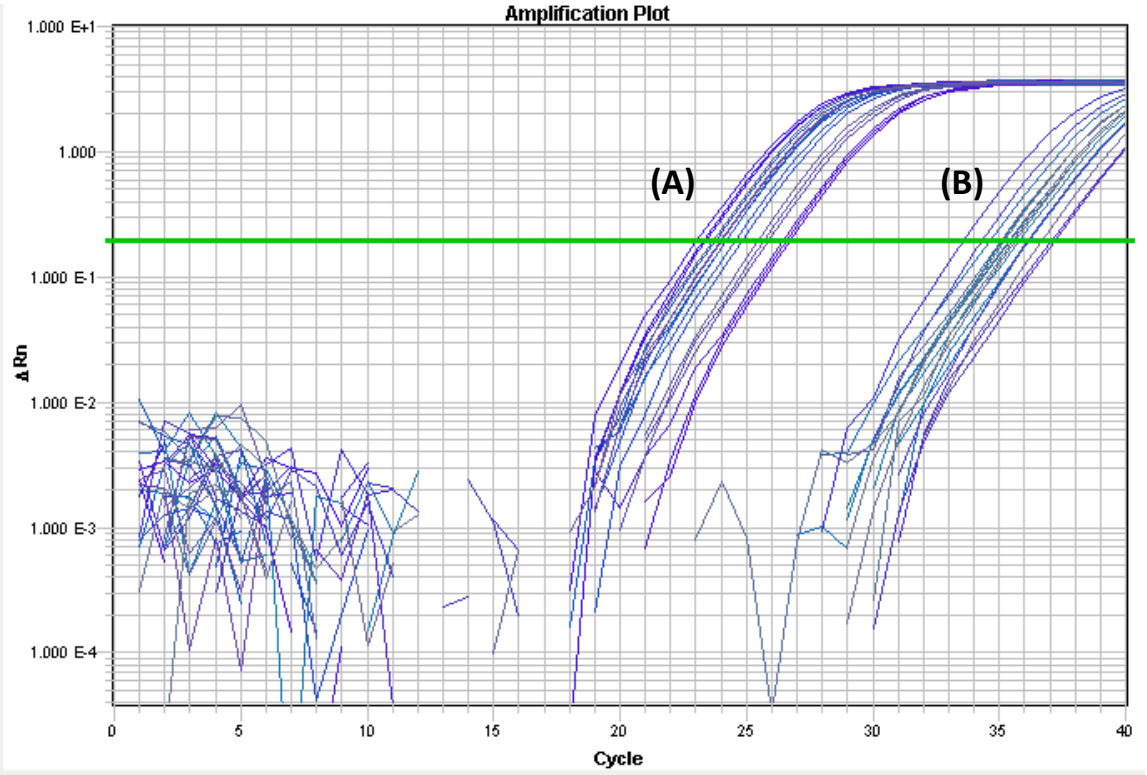

Figure 2.4 QPCR amplification plot for ADM in PaCa cell lines (*y*-axis on log scale). (A) Reverse transcriptase positive samples. (B) Reverse transcriptase negative samples. Samples showed no band following endpoint PCR gel electrophoresis using ACTB primers. The threshold (green line) is set within the linear phase to interpolate the Ct values for each sample.

2.4 Western blotting

This method was used to detect RAMP-1, RAMP-2, RAMP-3 protein in the PaCa cell lines.

2.4.1 Protein extraction

Cells were grown to a confluency of 70% in a T75 flask before being used. The flask was kept on ice during the extraction. Halt™ Protease and Phosphatase inhibitor Cocktail diluted 1:100 in NP40 buffer (150mM NaCl, 50mM Tris Base pH 8.0 and 1% NP-40) were prepared to make a lysis buffer. The protease inhibitors in the lysis buffer were aprotinin, bestatin, E-64 and leupeptin which inhibit serine

and cysteine proteases. Phosphatase inhibitors prevent the degradation of sodium fluoride, sodium orthovanadate, sodium pyrophosphate and β-glycerophosphate in serine, threonine and tyrosine.

The cells were washed twice with ice cold PBS before 1 mL of the lysis buffer was added to the cells and left to incubate on ice for 5 minutes. Cells were then scraped from the bottom of the flask and the lysate was transferred into a 1.5 mL cold Eppendorf tube. The lysate was then sonicated for 30 seconds at input 60 and spun at 13,000 xg for 20 minutes at 4°C. The lysate was transferred to a new 1.5 mL Eppendorf and kept at -20°C until required for BCA assays or western blotting.

2.4.2 Bicinchoninic (BCA) assay

To measure the protein concentration of samples from the protein extraction, the colorimetric Biorad *DC* protein assay was used. The protein sample reacts with both alkaline copper tartrate and folin reagent. Initially the samples react with copper tartrate and then reduce the Folin reagent with the loss of 1-3 oxygen atoms. These oxygen atoms are typically associated with tryptophan and tyrosine producing a blue colour on reduction. This was detected at a wavelength of 750nm on the Ensight® Perkin Elmer plate reader.

A series of dilutions were prepared to generate a standard curve to determine protein concentrations using bovine serum albumin (BSA) diluted in NP-40 lysis buffer (Table 2.15). The standards were loaded in 5 µL triplicates into a 96 well plate. 5 µL of both neat and 1:10 diluted protein samples were also loaded in triplicate. To each well, 25 µL of working solution (a mix of solution A and S) was added. The working solution was prepared by adding 20 µL S for every 1 mL of solution A (containing alkaline copper tartrate). 200 µL of reagent B was added to each well and the plate was left to incubate for 15 minutes at room temperature. The plate was read on the Ensight® Perkin Elmer plate reader at 750nm. A standard curve was plotted (Figure 2.5) on GraphPad Prism, the protein sample concentrations were interpolated using the standard curve linear equation: $y = mx + c$

Table 2.15 Dilutions prepared to make a standard curve for BCA assay

Protein conc (mg/mL)	NP-40 lysis buffer (µL)	BSA (µL)
1.43	0.0	20.0
1.14	4.0	16.0
0.86	8.0	12.0
0.57	12.0	8.0
0.29	16.0	4.0
0.00	20.0	0.0

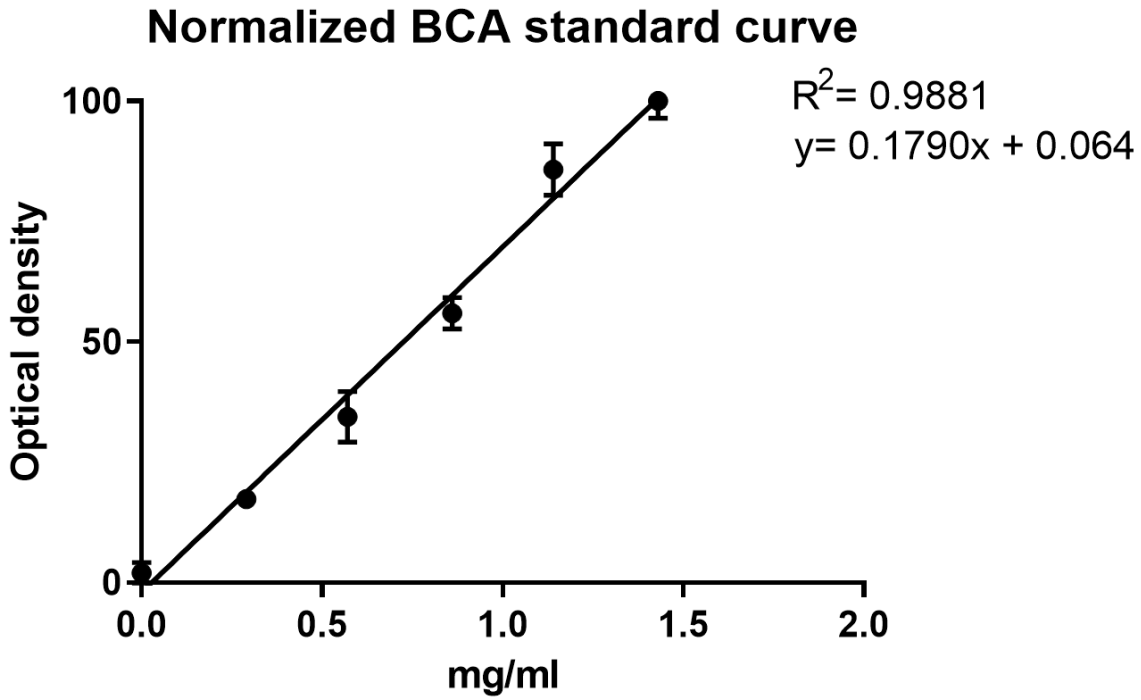

Figure 2.5 Normalized BCA assay standard curve

2.4.3 Western blotting: Gel electrophoresis and transfer

Western blotting is a method used to determine expression of different proteins in the samples using antibodies. Each sample was prepared using 5 µg protein. The samples are diluted in 4X laemmli buffer (LB) and 350 mM DTT (dithiothreitol). LB contains 2% sodium dodecyl sulphate (SDS) which aids in denaturing proteins and distributes a negative charge across protein samples. The buffer contains glycerol which increases the density of the sample for the gel electrophoresis, whilst the bromophenol blue within the buffer runs ahead of the protein to monitor its movement down the gel. DTT reduces

intra-molecular and inter-molecular bonds in the protein samples. The protein samples were separated by size when loaded onto an electrophoresis gel with a charge applied onto the gel. The protein was then transferred onto a membrane to be probed with antibodies. The membrane was blocked to prevent non-specific binding and the proteins were detected by a secondary antibody conjugated to horse-radish peroxidase. The bands were detected by chemiluminescence.

The samples were prepared to a final concentration of 5 µg with LB (65.8mM Tris-HCl pH 6.8, 26.3% glycerol, 2.0% SDS and 0.01% bromophenol blue), 350 mM DTT and water to make a final volume of 50 µL. The samples were heated to 95°C for 10 minutes to denature the protein sample. 10µL of Precision Plus Protein™ Dual Colour standards ladder was added into a 4-20% Mini-PROTEAN® TGX™ Precast Protein gel, along with 50 µL of each sample in the Biorad Vertical Electrophoresis Cell with 1X Tris/Glycine/SDS running buffer. The samples were run at 150V for 45 minutes and transferred onto a trans-blot PVDF membrane. The transfer was completed with the Trans-Blot® Turbo™ Rapid transfer system using pre-set conditions for mixed molecular weight proteins at 25V for 7 minutes.

2.4.4 Western blotting: Blocking and probing

The transfer membrane was blocked in the appropriate blocking buffer diluted in 1X TBS-T (150mM Tris, 20 mM Tris Base and 0.1% Tween) (Table 2.16) for 1 hour on a plate shaker at 600 rpm. Following blocking, the membrane was probed in a 50 mL falcon tube with the appropriate antibody concentration (Table 2.16) and left overnight at 4°C on a roller. The next day, the membrane was washed 3 times for 10 minutes each in 1X TBS-T before adding the appropriate secondary antibody in blocking buffer (Table 2.17) for 1 hour at room temperature on the roller. After 1 hour, the membrane was washed 3 times for 5 minutes in 1X TBS-T and 3 times for 5 minutes in water.

Table 2.16 Primary antibody dilutions and blocks

Target	Antibody type	Species	Code	Concentration	Block
RAMP-1	Monoclonal	Anti-rabbit	Abcam ab156575	1:1000	3% BSA + 0.01% Tween
RAMP-2	Monoclonal	Anti-mouse	Santa Cruz Biotechnology sc-365240	1:100	3% BSA + 0.01% Tween
RAMP-3	Monoclonal	Anti-mouse	Santa Cruz Biotechnology sc-365313	1:1000	5% skimmed milk + 0.01% Tween

Table 2.17 Secondary antibody dilutions

Secondary antibody	Antibody type	Code	Concentration
Goat IgG anti-rabbit HRP	Polyclonal	Dako P0449	1:15,000
Goat IgG anti-mouse HRP	Polyclonal	Dake P0447	1:2000

2.4.5 Western blotting: Detection

The protein was detected using the Thermo Fisher SuperSignal™ West Dura Extended Duration substrate. This assay consists of luminol-based enhanced chemiluminescence substrate (ECL) to detect HRP. It detects antigens by oxidising the ECL in the presence of HRP and peroxidase. 250 µL of ECL and peroxidase were mixed and added to the blot covered in the detection mix. The blot was placed in between transparent plastic film and visualised on the GelDoc XR+ Gel Documentation System.

2.8 Statistical analysis

All data shown in Chapters 3-6 are shown as mean and standard error of mean (SEM). Graphpad Prism, version 9.2.0 was used to analyse and display the data collected.

One-way ANOVA analysis was used for analysis of the effect a single independent variable (for example, a particular dose of a chemotherapy) on multiple groups (different cell types). In experiments where there was more than one variable (different chemotherapy doses and different cell types), two-way ANOVA analysis was used to identify interactions between different variables and to analyse the variables individually. Repeated measure two-way ANOVA analysis used for viability

assays specifically, where the data was time-course related. Tukey's multiple comparisons tests were used as post-hoc analysis for two-way ANOVA analysis. ROUT outlier tests were done to identify potential outliers however, no outliers were identified within data.

CHAPTER 3: PaCa CELL LINE CHARACTERISATION

3.1 Introduction

3.1.1 ADM and its receptors in PaCa

PaCa cancer is known to exhibit an aggressive phenotype and is associated with a poor patient survival. There is limited understanding on the molecules that drive this phenotype however, ADM and its receptor components have been shown to be elevated in other cancers. Evidence is growing that the CLR/RAMP-3 receptor may be the key driver in inducing pro-tumorigenic effects whilst the CLR/RAMP-2 receptor has been linked to more physiological functions. However, research within PaCa could implicate otherwise as discussed below.

Ishikawa *et al* (2003) show that ADM mRNA was expressed in 5 PaCa cell lines however, only 2 out of 5 expressed both RAMP-2 and CLR, two expressed RAMP-2 alone and one cell line expressed neither. RAMP-3 expression was not detected in any of the cell lines. Treating tumours with αAM antibody resulted in decreased tumour size and a decrease in the number of proliferating tumour cells. Furthermore, formation of large blood vessels was supressed which depleted the oxygen and nutrient supply to the tumour and inhibited its growth. The receptor through which this effect was mediated was not confirmed however, RAMP-2 has been associated with vessel growth and decreased tumour size in a study by Dai *et al* (2020).

Keleg *et al* (2007) also showed limited RAMP-3 expression with only 1 out of 5 PaCa cell lines expressing RAMP-3 at mRNA level. However, all the cell lines expressed ADM, CLR, RAMP-1 and RAMP-2. Median mRNA expression of ADM and its receptor components in normal pancreatic tissue and PDAC tissue showed an increase in ADM and CLR expression in PDAC. There was no difference in RAMP-2 mRNA expression and RAMP-1 and RAMP-3 showed a decrease in PDAC samples compared to normal tissue. Immunostaining of PDAC tissue showed co-localisation of CLR with RAMP-1 or RAMP-2 in malignant cells but no RAMP-3. These data also indicate that RAMP-3 may not have a direct effect on PDAC.

Ramachandran *et al* (2007) also explored the expression of ADM and its receptors in both cell lines and tissues. In tissues they showed that 43 out of 48 PDAC samples expressed ADM. Furthermore, all eight cell lines expressed ADM. However, CLR and RAMP-3 were not expressed in these cell lines but RAMP-1 and RAMP-2 were expressed in BxPC-3, Panc-1 and MiaPaCa-2 cells. However, the ADMR receptor (also known as L1-R) was expressed. Furthermore, silencing of ADMR resulted in reduced invasion and migration suggesting the invasive and migratory mechanisms may be induced through this receptor instead. Interestingly, pancreatic stellate cells (PSCs, a type of CAF) and HUVECS expressed both ADMR and CLR suggesting that the CLR/RAMP receptors may act on cells within the tumour microenvironment but not the PaCa cells themselves producing a more aggressive PaCa phenotype.

The role of ADM and its receptor components in cancer has largely been researched under the assumption that they induce direct effects on tumour cells. However, research in PaCa has shown evidence that ADM may induce its pro-tumorigenic effects by interacting with cells that enter the tumour microenvironment, as opposed to cancer cells themselves. Xu *et al* (2016) have shown evidence for this as they showed CLR, RAMP-2 and RAMP-3 expression in myelomonocytic cells (MMCs) associated with PDAC. They showed that PaCa cells secrete ADM and that MMCs express the receptors for ADM to bind to. *In vivo,* overexpression of ADM in PaCa cells resulted in increased recruitment of MMCs compared to controls.

Dai *et al* (2020) most recently demonstrated ADM interactions with cancer-associated fibroblasts (CAFs) in the tumour microenvironment. CAFs are cells found within the PaCa tumour microenvironment that have been shown to interact with multiple cells of the microenvironment and induce pro-tumorigenic effects (explained in more detail in Chapter 6). Dai *et al* (2020) showed the association between CAFs and increasing the tumorigenic and metastatic capacity of PaCa. RAMP-2 endothelial knockouts in mice showed that tumour masses significantly decreased and that angiogenesis was defective at both tumour and metastatic sites. They showed that in metastatic

sites, RAMP-3 expression was significantly elevated with ten times greater expression than RAMP-2. The increase in RAMP-3 expression correlated with increased α-SMA and PDPN expression which are markers of CAFs and lymphatic endothelial cells and associated with poorer prognosis in patients. They also generated RAMP-3 knockouts to investigate the association between RAMP-3 and CAFs further. They found that there was less fibrosis in metastatic livers and less expression of α-SMA/PDPN, suggesting that RAMP-3 may regulate metastasis in PaCa.

These data suggest a novel approach to PaCa therapy and give a new insight into our understanding and approach of ADM and RAMP-3 role in cancer. It has been widely accepted that RAMP-2 may have a physiological role within the human body and therefore any pathological conditions including cancer may be driven by RAMP-3 as there is limited understanding of the CLR/RAMP-3 receptor. However, research around PaCa suggests that RAMP-2 may have a direct role on PaCa tumours whilst RAMP-3 interacts with the cells that are part of the tumour microenvironment for example, CAFs, MMC cells and TAMs to make the tumour more aggressive and induce metastasis. These data confirm that ADM plays a key role in PaCa and that it utilises both RAMP-2/CLR and RAMP-3/CLR receptors to induce pro-tumorigenic effects. From a novel therapy perspective, targeting these receptors may be a challenge as RAMP-2 is important in regulating blood pressure however, targeting RAMP-3 may be more feasible. This may reduce metastasis and the formation of fibrosis around tumours making it easier for current therapies to access the target site. ADM_{22-52} has already shown promise in targeting the ADM receptor to treat cancer. This is an antagonist that targets both AM_1 and AM_2 receptors. Ishikawa *et al* (2003) showed how intra-tumoural injection of PCI-43 PaCa cells with AM_{22-52} resulted in decreased tumour growth that correlated with small blood vessel diameter. Furthermore, in a breast cancer xenograft model, Benyahia *et al* (2017) showed how treatment of MCF-7 cells with AM_{22-52} or αAMr resulted in decreased tumour volume. Treatment also induced disruption to tumour vasculature, induction of apoptosis and decreased tumour cell proliferation. These results show promise for developing an antagonist again the AM_2 receptor.

3.1.2 ADM and its receptors in other cancers

Expression of ADM and its receptor components is shown in Table 3.1, showing that it is expressed in a wide range of cancers. ADM does not necessarily have a direct role in causing cancer however, it does contribute to the pathogenesis of cancer. It has been shown to induce proliferation of cancer cells and inhibit apoptosis, induce angiogenesis and lymphangiogenesis and alter the phenotype of cancer cells to make them more aggressive (Berenguer-Daizé et al., 2013; Berenguer et al., 2008; Fritz-Six, Dunworth, Li, & Caron, 2008; Greillier & Tounsi, 2015; Hague et al., 2000; Ichikawa-shindo et al., 2008; Brekhman et al., 2011).

Multiple studies demonstrate how ADM expression is correlated with poorer prognoses and disease stage. Greillier & Tounsi (2015) showed 2-fold to 10-fold higher ADM tissue mRNA expression in malignant pleural mesothelioma (MPM) compared to normal pleural lung tissue suggesting that ADM has a role in making the cells more malignant. Mazzocchi *et al* (2004) also showed how increased ADM expression was shown in prostate carcinoma samples compared to prostate hyperplasia. Deville *et al* (2009) compared ADM expression in normal renal tissue to clear cell renal carcinoma and chromphobe renal carcinoma tissue samples, showing higher ADM mRNA expression in the malignant tissues. This correlated with increased VEGF expression suggesting that ADM may induce angiogenesis. Together, these data indicate that ADM is expressed more in malignant phenotypes compared to normal tissues.

Furthermore, higher ADM expression has been correlated with increased risk of relapse and metastases. Deville *et al* (2009) showed higher expression of ADM correlated with an increased chance of relapse following curative nephrectomy. In colorectal cancer, high ADM mRNA expression has been suggested to be a good marker of predicting high risk relapse and cancer-related death in patients who undergo curative resection. This has also been shown by Uemura *et al* (2011) who showed high expression of ADM correlated with cancer recurrence and liver metastasis. In epithelial ovarian cancer, Deng *et al* (2012) showed a correlation between high ADM expression, higher

incidence of metastases, larger residual size of tumour after chemotherapy, shorter disease free and overall survival time. These data combined indicate that ADM is associated with increased risk of cancer recurrence and metastases.

Ouafik *et al* (2002) demonstrate a correlation between more malignant phenotypes of brain tumours and ADM mRNA expression. In glioblastomas, ADM expression was high compared to low grade astrocytomas which had barely detectable levels of ADM mRNA. Rocchi *et al* (2001) showed a correlation between high ADM mRNA expression and Gleason score, with barely detectable levels of ADM in benign prostate hyperplasia but increasing ADM expression between Gleason scores of 6-9. Berenguer-Daizé *et al* (2013) also showed a correlation between ADM expression and increasing Gleason score. These data suggest that ADM expression correlates with a more aggressive cancer phenotype.

ADM can induce its pro-tumorigenic effects through multiple receptors including CLR/RAMP-2 and CLR/RAMP-3 receptors. Determining which receptor ADM induces its pro-tumorigenic effects could be valuable for designing therapeutic targets against ADM. Ouafik *et al* (2002) showed that CLR/RAMP-2 and CLR/RAMP-3 expression was increased in gliomas. Giacalone *et al* (2003) have shown that RAMP-2 and RAMP-3 are expressed in human ovarian cancer cell lines at mRNA level. Berenguer-Daizé *et al* (2013) showed CLR, RAMP-2 and RAMP-3 expression increased with increasing Gleason score in prostate cancer. CLR, RAMP-2 and RAMP-3 expression was dispersed amongst the stromal collagen septa and clusters of stromal cells. Furthermore, Mazzocchi *et al* (2004) showed that CLR and RAMP-2 were expressed at mRNA level in equal amounts in prostate hyperplasias and carcinomas however, RAMP-3 and ADM were expressed significantly more in prostate carcinomas. RAMP-3 immunostaining in renal cell carcinoma showed that RAMP-3 was located in inflammatory cells that infiltrated the tumour suggesting that RAMP-3 and ADM are also expressed in cells of the tumour microenvironment, not only tumour cells (Deville et al., 2009).These data are in line with

previous findings suggesting that RAMP-2 is more important in inducing physiological effects whilst RAMP-3 is associated with pathological effects.

Table 3.1 Summary of ADM and its receptor component expression. Expression was measured as mRNA and protein by western blot or immunostaining. Table adapted from Riveiro, Berenguer-daize, Kane, & Oua (2021)

Cancer	ADM	CLR	RAMP-1	RAMP-2	RAMP-3	References
Breast	+	+	NR	+	+	(Benyahia et al., 2017; Brekhman et al., 2011; Siclari et al., 2014)
Colorectal	+	+	NR	+	+	(Kaafarani et al., 2009; Nouguerède et al., 2013; Uemura et al., 2011; Wang et al., 2014)
Glioblastoma	+	+	NR	+	+	(Kaafarani et al., 2009; L. H. Ouafik et al., 2002)
Kidney	+	+	NR	+	+	(Deville et al., 2009; Ishimitsu, Nishikimi, et al., 1994; Michelsen et al., 2006)
Liver	+	+	NR	+	+	(Park et al., 2008)
Melanoma	+	+	NR	+	+	(Peiwen Chen, Huang, Bong, Ding, Song, & Wang, 2011)
Malignant pleural mesothelioma	+	+	NR	+	+	(Greillier & Tounsi, 2015)
Osteosarcoma	+	+	NR	+	+	(Dai et al., 2013; Wu et al., 2015)
Ovarian	+	+	NR	+	+	(Giacalone et al., 2003)
Pancreas	+	+	+	+	+	(Dai et al., 2020; Ishikawa et al., 2003; Keleg et al., 2007; Ramachandran et al., 2007; Xu et al., 2016)
Prostate	+	+	+	+	+	(Berenguer-daize et al., 2013; Rocchi et al., 2001; Mazzocchi et al., 2004)

NR: not reported

3.1.3 Hypothesis

The null hypothesis is that PaCa cell lines do not express ADM and its receptor components (CLR, RAMP-1, RAMP-2 and RAMP-3) and have no functional role in PaCa. Therefore, ADM and its receptor components are not involved in PaCa development and progression.

3.1.4 Aims and objectives

The aim of the characterisation of the PaCa cell lines was to determine the expression of ADM and its receptors for *in vivo* and *in vitro* experiments. Confirmation of receptor expression and functional role was used to select suitable cell lines to develop ADM and RAMP-3 knockdowns to determine their role in PaCa cancer progression.

Endpoint PCR and QPCR were used to characterise the PaCa cell lines at mRNA level. Western blotting was used to determine expression of the RAMPs at protein level. cAMP assays were important to determine the functional role of ADM and other calcitonin peptides (CGRP and IMD), this helped identify cell lines most suitable for determining the effects of ADM and RAMP-3 knockdowns.

3.2 Methods

3.2.1 Cell culture

Chapter 2, Section 2.1 outlines how PaCa cells were cultured and the appropriate media and supplements used for each cell line (Table 2.1). Cells were seeded or sub-cultured at a confluency of 70-80%. Cells were seeded for experiments at passages 45 or less to ensure cells maintained the same morphology, growth rate, protein expression and transfection efficiency.

3.2.2 Endpoint PCR

Chapter 2, Section 2.2 describes how PaCa cell lines were characterised for mRNA from RNA extraction to endpoint PCR. RNA was first extracted using the Promega ReliaPrep™ Cell Miniprep system and the amount of RNA in samples was quantified using the NanoDrop™ 2000 (Thermo Fisher) as described in Section 2.2.1 and 2.2.2. Once the RNA concentration was determined, 1.0 µg of cDNA was prepared using Thermo Fisher high capacity RNA-to-cDNA™ kit as described in Section 2.2.3. The synthesised cDNA was used to analyse ADM, CLR and RAMP 1-3 mRNA expression using the Promega GoTaq® HotStart polymerase kit and the primers specified in Table 2.9 (Section 2.2.4). The samples were run on a 1.5% agarose gel with ethidium bromide and mRNA bands were visualised using the Gel Doc XR+ System (Section 2.2.5). To confirm that the bands corresponded to ADM, CLR, RAMP 1-3 mRNA samples were sequenced by the Sheffield Core Genomic facility and analysed using FinchTV (Section 2.2.6)

3.2.3 QPCR

QPCR was used to quantify levels of RNA in PaCa cell lines. 1.5 µg cDNA was prepped using Primerdesign Precision nanoScript2 reverse transcription kit. The two-step process (annealing and extension) was described in Section 2.3.1. RAMP-1 and ADM levels were quantified using the Primerdesign PrecisionPlus buffer with ROX reference dye and the primers listed in Table 2.3. The

primers had a double dye hydrolysis probe with a FAM reporter. The hydrolysis probe was a TaqMan style probe (Section 2.3.2)

3.2.4 Western blot

Western blotting was used to determine protein expression in the seven PaCa cell lines outlined in Chapter 2, Section 2.1.1. First, protein was extracted using NP40 lysis buffer described in section 2.4.1. To determine the protein concentration, Biorad *DC* protein assay was used to determine the volume of protein needed to make a final concentration of 5 µg protein (Section 2.4.2). The protein was probed for RAMP-1, RAMP-2 and RAMP-3 (Table 2.15) and visualised on the GelDoc XR+ Gel documentation system (Chapter 2, Section 2.4).

3.2.5 cAMP assays

To further characterise the 7 PaCa cell lines and determine if they had functional ADM receptors, the LANCE® cAMP 384 kit was used. Downstream of CLR (GPCR) is the cAMP pathway, following ligand binding (ADM, CGRP and IMD), adenosine triphosphate is converted to cAMP following activation of adenylyl cyclase.

The LANCE cAMP assay is a time resolved fluorescence energy transfer (TR-FRET) immunoassay that measures cAMP production after GPCR stimulation following ligand binding. The assay is based on competition between a Europium-labelled cAMP tracer complex (formed by tight interactions between biotin-cAMP and EU-streptavidin) and cAMP in the samples for binding sites on cAMP-specific antibody. The cAMP-specific antibody is labelled with AlexaFluor 647 dye.

When Europium labelled-cAMP tracer complex is excited at a wavelength of 320 nm, it transfers energy to the Alexa-Fluor-labelled antibody. Fluorescence released following the energy transfer is measured at 665 nm. The more cAMP in the cell sample, the lower the amount of fluorescence at 665 nm as there is less of the Europium-labelled complex available to bind to the Alexa Fluor

antibody. This is a competition assay therefore, the signal produced is inversely proportional to the amount of cAMP in the cells (Figure 3.1).

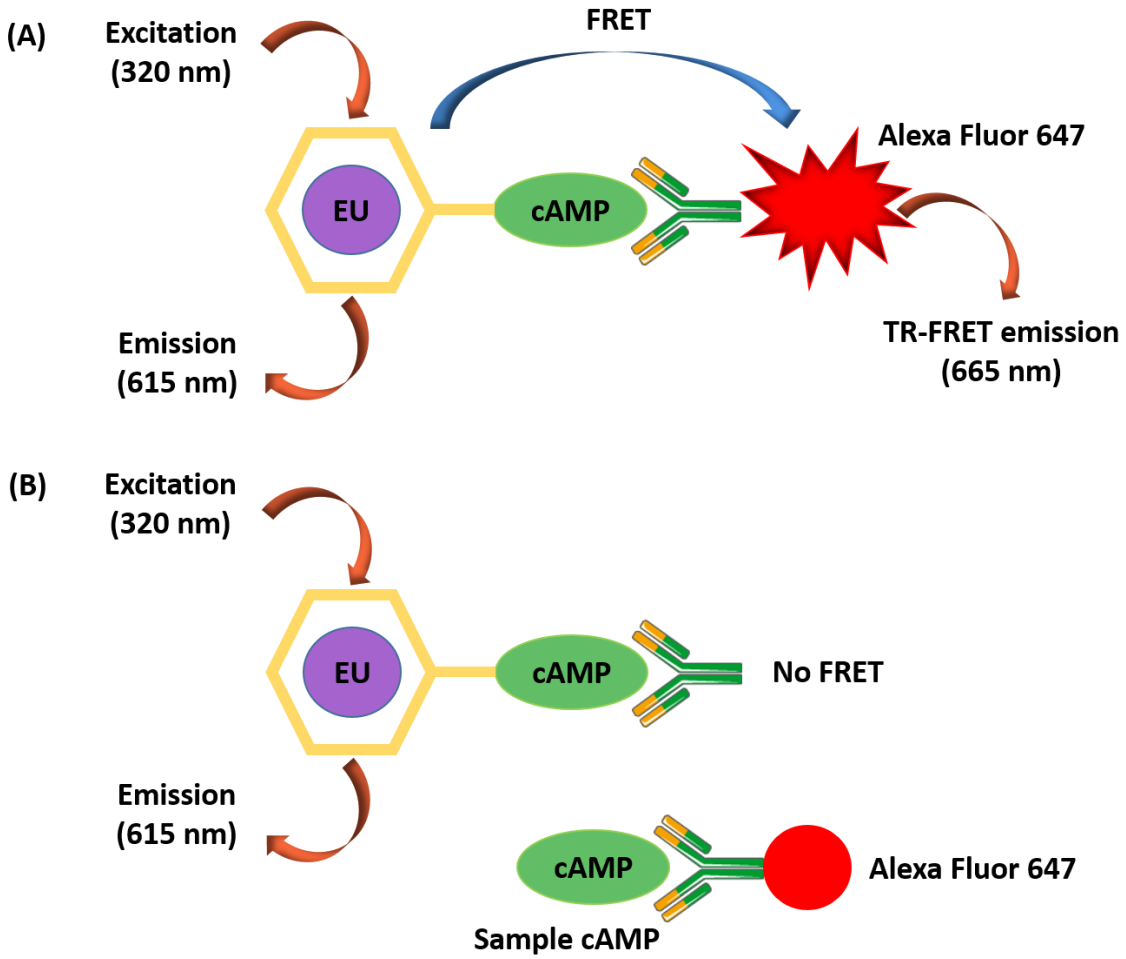

Figure 3.1 Principles of the LANCE cAMP assay. (A) When the Europium labelled cAMP tracer complex is excited at 320 nm and bound to the Alexa Fluor 647 antibody, energy is transferred from the Europium complex to the antibody. This releases a fluorescent signal (TR-FRET) at 665 nm. (B) However, in the presence of a sample containing cAMP Alexa Fluor binds to the sample cAMP instead of the Europium complex. This results in a lower TR-FRET signal which is inversely proportional to the amount of cAMP produced by the sample of interest.

A stimulation buffer was made with HBSS with Ca^{2+} and Mg^{2+} according to Table 3.2 (pH adjusted to 7.4 with 0.1 M NaOH) and used as a diluent for ligands as specified by the manufacturers protocol. To prepare cells, HBSS without Ca^{2+} and Mg^{2+} was used to prevent clumping and to ensure equal

distribution of cells between wells. IBMX was used to inhibit phosphodiesterase degradation of cAMP and BSA was used to stabilise the antibody used in the assay.

Table 3.2 Stimulation buffer recipe for cAMP assays

Reagent	Stock concentration	Volume added	Final concentration
HBSS	-	15 mL	-
HEPES	1 M	75 µL	5 mM
BSA Stabiliser	7%	200 µL	0.1%
IBMX	250 mM	30 µL	0.5 mM

HBSS: Hank's buffered saline solution; HEPES: 4-(2-hydroxyethyl)-1-piperazineethanesulfonic acid; BSA: bovine serum albumin; IBMX: 3-isobutyl-1-methylxanthine

In each well prepared, 6 µL cells, 6 µL agonist and 12 µL detection mix was added respectively. Half-log dilutions of ADM, CGRP, IMD were prepared using the VIAFLO 125 multichannel pipette on the ASSIST automated pipette platform in 96 well plates. Forskolin was used as a positive control as it directly activates adenylyl cyclase. Both ligand and forskolin dilutions were prepared according to Table 3.3 and Table 3.4. Once ligands were prepared and cells were seeded as described below, 6 µL of the ligand agonists were added in 384-well Optiplates.

Table 3.3 Half-log serial dilution of calcitonin family peptides for cAMP assay

Dilution	2x conc (M)	Final conc (M)	Volume of dilution	Diluent
1	2.00E-06	1.00E-06	4 µL of 60 µM	116 µL
2	6.32E-07	3.16E-07	30 µL of 1	70 µL
3	2.00E-07	1.00E-07	30 µL of 2	60 µL
4	6.32E-08	3.16E-08	30 µL of 3	70 µL
5	2.00E-08	1.00E-08	30 µL of 4	60 µL
6	6.32E-09	3.16E-09	30 µL of 5	70 µL
7	2.00E-09	1.00E-09	30 µL of 6	60 µL
8	6.32E-10	3.16E-10	30 µL of 7	70 µL
9	2.00E-10	1.00E-10	30 µL of 8	60 µL
10	6.32E-11	3.16E-11	30 µL of 9	70 µL
11	2.00E-11	1.00E-11	30 µL of 10	60 µL
Blank	-	-	-	70 µL

Conc: concentration; stimulation buffer was used as the diluent

Table 3.4 Half-log serial dilutions of forskolin for cAMP assay

Dilution	2x conc (M)	Final conc (M)	Volume of dilution	Diluent
1	2.00E-04	1.00E-04	80 µL of 150 µM	40 µL
2	6.32E-05	3.16E-05	30 µL of 1	70 µL
3	2.00E-05	1.00E-05	30 µL of 2	60 µL
4	6.32E-06	3.16E-06	30 µL of 3	70 µL
5	2.00E-06	1.00E-06	30 µL of 4	60 µL
6	6.32E-07	3.16E-07	30 µL of 5	70 µL
7	2.00E-07	1.00E-07	30 µL of 6	60 µL
8	6.32E-08	3.16E-08	30 µL of 7	70 µL
9	2.00E-08	1.00E-08	30 µL of 8	60 µL
10	6.32E-09	3.16E-09	30 µL of 9	70 µL
11	2.00E-09	1.00E-09	30 µL of 10	60 µL
Blank	-	-	-	70 µL

Conc: concentration; stimulation buffer was used as the diluent

Frozen cell aliquots were thawed and counted as described in Section 2.1.3 and 2.1.4 and Alexa Fluor anti-cAMP was added 1:100 to cell suspension before being seeded into wells (2,500 cells in 6 µL). The remainder of the experiment was completed in darkness. Cells were stimulated for 30 minutes by the diluted ligands at room temperature and 12 µL detection mix (europium-labelled CAMP tracer complex) was added to each well which was prepared 30 minutes before its use. After an hour, the plate was read on the EnSight Multimode Plate Reader (PerkinElmer) at 320/340 nm excitation and 615/665 nm emission. Both forskolin-stimulated (0.1 mM) and vehicle-control wells were used as controls for 100% and 0% cAMP stimulation respectively.

3.3 Results

3.3.1 PaCa Cell morphology

PaCa cell lines were cultured *in vitro* and imaged to determine morphology of the cells and ensure that the cells were healthy (Figure 3.2). The morphology of the panel of 7 PaCa cell lines was compared to the images on ATCC where the cells were supplied from. The panel of 7 PaCa cell lines outlined in Table 2. 1 were selected as they represent pancreatic adenocarcinomas with different characteristics including different mutations, genders and stages of cancer (either primary or metastatic). Using a panel of cell lines with these different characteristics could inform whether specific characteristics effected expression of AM and its receptor components, the functionality of the receptor (cAMP) and changes in viability and apoptosis.

AsPC-1 cells are adherent cells that have a round and elongated morphology. As the cells become more confluent, they begin to grow in clusters of proliferating cells to form a single monolayer. BxPC-3 cells have an epithelial morphology, are adherent and also form a monolayer. BxPC-3 cells appear slightly bigger in size compared to AsPC-1 cells and also form clusters of proliferating cells forming a single monolayer.

Capan-2 cells are adherent, polygonal epithelial cells that grow in clusters. These cells differ to AsPC-1 and BxPC-3 cells as they grow in separate clusters with large empty spaces in between. CFPAC-1 cells have a more mesenchymal morphology and polarisation making the cells appear round and elongated. They grow in monolayers similar to the other cell types however, they have a disorganised pattern of growth. After the cells have established and become more confluent, they distribute evenly and form clusters of proliferating cells similar to AsPC-1 and BxPC-3 cells.

HPAF-II cells have epithelial morphology and are adherent. The cells are pleomorphic and form a single monolayer. Similar to Capan-2 cells, they form distinct clusters of cells with large empty spaces between with a few smaller clusters of proliferating cells. They also form giant multinucleated cells with some smaller mononucleated cells.

Panc 10.05 form epithelial monolayers and are similar to BxPC-3 cells in appearance with round and polygonal cell types. However, they grow in similar patterns to Capan-2 and HPAF-II cells forming large clusters and empty spaces in between. Furthermore, they form both multinucleated and mononuclear cells similar to HPAF-II. SW1990 cells are epithelial in morphology and have a mix of polygonal and round cells. They form a monolayer with smaller clusters of proliferating cells. They also have a mix of multinucleated and mononuclear cells.

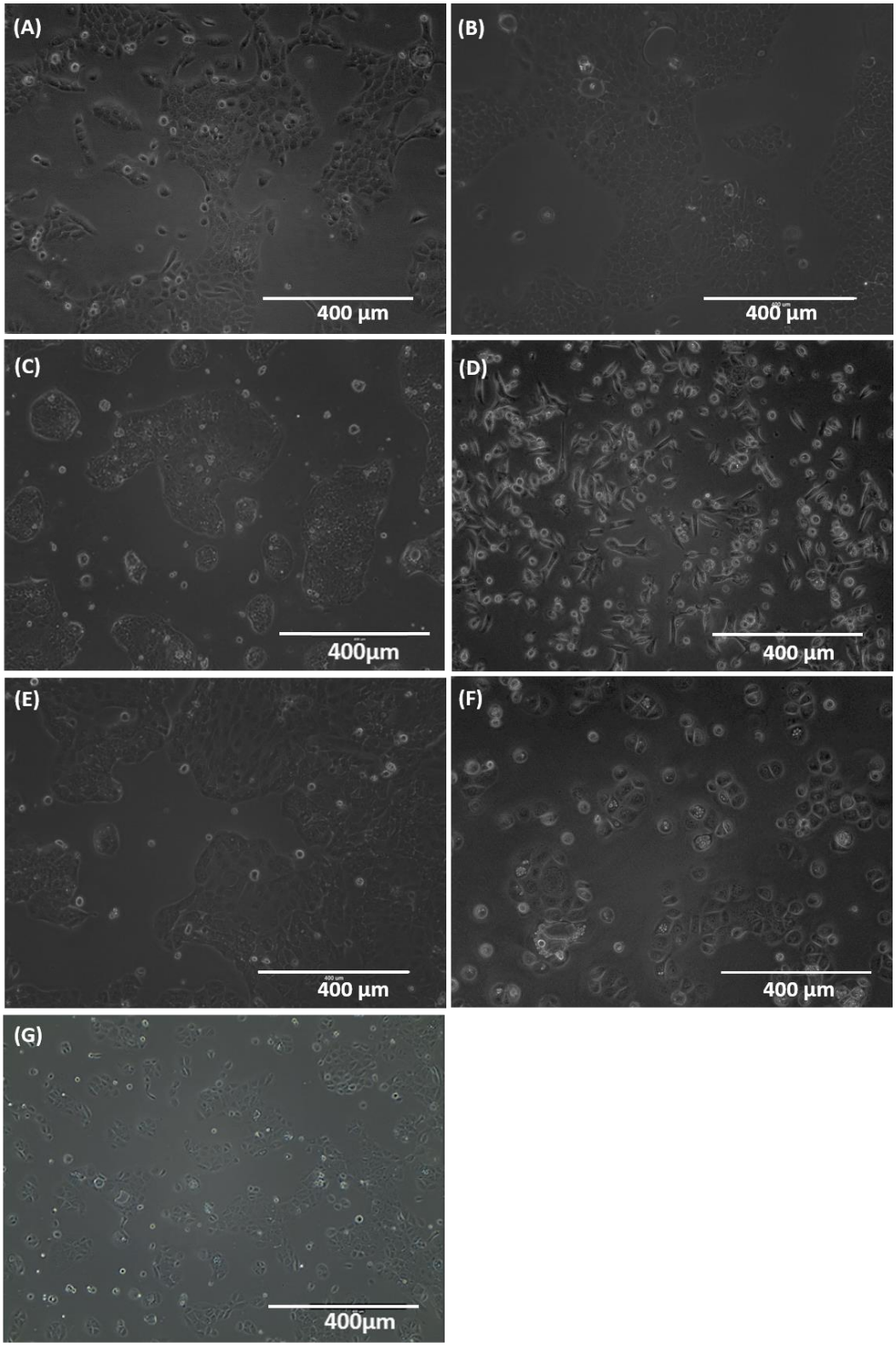

Figure 3.2 Phase-contrast images of a panel of seven pancreatic cell lines from American Type Culture Collection (ATCC). (A) AsPC-1, (B) BxPC-3, (C) Capan-2, (D) CFPAC-1, (E) HPAF-II, (F) Panc 10.05 and (G) SW1990. Images were taken at 100x magnification.

3.3.2 mRNA expression of ADM/CLR/RAMPs

To determine if PaCa cell lines express ADM and its receptor components including CLR and RAMP 1 to 3, mRNA expression was determined by endpoint PCR and QPCR. Determining ADM and its receptor expression was important to identify which cell lines produce ADM and RAMP-3 KDs in.

Figure 3.3, Figure 3.5, Figure 3.7, Figure 3.9 and Figure 3.11 show endpoint expression of RAMP-1-3, CLR and ADM across the seven different PaCa cell lines. Figure 3.3 shows that all the cell lines express RAMP-1 with bands at a height of 193 base pairs (BP), including in the CGRP receptor control cells. The expression of RAMP-1 was further confirmed by the sequencing data shown in Figure 3.4 with a sequence similarity of 77%, suggesting low homology due to a poor sequencing read RAMP-1 expression was confirmed in AsPC-1, BxPC-3, Capan-2, CFPAC-1, HPAF-II, Panc 10.05 and SW1990 cells. RAMP-2 expression was also confirmed by endpoint PCR with bands at 256 BP (Figure 3.5). The results showed a more varied degree in expression across the cell lines with fainter bands in ASPC-1 and Panc 10.05 and a strong band in SW1990 and the AM1 control. The expression of RAMP-2 was confirmed by sequencing data with a sequence similarity of 91% (Figure 3.6). RAMP-3 was also expressed in most cell lines including AM2 control cells. BxPC-3 did not show a band at the height of 226 BP (Figure 3.7). RAMP-3 endpoint PCR gel electrophoresis also showed multiple bands that were below 226 BP, including BxPC-3. Expression of RAMP-3 was confirmed following excision of the band at 226 BP and by sequencing data, showing 99% similarity to the RAMP-3 gene (Figure 3.8). Figure 3.9 shows expression of ADM in all seven PaCa cell lines with a band at a height of 197 BP which was also shown in AM2 control cells. This result was confirmed by sequencing data with a sequencing similarity of 98% (Figure 3.10). CLR is also expressed across all the cell lines with a band at 302 BP including in the control cells (Figure 3.11). The expression of CLR was confirmed by sequencing with a sequencing similarity of 97% (Figure 3.12).

To determine quantitative levels of mRNA expression, QPCR was used to determine expression levels of ADM, RAMP-1, RAMP-2 and RAMP-3. ADM mRNA expression was confirmed across all the

cell lines was similar with Ct values ranging from 22.5 in BxPC-3 cells to 26.0 in SW1990 (Table 3.). RAMP-1 mRNA expression confirmed in all seven PaCa cell lines. Ct values ranged from 23.0 in HPAF-II to 27.5 in Capan-2 (Table 3.5). RAMP-2 and RAMP-3 mRNA expression was not shown in the 7 PaCa cell lines however, AM1 and AM2 cell controls were shown to express RAMP-2 and RAMP-3 with Ct values of 18.3 and 16.3 respectively. A Ct value above 35 was used as the cycle cut-off value.

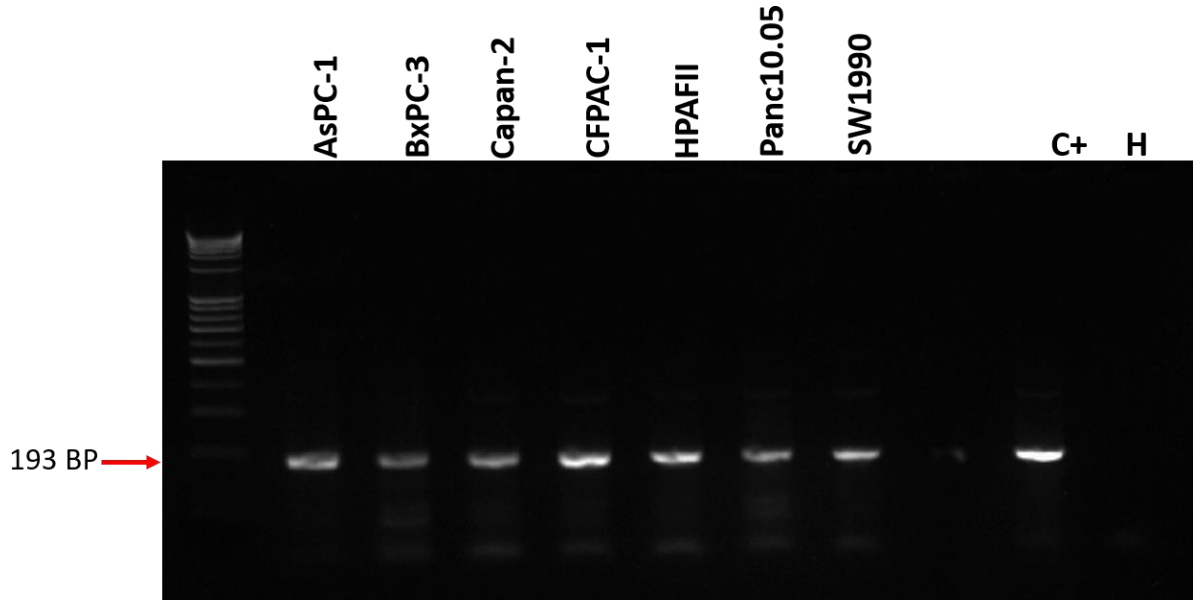

Figure 3.3 RAMP-1 endpoint PCR. RAMP-1 mRNA expression in seven PaCa cell lines with bands at 193 base pairs (BP) representing RAMP-1. CGRP cells were used as a positive control and water was used as a negative control as it has no DNA template. The data shown is representative of three independent experimental repeats.

(A)

PREDICTED: Homo sapiens receptor activity modifying protein 1 (RAMP1), transcript variant X3, mRNA

Sequence ID: XM_017003156.2 Length: 1002 Number of Matches: 1

Range 1: 540 to 650 GenBank Graphics Next Match Previous Match

Score	Expect	Identities	Gaps	Strand
100 bits(110)	1e-17	85/111(77%)	1/111(0%)	Plus/Plus

```
Query  31   ATCTCANGCANGGCCGNGCGGNACCNNCCCGGCA-CAACNTCNACCCCTTCATCNTGNTC  89
            |||||| ||| ||||| |||| |||  ||||||| || | || |||||||||| || ||
Sbjct  540  ATCTCAGGCAGGGCCGTGCGGGACCCGCCCGGCAGCATCCTCTACCCCTTCATCGTGGTC  599

Query  90   NCCATCNNNGTGACACTGCTGGTNACNGCANTNGTGGNCNNGCACAGCNAG  140
             |||||   ||||| |||||||| || ||| | |||| |  ||| ||| ||
Sbjct  600  CCCATCACGGTGACCCTGCTGGTGACGGCACTGGTGGTCTGGCAGAGCAAG  650
```

(B)

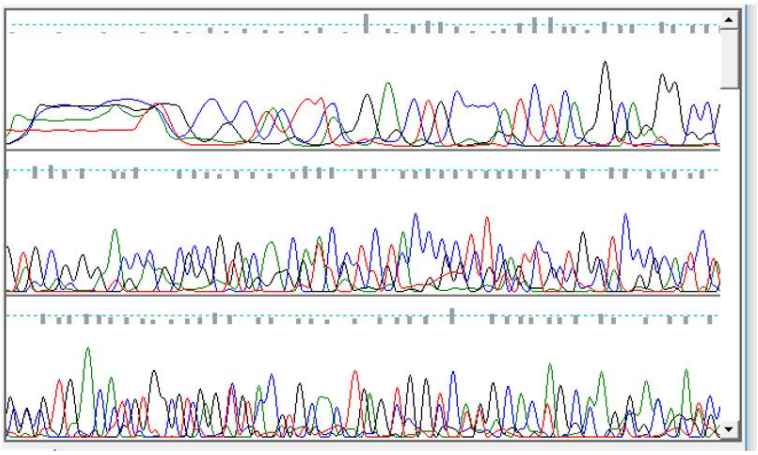

Figure 3.4 RAMP-1 sequencing data from CFPAC-1 PaCa RNA sample. **(A)** NCBI Blast alignment was used to identify the sequence obtained from FinchTV software after Sanger sequencing was completed on PCR sample **(B)** FinchTV software was used to identify the sequence in the sample and determine if the band at a height of 193 BP in Figure 3.3 correlated to RAMP-1 expression using NCBI Blast alignment.

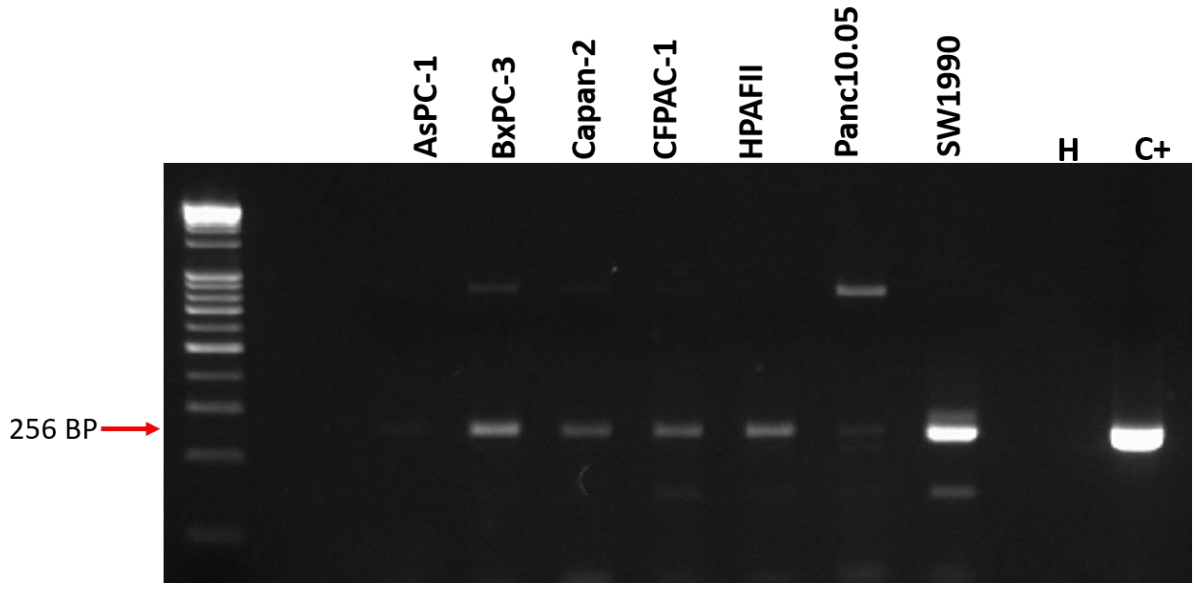

Figure 3.5 RAMP-2 endpoint PCR. RAMP-2 mRNA expression in seven PaCa cell lines with bands at 256 base pairs (BP) representing RAMP-2. AM1 cells were used as a positive control and water was used as a negative control as it has no DNA template. The data shown is representative of three independent experimental repeats.

(A)

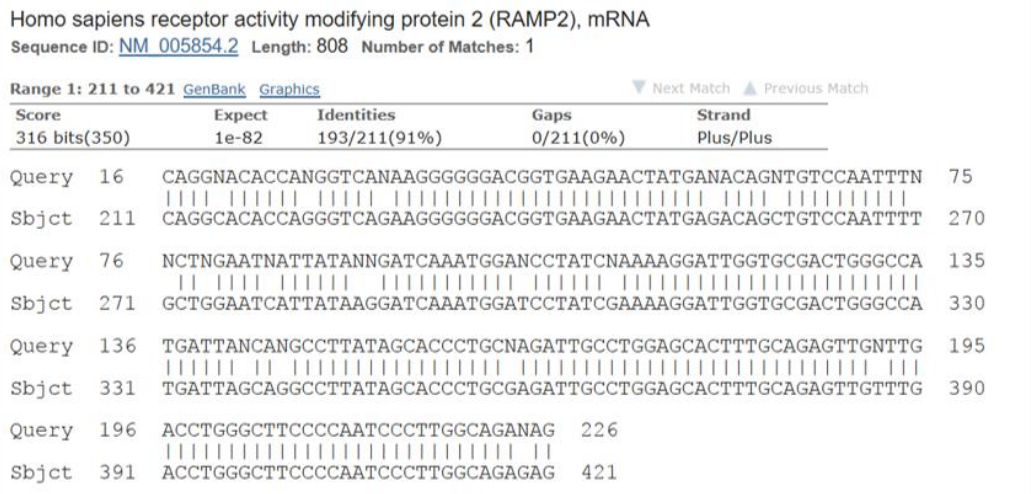

Homo sapiens receptor activity modifying protein 2 (RAMP2), mRNA

Sequence ID: NM_005854.2 Length: 808 Number of Matches: 1

Range 1: 211 to 421 GenBank Graphics Next Match Previous Match

Score	Expect	Identities	Gaps	Strand
316 bits(350)	1e-82	193/211(91%)	0/211(0%)	Plus/Plus

```
Query  16   CAGGNACACCANGGTCANAAGGGGGGACGGTGAAGAACTATGANACAGNTGTCCAATTTN  75
            ||||  ||||||  |||||  ||||||||||||||||||||||  ||||  ||||||||||
Sbjct  211  CAGGCACACCAGGGTCAGAAGGGGGGACGGTGAAGAACTATGAGACAGCTGTCCAATTTT  270

Query  76   NCTNGAATNATTATANNGATCAAATGGANCCTATCNAAAAGGATTGGTGCGACTGGGCCA  135
            ||  ||||  ||||||  ||||||||||  ||||||  ||||||||||||||||||||||
Sbjct  271  GCTGGAATCATTATAAGGATCAAATGGATCCTATCGAAAAGGATTGGTGCGACTGGGCCA  330

Query  136  TGATTANCANGCCTTATAGCACCCTGCNAGATTGCCTGGAGCACTTTGCAGAGTTGNTTG  195
            ||||||  ||  ||||||||||||||||  ||||||||||||||||||||||||||| |||
Sbjct  331  TGATTAGCAGGCCTTATAGCACCCTGCGAGATTGCCTGGAGCACTTTGCAGAGTTGTTTG  390

Query  196  ACCTGGGCTTCCCCAATCCCTTGGCAGANAG  226
            ||||||||||||||||||||||||||||  ||
Sbjct  391  ACCTGGGCTTCCCCAATCCCTTGGCAGAGAG  421
```

(B)

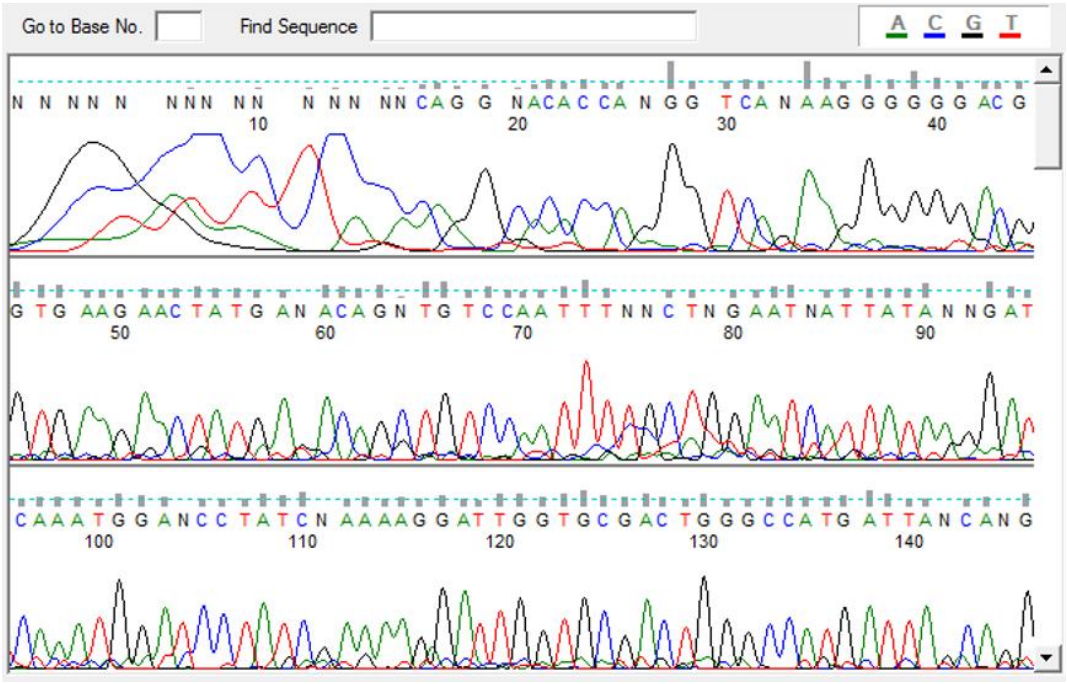

Figure 3.6 RAMP-2 sequencing. RAMP-2 sequencing data from CFPAC-1 PaCa RNA sample. **(A)** NCBI Blast alignment was used to identify the sequence obtained from FinchTV software after Sanger sequencing was completed on PCR sample **(B)** FinchTV software was used to identify the sequence in

the sample and determine if the band at a height of 256 BP in Figure 3.5 correlated to RAMP-2 expression using NCBI Blast alignment.

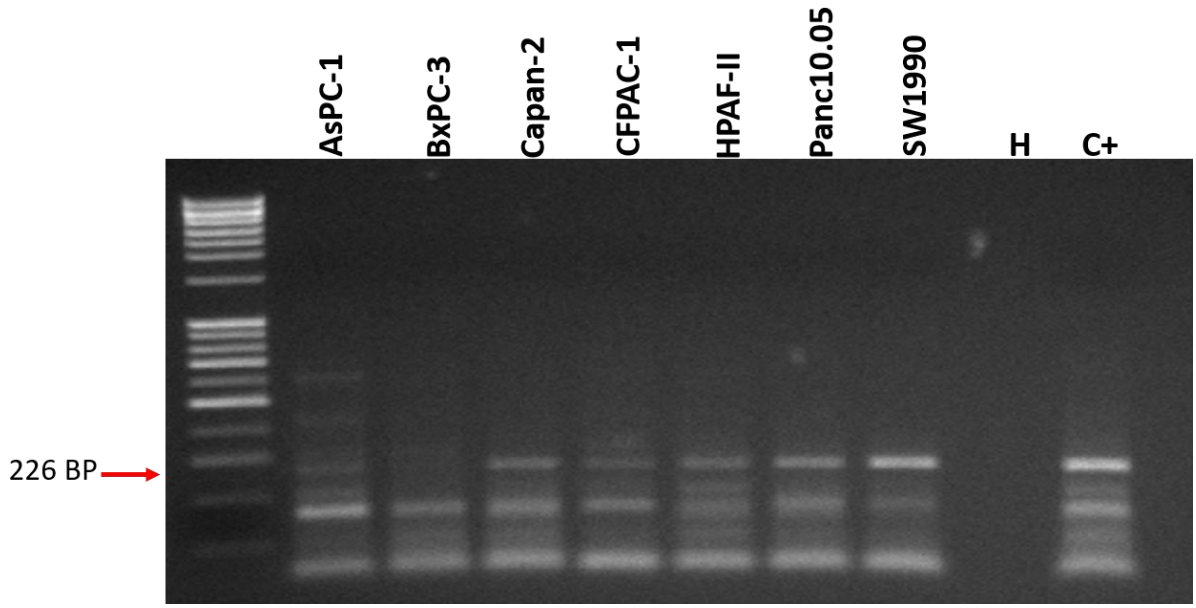

Figure 3.7 RAMP-3 endpoint PCR. RAMP-3 mRNA expression in seven PaCa cell lines with bands at 226 base pairs (BP) representing RAMP-3. AM2 cells were used as a positive control and water was used as a negative control as it has no DNA template. The data shown is representative of three independent experimental repeats.

(A)

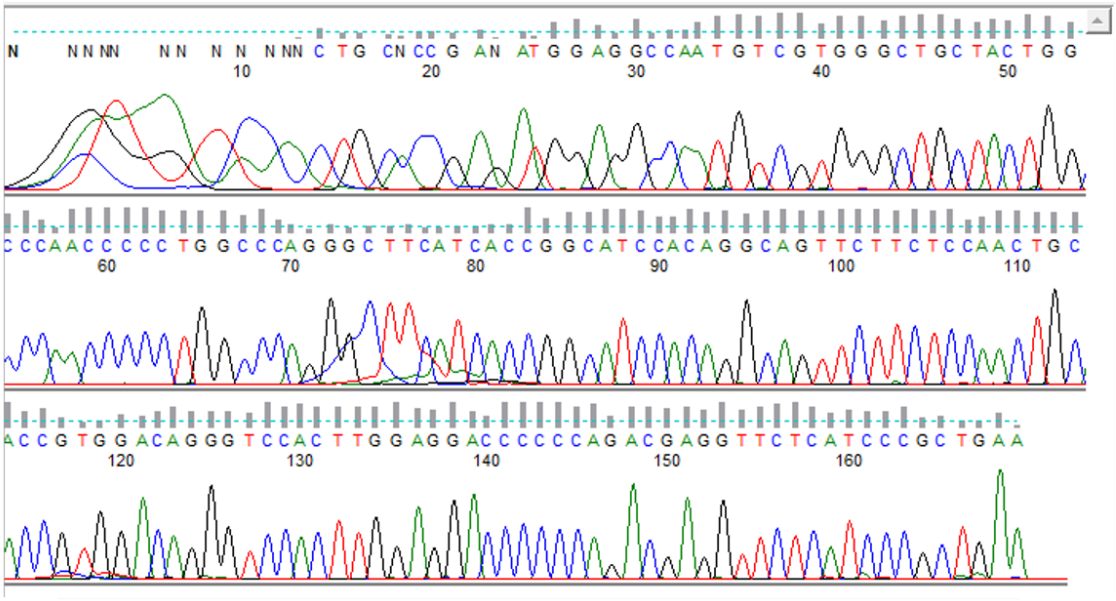

(B)

Homo sapiens receptor activity modifying protein 3 (RAMP3), mRNA

Sequence ID: NM_005856.3 **Length:** 1323 **Number of Matches:** 1

Range 1: 251 to 405 GenBank Graphics ▼ Next Match ▲ Prev

Score	Expect	Identities	Gaps	Strand
273 bits(302)	2e-69	153/155(99%)	0/155(0%)	Plus/Plus

```
Query  14   CTGCNCCGANATGGAGGCCAATGTCGTGGGCTGCTACTGGCCCAACCCCCTGGCCCAGGG  73
            |||| |||| ||||||||||||||||||||||||||||||||||||||||||||||||||
Sbjct  251  CTGCACCGAGATGGAGGCCAATGTCGTGGGCTGCTACTGGCCCAACCCCCTGGCCCAGGG  310

Query  74   CTTCATCACCGGCATCCACAGGCAGTTCTTCTCCAACTGCACCGTGGACAGGGTCCACTT  133
            ||||||||||||||||||||||||||||||||||||||||||||||||||||||||||||
Sbjct  311  CTTCATCACCGGCATCCACAGGCAGTTCTTCTCCAACTGCACCGTGGACAGGGTCCACTT  370

Query  134  GGAGGACCCCCCAGACGAGGTTCTCATCCCGCTGA  168
            |||||||||||||||||||||||||||||||||
Sbjct  371  GGAGGACCCCCCAGACGAGGTTCTCATCCCGCTGA  405
```

Figure 3.8 RAMP-3 sequencing. RAMP-3 sequencing data from CFPAC-1 PaCa RNA sample. **(A)** NCBI Blast alignment was used to identify the sequence obtained from FinchTV software after Sanger sequencing was completed on PCR sample **(B)** FinchTV software was used to identify the sequence in the sample and determine if the band at a height of 226 BP in Figure 3.7 correlated to RAMP-3 expression using NCBI Blast alignment.

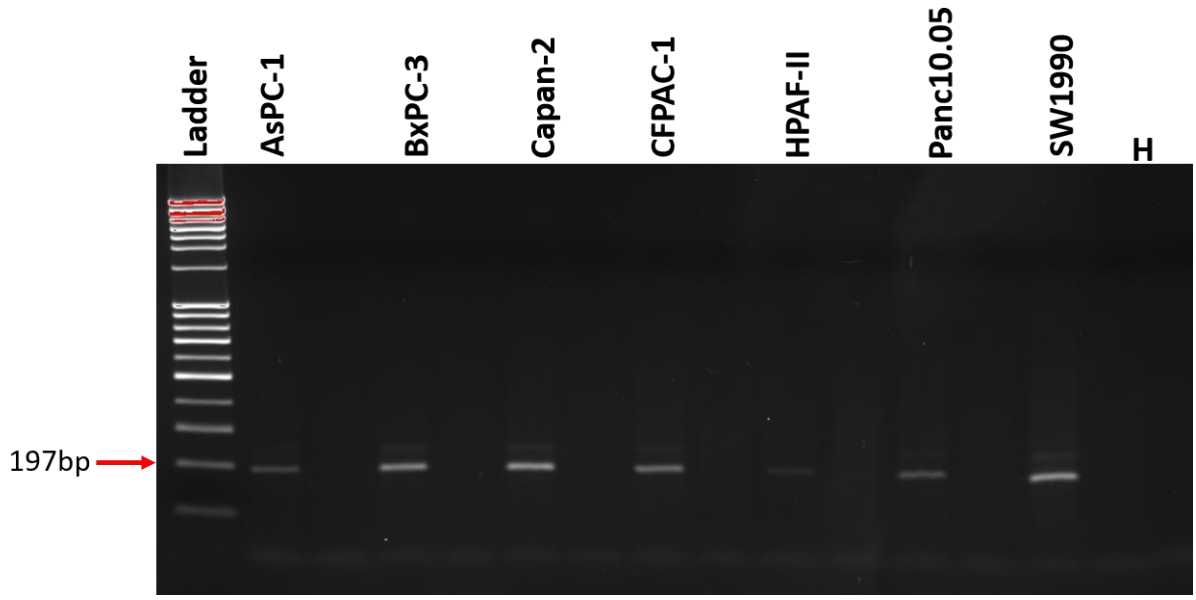

Figure 3.9 ADM endpoint PCR. ADM mRNA expression in seven PaCa cell lines with bands at 197 base pairs (BP) representing ADM. AM2 cells were used as a positive control and water was used as a negative control as it has no DNA template. The data shown is representative of three independent experimental repeats.

(A)

Homo sapiens adrenomedullin (ADM), mRNA

Sequence ID: NM_001124.2 Length: 1606 Number of Matches: 2

Range 1: 338 to 489 GenBank Graphics ▼ Next Match ▲ Previous Match

Score	Expect	Identities	Gaps	Strand
264 bits(292)	8e-67	149/152(98%)	0/152(0%)	Plus/Plus

```
Query  16   CGGTTGGATGTCGCGTCGGAGTTTCGAAAGAAGTGGAATAAGTGGGCTCTGAGTCGTGGG  75
            ||||||||||||||||||||||||||||||||||||||||||||||||||||||||||||
Sbjct  338  CGGTTGGATGTCGCGTCGGAGTTTCGAAAGAAGTGGAATAAGTGGGCTCTGAGTCGTGGG  397

Query  76   NNGAGGGAACTGCGGATGTCCAGCAGCTACCCCACCGGGCTCGCTGACGTGAAGGCCGGG  135
             ||||||||||||||||||||||||||||||||||||||||||||||||||||||||||||
Sbjct  398  AAGAGGGAACTGCGGATGTCCAGCAGCTACCCCACCGGGCTCGCTGACGTGAAGGCCGGG  457

Query  136  CCTGCCCAGACCCTTATTCGGCCCNAGGACAT  167
            |||||||||||||||||||||| |||||||
Sbjct  458  CCTGCCCAGACCCTTATTCGGCCCCAGGACAT  489
```

Range 2: 370 to 396 GenBank Graphics ▼ Next Match ▲ Previous Match ▲ First Match

Score	Expect	Identities	Gaps	Strand
42.8 bits(46)	4.8	25/27(93%)	0/27(0%)	Plus/Plus

```
Query  198  GTGGAATAAGTGGGCTCTGNGTCGNGG  224
            |||||||||||||||||| |||| ||
Sbjct  370  GTGGAATAAGTGGGCTCTGAGTCGTGG  396
```

(B)

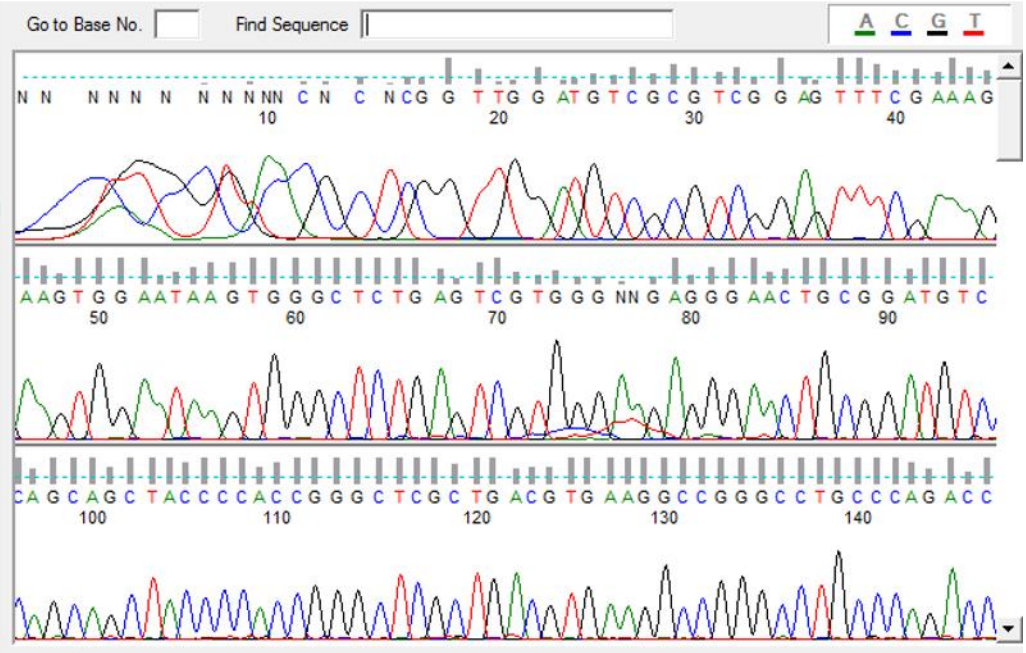

Figure 3.10 ADM sequencing. ADM sequencing data from CFPAC-1 PaCa RNA sample. **(A)** NCBI Blast alignment was used to identify the sequence obtained from FinchTV software after Sanger sequencing was completed on PCR sample **(B)** FinchTV software was used to identify the sequence in the sample and determine if the band at 196 BP in Figure 3.9 correlated to ADM expression using NCBI Blast alignment.

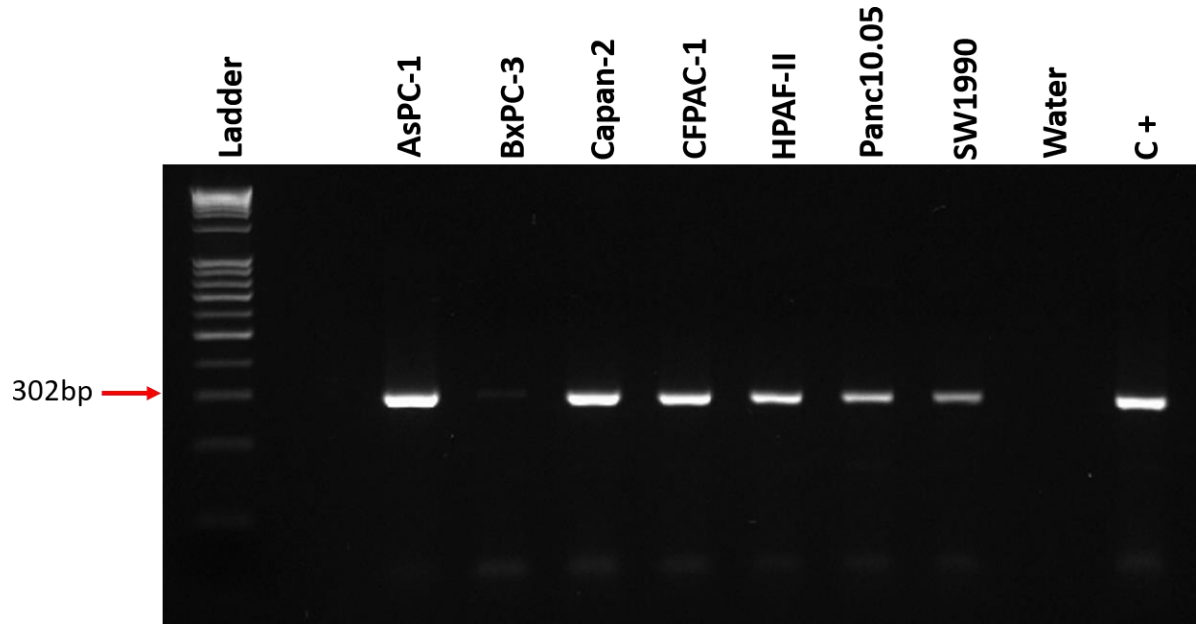

Figure 3.11 CLR endpoint PCR. CLR mRNA expression in seven PaCa cell lines with bands at 302 base pairs (BP) representing CLR. AM2 cells were used as a positive control and water was used as a negative control as it has no DNA template. The data shown is representative of three independent experimental repeats.

(A)

Homo sapiens calcitonin receptor like receptor (CALCRL), transcript variant 1, mRNA

Sequence ID: NM_005795.5 Length: 6155 Number of Matches: 1

Range 1: 1373 to 1621 GenBank Graphics ▼ Next Match ▲ Previous Match

Score	Expect	Identities	Gaps	Strand
421 bits(466)	6e-114	241/249(97%)	0/249(0%)	Plus/Plus

```
Query  25    CTTATATTACAATGACAATTGCTGGATCAGTTCTGATACCCATCTCCNCNNCNTTATCCA  84
             ||||||||||||||||||||||||||||||||||||||||||||||| |   | |||||||
Sbjct  1373  CTTATATTACAATGACAATTGCTGGATCAGTTCTGATACCCATCTCCTCTACATTATCCA  1432

Query  85    TGGCCCAATTTGTGCTGCTTTACTGGTGAATCttttttttCTTGTTAAATATTGTACGCGT  144
             ||||||||||||||||||||||||||||||||||||||||||||||||||||||||||||
Sbjct  1433  TGGCCCAATTTGTGCTGCTTTACTGGTGAATCTTTTTTTCTTGTTAAATATTGTACGCGT  1492

Query  145   TCTCNTCACCAAGTTAAAAGTTACACACCAAGCGGAATCCAATCTGTACATGAAAGCTGT  204
             |||| ||||||||||||||||||||||||||||||||||||||||||||||||||||||||
Sbjct  1493  TCTCATCACCAAGTTAAAAGTTACACACCAAGCGGAATCCAATCTGTACATGAAAGCTGT  1552

Query  205   GAGAGCTACTCTTATCTTGGTGCCATTGCTTGGCATTGAATTTGNGCTGATTCCATGGCN  264
             |||||||||||||||||||||||||||||||||||||||||||| ||||||||||||||
Sbjct  1553  GAGAGCTACTCTTATCTTGGTGCCATTGCTTGGCATTGAATTTGTGCTGATTCCATGGCG  1612

Query  265   ANCTGAAGG  273
             | |||||||
Sbjct  1613  ACCTGAAGG  1621
```

(B)

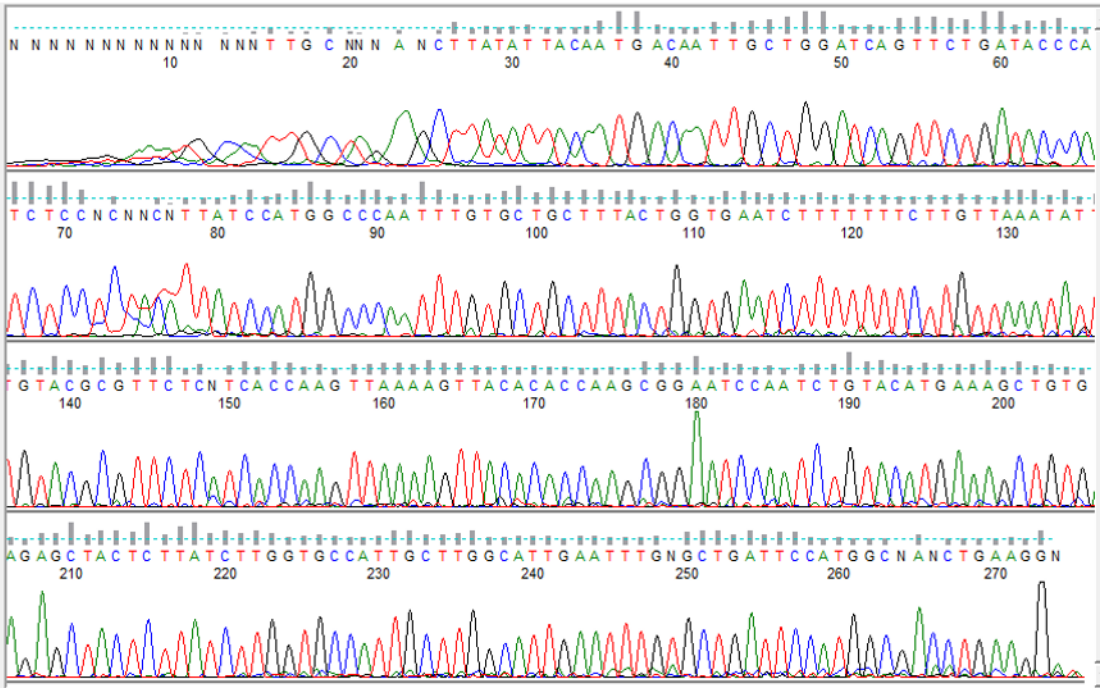

Figure 3.12 CLR sequencing. CLR sequencing data from CFPAC-1 PaCa RNA sample. (A) NCBI Blast alignment was used to identify the sequence obtained from FinchTV software after Sanger sequencing was completed on PCR sample (B) FinchTV software was used to identify the sequence in the sample and determine if the band at a height of 302 BP in Figure 3.11 correlated to CLR expression using NCBI Blast alignment.

Table 3.5 ADM and RAMP-1 mRNA expression in seven PaCa cell lines detected by quantitative real-time polymerase chain reaction (QPCR). Data is presented as 3 independent experimental repeats and presented as mean±SD.

Cell line	ADM Ct value	RAMP-1 Ct value
AsPC-1	23.5±0.61	24.0±1.27
BxPC-3	22.5±0.58	26.8±0.42
Capan-2	23.5±1.06	27.5±1.06
CFPAC-1	23.1±0.74	23.3±1.56
HPAF-II	24.4±1.91	23.0±0.21
Panc 10.05	22.9±0.82	24.9±1.77
SW1990	26.0±1.26	26.6±0.11

Ct: Cycle threshold. This is the number of cycles required for the fluorescent signal to cross the background fluorescent threshold.

3.3.3 Protein expression of RAMPs

The expression of RAMP-1, RAMP-2 and RAMP-3 was also determined at protein level in the seven PaCa cell lines. RAMP-1 was expressed across all the cell lines as shown by the band at 17 kDa (Figure 3.13). RAMP-2 was also expressed in all cell lines with a single band at 17 kDa. The strongest band was in BxPC-3 (Figure 3.14). Figure 3.15 shows RAMP-3 expression in all cell lines with a band at 34 kDa (RAMP-3 dimer). These results show that all the RAMPs are expressed at protein level across the 7 different PaCa cell lines.

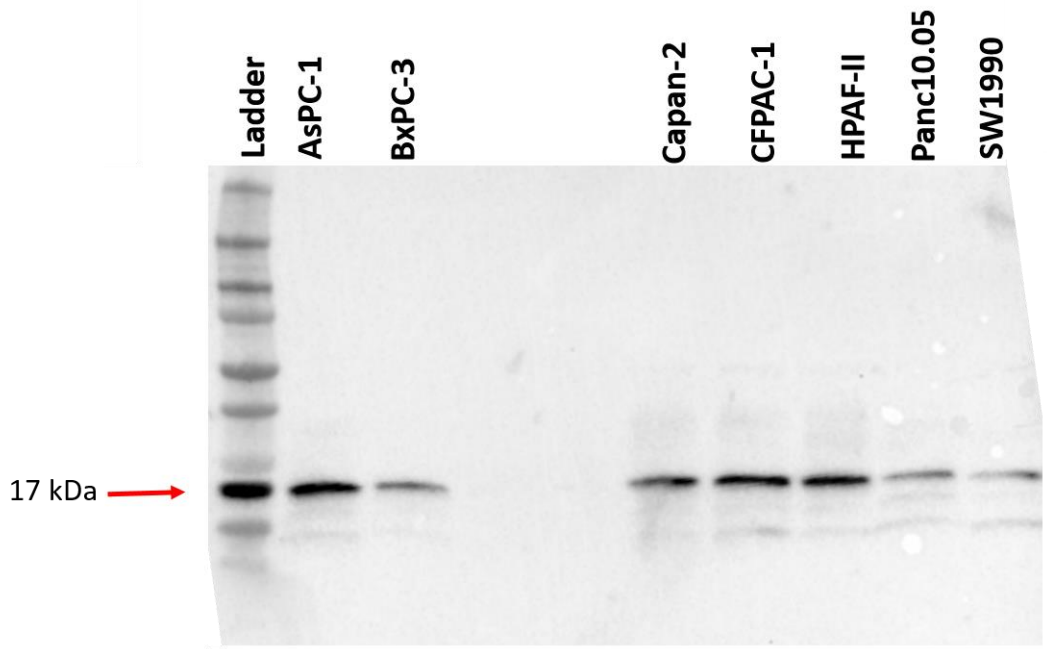

Figure 3.13 RAMP-1 protein expression determined by western blotting. RAMP-1 protein expression in seven PaCa cell lines with bands at 17 kDa representing RAMP-1. The data shown is representative of three independent experimental repeats.

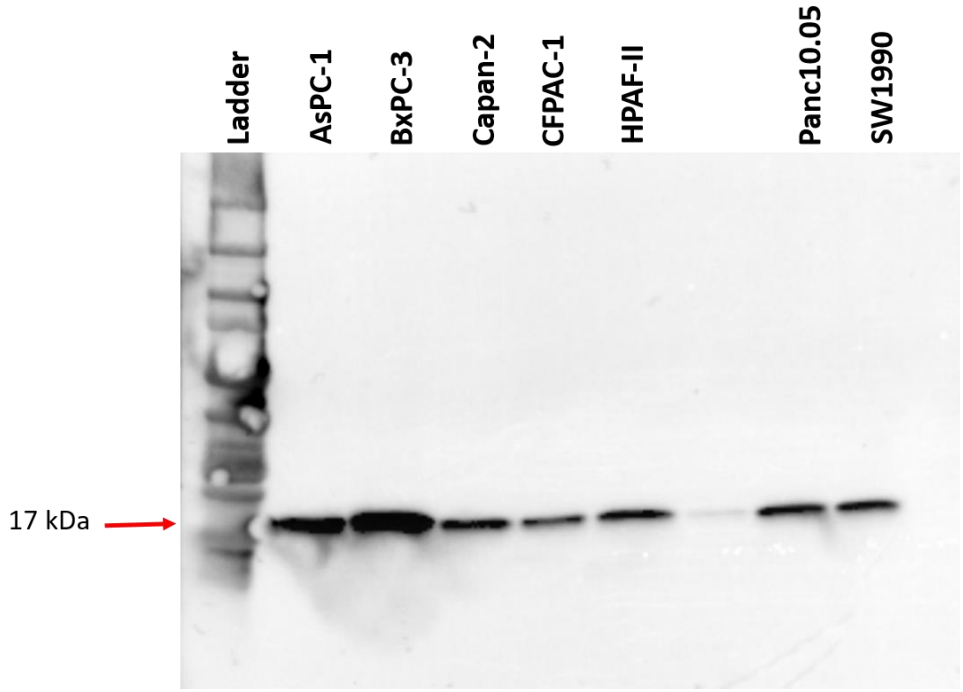

Figure 3.14 RAMP-2 protein expression determined by western blotting. RAMP-2 protein expression in seven PaCa cell lines with bands at 17 kDa representing RAMP-2. The data shown is representative of three independent experimental repeats.

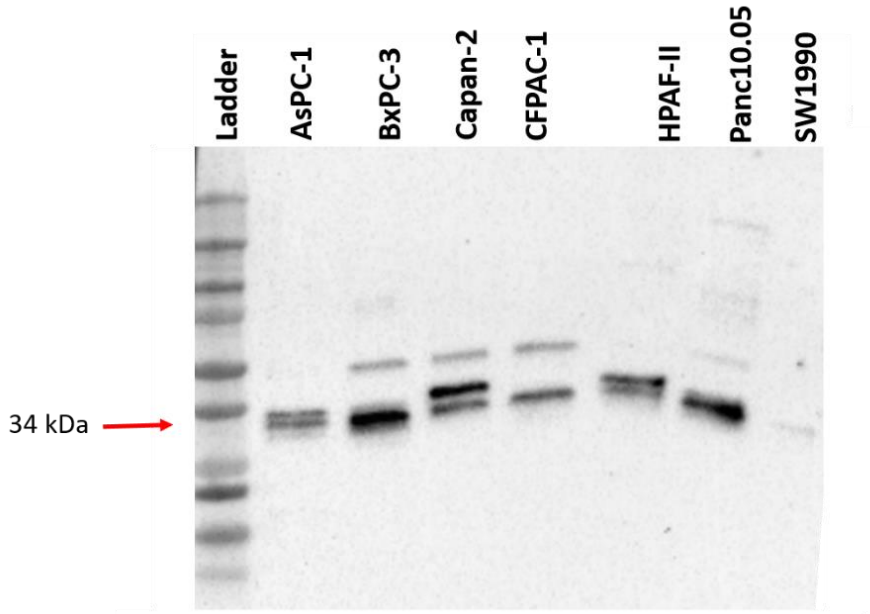

Figure 3.15 RAMP-3 protein expression determined by western blotting. RAMP-3 protein expression in seven PaCa cell lines with bands at 34 kDa representing RAMP-3. The data shown is representative of three independent experimental repeats.

3.3.4 Stimulation of PaCa cells with calcitonin superfamily

To determine if the cell lines are functional in the 7 PaCa cell lines, cAMP assays were completed. These were important to inform which cell lines would be used to develop ADM and RAMP-3 KDs (Chapter 4). Figure 3.16 shows the response of PaCa cell lines when stimulated by ADM, CGRP and IMD when stimulated at concentrations between 1 µM and 10 pM. Six out of the seven cell lines were stimulated by CGRP with EC_{50} doses ranging between 3.43 nM and 57.1 nM. CGRP stimulation efficacy varied between 20-100% when normalised to forskolin. Five out of the cell lines were stimulated by ADM with EC_{50} ranging between 288 nM and 682 nM, the efficacy ranged between 40-

100%. IMD also stimulated cAMP production in five out of the seven cell lines. SW1990 was not stimulated by any of ligands.

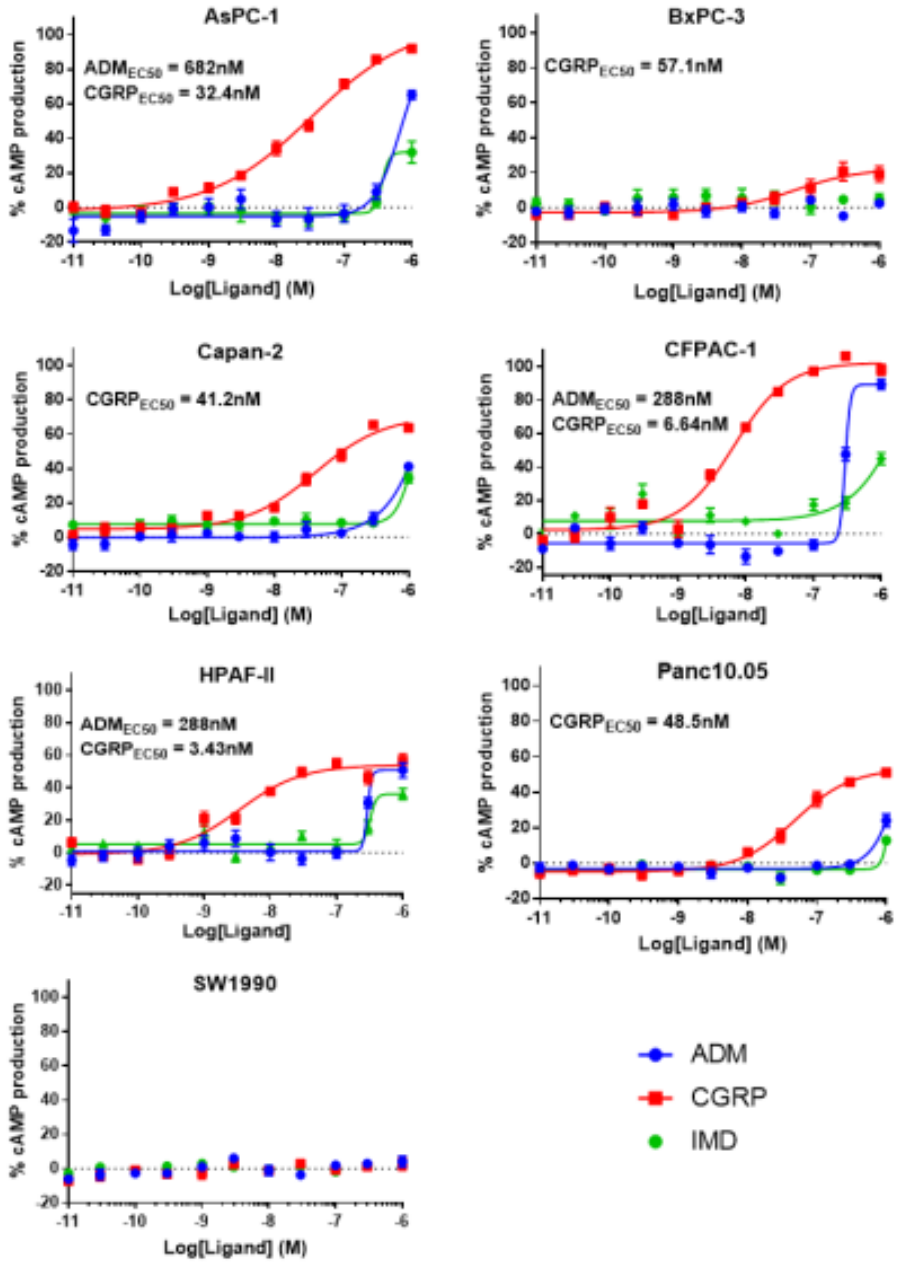

Figure 3.16 Effect of calcitonin peptides (ADM, CGRP, IMD) on cAMP production of seven PaCa cell lines. Cells were stimulated for 30 minutes with different concentrations of peptide and cAMP levels were measured. SW1990 cells were not stimulated by the peptide concentrations prepared. BxPC-3 was stimulated by CGRP, and the remainder of cells were stimulated at different potencies and

efficacies by all peptides. These data were collected as three independent repeats and presented as mean ±SEM. The data was normalised to 100 µM forskolin and blank representing 100% and 0% stimulation respectively. Dose response curves were analysed using four-parameter logistic curve and only unambiguous EC_{50} values are shown. This experiment and data was completed by Dr Ameera Jailani and was presented in her thesis (March 2019).

3.4 Discussion

ADM and its receptor components (CLR, RAMP-1, RAMP-2 and RAMP-3) have been previously shown to be expressed in PaCa and other cancer cell lines including prostate cancer, colorectal cancer, endometrial cancer and glioblastomas. Furthermore, these studies have shown ADM to induce pro-tumorigenic effects including proliferation, inhibiting apoptosis and immunosuppression (Abasolo, et al., 2004; Berenguer-Daizé et al., 2013; Berenguer et al., 2008; Ishikawa et al., 2003; Keleg et al., 2007; Oehler et al., 2003; Ouafik et al., 2002; Wang et al., 2014). These studies provide the basis for investigating the role of ADM and its receptor components in the PaCa. Therefore, a panel of 7 PaCa cell lines were characterised at mRNA and protein to determine whether ADM, CLR, RAMP-1, RAMP-2 and RAMP-3 are expressed in PaCa as this has not previously been done. Furthermore, cAMP data was collected to determine whether the cell lines had functional receptors. These experiments and data were important to determine subsequent experiments shown in chapter 4 to chapter 6.

3.4.1 PaCa cell line morphology

Understanding the characteristics of PaCa cell lines was important to determine the most suitable cell lines to generate ADM and RAMP-3 knockdowns for both *in vivo* and *in vitro* assays. Therefore, a panel of 7 PaCa cell lines were analysed for morphology, ADM and its receptor mRNA and protein expression and cAMP stimulation by ADM and calcitonin superfamily peptides.

The cell lines can be subdivided by multiple characteristics including, cobblestone appearance, epithelial appearance, polygonal, elongated or round cells, mononuclear or multinucleated. The majority of the cells appear to have a cobblestone epithelial appearance, with the exception of CFPAC-1 and AsPC-1. CFPAC-1 in particular has a more mesenchymal appearance with elongated and round cells, AsPC-1 has some of these characteristics but presented more subtly. These cells also grow in a more disorganised pattern. Capan-2, Panc 10.05 and SW1990 all have polygonal shapes, whilst BxPC-3 cells have a more distinct round shape. HPAF-II are pleomorphic with a mix of polygonal and round shapes (Figure 3.2).

Distinguishing between epithelial and mesenchymal morphologies of cells can be indicative of cell line characteristics. Epithelial cells are more rounded and have previously been shown to express more E-cadherin and low vimentin, whilst mesenchymal cells have been associated with high expression of vimentin and low expression of E-cadherin. Both these markers are important markers of epithelial-to-mesenchymal transition (EMT) which can lead to metastases. Minami *et al* (2021) showed that low E-cadherin expression in two PaCa cell lines (Panc-1 and KP4) correlated with a more mesenchymal appearance including more elongated and spindle shaped cells. These cell lines also had more invasive capacities. Mesenchymal cells also have increased migratory capacity, resistance to apoptosis and increased expression of ECM components which aids in the development of fibrosis around PaCa tumours (Kalluri & Neilson., 2016). Both AsPC-1 and CFPAC-1 are metastatic derived cell lines therefore, their mesenchymal cell appearance correlates with their metastatic status. However, HPAF-II and SW1990 cells are also metastatic cell lines and have more epithelial features with round and polygonal cells suggesting spindle shaped mesenchymal cells do not necessarily correlate with metastatic potential of cells. Dai *et al* (2020) and Zhou *et al* (2015) have both shown the involvement of ADM and RAMP-3 in EMT. Dai *et al* (2020) showed that RAMP-3 KOs in PAN02 cells resulted in decreased vimentin expression and migratory capacity. Zhou *et al* (2015) showed that ADM KDs in chollangiocellular carcinoma resulted in reversal of EMT.

Cells can also be characterised as mononuclear or multinucleated; HPAF-II, Panc 10.05 and SW1990 have a mix of mononuclear and multinucleated cells, whilst ASPC-1 cells present as mononuclear. There are also two distinct patterms that the cells grow in, *in vitro*, either as a single monolayer covering all space or in clusters with large empty spaces. ASPC-1, BxPC-3, CFPAC-1 and SW1990 all grow as a single monolayer with no spaces in between. However, Capan-2, HPAF-II and Panc 10.05 all grow as clusters with large empty spaces between. Hasegawa *et al* (2017) have shown that metastatic PaCa cells contained more multinucleated cells compared to primary tumour cells. HPAF-II and SW1990 cells are both metastatic derived cell lines and showed multinucleated cell

morphologies therefore, although the cells do not have a mesenchymal appearance, their metastastic potential may be driven by multinucleated cells.

3.4.2 PaCa cell lines express ADM and its receptor components

It was essential to characterise the panel of the seven PaCa cell lines for both ADM and its receptor components (RAMP-1, RAMP-2, RAMP-3 and CLR) to select appropriate cell lines for ADM and RAMP-3 knockdown development. Endpoint PCR, QPCR and western blots confirmed expression of ADM, RAMPs and CLR in all the cell lines cultured under optimal conditions at both mRNA and protein level (only RAMPs were characterised at protein level). These data were significant as they confirmed that ADM and its receptors may play a role in PaCa development.

Although the data presented and other studies researching mRNA expression of ADM, RAMP and CLR expression in glioblastomas, ovarian cancer, renal cancers and prostate cancer all show mRNA and protein expression of RAMP-3 (Berenguer-Daizé et al., 2013; Deville et al., 2009; Giacalone et al., 2003; Ouafik et al., 2002), current PaCa cancer research shows limited evidence of RAMP-3 expression. Ishikawa *et al* (2003) studied 5 PaCa cell lines and showed ADM mRNA expression in all the cell lines however, there was no RAMP-3 mRNA expression in any of the cell lines including BxPC-3 which is also shown in Figure 3.7. However, they did show that BxPC-3 expresses CLR and RAMP-2 similar to Figure 3.5 and Figure 3.11 together with another PaCa cell line, PCI-35. Two other cell lines expressed only RAMP-2 alone and another cell line expressed only ADM alone but none of the CLR/RAMP receptor components. Keleg *et al* (2007) measured mRNA expression in 5 PaCa cell lines and found them all to express ADM, CLR, RAMP-1 and RAMP-2 however, only one cell line expressed RAMP-3. Furthermore, analysis of PaCa tissue showed co-localisation of CLR with RAMP-1 and RAMP-2 in tissue but no RAMP-3. Ramachandran *et al* (2007) also analysed mRNA expression in 8 cell lines including BxPC-3, AsPC-1 and CFPAC-1 finding that all expressed ADM but there was no evidence of CLR or RAMP-3 expression. BxPC-3 did express RAMP-1 and RAMP-2 which mimics the results shown in Figure 3.3, Table 3.5 and Figure 3.5. However what is clear from the literature is

that RAMP-3 expression is more prevalent in cells that infiltrate the tumour as demonstrated by Chen *et al* (2011), Dai *et al* (2020), Kaafarani *et al* (2009), Xu *et al* (2016) Deville *et al* (2009) and Ramachandran *et al* (2007).

In melanoma, Chen *et al* (2011) showed that CLR was expressed in melanoma cells but RAMP-2 and RAMP-3 were not. However, infiltrating TAMs expressed ADM, CLR, RAMP-2 and RAMP-3 and co-localisation of ADM and the RAMP/CLR complexes was also found in macrophages. Furthermore, melanoma cells treated *in vivo* treated with ADM receptor antagonist showed a decreased percentage of M2 phenotype macrophages. In renal cell carcinoma, Deville *et al* (2009) showed that RAMP-3 was only expressed in inflammatory cells that were infiltrating the tumours suggesting that RAMP-3 may play an important role in the crosstalk between tumour cells and infiltrating cells.

Whilst, Kaafarani *et al* (2009) showed that CLR/RAMP-2 and CLR/RAMP-3 promote ADM in matrigel plugs to induce angiogenesis by promoting the recruitment of pericytes, endothelial cells, myeloid precursor cells and macrophages which work together to promote channel formation. Ramachandran *et al* (2007) revealed that ADM and its receptors interact with cells of the stromal microenvironment (CAFs and HUVECs) to induce pro-tumorigenic effects.

Xu *et al* (2016) showed PaCa cells secreted high levels of ADM however, receptors for ADM were only found on MMC cells. ADM enhanced MMC cell invasion and migration and promoted adhesion and transendothelial migration of MMC cells by increasing VCAM-1 and ICAM-1 expression in endothelial cells. These molecules work together to promote EMT and create a more aggressive phenotype. Furthermore, ADM had an impact on macrophages and myeloid derived suppressor cells (MDSC) by promoting expression of a more pro-tumour phenotype. These data combined with Dai *et al* (2020) research that provides evidence that RAMP-3 has a key role in promoting metastasis in PaCa by increasing expression of RAMP-3 in CAFs, show that ADM and RAMP-3 work synergistically to integrate the complex network of molecules that form the PaCa tumour microenvironment. In

future, research around expression of ADM and its receptors in cells found in the PaCa tumour microenvironment may be a field of research to consider.

There are few studies describing the characterisation of cell lines for RAMPs and CLR at protein level using western blotting. The data shown in Section 3.3.3 shows bands at 17 kDa (monomer) across the panel of seven PaCa cell lines for RAMP-1 and RAMP-2. RAMP-3 expression is shown as a dimer with a band at 34 kDa, this blot also shows multiple other uncharacterised bands. Berenguer-Daizé *et al* (2013) have shown protein expression of CLR, RAMP-2 and RAMP-3 in DU145 cells with a band at 48 kDa (CLR) and 28 kDa (RAMP-2 and RAMP-3) and additional bands at 50 kDa and 73 kDa which they suggest are homo- and hetero- dimers. However, there is limited western blot data characterising PaCa cells or other cancer cell available. Hay & Pioszak (2016) suggest that there are few antibodies available that have undergone rigorous testing and what is often assumed as a homodimer and heterodimer has been shown to artifact. These data suggest that more research needs to be done into developing antibodies specific to ADM and its receptor components to be sure that the bands seen correlate to the proteins.

It is important to consider the different RAMP-2 and RAMP-3 mRNA expression data collected by endpoint PCR and QPCR. Endpoint PCR data shows that the PaCa cell lines express both RAMP-2 and RAMP-3 however, QPCR data only showed expression of RAMP-2 and RAMP-3 in AM1 and AM2 controls. QPCR is a method that detects mRNA in the exponential phase of PCR, whilst endpoint PCR detects mRNA in the plateau phase of PCR. Therefore, if expression of RAMP-2 and RAMP-3 is low (RAMP-3 endpoint PCR cycle number was of 40), then QPCR may not detect mRNA expression. To date, there is still no set maximum cycle number that is used for mRNA detection in QPCR and there is much debate over which cycle numbers detect false positives. Too low cycle cut-off points may not detect true positive numbers whilst too high cycle numbers (50-60 cycles) may detect false positives (Burns et al, 2005; Burns & Valdivia, 2008; Bustin et al., 2009). The Applied Biosystems 7900 HT Fast Real-Time PCR instrument used to collect RAMP-2 and RAMP-3 data detected up to 39 cycles,

anything above was classed as 'undetermined'. Increasing the cycle number may have detected RAMP-2 and RAMP-3, particularly as RAMP-3 required a minimum of 40 cycles for detection by endpoint PCR. However, at 40 cycles the RAMP-3 endpoint PCR detected non-specific bands. It has been suggested that too many cycles can increase error and result in multiple band detection following gel electrophoresis (Figure 3.7). The concentration of primer was also higher in the RAMP-3 mastermix which could have caused primer dimers. Furthermore, this may explain why BxPC-3 samples showed no RAMP-3 expression, a higher cycle number may have detected expression however, this may have resulted in further non-specific bands (Figure 3,7). Sequencing the lower molecular weight in future would help determine other genes being detected. The concentration of primer was also higher in the RAMP-3 mastermix which can also cause primer dimers. $MgCl_2$ concentration, addition of DMSO, increasing primer concentration and altering annealing temperatures were optimised to try and produce single band gels. However, expression of RAMP-3 was confirmed by sequencing which suggests RAMP-3 is expressed at mRNA level in the seven PaCa cell lines (Figure 3.8). Furthermore, western blotting confirmed the expression of RAMP-2 and RAMP-3 (Figure 3.14 and Figure 3.15) which suggests the 7 PaCa cell lines express mature protein.

Another important consideration is the presence of multiple bands following RAMP-2 endpoint PCR shown in Figure 3.5, BxPC-3 and Panc 10.05 samples showed higher bands. RAMP-2 primers were not designed across intron-exon boundaries as primers that crossed these boundaries did not have a suitable GC content (40-60%), annealing temperature or primer length (18-30bp). Designing primers that cross intron-exon boundaries would have confirmed that the higher bands in Figure 3.5 may be as a result of genomic contamination. Lower bands in all RAMP-2 and CLR PCR gels (Figure 3.5 and Figure 3.11 respectively) may be explained by primer dimers which can be caused by too low annealing temperatures or too long extension time.

3.3.3 PaCa cell lines are stimulated by ADM, CGRP and IMD to produce cAMP

Having shown that a panel of 7 PaCa cell lines all express ADM and its receptor components, it was important to determine if the receptor components are functional. Section 1.2.3 outlines the signalling pathways ADM induces that are associated RAMP/CLR receptors including the cAMP pathway (McLatchie et al., 1998). Therefore, cAMP assays were used to determine the functionality of RAMP/CLR receptors. The purpose of these experiments was to identify suitable cell lines to generate ADM and RAMP-3 knockdowns in future for *in vivo* and *in vitro* experiments described in Chapters 5 and 6. The data described in Section 3.3.4 also shows CGRP and IMD ligand data as they can also bind to the same receptor complexes ADM.

Three of the cell lines (AsPC-1, CFPAC-1 and HPAF-II) were stimulated by ADM with CFPAC-1 and HPAF-II being the most potent with a EC_{50} of 288 nM compared to 682 nM in AsPC-1. CFPAC-1 cells were more efficacious with 100% maximum response compared to 60% in HPAF-II. Six of the seven cell lines were stimulated by CGRP with HPAF-II being the most potent at 3.43 nM however it was 60% efficacious compared to CFPAC-1 which was slightly less potent at 6.64 nM but had 100% efficacy. Based on the higher efficacy of ADM and CGRP and confirmed expression of ADM and RAMP-3 at RNA and protein level (RAMP-3 only), CFPAC-1 was selected to generate the ADM and RAMP-3 knockdowns described in Chapter 4.

Based on the characteristics outlined by ATCC, it was the three metastatic cell lines that responded to stimulation by ADM with the exception of SW1990. SW1990 may induce pro-tumorigenic actions through other pathways including MAPK or PI3K kinase pathways. Furthermore, Xu *et al* (2016) showed that SW1990 had the lowest ADM expression which may also explain the lack of stimulation. BxPC-3, Capan-2 and Panc 10.05 are all primary tumours and only showed CGRP stimulation but not ADM. These data suggest that ADM has a role in making tumours metastatic as opposed to being involved in establishing the initial tumour. This is further supported by data on PaCa from Dai *et al* (2020), Ramachandran *et al* (2007) and Xu *et al* (2016) that showed ADM and RAMP-3 roles in

metastasis and their expression in cells found within the tumour microenvironment including TAMs and MMCs cells.

3.5 Conclusion

The morphology of the cell lines was characterised to understand the different characteristics of the cells. This was to ensure that any morphological changes could be recognised which may indicate unhealthy cells *in vitro* together with regular mycoplasma tests. Culture conditions and doubling times had previously been optimised for *in vitro* experiments including RNA and protein collection.

All seven PaCa cell lines were characterised at mRNA and protein level to determine the expression of ADM, CLR and RAMPs. These receptor components were all detected in the seven cell lines and confirmed by sequencing. This data confirmed that ADM and its receptor components may have a role in PaCa progression and therefore, would be a suitable peptide and receptor to investigate further for its stromal and tumorigenic effects.

Six out of seven cell lines were stimulated by calcitonin family peptides (ADM, CGRP and IMD) which suggests that ADM and its receptor components have a functional role PaCa cells. These data suggest ADM mediates downstream signalling pathways of cAMP involved in PaCa progression and development.

CHAPTER 4: KNOCKDOWN CHARACTERISATION AND VALIDATION

4.1 Introduction

The physiological role of ADM and RAMP-3 and their role in cancer have been discussed in depth in Chapters 1 and 3. These chapters highlight the limited understanding of the exact roles of ADM and RAMP-3 in PaCa. However, Dai *et al* (2020) provide a new insight into the roles of these genes and show the value of knockout (KO) studies.

For this study, SMARTvector inducible lentiviral shRNA was chosen to develop knockdowns (KD). This is a highly efficient method of transduction as viral particles are used to infect the cells of interest which results in a KD (explained in Section 4.2.1). This tool enables the switching on and off of knockdowns instead of permanently knocking down which is beneficial in cases where permanent KD may be lethal to cells, or *in vivo* where research scientists may be interested in how tumour growth is effected by switching on and off the inducible gene. Further benefits to lentiviral KDs is that they have a high transduction efficiency and are very scalable for this reason. KOs completely silence the of a gene of interest however, development can be time consuming. They also often require isolating single clones and scaling them up before determining if the KO has been successful by PCR and sequencing. KD and KO studies provide a useful insight into the role of genes in different disease including cancer and their effect on pro-tumorigenic pathways including proliferation, apoptosis and angiogenesis.

In this chapter, Section 4.3.1 will show the development of inducible lentiviral KDs of ADM, RAMP-3 and scrambled controls in CFPAC-1 cells. Whilst Section 4.3.2 will show results of successful transduction of ADM KDs and scrambled control with firefly luciferase (Luc-RFP). The effect of CFPAC-1 ADM KDs and RAMP-3 KDs on proliferation will also be discussed. Development of these KDs will be used for future *in vitro* and *in vivo* experiments discussed in Chapters 5 and 6.

4.1.1 ADM knockdown studies

ADM KDs have been used in numerous studies to investigate cancer and other disease models such as diabetes. Li *et al* (2014) developed ADM KDs and scrambled controls in hepatocellular carcinoma cells,

showing an increase in apoptosis when ADM was knocked down. *In vivo* they combined cisplatin (chemotherapy) with ADM KD in SMMC-7221 cells and showed a 77.2% decrease in tumour growth compared to 39.2% with cisplatin alone showing the therapeutic potential of antagonising ADM in cancer.

Wang *et al* (2014) also analysed the effects of ADM KDs in colorectal cancer tumour xenografts showing a block in angiogenesis, activation of apoptosis and tumour growth suppression. In bladder cancer and osteosarcoma, ADM KDs in cell lines also showed an increase in apoptosis and inhibition of cancer cell proliferation (Dai, et al., 2013; Liu et al., 2013). Angiogenesis has also been shown to be regulated by ADM following KD studies in CAOV3 ovarian cancer cells, where HIF-1α and VEGF mRNA were shown to decrease following ADM KD. These molecules are tightly associated with hypoxia and angiogenesis therefore it was concluded that ADM is an important regulator of this process (Zhang et al., 2017).

Zhou *et al* (2015) were able to show the role of ADM in metastasis in intrahepatic cholangiocellular carcinoma. ADM KDs in these cells resulted in the reversal of EMT which is an important process for metastasis. Zudaire *et al* (2006) developed ADM KDs in mast cells which supressed anchorage dependent and independent growth of A549 lung cancer cells. Whilst Pang *et al* (2013) showed how ADM KDs in ovarian cancer cells effects macrophage polarisation. There was a significant increase in macrophage M2 marker, CD206, in non-transduced ovarian H08910, whereas there was a decrease in CD206 in KD cells. There was also a decrease in macrophage migration, stress fibre formation and cytoskeleton rearrangement when macrophages were co-cultured with HO8910 ADM KD cells.

Aggarwal *et al* (2012) looked at the effects of ADM KDs in PANC-1 cells on insulin secretion from INS-1 cells (insulin secreting β-cells). They showed that ADM KDs resulted in increased insulin secretion (174% insulin secretion) compared to scrambled controls (100% insulin secretion). This result was also replicated when ADM KDs were generated in mouse islets. These data show that ADM KDs inhibit glucose stimulated insulin secretion.

Overall, these results demonstrate the diversity of ADM and how KDs provide useful insights in both cancer models and processes including insulin secretion from pancreatic β cells. Furthermore, the data shows that KDs can be used for both *in vitro* and *in vivo* applications.

4.1.2 RAMP-3 knockdown studies

Research relating to RAMP-3 is very limited, it has only been more recently that research around the significance of RAMP-3 at a pathological level has been investigated. RAMP-1 has been widely studied and characterised relating to its association with migraines, RAMP-2 is well understood and been most notably been associated with regulation of blood pressure and embryo lethality following knockdown. However, there is limited research available of RAMP-3 and therefore, more research needs to be conducted around the role of RAMP-3. Expression of RAMP-3 has been shown in many cancer studies discussed in Chapters 1 and 3, and also mRNA and protein expression has been shown in the panel of seven PaCa cell lines investigated in this study (Chapter 3).

Dai *et al* (2020) show the potential significance of RAMP-3 in PaCa where RAMP-3 KOs in mice showed decreased PaCa metastasis. The study also showed how co-culture of RAMP-3 KO CAFs with PaCa tumour cells resulted in decreased migration, proliferation and metastasis. This is some of the first evidence showing the significant role of RAMP-3 in tumorigenesis in PaCa, showing that it is important to consider cells of the tumour microenvironment, not the cancer cells alone when focussing on RAMP-3.

Venkatanarayan *et al* (2015) looked at the role of amylin (IAPP), a peptide hormone co-secreted with insulin from β-cells of the pancreas, RAMP-3 and CLR in non-small cell lung carcinoma. RAMP-3 KDs in lung adenocarcinoma cells, H1299, showed that KD of RAMP-3 did not inhibit glycolysis and reactive oxygen species (ROS) and apoptosis were not induced following treatment with H1299 media secreting IAPP. These data suggest that RAMP-3 expression is critical for IAPP role in inhibiting glycolysis and inducing ROS and apoptosis in lung cancer cells showing that RAMP-3 has a positive

effect in these cancers. Furthermore, using basal cancer cell patient samples, RAMP-3 expression was associated with better patient survival determined by a Kaplan Meier curve.

RAMP-3 KD studies have shown its role in inducing cAMP production in mesenteric artery smooth muscle cells. RAMP-3 KDs resulted in inhibited cAMP production (Chauhan et al., 2015). These results demonstrate that RAMP-3 has diverse roles, one study showing that RAMP-3 is involved in pro-tumorigenic pathways, whilst the other demonstrates improved patient survival in breast cancer. However, it is important to consider that this is with amylin as the ligand, not ADM. Furthermore, RAMP-3 has been shown to have some association with vascular smooth muscle cells which could be significant when considering developing AM2 receptor specific therapies.

Overall, the combined ADM and RAMP-3 KD studies show how useful KD and KO studies can be in finding out the roles of genes in multiple pathways. It is evident that more research has been conducted into the consequences of ADM KDs in a variety of cancers. In particular, it highlights that research into ADM KDs in cells other than just tumour cells alone, could provide novel insights into the role of ADM and RAMP-3 in PaCa. The limited studies involving RAMP-3 KDs show that more research needs to be done into the role of RAMP-3 both physiologically and pathologically.

4.1.3 Aims and Objectives

The main aim of the project was to develop ADM and RAMP-3 KDs that could be used for future *in vitro* and *in vivo* experiments. The second aim was to transduce the KDs with firefly luciferase (Luc-RFP) so cells could be used for *in vivo* orthotopic experiments. Validating the KDs by QPCR was important for *in vivo* experiments. Furthermore, showing green fluorescent protein (GFP) induction and red fluorescent protein (RFP) induction by imaging and on the plate reader also contributed to validating successful transductions. This was important as cells were to be used for experiments showing the role of ADM and RAMP-3 in the pathogenesis of PaCa. Proliferation of KD cells compared to WT cells was also determined as part of the characterisation to see whether KDs had an impact on CFPAC-1 proliferation.

4.2 Methods

4.2.1 Transduction of ADM/RAMP-3 with SMARTvector inducible lentiviral shRNA

To generate ADM/RAMP-3 KDs in CFPAC-1 cells, Dharmacon™ SMARTvector™ Inducible Lentiviral shRNA particles were used (Figure 4.1) and scrambled shRNA (scrshRNA) was used as the control. This method of transduction utilises the activation of a Tet-On®3G bipartite induction system. The system includes an inducible RNA polymerase II promoter (mCMV) that has been optimised for minimal basal induction and potent activation upon induction with doxycycline. When doxycycline is added, the TRE3G (tetracycline responsive element) inducible promotor is bound and activated by the Tet-On 3G transactivator protein that is encoded within the inducible shRNA vector. The TRE3G promoter and Tet-On 3G protein work together to tightly regulate shRNA expression. Within the vector, there is also a puromycin resistance gene that is used for selection of cells that have been successfully transduced. The vector also includes a TurboGFP reporter which can be used to monitor successful transduction and expression when doxycycline is added to the cells. Successful transduction results in an increase in GFP expression which can be detected using a microscope.

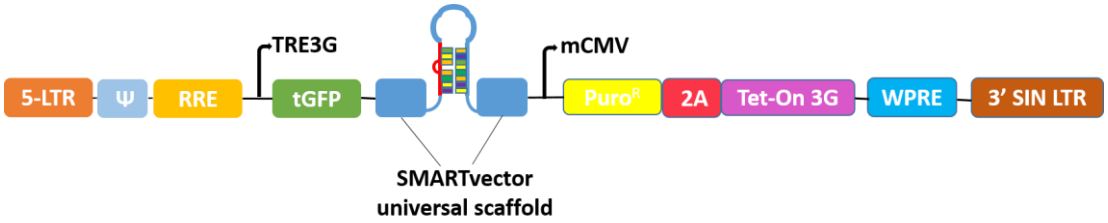

Vector element	Utility
5-LTR	5' long terminal repeat-needed for lentiviral production and integration of the construct into host cell genome
Ψ	Psi packaging sequence allows lentiviral genome packaging using lentiviral packaging systems
RRE	Rev response element increases packaging efficiency of full length lentiviral genome which enhances titre
TRE3G	Inducible promoter with tetracycline response elements which are activated by Tet-On 3G protein in the presence of doxycycline
tGFP	Turbo GFP reporter for visual tracking of transduction and expression upon doxycycline induction
SMARTvector universal scaffold	Scaffold based on native primary microRNA in which gene targeting sequence is embedded
mCMV	Murine cytomegalovirus- RNA polymerase II promoter
Puro^R	Puromycin resistance gene which permits antibiotic selection of transduced cells
2A	Self-cleaving peptide that enables expression of both Puro^R and Tet-On 3G transactivator from a single RNA polymerase II promoter
Tet-On 3G	Encodes doxycycline regulated transactivator protein which binds to TRE3G only when doxycycline is added
WPRE	Woodchuck Hepatitis Post-transcriptional Regulatory element which enhances transgene expression in target cells
3' SIN LTR	3' self-inactivating Long Terminal Repeat for generation of replication-incompetent lentiviral particles after integration

Figure 4.1 Dharmacon SMARTvector Inducible Lentiviral shRNA vector structure and table describing the individual vector elements adapted from the Dharmacon SMARTvector technical manual. The lentiviral knockdowns are induced by doxycycline which activates TRE3G inducible promoter. The SMARTvector universal scaffold encodes the gene targeting sequence of interest (ADM, RAMP-3 or scrambled). Turbo GFP is downstream of promoter and is used as a visual tracker of transduction after

addition of doxycycline. Puromycin resistance gene is incorporated into the vector to allow selection of transduced cells.

For both ADM and RAMP-3 knockdowns, a combination of 3 shRNA were combined (Table 4.1) (Figure 4.2 and Figure 4.3) to make a final MOI (multiplicity of infection) of 1.8. The MOI is the ratio of the number of viral particles to the number of cells. For the scrshRNA control, an MOI of 0.5 was prepared as recommended by Dharmacon.

Table 4.1 SMARTvector inducible lentiviral shRNA clone ID for ADM, RAMP-3 and scrambled control. The table includes the gene target sequence and the titre provided to for each individual vector. For ADM and RAMP-3, the 3 vectors were combined to make a final MOI of 1.8.

Clone ID	Vector	Gene	Gene Target Sequence	Titre (TU/well)
V3IHSMCG_5097476	piSMART mCMV/TurboGFP	ADM	GCGTCGGAGTTTCGAAAGA	8.88E+07
V3IHSMCG_5154731	piSMART mCMV/TurboGFP	ADM	ACCTGGGTTCGCTCGCCTT	1.49E+07
V3IHSMCG_9181061	piSMART mCMV/TurboGFP	ADM	GGTCGGACTCTGGTGTCTT	3.45E+07
V3IHSMCG_5735531	piSMART mCMV/TurboGFP	RAMP-3	TGGGAAGGCTTTCGCAGAC	6.63+07
V3IHSMCG_6204461	piSMART mCMV/TurboGFP	RAMP-3	CAATGTCGTGGGCTGCTAC	8.47+E07
V3IHSMCG_8049887	piSMART mCMV/TurboGFP	RAMP-3	CACAGGCAGTTCTTCTCCA	1.33+08
VSC6584	Non-targeting Control mCMV—TurboGFP	Scrambled		1.25+08

actcagtggtttcttggtgacactggatagaacagctcaagccttgccacttcgggcttc
tcactgcagctgggcttggacttcggagttttgccattgccagtgggacgtctgagactt
tctccttcaagtacttggcagatcactctcttagcaggtaggtgccgcagaccctgcggg
ttaagaggtggggtgggggggcagtgcttgccaaggccctaaactgggagcgctgggtgag
gggaacaacccactttggagggttctctgagagatagatacaccccatatcctgggccca
gctcgtgcacacagctggaggtccagagacccagtcccctctgctccgtcagccaagttc
caagaagttgagcagagaccctctgggagcctggcggggtgcagcggcctcccctgcggg
gcctgtcacccggccggcgcgtgcaaacgcctctggcgcctctctgcgcggagggagata
agcgtctgagccagggaaagcgcgggctaaacccgcctcgccggggcccctgcccgccct
ccgtgccccgcccgggcggtgcagctggcccgggtgctcacgctcgactctctttcttct
tttccagggtctgcgcttcgcagccgggatgaagctggtttccgtcgccctgatgtacct
gggttcgctcgccttcctaggcgctgacaccgctcggttggatgtcgcgtcggagtttcg
aaagaagtgagtccgggcagcgccttccccttgctggtacctggcaggcaaggggaact
gaccgttggtcccgaaggtctagaagtgaatgggagcagggacaggcctgggcgtcacct
gaacgcacgcgaatcgggtctgcttgtgttttccaggtggaataagtgggctctgagtcg
tgggaagagggaactgcggatgtccagcagctaccccaccgggctcgctgacgtgaaggc
cgggcctgcccagacccttattcggccccaggacatgaagggtgcctctcgaagccccga
agacaggtaactacgccctgtgctgtccagggacgggagggaaggaaggtgtgcgggagg
agttctctgtctccactcccctggcccgggggatcgtcggggctggaccgcagctcagat
ggcgcgagcagtttccagctccctctggctctagaatggctcccgttcccggtgttgggg
ccaaagctctgcttgatggggtctcaagttgcctttcttcccccctcccccgcccgcagc
agtccggatgccgcccgcatccgagtcaagcgctaccgccagagcatgaacaacttccag
ggcctccggagctttggctgccgcttcgggacgtgcacggtgcagaagctggcacaccag
atctaccagttcacagataaggacaaggacaacgtcgccccccaggagcaagatcagcccc
cagggctacggccgccggcgccggcgctccctgcccgaggccggcccggtcggactctg
gtgtcttctaagccacaagcacacggggctccagccccccgagtggaagtgctccccac
tttctttaggatttaggcgcccatggtacaaggaatagtcgcgcaagcatcccgctggtg
cctcccgggacgaaggacttcccgagcggtgtggggaccgggctctgacagccctgcgga
gaccctgagtccgggaggcaccgtccggcggcgagctctggctttgcaagggcccctcct
tctgggggcttcgcttccttagccttgctcaggtgcaagtgccccaggggcggggtgca
gaagaatccgagtgtttgccaggcttaaggagaggagaaactgagaaatgaatgctgaga
cccccggagcaggggtctgagccacagccgtgctcgcccacaaactgatttctcacggcg
tgtcaccccaccagggcgcaagcctcactattacttgaactttccaaaacctaaagagga
aaagtgcaatgcgtgttgtacatacagaggtaactatcaatatttaagtttgttgctgtc
aagatttttttgtaacttcaaatatagagatattttgtacgttatatattgtattaag
ggcattttaaaagcaattatattgtcctcccctattttaagacgtgaatgtctcagcgag
gtgtaaagttgttcgccgcgtggaatgtgagtgtgtttgtgtgcatgaaagagaaagact
gattacctcctgtgtggaagaaggaaacaccgagtctctgtataatctatttacataaaa
tgggtgatatgcgaacagcaaaccaataaactgtctcaatgctga

Figure 4.2 ADM sequence from NCBI GenBank. SMARTvector inducible lentiviral shRNA sequences for ADM are highlighted in yellow, green and pink.

gagcgtgacccagctgcggccggccagccatggagactggagcgctgcggcgcccgcaac
ttctcccgttgctgctgctgctctgcggtgggtgtcccagagcaggcggctgcaacgaga
caggcatgttggagaggctgcccctgtgtgggaaggctttcgcagacatgatgggcaagg
tggacgtctggaagtggtgcaacctgtccgagttcatcgtgtactatgagagtttcacca
actgcaccgagatggaggccaatgtcgtgggctgctactggcccaacccccctggcccagg
gcttcatcaccggcatccacaggcagttcttctccaactgcaccgtggacagggtccact
tggaggacccccagacgaggttctcatcccgctgatcgttatacccgtcgttctgactg
tcgccatggctggcctggtggtgtggcgcagcaaacgcaccgacacgctgctgtgagggt
cccggtgagatggagtgggtcacacctggcaagctggaagaaagttccctggggatggga
gatcgggtgggtgctgccaatctccagctactgtggccacaccccacctggtcatgggca
gacccctcccttcctgggctgacctgctccctcgaggccagcctgctccctggctgaggc
tcaggctatccgcccaagctctttgctcattctagggccagtggaggaaaatgtgataag
gccagagcttgtgtgctgggcaagaaatcacctgctgcatcctgtgctccgcaggctggg
ccggaagcctctgcctgcaggtttctatgctgtttcttagcacagaatccagcctagcct
tagccgcagtctaggccctgcttggactaggactccttgcttgaccccatctctggttcc
tgccctggctcctgcaccagccccagctcctgcctacatccaggcagaaatataggcagg
ggctcttggaagacgttccgtgctgtgacctccgagccctcctggtgggaagacagctgg
aaaggctgggaggagaagggagggggctgggggttcccaggagccatgcgtggcctgcaga
gtccattccatcatgatgctgtgcccgctatgggctgtgtccatgaccagaggctggagt
gggggtgtgttatagcccctcaccgggacttgctgtgcggatggggcctgggcctccttc
ctacaggggctcctctgtgggtgaggggccctctggaatggcatcccatgagcttgtggc
ctctatctgctaccatctgtgttttatctgagtaaagttaccttacttctgg

Figure 4.3 RAMP-3 sequence from NCBI GenBank. SMARTvector inducible lentiviral shRNA sequences for RAMP-3 are highlighted in yellow, green and pink.

Before transduction, cells were grown to a confluency of ~70% in a T75 flask. Cells were seeded in a 6 well plate at a density of 250,000 cells per well in 2 mL of warmed full serum media using the methods described in Section 2.1.1. and 2.1.4. The next day, transduction media containing 1 mL full serum media, lentiviral particles (MOI 1.8 or 0.5 for ADM/RAMP-3 and scrshRNA respectively) and 8µL 1 mg/mL polybrene was prepared. The transduction media was left to stand at room temperature for 20 minutes, the cells were washed twice with PBS before the transduction media was added to the cells seeded the previous day. Three days after transduction, the cells were sub-cultured into a T25 flask and the media was changed to selection media containing 2 µg/mL puromycin the following days. Puromycin selection continued for a week before 500 ng/mL doxycycline was added to the cells for a week to induce the transduction before cell sorting (Section 4.2.2).

4.2.2 Optimising concentration of doxycycline for induction of CFPAC-1 ADM, CFPAC-1 RAMP-3 and CFPAC-1 scrshRNA

An increase in GFP expression is a marker of successful induction of inducible lentiviral KDs therefore, a black clear bottomed 96 well plate was used to measure changes in GFP and determine the optimal doxycycline concentration. CFPAC-1 ADM KDs, CFPAC-1 RAMP-3 KDs and CFPAC-1 scrshRNA were seeded in a 96 well black clear bottomed plate (2,000 cells/well). The cells were treated every two days with either no doxycycline, 10 ng/mL doxycycline, 100 ng/mL doxycycline or 500 ng/mL doxycycline. The amount of GFP expression was measured using the Ensight ® Perkin Elmer plate reader (excitation 482 nm and emission 502 nm) daily. Data was plotted using GraphPad, version 9.2.0.

4.2.3 GFP cell sort of CFPAC-1 ADM/RAMP-3 knockdowns

The KD cells and scrshRNA cells treated with 500 ng/mL doxycycline for a week and sub-cultured into a T75 flask until they reached a confluency of 70%. Negative control T75 flasks were also prepared containing the KD cells and scrshRNA with media without doxycycline. The cells without doxycycline in the media did not express GFP, any cells that were more fluorescent than the control cells were sorted.

To sort the cells, the cells were detached and counted using methods described in Section 2.1.1 and 2.1.4 to ensure there were no more than $10e^6$ cells/mL. The counted cells were filtered through a 100 µM Nylon cell strainer before being sorted for GFP positive cells with mid and high GFP expression using fluorescence activated cell sorting (FACS) (excitation 482 nm, emission 502 nm). FACSAria was operated by a technician in the Core Flow Cytometry facility to sort the cells. After the sort, the cells were centrifuged at 250 x g for 5 minutes and resuspended in full serum media in a 6 well plate. Cells were sub-cultured into a T75 flask and induced with 500 ng/mL doxycycline for a week before use in *in vitro* experiments.

4.2.4 ADM knockdown validation by QPCR

To determine if ADM KD were successful, QPCR using ADM and ACTB (housekeeper) primers was completed. The samples outlined in Table 4.2 were RNA extracted as described in Section 2.2.1 before the RNA samples were quantified using the NanoDrop 2000, cDNA was synthesised and the QPCR was run (Section 2.2.2 and 2.3). Before collecting the RNA, cells were seeded in a 6 well plate in duplicates at a density of 350,000 cells/well (Day 1 RNA collection) and 100,000 cells/well (Day 7 RNA collection) to ensure RNA was collected when cells were 60-70% confluent, half the cells were induced with 500 ng/mL doxycycline, whilst the other half of cells were treated with normal full serum media. RNA was collected either after 1 day of doxycycline induction or after 7 days of doxycycline induction. CFPAC-1 WT cells and AM2 overexpressing cells were seeded at 350,000 cells/well and the RNA was collected when they reached 70% confluency. Before RNA collection the cells were visualised using the microscope and images were taken to show cells expressing GFP following induction with doxycycline.

Table 4.2 A list of the samples that were RNA extracted to validate the knockdown of ADM in CFPAC-1 cells.

Sample	Doxycycline induced (0.5 mg/mL)?
AM2 overexpressing cells	No
CFPAC-1 scrshRNA controls	Yes
Day 1 CFPAC-1 ADM knockdown	Yes
Day 7 CFPAC-1 ADM knockdown	Yes
Day 1 CFPAC-1 ADM knockdown	No
Day 7 CFPAC-1 ADM knockdown	No

The differences in ADM mRNA expression was determined by calculating the delta-delta Ct ($2^{-\Delta\Delta Ct}$). This is used to calculate the relative fold change gene expression of samples. The calculation was relative to doxycycline induced CFPAC-1 scrshRNA controls. Doxycycline induced CFPAC-1 scrshRNA controls were used as the control to calculate the fold change. Following $2^{-\Delta\Delta Ct}$ calculations, the

percentage difference in ADM expression relative to CFPAC-1 scrshRNA control was calculated. Data was plotted using GraphPad, version 9.2.0.

4.2.5 Lentiviral transduction of ADM knockdown cells and ScrshRNA cells with firefly luciferase (Luc-RFP)

CFPAC-1 ADM KD and CFPAC-1 scrshRNA cells were transduced with a lentiviral vector containing firefly luciferase, red fluorescent protein (RFP) marker and an antibiotic resistance gene for blasticidin (Figure 4.4) for use in *in vivo* orthotopic models. Luc-RFP transduction of cells allows live monitoring of tumour cells in mice for primary tumour size and metastasis. To transduce the cells, CFPAC-1 ADM KDs and CFPAC-1 scrshRNA were seeded in a 24 well plate so cells were 70% confluent the following day. The following day, the cells were transduced with an MOI of 3. Once the cells had established, cells were selected in 20 µg/mL blasticidin for a week. The cells were monitored for fluorescence under the microscope and sub-cultured until they reached a confluency of 70% in a T75 flask. The Luc-RFP transduced KDs and KDs without Luc-RFP were seeded in a 6 well plate at 300,000 cells/well and treated with D-luciferin prior starting the *in vivo* experiment to ensure the cells were successfully transfected using IVIS (In Vivo Imaging System). D-luciferin is the substrate to luciferase and produces a bioluminescent signal. Luc-RFP transduced and un-transduced KD cells were also seeded at 2,000 cells/well in a 96-well clear black bottom plate and treated with 5 µL D-luciferin for 30 minutes to measure luminescence on the Ensight® Perkin Elmer plate reader.

Cppt; Central polypurine tract (cppt) increases lentivirus mediated gene transfer efficiency, WPRE; Woodchuck Heptatis Virus Post-transcriptional Regulatory Element creates a tertiary structure enhancing expression of gene of interest.

Figure 4.4 Firefly Luciferase vector adapted from the Amsbio manual. EF1a is a promoter upstream of luciferase and red fluorescent protein (RFP) which are constitutively expressed as individual proteins. Blasticidin (Bsd) resistance gene permits antibiotic selection of transduced cells and is downstream of the Rsv promoter.

4.2.6 CFPAC-1 ADM KD, RAMP-3 KD, scrshRNA and WT viability assay

To determine whether transduction of CFPAC-1 cells with inducible lentiviral ADM shRNA, RAMP-3 shRNA and scrshRNA had an effect on viability of cells compared to WT cells, the RealTime Glo™ MT cell viability assay was used. The RealTime Glo™ MT cell viability assay is a bioluminescent method used to measure cell viability. It determines the number of viable cells by measuring the reducing potential of them.

The assay measures the reducing potential of cells and their metabolism. The reaction involves the addition of a cell permeant pro-substrate and NanoLuc® luciferase to cells in culture. Viable cells will reduce the pro-substrate and release it into the surrounding media. The NanoLuc® substrate that is produced reacts with NanoLuc® luciferase in the media and generates a luminescent signal (Figure 4.5). The enzyme/substrate mix remains stable in the media for 72 hours at 37°C. If cells are dead, there will be no luminescent signal as the MT cell viability substrate will not be reduced by the cells.

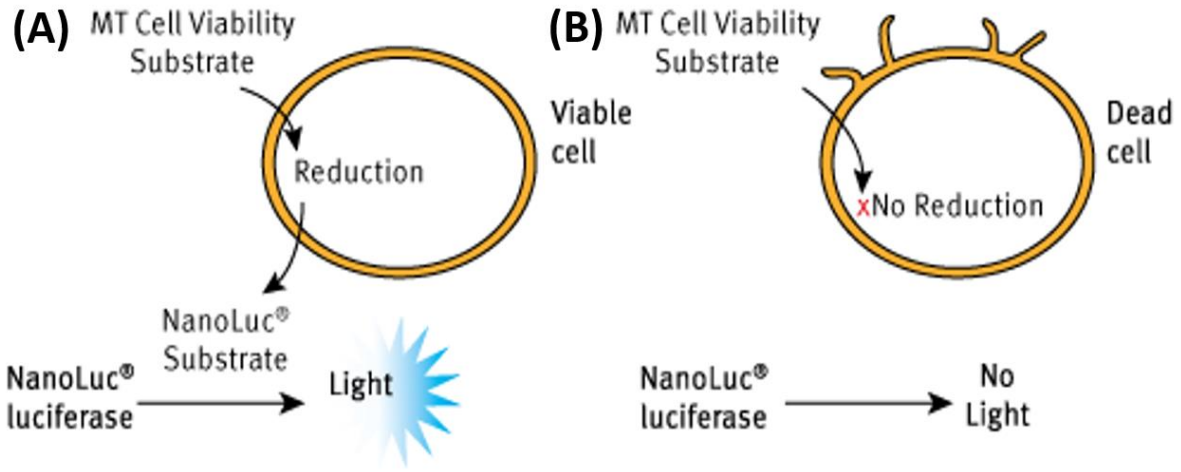

Figure 4.5 Principles of the RealTime Glo™ MT Viability assay. (A) Metabolically active cells (viable cells) will reduce the cell viability substrate which reacts with NanoLuc luciferase ® to produce a luminescent signal. (B) Dead cells are unable to reduce the substrate and therefore no luminescent signal is released (Promega, 2016).

Cells were seeded at a density of 2,000 cells per well (100 µL optimal growth media per well) in a clear white bottomed 96 well plate and left overnight in the incubator at 37°C. The following day, the MT cell viability substrate and NanoLuc® enzyme were heated to 37°C with 5% media for 10 minutes. The enzyme and substrate (1:1000 dilution) were added 5% media and shaken vigorously. The cells in the plate were first washed twice with 100 µL PBS and then 100 µL of the reagent mix was added. The cells were left to incubate for 1 hour at 37°C before taking the baseline luminescence reading on the plate reader with the lid removed and a plastic film placed on top. The luminescence was measured every 24 hours for 72 hours. Data was normalised to day 0 luminescence, plotted and analysed using GraphPad, version 9.2.0. Two-way ANOVA analysis and Tukey's multiple comparison test were used to determine any significant differences between CFPAC-1 KDs, scrshRNA controls and WT cells.

4.3 Results

4.3.1 Knockdown validation

CFPAC-1 ADM KDs, CFPAC-1 RAMP-3 KDs and scrshRNA controls were developed using inducible lentiviral shRNA to compare effects of KD, scrshRNA control and WT cells *in vitro* and *in vivo.* The data shown in this chapter describes the development and validation of the KDs. It also includes data on how viability of cells if effected by KD of ADM and RAMP-3.

4.3.3.1 CFPAC-1 ADM Knockdown doxycycline induction

As described in section 4.2.1 for successful KD, the KD cells must be induced by doxycycline (dox). CFPAC-1 ADM KD cells were seeded in a 6 well plate and treated with media containing different concentrations of doxycycline every two days (no dox, 10 ng/mL, 100 ng/mL and 500 ng/mL), at day 1 and day 7 images were taken on the microscope (Figure 4.6) and RNA was collected. The amount of fluorescence was also measured over a 7-day period and plotted to monitor any changes as described in section 4.2.2 (Figure 4.7). Figure 4.6 shows that when full serum media without doxycycline was added to cells, there was no change in GFP expression at day 1 (panel A) and day 7 (panel B). The same result was replicated in CFPAC-1 ADM KDs treated with full serum media containing 10 ng/mL doxycycline, there was no difference between day 1 (panel C) and day 7 (panel D). At a concentration of 100 ng/mL on both day 1 (panel E) and day 7 (panel F), there was GFP expression with an increase seen at day 7. Figure 4.7 also shows that GFP fluorescence in CFPAC-1 ADM KDs increased by 26% increase from day 1 to day 7. CFPAC-1 ADM KDs treated with media containing 500 ng/mL doxycycline showed a clear increase in GFP expression of 46.8% between day 1 and day 7 of 46.8% (Figure 4.7). This was also captured on the microscope as shown by Figure 4.6 where there is an increase in GFP as doxycycline concentration increases.

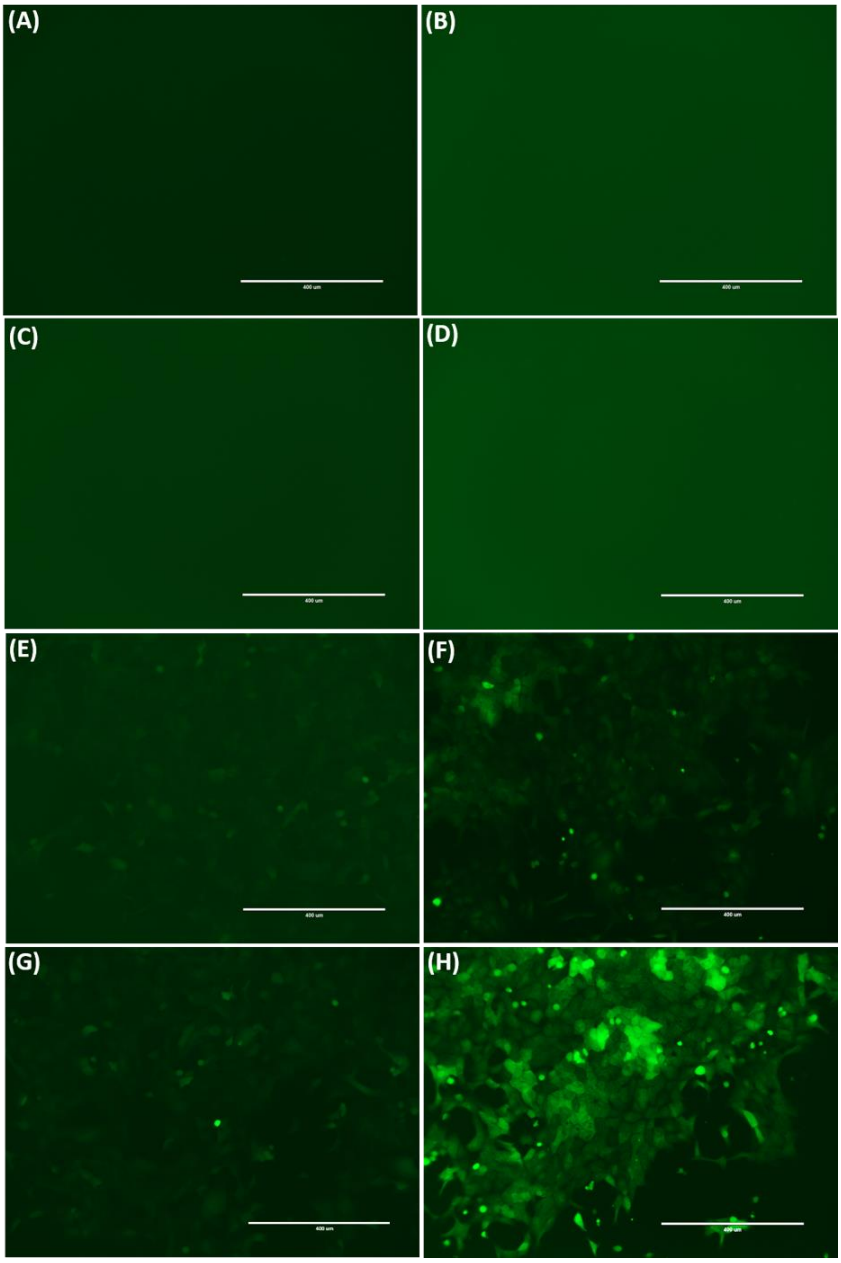

Figure 4.6 Day 1 and Day 7 CFPAC-1 ADM inducible lentiviral shRNA KD induction. ADM KDs were induced over 7 days with different concentrations of dox **(A)** Day 1 CFPAC-1 ADM inducible KD without dox induction **(B)** Day 7 CFPAC-1 ADM inducible KD induced without dox **(C)** Day 1 CFPAC-1 ADM inducible KD with 10 ng/mL dox **(D)** Day 7 CFPAC-1 ADM inducible KD with 10 ng/mL dox **(E)** Day 1 CFPAC-1 ADM inducible KD with 100 ng/mL dox **(F)** Day 7 CFPAC-1 ADM inducible KD with 100 ng/mL dox **(G)** Day 1 CFPAC-1 ADM inducible KD with 500 ng/mL dox **(H)** Day 7 CFPAC-1 ADM inducible KD with 500 ng/mL dox.

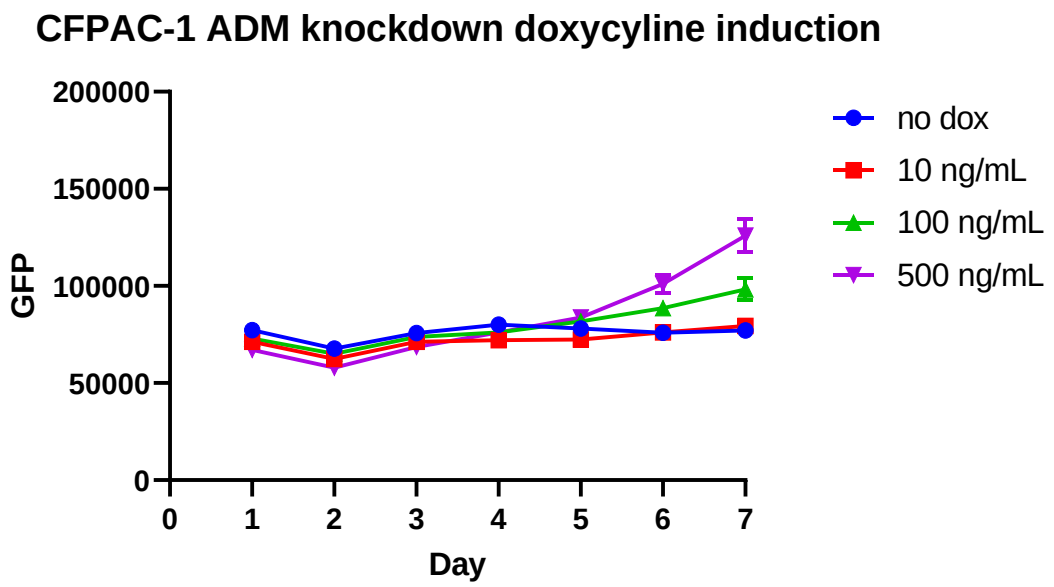

Figure 4.7 CFPAC-1 ADM KD doxycycline (dox) induction over seven days. CFPAC-1 ADM KDs were induced at different dox concentrations (no dox, 10 ng/mL, 100 ng/mL, 500 ng/mL) and GFP was measured an excitation of 482 nm and emission of 502 nm. One-way ANOVA analysis confirmed a significant difference between different dox conditions on day 7 (p= 0.01).

4.3.3.2 CFPAC-1 RAMP-3 Knockdown doxycycline induction

CFPAC-1 RAMP-3 KDs were also developed to determine the effect in *in vitro* assays (Chapter 5). Figure 4.8 shows similar results to the CFPAC-1 ADM KDs described in Section 4.3.3.1. There was no difference in day 1 and day 7 GFP in untreated and 10 ng/mL doxycycline RAMP-3 KDs (panel A, B, C and D). There was a 35% increase in GFP between day 1 and day 7 (Figure 4.9) in RAMP-3 KDs treated with media containing 100 ng/mL doxycycline (Figure 4.8 panel E and F). At 500 ng/mL there was a 57% increase in GFP expression between days 1 and 7 (Figure 4.9) and panel G and H also visually show the increase in GFP expression in images taken prior to RNA extraction (Figure 4.8).

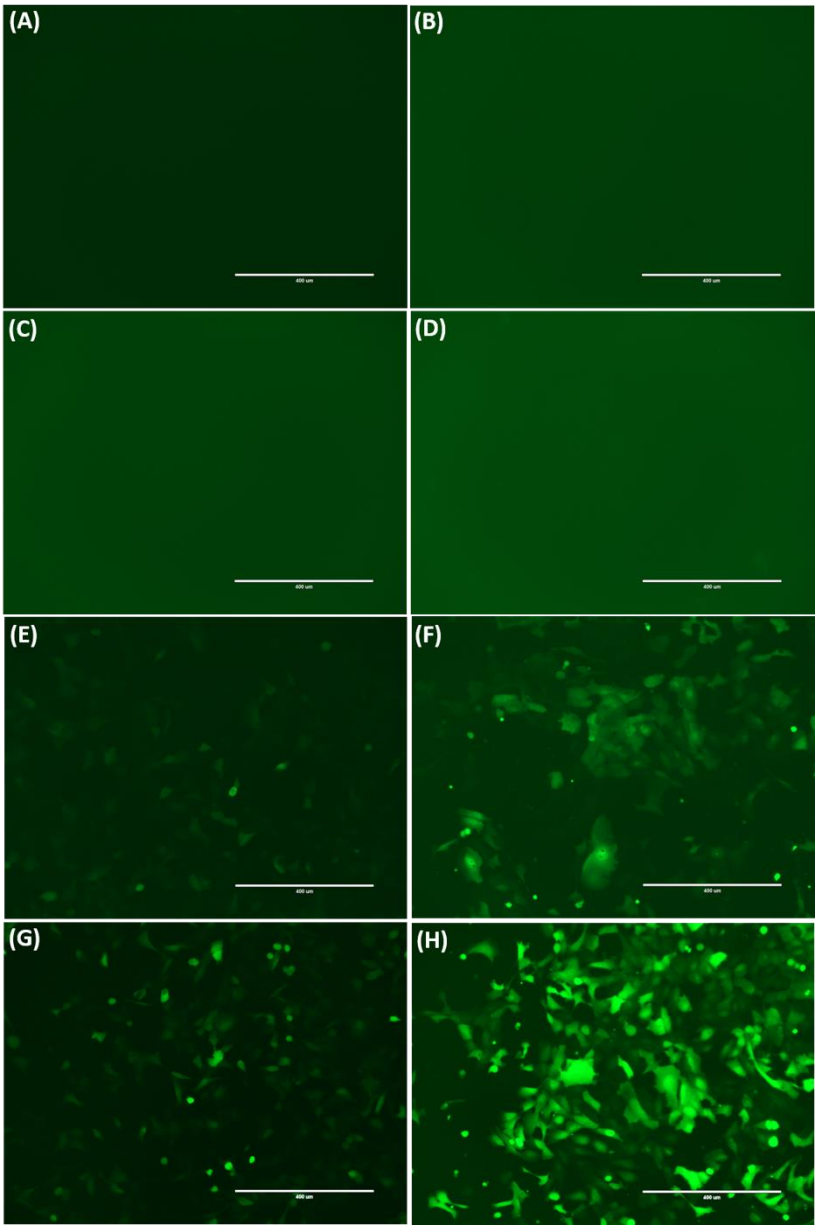

Figure 4.8 Day 1 and Day 7 CFPAC-1 RAMP-3 inducible lentiviral shRNA KD induction. RAMP-3 KD were induced over 7 days with different concentrations of doxycycline **(A)** Day 1 CFPAC-1 RAMP-3 inducible KD without dox induction **(B)** Day 7 CFPAC-1 RAMP-3 inducible KD induced without dox **(C)** Day 1 CFPAC-1 RAMP-3 inducible KD with 10 ng/mL dox **(D)** Day 7 CFPAC-1 RAMP-3 inducible KD with 10 ng/mL dox **(E)** Day 1 CFPAC-1 RAMP-3 inducible KD with 100 ng/mL dox **(F)** Day 7 CFPAC-1 RAMP-3 inducible knockdown with 100 ng/mL dox **(G)** Day 1 CFPAC-1 RAMP-3 inducible KD with 500 ng/mL dox **(H)** Day 7 CFPAC-1 RAMP-3 inducible KD with 500 ng/mL dox.

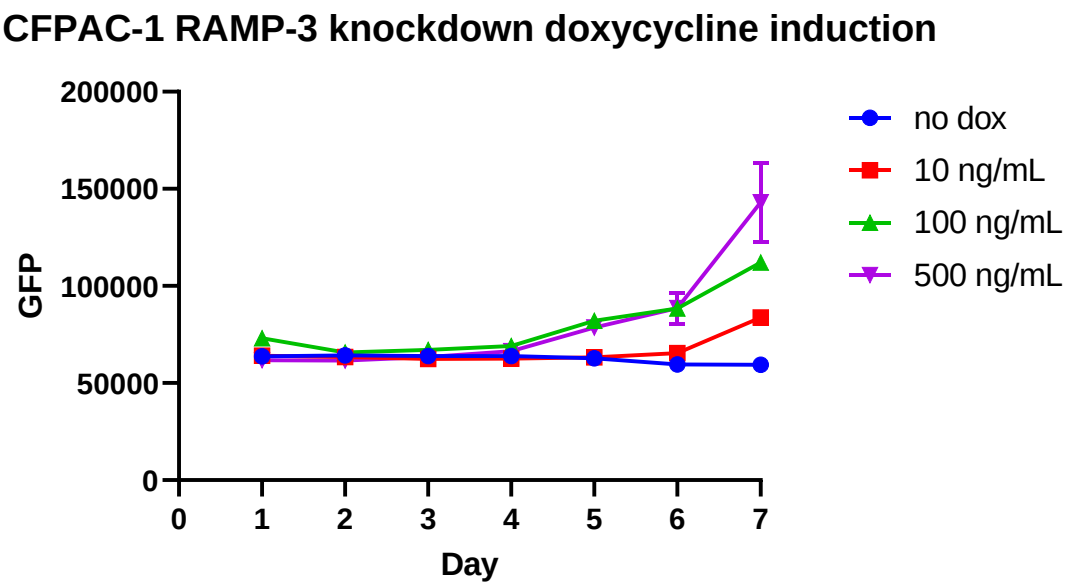

Figure 4.9 CFPAC-1 RAMP-3 knockdown doxycycline (dox) induction over seven days. CFPAC-1 RAMP-3 KDs were induced at different dox concentrations (no dox, 10 ng/mL, 100 ng/mL, 500 ng/mL) and GFP was measured an excitation of 482 nm and emission of 502 nm. One-way ANOVA analysis confirmed a significant difference between different concentrations of dox on day 7 (p= 0.002).

4.3.3.3 CFPAC-1 scrambled shRNA (scrshRNA) control doxycycline induction

CFPAC-1 scrshRNA control cells were developed to compare *in vitro* and *in vivo* results from ADM and RAMP-3 KDs. ScrshRNA is when an shRNA sequence has its nucleotides randomly rearranged to generate a random sequence. Figure 4.10 shows the results for doxycycline induction of the scrshRNA controls, as with ADM and RAMP-3 KDs, there was no GFP expression in untreated cells at both day 1 and day 7 (panel A and B). Cells treated with 10 ng/mL doxycycline showed GFP expression at day 7 from day 1 (panel C and D), showing only a small increase of 8% (Figure 4.11). CFPAC-1 scrshRNA treated with 100 ng/mL doxycycline show a clear increase in GFP expression in Figure 4.10 (panel E and F) however, Figure 4.11 only showed a 10.8% increase in doxycycline when cells were read on the plate reader. CFPAC-1 scrshRNA treated with 500 ng/mL doxycycline showed an increase of 42.2% GFP expression from day 1 to day 7 which is also shown in panel G and H of Figure 4.10.

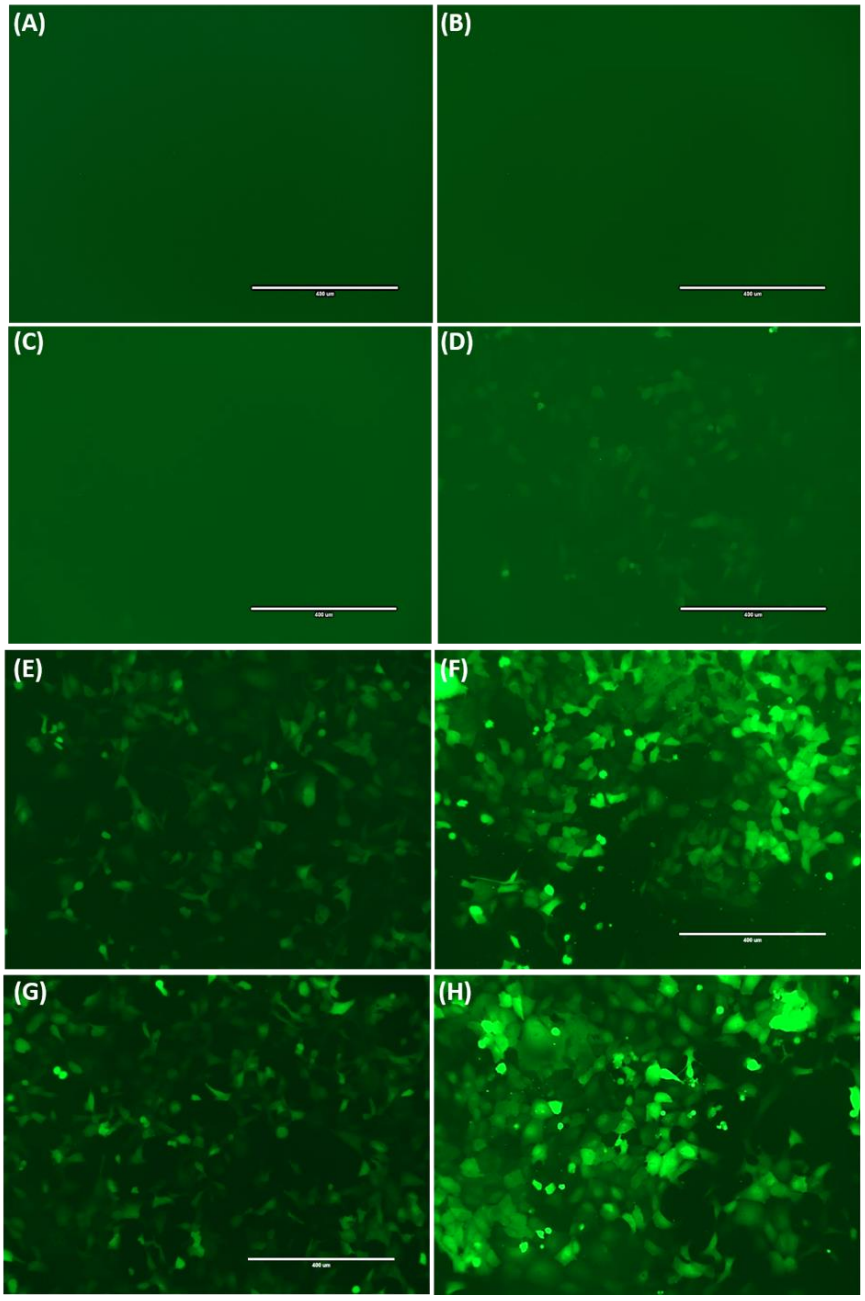

Figure 4.10 Day 1 and Day 7 CFPAC-1 inducible scrambled shRNA (scrshRNA) control dox induction. CFPAC-1 scrshRNA cells were induced over 7 days with different concentrations of dox (A) Day 1 CFPAC-1 scrshRNA without dox induction (B) Day 7 CFPAC-1 scrshRNA without dox (C) Day 1 CFPAC-1 scrshRNA with 10 ng/mL dox (D) Day 7 CFPAC-1 scrshRNA with 10 ng/mL doxycycline (E) Day 1 CFPAC-1 inducible scrshRNA with 100 ng/mL dox (F) Day 7 CFPAC-1 scrshRNA with 100 ng/mL dox (G) Day 1 CFPAC-1 inducible scrambled control with 500 ng/mL doxycycline (H) Day 7 CFPAC-1 scrshRNA with 500 ng/mL dox.

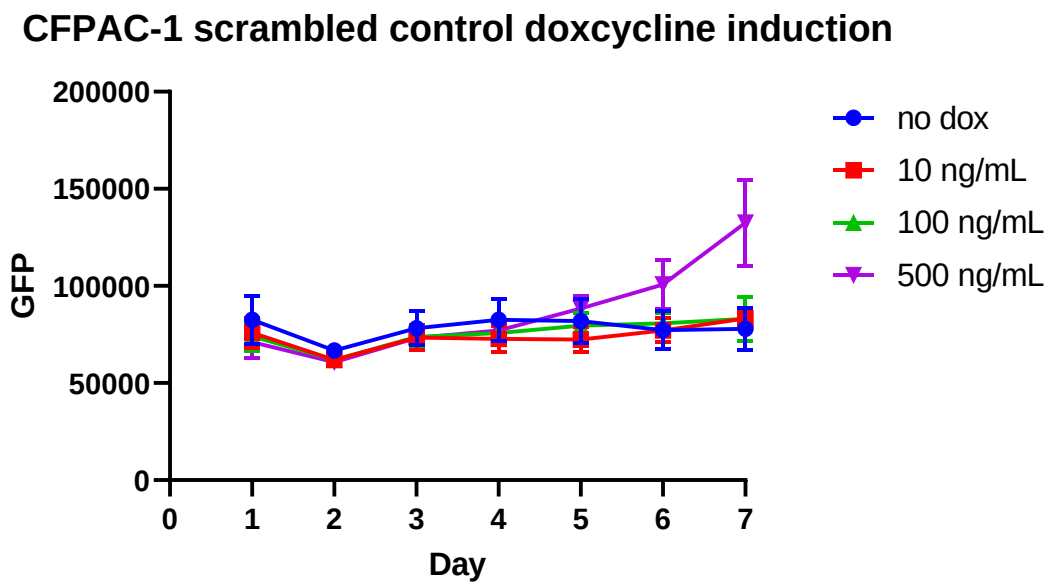

Figure 4.11 CFPAC-1 scrshRNA doxycycline (dox) induction over seven days. CFPAC-1 scrshRNA cells were induced at different dox concentrations (no dox, 10 ng/mL, 100 ng/mL, 500 ng/mL) and GFP was measured an excitation of 482 nm and emission of 502 nm. One-way ANOVA analysis confirmed a significant difference between different dox concentrations on day 7 (p= 0.0009).

4.3.3.4 QPCR validation

QPCR was used to validate the successful KD of ADM for use of cells *in vivo.* Figure 4.12 shows the delta-delta Ct values calculated relative to CFPAC-1 scrshRNA controls. The data shows that following one day of doxycycline induction at a concentration of 500 ng/mL, there was a 43% decrease in ADM expression relative to CFPAC1-1 scrshRNA control (p= 0.002). CFPAC-1 ADM KDs not induced with doxycycline on day 1 had a larger decrease in ADM expression relative to CFPAC-1 scrshRNA of 69% (p< 0.0001). After no doxycycline induction of CFPAC-1 ADM KDs for 7 days, there was an 81% decrease in ADM expression relative to CFPAC-1 scrshRNA (p<0.0001). CFPAC-1 ADM KDs induced with 500 ng/mL doxycycline showed a 71% decrease in ADM expression following 7 days of induction relative to CFPAC-1 scrshRNA (p< 0.0001). Overexpressing AM2 cells showed a 299% increase in ADM expression relative to CFPAC-1 scrshRNA.

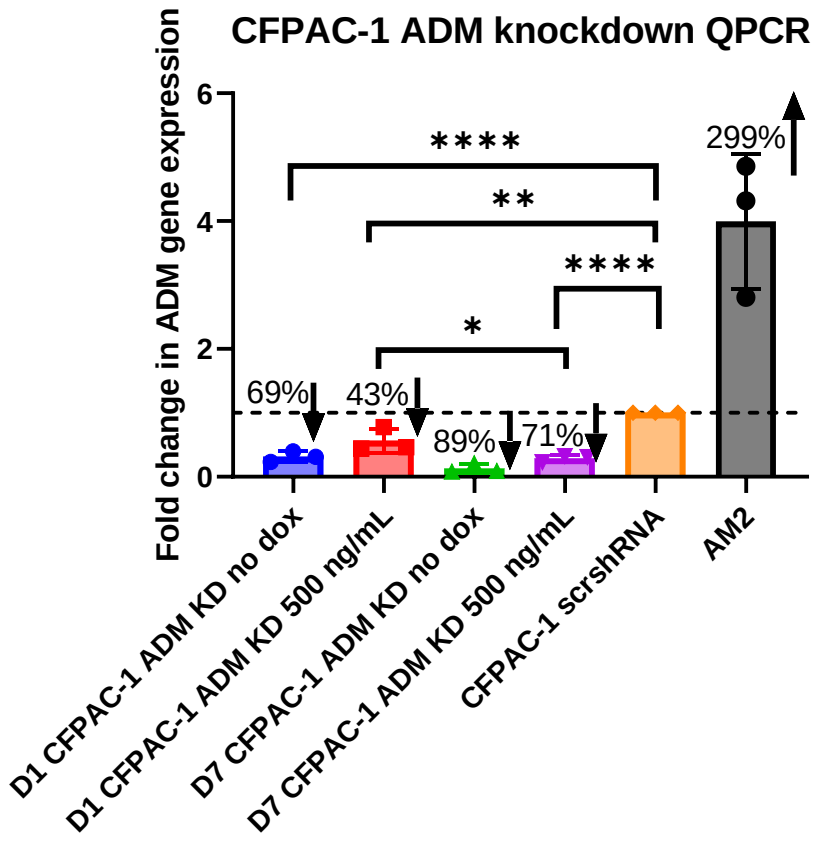

Figure 4.12 Fold change in expression of ADM in CFPAC-1 ADM KD relative to CFPAC-1 scrshRNA determined by QPCR. Delta delta Ct ($2^{-\Delta\Delta Ct}$) was used to calculate the fold change in ADM expression in CFPAC-1 ADM KDs relative to scrshRNA controls. Day 1 CFPAC-1 ADM KD no dox and 500 ng/mL dox induction, showed a 69% decrease and 43% decrease in ADM expression relative to CFPAC-1 scrshRNA respectively. Day 7 CFPAC-1 ADM KD no dox and 500 ng/mL dox induction, showed an 89% and 71% decrease in ADM expression relative to CFPAC-1 scrshRNA respectively. AM2 control cells showed a 189% increase in ADM expression relative to CFPAC-1 scrshRNA. The fold change ($2^{-\Delta\Delta Ct}$) was 0.31, 0.57, 0.11, 0.29, and 3.9 for day 1 CFPAC-1 ADM KD no dox and 500 ng/ml dox, day 7 CFPAC-1 ADM KD no dox and 500 ng/ml dox and AM2 respectively. One-way ANOVA analysis showed a significant difference ($p < 0.0001$) between CFPAC-1 ADM KDs at day 1 and day 7 and CFPAC-1 scrshRNA. Tukey's multiple comparison post-hoc test showed more specific significant differences shown in the graph.

4.3.3.5 Effect of CFPAC-1 ADM KD and RAMP-3 KD on viability of cells

The viability of CFPAC-1 cells was compared to determine whether KD of ADM or RAMP-3 had an impact on the viability of CFPAC-1 cells following doxycycline induction. The percentage viability was calculated relative to day 0. The data shown in Figure 4.13 shows that CFPAC-1 WT cells had the biggest increase in viability relative to day 0 (1469.9% on day 3) and that CFPAC-1 scrshRNA cells had the smallest increase in viability (307.6% on day 3). Two-way ANOVA analysis showed that there was a statistical difference between the percentage viability of all the cell lines (p= 0.0002). On day 3, Tukey's multiple comparison test shows that there is a significant difference between CFPAC-1 ADM KDs (662.2% day 3) and CFPAC-1 WT cells (1569.9% day 3) (p= 0.03) and CFPAC-1 scrshRNA (407.6% on day 3) and CFPAC-1 WT cells (p= 0.02). There were no significant differences between CFPAC-1 RAMP-3 KDs and WT cells on day 3, although the percentage viability was lower in CFPAC-1 RAMP-3 KDs (1021.1%). There were also no significant differences between CFPAC-1 ADM KDs/RAMP-3 KDs and CFPAC-1 scrshRNA.

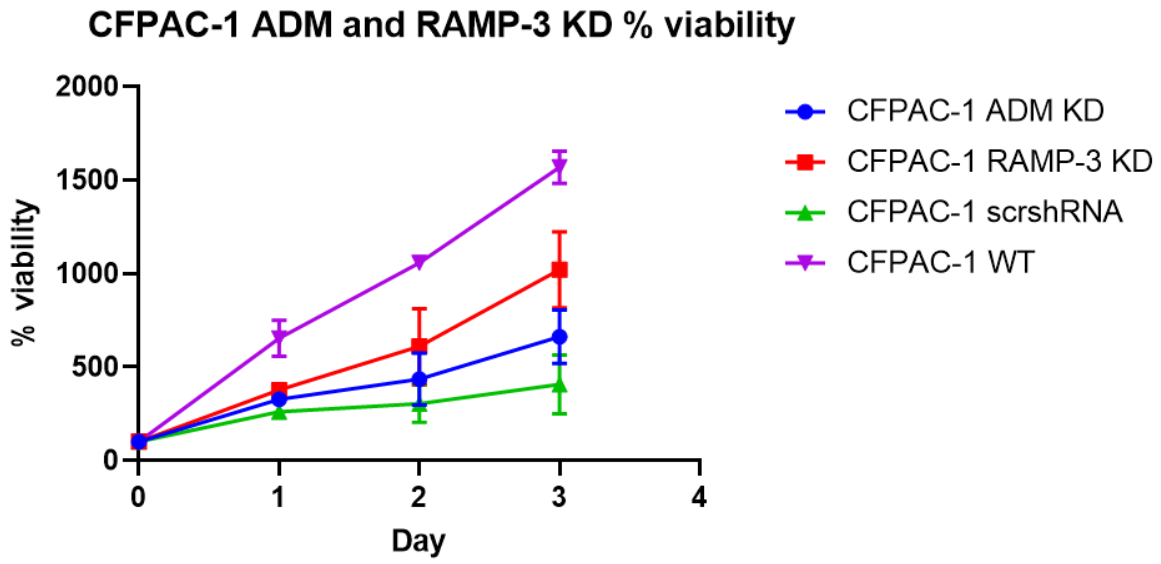

Figure 4.13 CFPAC-1 ADM KD, RAMP-3 KD, scrshRNA and WT percentage viability relative to baseline day 0 read. Cells were induced with 500 ng/mL doxycycline for 7 days before viability of the cells was measured. Results are based on 3 independent repeats and presented as mean±SEM. One-way

ANOVA analysis showed a significant difference between CFPAC-1 ADM KDs, CFPAC-1 RAMP-3 KDs, CFPAC-1 scrshRNA and CFPAC-1 WT at day 3 (p= 0.002).

4.3.2 Lentiviral transduction of KD cells with firefly luciferase (Luc-RFP)

4.3.2.1 Luc-RFP transduction validation

CFPAC-1 ADM KDs and CFPAC-1 scrshRNA cells were transduced with Luc-RFP to be able to monitor tumour growth *in vivo* following orthotopic injection. To ensure that the KD cells were successfully transduced with Luc-RFP, cells were treated with D-luciferin substrate to measure luminescence of cells on the on the plate reader and cells were also visualised using IVIS (Section 4.2.4). Figure 4.14 shows that the KDs with Luc-RFP had higher levels of luminescent signal than, CFPAC-1 ADM KD, scrshRNA and media without Luc-RFP transduction. CFPAC-1 ADM KD transduced with Luc-RFP had higher luminescent signal which is also shown in Figure 4.15 by the luminescent signal detected by IVIS. CFPAC-1 ADM KD transduced with Luc-RFP showed a signal of 1.897 E07 (p/sec) compared to CFPAC-1 scrshRNA which has a signal of 1.316 E07 (p/sec). CFPAC-1 ADM KDs and CFPAC-1 scrshRNA cell lines without Luc-RFP showed no luminescent signal.

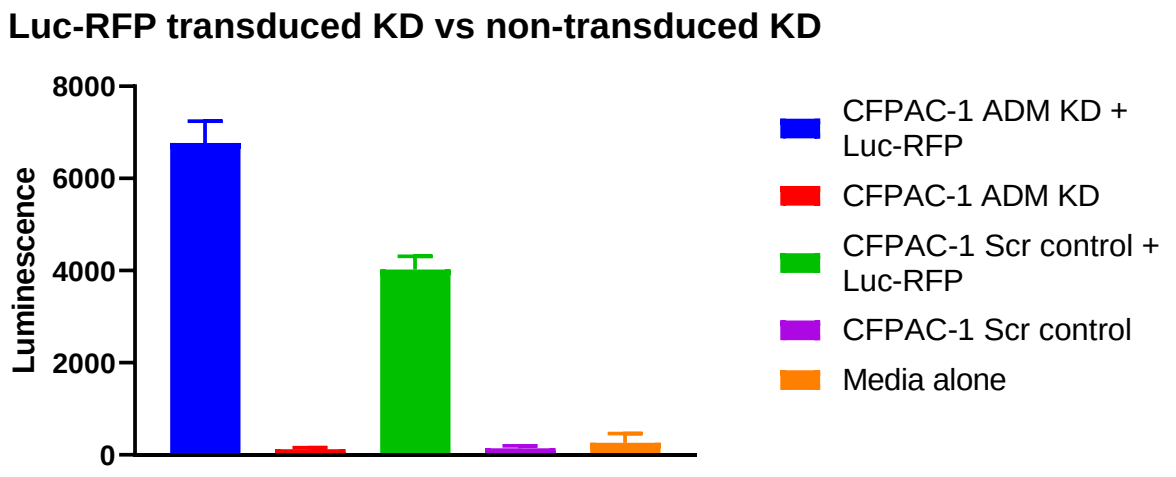

Figure 4.14 Luminescence of CFPAC-1 ADM KD and CFPAC-1 scrshRNA (Scr) controls transduced with Luc-RFP. Luminescence of Luc-RFP transduced CFPAC-1 ADM KD and CFPAC-1 scrshRNA cells was compared to CFPAC-1 ADM KDs and CFPAC-1 scrshRNA that had not been transduced with Luc-RFP.

All cells were induced with D-luciferin before luminescence was measured on the Ensight Perkin Elmer plate reader. Luminescence of media was also measured as a control.

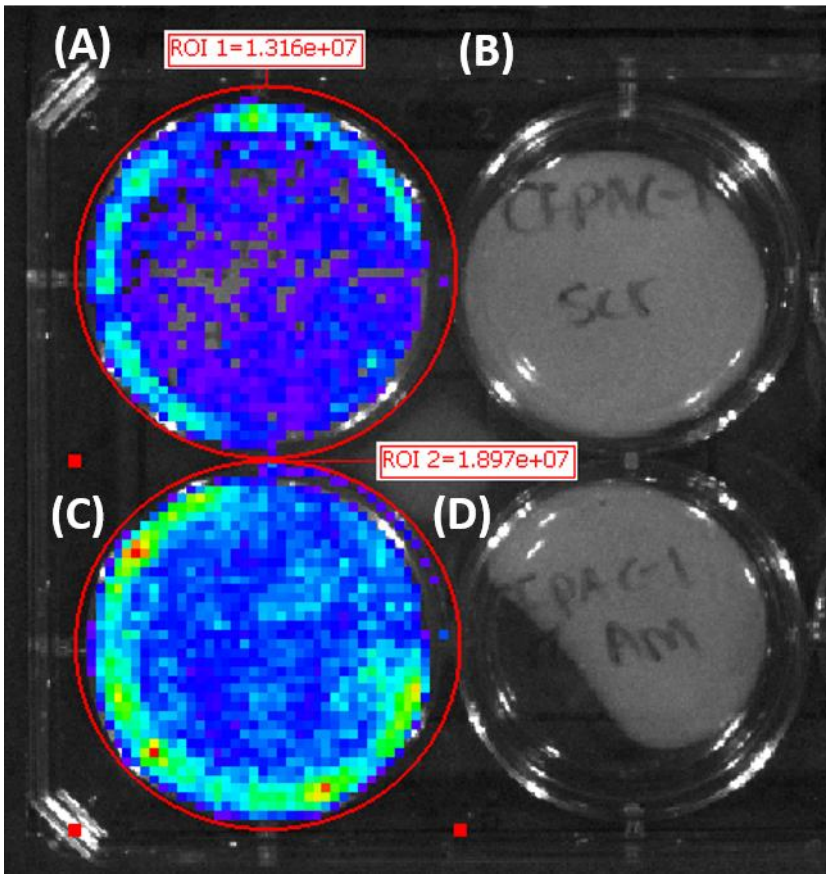

Figure 4.15 Luciferase expression in CFPAC-1 ADM KD-LucRFP and CFPAC-1 scrshRNA-LucRFP cells imaged before *in vivo* orthotopic experiment following addition of D-luciferin substrate. (A) CFPAC-1 scrshRNA-LucRFP transduced cells (B) CFPAC-1 scrshRNA cells (C) CFPAC-1 ADM KD-LucRFP transduced cells (D) CFPAC-1 ADM KD cells. The region of interest (ROI) was selected on Living Image software and total flux (p/sec) was determined.

4.4 Discussion

CFPAC-1 ADM and CFPAC-1 RAMP-3 KDs were developed for both *in vitro* and *in vivo* experiments to determine the effects of these genes in the development of PaCa. CFPAC-1 cells were chosen to develop KDs in as they showed mRNA expression of both RAMP-3 and ADM which was confirmed further by sequencing data (Chapter 3, Figure 3.7 to Figure 3,9 and Table 3.5). RAMP-3 expression was also shown at protein level in CFPAC-1 cells as a dimer (Chapter 3, Figure 3.15). cAMP assays showed that ADM activated cAMP production in CFPAC-1 cells with 100% efficacy and a potency of 288 nM (Figure 3.16). These cells were also selected based on previous data obtained from the lab group showing successful establishment of CFPAC-1 cells subcutaneously and in orthotopic experiments. The experimental parameters of these *in vivo* models were based on Shi *et al* (2016) paper.

To generate KDs, inducible lentiviral shRNA was used which is a tool that can be used to switch on and off KD of genes. The advantages of this system is that it allows for a stable transfection and long term usage by retroviral delivery compared to using siRNA. It also has a higher transfection efficiency, infecting nearly any cells type with the ability to integrate into both dividing and non-dividing cells. The ability to switch the KD of a gene on and off also provides a useful advantage in cells where the KD of the gene may be lethal. Furthermore, it provides the option of using non-induced cells as a control instead of developing a separate control cell line.

4.4.1 CFPAC-1 ADM knockdowns are validated, whilst RAMP-3 knockdowns need further validation

The results in Figure 4.6 and Figure 4.7 show induction of ADM KDs at concentrations of 100 ng/mL and 500 ng/mL doxycycline, with higher levels of GFP expression at 500 ng/mL. These results are mimicked in CFPAC-1 RAMP-3 KDs and in CFPAC-1 scrshRNA controls (Figure 4.8, Figure 4.9, Figure 4.10 and Figure 4.11). Based on the principles of the inducible lentiviral shRNA described in Section 4.2.1, the induction of KDs was successful as the addition of doxycycline to cells resulted in the activation of the lentiviral promoter and activation of downstream GFP. One limitation to this is that

the GFP images presented in Figure 4.6, Figure 4.8 and Figure 4.10 do not represent the GFP measurements in Figure 4.7, Figure 4.9 and Figure 4.11. The images presented are not be directly comparable to the GFP readings from the plate reader, intensity of GFP under the microscope is regulated by exposure. The small differences in GFP expression between no doxycycline and 500 ng/mL may be due to auto-fluorescence of the cells in the no doxycycline group.

However, to further validate this, QPCR was completed on CFPAC-1 ADM KDs and CFPAC-1 scrshRNA cells (Figure 4.12) showing the fold change in expression and the percentage decrease or increase in ADM expression relative to the scrshRNA. Induced scrshRNA was used as expression of ADM in these cells should not be effected. In future, CFPAC-1 WT cells could be used as an alternative control. As RAMP-3 was not detected using RAMP-3 QPCR primers as shown in the Chapter 3, RAMP-3 KD was not able to be validated by QPCR and therefore, were not used for *in vivo* experiments. The QPCR results for CFPAC-1 ADM KDs (Figure 4.12) show that on day 1, the KD cells that were not induced by doxycycline had a 69% decrease in ADM expression compared to scrshRNA, whilst the CFPAC-1 ADM knockdowns induced with 500 ng/mL doxycycline, had a 43% decrease in ADM expression at day 1. At day 7, cells without doxycycline treatment or induced with 500 ng/mL doxycycline had a further decrease in ADM expression to 89% and 71% respectively. There was a bigger change in expression over 7 days in the 500 ng/mL doxycycline induced CFPAC-1 ADM KD cells compared to the non-induced cells. Notable significant differences were seen between day 1 ADM KD with no doxcycline and scrshRNA ($p< 0.0001$), day 7 ADM KD no doxycycline and scrshRNA ($p< 0.0001$), day 1 doxycycline induced CFPAC-1 ADM KD and day 7 induced CFPAC-1 ADM KDs ($p= 0.05$), day 1 doxycycline induced and scrshRNA ($p= 0.002$) and day 7 doxycycline induced scrshRNA ($p< 0.0001$).

The larger decrease in ADM expression in the non-induced cells could be attributed to leakiness of the inducible promoter with GFP. Nash & Lever (2004) showed 3 days after transduction of 293T cells with either a lentiviral vector or control plasmid without viral packaging and GFP, both had a high percentage of GFP positive cells. Kozlova *et al* (2020) have suggested that cells naturally have some

auto-fluorescence when live or dead, this can be from endogenous fluorophores originated from mitochondria and lysosomes, also flavaproteins, NADPH, lipo-pigments and aromatic amino acids. Therefore, the high GFP expression levels may not completely correlate with successful transduction and may explain the similar levels of ADM expression in non-induced and induced KDs. Treating WT cells with doxycycline and measuring the impact this has on GFP expression could be completed in future. This data could be used to normalise the fluorescence detected in KD cells compared to WT cells.

Furthermore, basal leakiness is a reoccurring issue in Tet systems which results in mRNA expression in non-induced cells being similar to that in doxycycline induced cells. This can be from cryptic promoters or false promoters that lead to leaky expression in non-induced cells. Meyer-ficca *et al* (2004) tested different vector systems and showed promoter leakiness, both induced and non-induced promoters showed similar protein and luciferase activity following induction. Another important of consideration is that fetal bovine serum (FBS) added to media may contain traces of tetracycline including doxycycline as it is widely administered to animals by vets. This may explain the similar levels in ADM expression between induced and non-induced KDs. Using tetracycline free FBS in future would reduce unintentional induction of KDs.

Another important consideration is that the selection process may have selected a subpopulation of cells that intrinsically express less ADM than the parent population. Without the limitations of COVID-19, multiple CFPAC-1 ADM KD cells could have been developed to generate multiple KD strains or isolate individual clones to compare different ADM KDs. This would have allowed for selection of KD cells that intrinsically express more ADM. This would have shown more distinct differences in ADM mRNA expression between CFPAC-1 ADM KDs, CFPAC-1 scrshRNA and CFPAC-1 wild-type cells. Furthermore, there may have been more defined differences in viability/apoptosis assays and in tumour growth, immune cell populations, Ki67/α-SMA/endomucin expression in future experiments.

Following ADM KD validation, Luc-RFP was transduced into CFPAC-1 ADM KD cells and CFPAC-1 scrshRNA controls for use *in vivo*. Transducing the cells with RFP and luciferase allows for visualisation *in vitro* and *in vivo* (Figure 4.14 and Figure 4.15). *In vitro,* differences in luminescence between Luc-RFP transduced and Luc-RFP non-transduced KDs were measured. This showed a clear increase in luminescent signal in transduced cells. This was also shown when the cells were treated with D-luciferin and the bioluminescence of the cells was measured using IVIS. D-luciferin acts as an enzyme to the luciferase and produces a bioluminescent signal (Chapter 6). CFPAC-1 ADM KD and CFPAC-1 scrshRNA cells were the only cell lines selected for *in vivo* applications as they had more validation than RAMP-3, this decision complies with the 3R's (replacement, reduction and refinement) that ensure animals are treated in the most humane way. Further validation including a QPCR would be needed to use RAMP-3 KD *in vivo* to ensure that the decrease in RAMP-3 expression was significant.

The development of the KDs with or without Luc-RFP provide potential to develop *in vitro* and *in vivo* assays to compare the effects reduced levels of ADM/RAMP-3 to normal expression levels. Previous studies have shown the potential implications of ADM and RAMP-3 KDs. For example, ADM KDs have resulted in increased apoptosis in hepatocellular carcinoma, colorectal cancer and osteosarcoma (Dai et al., 2013; Li et al., 2014; Wang et al., 2014). ADM KDs have also been shown to regulate angiogenesis by decreasing expression of VEGF and inhibiting angiogenesis in ovarian and colorectal cancer (Wang et al., 2014; Zhang et al., 2017). Furthermore, ADM has been to promote metastasis, for example, KDs resulted in the reversal of EMT in intrahepatic cholangiocellular carcinoma (Zhou et al., 2015). ADM has also been shown to regulate mast cells and macrophage polarisation in other studies (Pang et al., 2013; Zudaire et al., 2006). There are significantly fewer studies investigating the role of RAMP-3 KDs in cancer however, most recently Dai *et al* (2020) showed RAMP-3 KOs in PaCa cells reduced metastasis. Overall, these data show that more research is needed investigating the role of RAMP-3 in cancer and that there is also a gap in ADM KD studies relating to PaCa.

4.4.2 CFPAC-1 ADM KD and CFPAC-1 RAMP-3 KD reduce cell viability compared to CFPAC-1 WT cells

The data collected shows that KD of ADM and RAMP-3 reduces the viability of cells compared to CFPAC-1 WT cells (Figure 4.13). However, CFPAC-1 scrshRNA cells were shown to have the lowest viability out of all the cell types. This suggests that transducing the cells with inducible lentiviral shRNA has an impact on viability regardless of KD of a specific gene. The large increases in viability from day 0 to day 3 as the calculations are based on normalising the luminescence of each individual cell line (CFPAC-1 ADM KD, CFPAC-1 RAMP-3 KD, CFPAC-1 scrshRNA and CFPAC-1 wild-type cells) to day 0. As the cells proliferated over 72 hours, the number of viable cells detected increases relatively. In future, normalising the viability to wild-type cells on each day would show how proliferation of KD cells and scrshRNA controls changes relative to wild-type cells. There is currently limited literature in relation to KD of ADM and RAMP-3 in PaCa cells and the effect on proliferation. However, Ishikawa *et al* (2003) showed that addition of ADM antagonist to BxPC-3 cells and PCI-35 cells which were both shown to express CLR and RAMP-2, had no effect on proliferation *in vitro.* However, *in vivo* administration of ADM antagonist to PCI-35 tumours showed a decrease in tumour growth. This however, could be due to effects on other cells within in the tumour microenvironment, not the PaCa cell themselves. This is supported by Dai *et al* (2020) where RAMP-3 knockouts (KOs) developed in cancer associated fibroblasts (CAFs) were co-cultured with PAN02 PaCa cells which resulted in a decrease in *in vitro* cell proliferation. This suggests that CAFs may regulate PaCa proliferation. Keleg *et al* (2007) showed that addition of ADM to 5 PaCa cells had an inhibitory effect on 2 out of 5 cell lines whilst the remaining 3 had no change in proliferation.

In other cancer cell lines ADM KDs have also been shown to reduce the proliferation of cancer cells. Wang *et al* (2014) showed that silencing ADM in colorectal SW480 cells resulted in decreased cell proliferation *in vitro.* This was also shown by Yao *et al* (2019) where KD of ADM in osteosarcoma cells decreased cell proliferation. Addition of exogenous ADM to osteosarcoma cells significantly increased

proliferation. In prostate cancer cell lines, Abasolo *et al* (2004) showed that overexpression of ADM in PC-3 and LNCaP cells inhibited proliferation and that proliferation of DU145 cells was not affected. Whilst addition of exogenous ADM to DU145 cells increased proliferation by 25% and had no effect on PC-3 and LNCaP cells (Rocchi et al., 2001). Furthermore, Berenguer-Daizé *et al* (2013) showed that addition of αAM to DU145 cells inhibited proliferation of cells in a dose dependent manner. After 8 days of treatment, proliferation decreased by 52% at the highest dose of αAM compared to IgG controls. These data suggest DU145 respond to ADM in a paracrine manner, whilst inhibition of PC-3 and LNCaP proliferation may have been induced by autocrine effects.

Together these data show that CFPAC-1 ADM KDs and RAMP-3 KDs have a decrease in cell viability. KD of ADM has also shown to decrease proliferation of both osteosarcoma cells and colorectal cancer cells suggesting that ADM does influence cancer cell proliferation. However, other studies have demonstrated that cancer cell lines were not affected by exogenous inhibition or stimulation of ADM, including PaCa cells. It is important to consider that these studies were not KD studies and that some cell lines may respond to autocrine ADM and others to paracrine stimulation by ADM. More research into the effect of ADM and RAMP-3 in PaCa cell lines is needed, although the recent study by Dai *et al* (2020) suggests that other cells of the tumour microenvironment (CAFs) may have an effect on proliferation.

4.5 Conclusion

These data show successful development of inducible lentiviral ADM KDs and CFPAC-1 scrshRNA controls. Induction of ADM, RAMP-3 and scrshRNA KDs using doxycycline at different concentrations resulted in a dose dependent increase in GFP expression (Figure 4.7, Figure 4.9, Figure 4.11). ADM KDs were validated using QPCR to calculate the fold change in ADM mRNA expression and percentage decrease in ADM mRNA expression relative to CFPAC-1 scrshRNA control cells. This showed an 89% and 71% decrease in ADM expression by day 7 without doxycycline and with 500 ng/mL doxycycline respectively (Figure 4.12). CFPAC-1 ADM KDs were also shown to have decreased proliferation compared to CFPAC-1 WT cells (Figure 4.13). RAMP-3 KDs were successfully induced by doxycycline as shown in Figure 4.8 and Figure 4.9 however, QPCR validation was not completed. High cycle numbers required to detect RAMP-3 mRNA expression (Chapter 3), made it difficult to quantify percentage decreases in expression. Viability assays comparing the effect of CFPAC-1 RAMP-3 KDs compared to CFPAC-1 WT cells and CFPAC-1 scrshRNA, showed that proliferation of CFPAC-1 RAMP-3 KDs decreased relative to CFPAC-1 WT cells but not CFPAC-1 scrshRNA. CFPAC-1 scrshRNA had the lowest percentage viability (Figure 4.13). As RAMP-3 KDs were not validated by QPCR, they were used for *in vitro* applications including viability assays and apoptosis assays (Chapter 5). ADM KD and scrshRNA control cells were successfully transduced with Luc-RFP for *in vivo* applications (Chapter 6) as shown by Figure 4.14 and Figure 4.15.

Overall, these data show that RAMP-3 KDs would need further validation for *in vivo* applications. CFPAC-1 ADM KDs have been successfully developed and validated for use in both *in vitro* and *in vivo.* In future, ADM and RAMP-3 KDs should be developed in other cell lines to see if the different characteristics of cells described in Chapter 3 might cause cells to respond differently to ADM and RAMP-3 KDs *in vitro* and *in vivo*.

CHAPTER 5: EFFECTS OF ADM AND RAMP-3 KNOCKDOWNS ON PROLIFERATION AND APOPTOSIS

5.1 Introduction

5.1.1 The use of gemcitabine and 5-FU in PaCa treatment

Gemicitabine and 5-FU are currently used as part of the treatment regime for PaCa in both late stages and advanced stage. One of the main difficulties in treating PaCa is that is often diagnosed in late stages, finding the right treatment for later stage patients can be difficult as patients may not be fit enough (determined by their ECOG status) for more intense treatments including FOLFIRINOX. In early stages, gemcitabine is offered alone or in combination with other therapies including 5-FU (Chapter 1, section 1.1.6) following tumour resection. Despite the availability of these treatments, median overall survival is similar with gemcitabine alone or gemcitabine in combination with 5-FU.

Neoptolemos *et al* (2010) have shown that there is not a significant difference in median between PDAC patients who had undergone surgical resection followed by treatment with either 5-FU in combination with folinic acid or gemcitabine alone. Median survival was 23 months and 23.6 months respectively. However, patients treated with 5-FU did have more adverse effects than patients treated with gemcitabine alone. Multiple studies comparing median survival between gemcitabine therapy alone and gemcitabine in combination with 5-FU or the pro-drug to 5-FU, capecitabine did not show significant differences in survival showing that neither has a survival advantage (Costanzo et al., 2005; Cunningham et al., 2005; Scheithauer et al., 2003). Ueno *et al* (2009) showed that in patients who have undergone both surgery and gemcitabine chemotherapy overall survival was 22.3 months vs 18.4 months. Disease free survival was also longer in patients who received gemcitabine compared to surgery alone (11.4 months vs 5 months).

FOLFIRINOX is also a therapy that is used for PaCa treatment dependent on the patients ECOG status which determines how fit and well the patient is. This is offered to patients with early diagnosis and resectable tumours or as a first line of treatment if patients have metastasis and are fit enough. Conroy *et al* (2018) have shown median overall survival to be 54.3 months in patients treated with FOLFIRNOX compared to 35 months in patients treated with gemcitabine alone following tumour resection.

However, adverse events are more prevalent in patients treated with FOLFIRINOX with 75.9% patients experiencing adverse effects compared to 52.9% in gemcitabine treated patients. In patients with metastatic cancer, median overall survival was 11.1 months following FOLFIRINOX treatment and 6.8 months in patients treated with gemcitabine. There were more adverse events in FOLFIRINOX treated patients however, definitive degradation in quality of life after 6 months of treatment was more common in patients treated with gemcitabine (66% with gemcitabine treatment vs 31% in FOLFIRINOX patients).

These data demonstrate the difficulty in finding a treatment that improves PaCa patient survival and that does not have serious adverse effects for already unfit patients. It shows that the regime for PaCa treatment may need reassessing or novel approaches to treating patients need to be developed. Therefore, understanding the PaCa tumour microenvironment and the key molecules involved in PaCa development could provide useful insights into how to improve response to current chemotherapies. Furthermore, understanding this may provide novel targets for PaCa treatment. One of the main issues in PaCa treatment is that often chemotherapies are unable to reach the target site due to the dense stromal environment that develops. PSCs are one of main cell types found within the PaCa tumour microenvironment and have been shown to promote tumorigenesis. Hwang *et al* (2008) showed that apoptosis of BxPC-3 cells was significantly lower in cells treated with human PSC conditioned media compared to cells BxPC-3 cells cultured in serum free media (9.4% and 38.9% apoptosis respectively). These data show that targeting cells other than the tumour cells themselves could provide a novel approach to PaCa therapy and improve the effectiveness of currently available chemotherapies including gemcitabine and 5-FU.

5.1.2 ADM and proliferation of cancer cells

Dysregulation of proliferation is one of the main hallmarks of cancer described by Hanahan & Weinberg (2000). In normal tissue, proliferation is tightly regulated by the production and release of growth promoting signals which ensure the homeostasis of cell number, ensuring normal tissue

architecture and function. In cancer, the regulation of growth promoting signals and the cell cycle is dysregulated. One of the main aims of chemotherapy is to alter the proliferation of cancer cells to prevent the tumours from getting larger and spreading. ADM has been shown to induce proliferation in different cancers including PaCa, prostate, glioblastoma, colorectal, renal and gastric cancer (Abasolo et al., 2004; Berenguer-Daizé et al., 2013; Deville et al., 2009; Keleg et al., 2007; Nouguerède et al., 2013; Ouafik et al., 2002; Qiao et al., 2017).

There are few studies investigating the role of ADM in proliferation of PaCa however, Keleg *et al* (2007) showed the role of ADM in proliferation *in vitro*. They showed that treating 5 different PaCa cell lines with recombinant ADM resulted in ~20% inhibition in 2 cell lines. There was no significant effect in other cell lines. They also treated the panel of PaCa cells with a CLR antagonist finding an increase in proliferation in Colo-387 cells at a concentration of 4 nM, however, in other cell lines there were no growth inhibitory or stimulatory effects. Overall, the results showed that ADM only has slight growth inhibitory effects in two of the PaCa cell lines however, this study showed ADM to have more of a role in inducing invasion of PaCa cells and inducing angiogenesis. *In vivo,* Dai *et al* (2020) have shown a reduction in Ki67 positive cells in mouse tumours and RAMP-3 KO CAFs compared to RAMP-3 overexpressing CAFs. These data suggest that CAFs expressing ADM may induce proliferation of tumour cells.

Abasolo *et al* (2004) showed that ADM has a growth inhibitory effects in prostate cancer cell lines. Overexpressing ADM in PC-3 and LNCaP cells resulted in growth inhibition of the cells and addition synthetic ADM peptide to WT PC-3 cells and LNCaP cells resulted in 20% and 50% inhibition respectively at concentrations of 10-1000 nM ADM peptide. WT and overexpressing Du145 cells however, showed no significant effect on proliferation except when treated with 1000 nM ADM peptide. In contrast, Berenguer-Daizé *et al* (2013) showed that ADM stimulated DU145 cell proliferation *in vitro*. Treatment of the cells with αAM resulted in inhibition of proliferation of DU145 and PC-3 cells.

These results are closely mirrored in U87 glioblastoma cells where treatment with an anti-ADM antibody resulted in decreased proliferation of the glioma cells by 16%, 28% and 33% at days 4, 6 and 8. Whilst addition of ADM resulted in a 13% and 12% increase in proliferation after 6 and 8 days of treatment (Ouafik et al., 2002). In colorectal cancer cells treated with ADM, proliferation increased by 20% and treatment of these cells with anti-CLR/RAMP-2 and anti-CLR/RAMP-3 antibodies resulted in 70% and 80% inhibition of proliferation respectively. 70% inhibition of proliferation was also seen when cells were treated with AM_{22-52} (Nouguerède et al., 2013). In renal cell carcinoma, anti-ADM antibody treatment resulted in 60% and 20% inhibition of proliferation in BIZ and 786-O cells. AM_{22-52} resulted in 40% inhibition of BIZ. These data suggest that ADM may induce its proliferative effects in an autocrine manner in the different cancer cell lines.

Overall, these data show the lack of research around ADMs role in inducing proliferation in PaCa. The data suggests that ADM has an inhibitory effect on proliferation of PaCa cells which is also supported by Abasolo *et al* (2004) showing the same results in two prostate cancer cell lines. However, other studies have shown that ADM induces proliferation in an autocrine manner. Therefore, in PaCa and in the prostate cancer cell lines that showed inhibitory effects of ADM on proliferation, induction of proliferation may be paracrine. This is supported by the *in vivo* study by Dai *et al* (2020) who showed RAMP-3 K0 CAFs to induce proliferation of PAN02 cells.

5.1.3 The role of ADM in regulating apoptosis in cancer and resistance to chemotherapy

Apoptosis is an important physiological process used to regulate cell death. In cancer, this system often becomes dysregulated, resulting in the survival of cancer cells and establishment of primary tumours. One of the key factors contributing to PaCa prognosis, is resistance to apoptosis which makes it unresponsive to the conventional chemotherapies used in the treatment of cancers. Schniewind *et al* (2004) have shown one of the mechanisms by which PaCa resists gemcitabine by altering apoptosis. They overexpressed Bcl-x_L (anti-apoptotic) and Bax (pro-apoptotic) in Colo357 cells and treated them with gemcitabine. Cells treated with gemcitabine had 80% intact DNA when Bcl-x_L was overexpressed,

compared to 20% intact DNA in WT and Bax overexpressing cells *in vitro*. Furthermore, *in vivo* treatment of Bcl-x_L overexpressing cells with or without gemcitabine showed no changes in tumour size, suggesting that this molecule is involved in preventing apoptosis in PaCa. Bold, Chandra, & Mcconkey (1999) also showed a correlation between enhanced chemo-resistance in PaCa and overexpression of Bcl-2.

5-FU induces DNA damage which should activate DNA repair systems and induce apoptosis. However, lack of sensitivity to 5-FU is common in PaCa, Shi *et al* (2002) showed this in 4 PaCa cell lines. They showed that PaCa cell lines are more sensitive to gemcitabine over 5-FU. PaCa cell lines had a range of responses to 5-FU with IC_{50} ranging from 0.22-4.63 µM compared to 11.51-42.2 nM when treated with gemcitabine. Following repeated treatment, the IC_{50} increased in two of the cell lines treated with 5-FU and one cell line treated with gemcitabine. Furthermore, mRNA expression of pro-apoptotic molecules of the Bcl-2 family corresponded with responsiveness to chemotherapies. Capan-1 cells had lower basal levels of Bcl-x_L and mcl-1 mRNA (anti-apoptotic molecules) and higher sensitivity to 5-FU and gemcitabine. Whilst MiaPaCa-2 and AsPC-1 cells displayed higher basal levels of these molecules and more resistance to 5-FU and gemcitabine. Oehler, Norbury, Hague, Rees, & Bicknell (2001) have shown a relationship between ADM upregulation in endometrial cancer under hypoxic conditions which induces the upregulation of Bcl-2, causing resistance to apoptosis. Ishikawa cells (endometrial cancer cells) were transfected with ADM or treated with ADM showing an increased resistance to hypoxia induced apoptosis. After 36 hours of ADM treatment at a concentration of 10^{-6} M, there was a 40% decrease in hypoxic induced cell death. Li, Takeuchi, Ohara, & Maruo, (2003) also showed this in cervical invasive carcinoma, where higher expression of Bcl-2 and ADM, correlated with increased apoptosis resistance compared to carcinoma in situ and normal cervical tissue.

Further evidence of the role of ADM in causing resistance to apoptosis in cancer has been shown by Martinez *et al* (2002). Overexpression of ADM in T47D and MCF-7 cell lines resulted in decreased apoptosis. Deville *et al* (2009) also correlated high levels of ADM staining with low levels of apoptosis

detected through caspase-3 in renal cell carcinoma. In colon cancer models, KD of ADM *in vivo* was associated with increased apoptosis represented by an increase in number of cleaved caspase-3 cells in tumour xenografts compared to control tumours (Wang et al., 2014). ADM KDs in osteosarcoma also showed an increase in apoptosis compared to control group (Dai et al., 2013) and in colorectal cancer, the apoptotic index was higher in tissue sections following treatment of tumours with an antibody against ADM.

Overall, the combined data shows a correlation between increased ADM expression in cancer and inhibition of apoptosis. ADM has been associated with regulating pro- and anti- apoptotic molecules in cancer and therefore may be partially responsible for causing resistance to gemcitabine and 5-FU in PaCa. Therefore, 5-FU and gemcitabine were selected to treat KD cells and determine the effects on apoptosis. Targeting ADM and RAMP-3 in combination with gemcitabine or 5-FU, could be a novel approach to treatment of pancreatic cancer.

5.1.4 Hypothesis

The null hypothesis is ADM and RAMP-3 have no involvement in regulating proliferation of PaCa cells and do not inhibit apoptosis. Therefore, ADM and RAMP-3 are not involved in promoting PaCa tumour proliferation and inhibition of apoptosis.

5.1.5 Aim and Objectives

The main aims were to determine the effects of chemotherapies (gemcitabine and 5-FU) on the viability and apoptosis of CFPAC-1 ADM KDs, CFPAC-1 RAMP-3 KDs, CFPAC-1 scrshRNA and CFPAC-1 WT cells. The objective was to see if knocking down ADM and RAMP-3 had an effect on the proliferation and apoptosis of cancer cells.

To determine whether CFPAC-1 KDs alter the response to gemcitabine and 5-FU chemotherapy and effect the proliferation of KD cells compared to scrshRNA and WT cells, promega Real-Time-Glo cell viability assays were completed. Furthermore, to determine if apoptosis is effected by knocking down ADM and RAMP-3 and whether KDs respond differently to gemcitabine and 5-FU compared to

scrshRNA and WT cells, promega caspase 3/7 apoptosis assays were completed. The data was plotted and analysed on GraphPad Prism, version 9.2.0. Two-way repeated measure ANOVA, one-way ANOVA and non-linear regression was used to determine any statistical significance within the data.

5.2 Methods

Cells used for viability and apoptosis assays were sub-cultured and counted as described in Chapter 2, Section 2.1.1 and Section 2.1.4. CFPAC-1 ADM KDs, CFPAC-1 RAMP-3 KDs and CFPAC-1 scrshRNA cells were transduced as described in Chapter 4, Section 4.2.1.

5.2.1 Gemicitabine and 5-FU Viability assay

The RealTime Glo™ MT cell viability assay was used as outlined in Chapter 4, Section 4.2.4 to determine the effects of current chemotherapies used to treat PaCa (gemicitabine and 5-FU) on CFPAC-1 ADM, CFPAC-1 RAMP-3, scrshRNA and WT cells. The cells were seeded in a white clear bottom 96-well plate at a density of 2,000 cells/well in 100 µL full serum media in triplicate (10% FCS). The following day, the viability substrate was added as described in Chapter 4, section 4.2.5 in 5% media and incubated for an hour before the baseline luminescence was read on the plate reader. 5% media was used as this is half the optimal concentration of FBS needed for growth of CFPAC-1 cells. This reduces bias in detecting any increases or decreases in viability of KD cells, scrshRNA and WT cells following treatment with gemcitabine and 5-FU, as the cells grow at 50% of their normal rate. After the baseline reading, the cells were treated with gemcitabine and 5-FU drug dilutions ranging from 1µM to 1nM. Readings were taken at 24 hours, 48 hours and 72 hours after addition of the RealTime Glo™ MT Viability Reagents. The stocks of gemcitabine and 5-FU were made up to 20 mM according to the manufacturers' guidelines. 50X aliquots were prepared and diluted in PBS so that 2 µL of treatment could be added to each well (100 µL total volume per well). An untreated control was also prepared containing DMSO. The treatment stocks and aliquots were stored at -20^{o}C. The data was plotted on GraphPad Prism version 9.2.0.

5.2.2 Gemicitabine and 5-FU Apoptosis assay

The Promega Caspase-Glo® 3/7 assay was used to determine late stage apoptosis in CFPAC-1 ADM KD, RAMP-3 KD, scrshRNA and WT cells following treatment with different concentrations of gemcitabine and 5-FU daily for 48 hours. This is an endpoint luminescent assay that measures caspase -3 and -7

activity in cells (Figure 5.1). The luminescence is proportional to the amount of caspase activity. To generate a luminescent signal, pro-luciferin substrate is cleaved by caspase 3/7 to produce aminoluciferin, a substrate to luciferase. Following cleavage, together with aminoluciferin, oxygen and magnesium bound adenosine triphosphate (ATP) produce oxyluciferin, carbon dioxide, adenosine monophosphate and disphosphate. Oxyluciferin decays and produces a photon of light producing the luminescent signal.

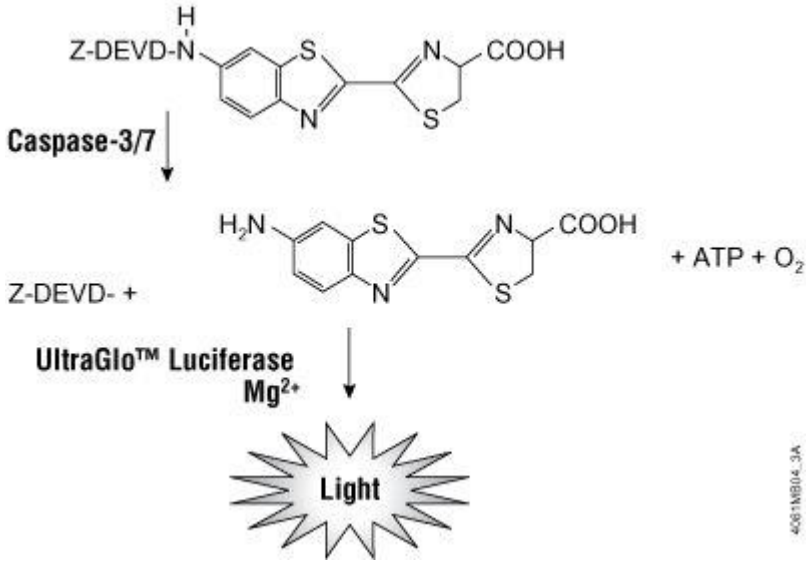

Figure 5.1 Schematic diagram of the Caspase 3/7 assay. After caspase cleavage of proluciferin-DEVD substrate, aminoluciferin a substrate for luciferin is released, resulting in a luminescent signal in the presence of ATP (Promega, 2019).

CFPAC-1 WT, scrshRNA and RAMP-3/ADM knockdown CFPAC-1 cells were used for this experiment. The cells were seeded at a density of 20,000 cells per well in a white clear bottom 96 well plate and left overnight at 37°C in 50 µL optimal growth media. The media was changed to serum free media to induce stress on the cells the following day and the cells were treated with different doses of gemcitibine of 5-FU (1µM- 1nM) daily 48 hours. Control wells containing full growth serum and 0% growth serum without cells were incubated as a baseline for negative and postive controls. After 48 hours of treatment, 50µL of the enzyme substrate reagent was added per well. The plate was

incubated at room temperature for an hour on a plate shaker. The luminescent signal was read on the Ensight® Perkin Elmer plate reader. The data was plotted on GraphPad Prism version 9.2.0.

5.3 Results

5.3.1 Effect of gemcitabine on viability and apoptosis of KD cells

Gemcitabine is a chemotherapy used for the treatment of PaCa and therefore, the effect of different doses of gemcitabine on viability and apoptosis of CFPAC-1 KD cells, scrshRNA controls and WT cells was compared. Figure 5.2 shows the change in viability of KD cells and controls over 3 days. Two-way ANOVA analysis of CFPAC-1 ADM KD viability assays shows a significant difference between the different doses of gemcitabine ($p< 0.0001$) and between the different days the cells were treated with gemcitabine ($p< 0.0001$). Following 3 days of treatment with 1 µM gemcitabine, there was a 68.2% decrease in viability compared to untreated cells ($p <0.0001$). At a concentration of 500 nM gemcitabine, there was a 67.5% decrease in viability compared to untreated cells and at a dose 100 nM gemcitabine, there was a 63.6% decrease in viability

Two-way ANOVA analysis shows a significant difference ($p <0.0001$) between drug concentration and day in CFPAC-1 RAMP-3 KD viability assays following gemcitabine treatment (Figure 5.2). There was also a significant difference between the different days alone and the different drug concentrations of gemcitabine alone ($p <0.0001$). One-way ANOVA analysis comparing CFPAC-1 ADM KDs, RAMP-3 KDs, scrshRNA and WT cells response to different concentrations of gemcitabine on day 3 shows no significant difference between different cell lines except at a dose of 100 nM. At 100 nM, there is a significant difference between CFPAC-1 ADM KD on day 3 and scrshRNA ($p= 0.009$) percentage viability. On day 3, CFPAC-1 ADM KDs had 36.4% viability compared to scrshRNA at 61.8%.

Figure 5.3 shows a gemcitabine dose response curve for CFPAC-1 ADM KD, RAMP-3 KD, scrshRNA and WT cells. The $\log IC_{50}$ was determined by non-linear regression to be -7.774, -7.919, -7.698, -7.553 in CFPAC-1 ADM KDs, CFPAC-1 RAMP-3 KDs, CFPAC-1 scrshRNA and CFPAC-1 WT cells respectfully.

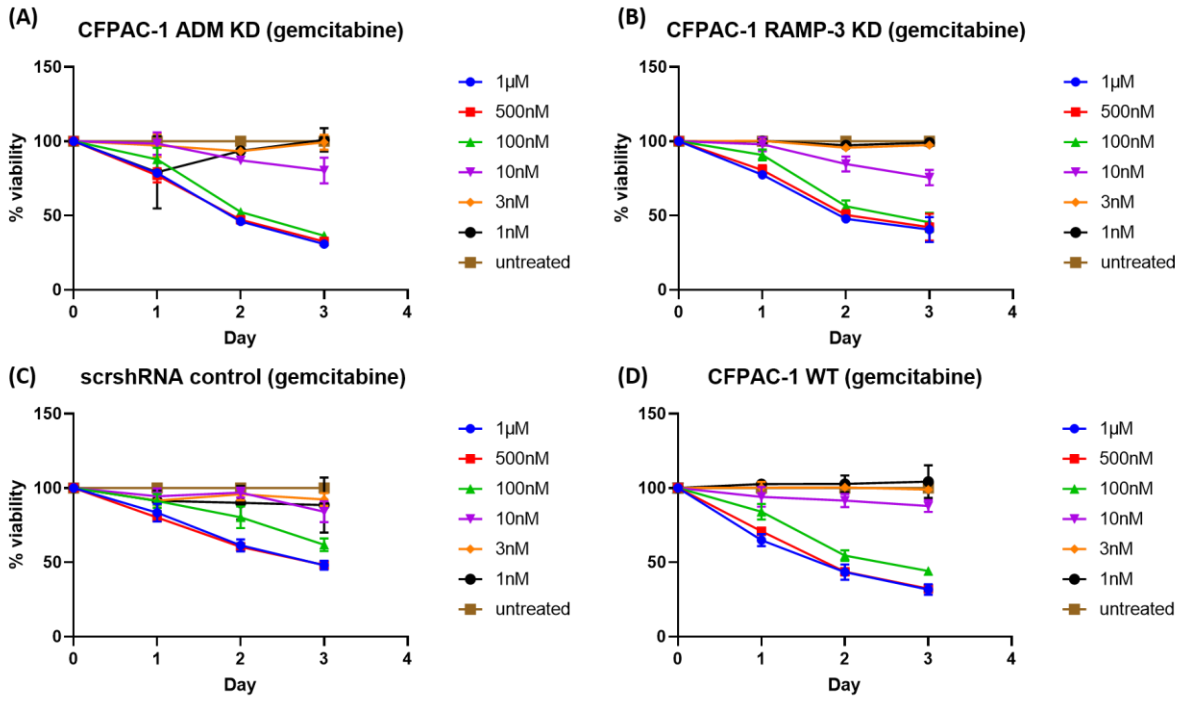

Figure 5.2 Effect of different doses of gemcitabine on percentage viability determined over 3 days. Two-way repeated measure ANOVA analysis showed that (A) CFPAC-1 ADM KDs treated with different doses of gemcitabine and induced with doxycycline showed a significant difference ($p > 0.0001$) in viability over 3 days of treatment (B) RAMP-3 KDs treated with gemcitabine and induced with doxycycline showed a significant difference ($p > 0.0001$) in viability following treatment with different doses of gemcitabine over 3 days. (C) CFPAC-1 scrshRNA treated with different doses of gemcitabine and induced with doxycycline showed a significant difference ($p > 0.0001$) in percentage viability following 3 days of treatment (D) CFPAC-1 WT cells treated with different doses of gemcitabine and induced with doxycycline showed a significant difference ($p > 0.0001$) in percentage viability following 3 days of treatment. One-way ANOVA analysis also showed a significant difference between CFPAC-1 RAMP-3 KD and CFPAC-1 scrshRNA treated with 100 nM gemcitabine at day 3. These results are based on the means of 3 independent repeats. Data was normalised against untreated cells which were calculated to have 100% viability. Data presented as mean ± SEM.

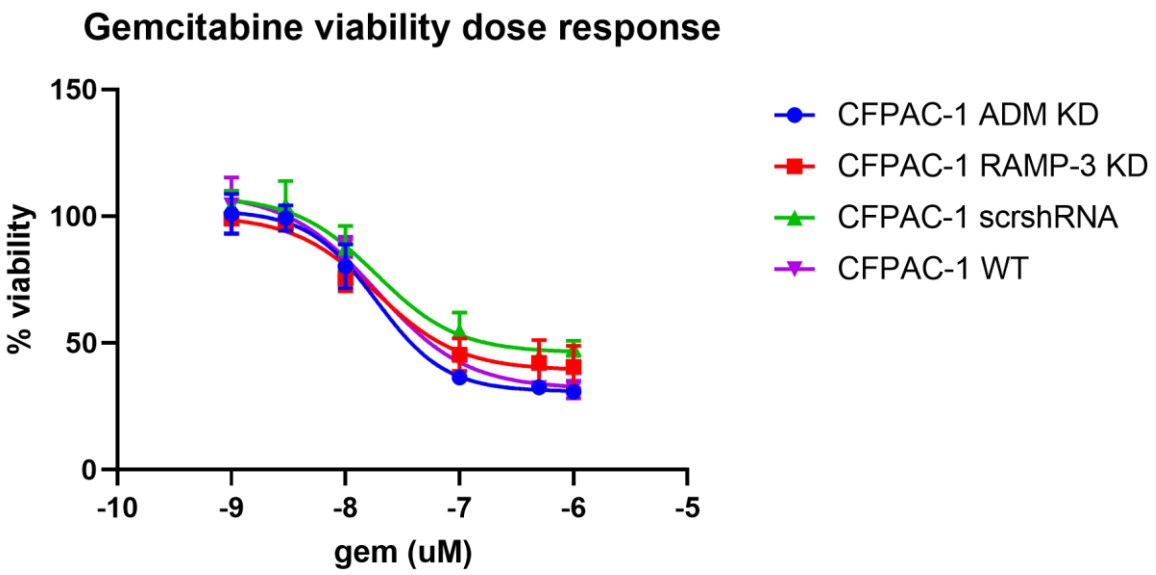

Figure 5.3 Day 3 gemcitabine viability dose response of CFPAC-1 ADM KD, CFPAC-1 RAMP-3 KD, CFPAC-1 scrshRNA, CFPAC-1 WT cells. Non-linear regression analysis showed that there is no difference in $logIC_{50}$ following 3 days of gemcitabine treatment (p= 0.5375) The $logIC_{50}$ for CFPAC-1 ADM KD, RAMP-3 KD, scrshRNA and WT cells was -7.774, -7.919, -7.698, -7.553 respectively. The data presented is based on the means of 3 independent repeats.

Figure 5.4 shows apoptosis in CFPAC-1 ADM KDs, CFPAC-1 RAMP-3 KDs, CFPAC-1 scrshRNA and WT cells following gemcitabine treatment. Following one-way ANOVA analysis of CFPAC-1 ADM KDs, there was a significant difference between untreated CFPAC-1 ADM KDs and 1 µM and 500 nM treated CFPAC-1 ADM KDs (Figure 5.4). Figure 5.4 shows a 1-fold increase and 1.3-fold increase in apoptosis following gemcitabine treatment at doses of 1 µM and 500 nM in CFPAC-1 ADM KDs compared to untreated cells. CFPAC-1 RAMP-3 KDs also showed a significant increase in apoptosis compared to untreated cells at doses of 1 µM, 500 nM and 100 nM gemcitabine (Figure 5.4). They showed a 1.1-fold, 1.6-fold and 1.7-fold increase in apoptosis respectively. CFPAC-1 RAMP-3 KDs treated with 100 nM gemcitabine, had the largest increase in apoptosis compared to all the cell lines (Figure 5.4). Furthermore, one-way ANOVA analysis confirmed that there is a statistically significant difference between CFPAC-1 RAMP-3 KDs and WT cells treated with 100 nM gemcitabine (p= 0.0002) (Figure 5.4).

CFPAC-1 scrshRNA shows an increase in apoptosis following gemcitabine treatment, with the largest increase at a dose of 100 nM showing a 1.1-fold increase in apoptosis compared to untreated cells (Figure 5.4 and Table 5.1). CFPAC-1 WT cells show the most apoptosis at higher doses of gemcitabine treatment with 2.1-fold, 2.4-fold and 1.5-fold apoptosis at 1 µM, 500 nM and 100 nM respectively.

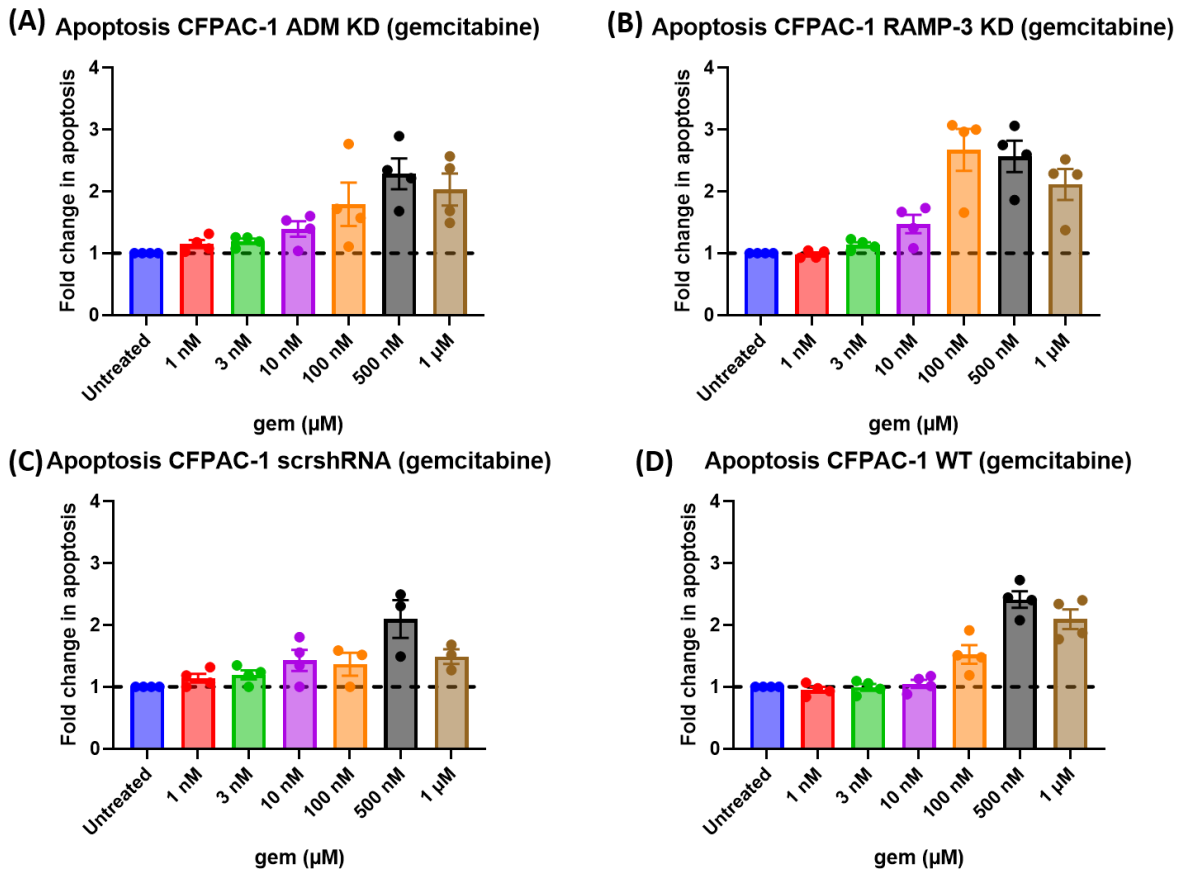

Figure 5.4 Effect of different doses of gemcitabine on apoptosis of KD cells. Fold change in apoptosis was calculated relative to untreated cells. (A) CFPAC-1 ADM KD (B) CFPAC-1 RAMP-3 KD (C) CFPAC-1 scrshRNA (D) CFPAC-1 WT cells. One-way ANOVA analysis and shows a significant difference following treatment of CFPAC-1 ADM KD ($p= 0.02$), CFPAC-1 RAMP-3 KD ($p<0.0001$), CFPAC-1 scrshRNA ($p <0.0004$) and CFPAC-1 WT cells ($p<0.0001$) with different doses of gemcitabine. Data presented is based on the means of 4 independent repeats. Data is presented as mean ± SEM.

5.3.2 Effect of 5-FU on viability and apoptosis of KD cells

5-FU is used as a monotherapy, in combination with gemcitabine or as part of a chemotherapy cocktail (FOLFIRINOX) in early and late stage PaCa. Therefore, the effect of different doses of 5-FU on viability and apoptosis of CFPAC-1 KD cells, scrshRNA controls and WT cells was compared. Figure 5.5 shows the change in viability of KD cells and controls over 3 days. CFPAC-1 ADM KDs, CFPAC-1 RAMP-3 KDs and CFPAC-1 scrshRNA show no significant changes in viability following treatment with different doses of 5-FU. In CFPAC-1 WT cells, there was some effect on viability following 5-FU treatment. There was a 13.2% decrease in viability at a dose of 500 nM 5-FU compared to 100 nM 5-FU treated CFPAC-1 WT cells at day 3 (p= 0.03). There was also a difference between 500 nM 5-FU treated and 3 nM treated 5-FU treated CFPAC-1 WT cells, showing 14.5% less viable cells at 500 nM (p= 0.02). However, the decrease in viability is significantly less than gemcitabine treated cells. Figure 5.6 shows that there is no significant difference between different doses and cell types following 3 days of treatment with 5-FU.

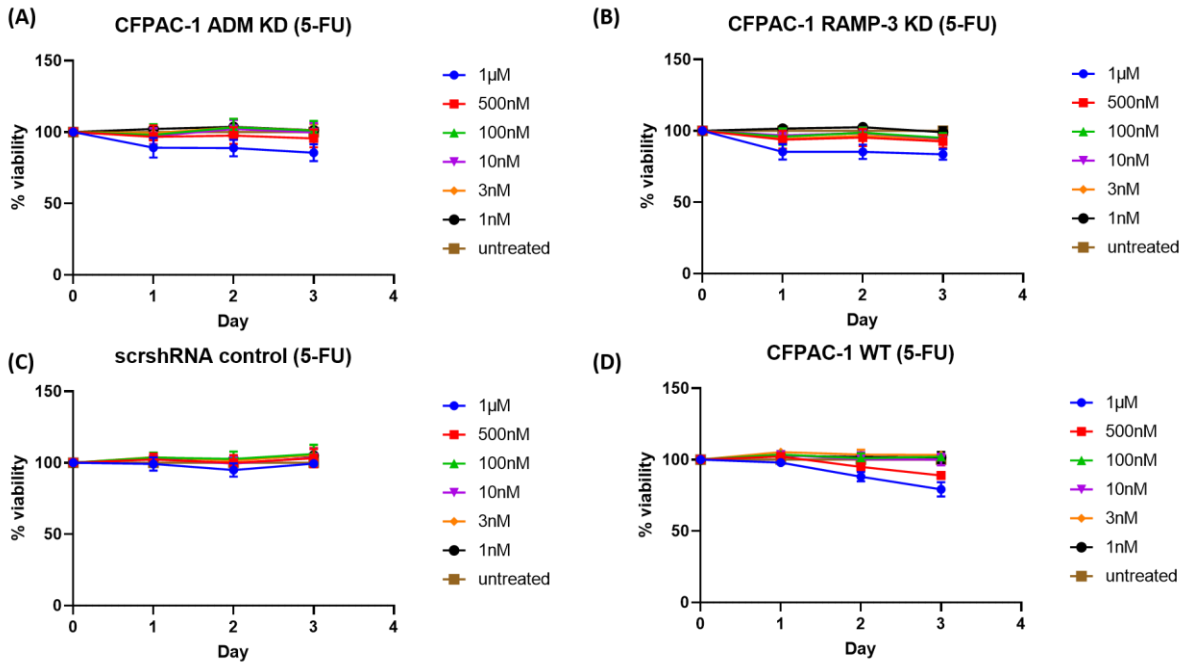

Figure 5.5 Effect of different doses of 5-FU on % viability over 3 days. Two-way repeated measure ANOVA analysis showed no significant difference between different doses of 5-FU and day of

treatment in (A) CFPAC-1 ADM KD (B) CFPAC-1 RAMP-3 KD and (C) CFPAC-1 scrshRNA. However, (D) CFPAC-1 WT cells showed a significant difference between different doses of 5-FU ($p < 0.0001$). These results are based on the means of 3 independent repeats. Data is presented as mean ± SEM.

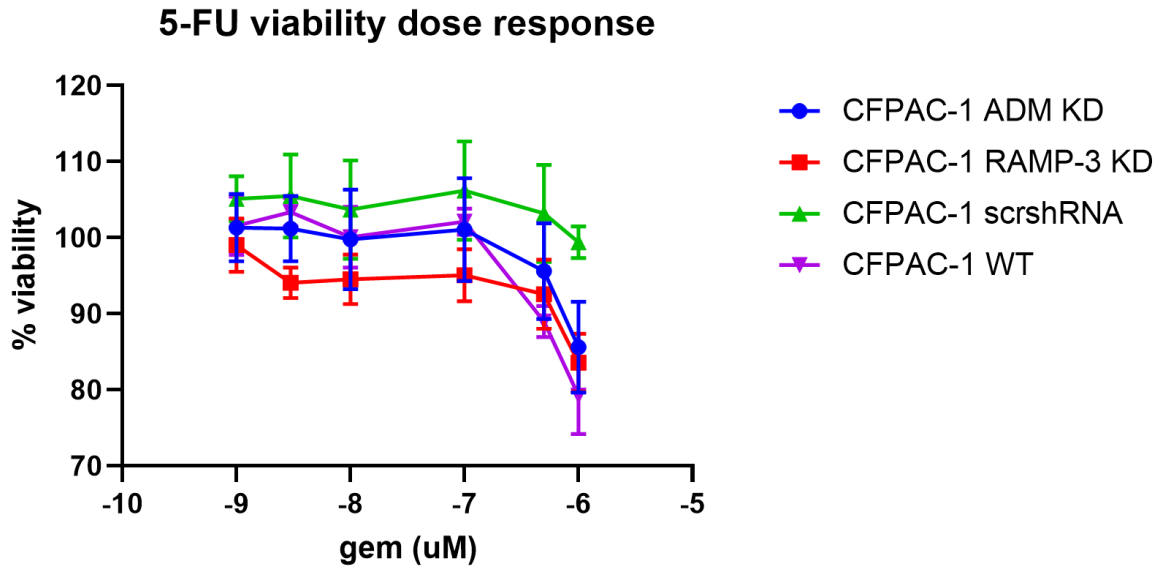

Figure 5.6 Day 3 5-FU % viability dose response of CFPAC-1 ADM KD, CFPAC-1 RAMP-3 KD, CFPAC-1 scrshRNA and CFPAC-1 WT cells. Two-way ANOVA analysis showed no significant difference in interactions between different doses of 5-FU and the different cell lines. There is a significant difference between drug concentrations alone ($p < 0.0001$) and between the different cell lines ($p = 0.001$), CFPAC-1 scrshRNA had the highest percentage viability on day 3 at -6 compared to the other cell lines. $LogIC_{50}$ could not be calculated with the data collected. The data presented is based on the means of 3 independent repeats and is shown as mean ± SEM

The apoptosis data shown in Figure 5.7 shows no significant difference in apoptosis between the different doses of 5-FU and untreated cells in CFPAC-1 ADM KD and RAMP-3 KDs. CFPAC-1 ADM KDs treated with 10 nM 5-FU showed the largest fold increase in apoptosis relative to untreated cells (0.1-fold increase) and at doses of 100 nM and 500 nM 5-FU, there was the smallest fold change in apoptosis compared to untreated cells (0.008-fold increase). This shows that there is no dose-dependent effect on apoptosis following apoptosis treatment in CFPAC-1 ADM KDs and that there is

no significant difference in apoptosis from untreated CFPAC-1 ADM KDs. CFPAC-1 ADM KDs cells had a 0.09-fold increase relative to untreated cells compared to WT cells (1.1-fold increase relative to untreated cells) at a dose of 1 µM 5-FU.

CFPAC-1 RAMP-3 KDs showed no significant difference between untreated RAMP-3 KDs and different doses of 5-FU (Figure 5.7). However, there was a significant difference at a dose of 1 µM 5-FU between CFPAC-1 RAMP-3 KDs and CFPAC-1 WT cells that showed a 0.3-fold and 1.1-fold increase in apoptosis respectively (relative to untreated cells) ($p= 0.001$) (Figure 5.7). At a dose of 500 nM 5-FU, CFPAC-1 RAMP-3 KDs cells showed 0.6-fold less apoptosis compared to CFPAC-1 WT cells treated with the same dose (Figure 5.7). There were similar levels of apoptosis between doses of 1-100 nM 5-FU. CFPAC-1 scrshRNA cells shown in Figure 5.7 showed a significant difference between different doses of 5-FU. ScrshRNA treated with 1 µM 5-FU showed a 0.2-fold decrease in apoptosis compared to untreated cells (Figure 5.7). At a dose of 3 nM 5-FU, there was a 0.2-fold increase in apoptosis compared to untreated cells (Figure 5.7). CFPAC-1 WT cells treated with 5-FU had the highest amount of apoptosis compared to the other cell types however, the percentage of apoptosis is far lower than gemcitabine (Figure 5.4 and Figure 5.7). One-way ANOVA analysis does confirm a statistically significant difference in apoptosis between the means of different doses of 5-FU ($p< 0.0001$). Treatment with 1 µM 5-FU showed the biggest response and fold increase in apoptosis with 1.1-fold more apoptosis compared to untreated cells . All other doses had a similar increase in apoptosis showing that the changes in apoptosis are not dose dependent following 48 hour 5-FU treatment.

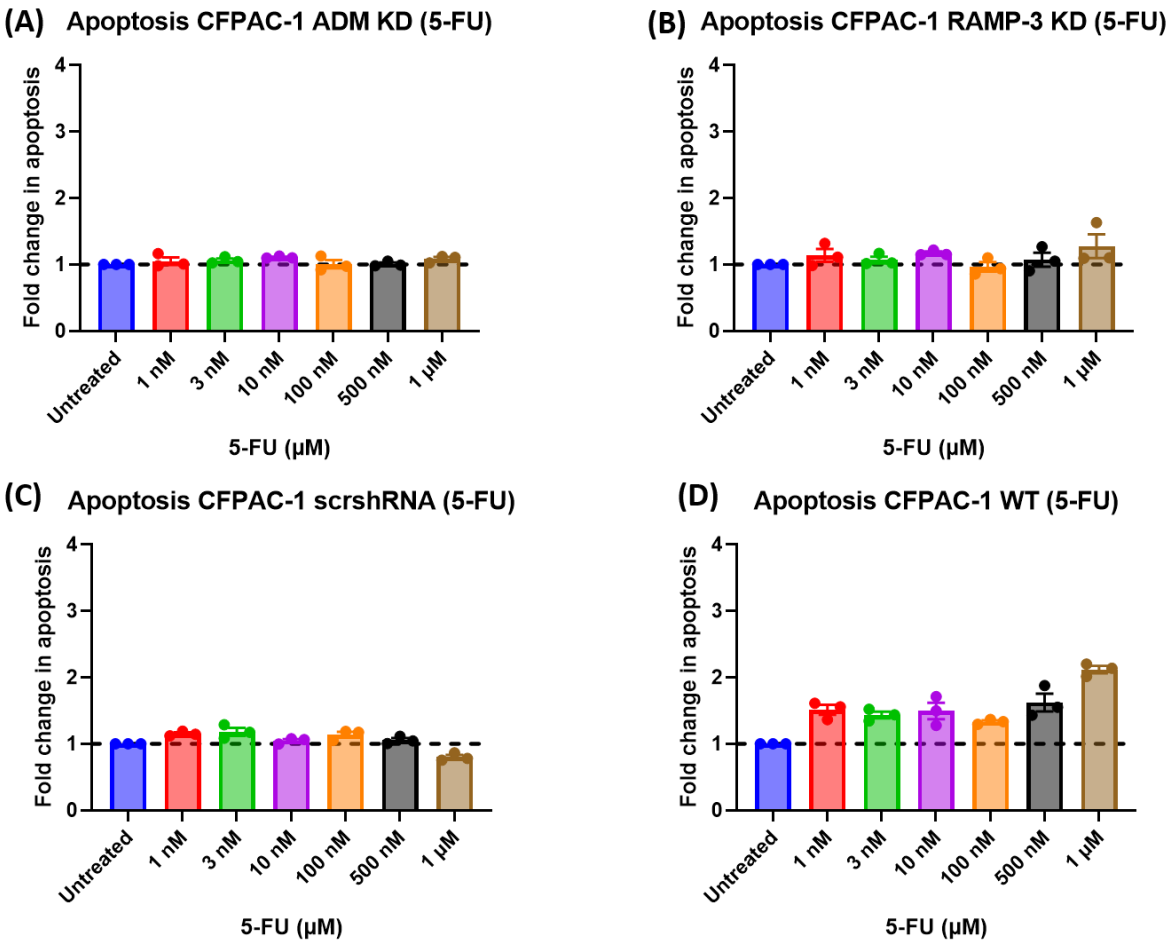

Figure 5.7 Effect of different doses of 5-FU on apoptosis of KD cells compared to controls. Fold change in apoptosis was calculated relative to untreated cells. (A) CFPAC-1 ADM KDs (B) CFPAC-1 RAMP-3 KDs (C) CFPAC-1 scrshRNA (D) CFPAC-1 WT cells. One-way ANOVA analysis shows no significant difference between different doses of 5-FU and apoptosis in CFPAC-1 ADM KDs and CFPAC-1 RAMP-3 KDs. CFPAC-1 scrshRNA showed a significant difference ($p< 0.0001$) between different doses of 5-FU untreated cells. CFPAC-1 WT cells also showed a significant difference between different doses of 5-FU and untreated cells ($p< 0.0001$). In all cell lines, there was a significant difference between the different cell lines at different doses of 5-FU. Data presented is based on means of 3 independent repeats. Data is presented as mean ± SEM.

5.4 Discussion

Gemcitabine and 5-FU are currently used for the treatment of PaCa, gemcitabine is used either alone or in combination with 5-FU as first line therapy or in advanced stages of PaCa. Both these chemotherapies work by inhibiting DNA synthesis by incorporating into the DNA of cancer cells, resulting in in DNA damage. In PaCa, treatment with these chemotherapies often results in resistance and therefore, unsuccessful treatment of patients unless the cancer is detected in early stages and tumour resection is an option.

Proliferation and dysregulation of apoptosis are key hallmarks of cancer that promote cancer cell survival. Increased proliferation of multiple cancer cell types including PaCa, prostate, glioblastoma, colorectal, renal and gastric cancer (Abasolo et al., 2004; Berenguer-Daizé et al., 2013; Deville et al., 2009; Keleg et al., 2007; Nouguerède et al., 2013; Ouafik et al., 2002; Qiao et al., 2017) has been shown to be linked with increased expression of ADM, which ultimately results in cancer cell survival and progression. Regulation of apoptosis is also important for development of cancer, apoptosis if often inhibited in cancer cells which promotes tumour survival. ADM overexpression has been associated with preventing apoptosis in different cancers including endometrial, ovarian, breast, renal, colon and bone cancer (Dai et al., 2013; Deville et al., 2009; Li et al., 2003; Martinez et al., 2002; Oehler et al., 2001; Wang et al., 2014). ADM has been linked to the Bcl-2 protein family which is associated with the regulation of apoptosis. The overall aim of this chapter was to determine if ADM and RAMP-3 KDs in PaCa cells alter response to gemcitabine and 5-FU treatment by measuring the viability (proliferation) and apoptosis of the cells.

5.4.1 CFPAC-1 KD cells respond to gemcitabine resulting in a decrease in PaCa proliferation

Analysis of CFPAC-1 ADM KD viability assays showed that there is a significant difference between different doses of gemcitabine and the day the cells are treated ($p < 0.0001$) (Figure 5.2). Following 3 days of treatment with gemcitabine, viability of cells decreased significantly at doses of 1 µM, 500 nM

and 100 nM gemcitabine compared to untreated cells (100% viability). The aforementioned doses of gemcitabine caused a decrease in viability of 68.2%, 67.5% and 63.6% respectively. The data show that CFPAC-1 ADM KDs do not increase or decrease sensitivity to gemcitabine as CFPAC-1 WT cells had similar responses at doses of 1 µM and 500 nM showing a 68.4% and 67.7% reduction in viability respectively (Figure 5.2). The similarity in results between CFPAC-1 ADM KDs and WT cells could be explained by Akada *et al* (2005) who show that CFPAC-1 cells were 1 of 3 PaCa cell lines in a panel of 15 PaCa cell lines that were the most sensitive to gemcitabine. After 72 hours of treatment with 25 ng/mL (95 nM) gemcitabine, CFPAC-1 cells showed less than 20% cell survival. Data collected in this study showed that after 72 hours at a dose of 100 nM, CFPAC-1 wild-type cells had 42.5% viability, whilst CFPAC-1 ADM KDs had 36.4% survival at 100 nM. Developing CFPAC-1 ADM KDs in one of the other cell lines characterised for ADM in Chapter 3, for example, AsPC-1 cells which were shown to be moderately sensitive to gemcitabine in this study, may provide a more useful insight into the role of ADM in proliferation and response to gemcitabine.

Analysis of CFPAC-1 RAMP-3 KDs treated with different doses of gemcitabine shows a significant difference ($p< 0.0001$) in percentage viability between drug concentration and the day of treatment (Figure 5.2). Compared to CFPAC-1 ADM KDs, the cells were slightly less sensitive to gemcitabine however, this was not significant as viability decreased by 59.5%, 57.9%. 54.6% at doses of 1 µM, 500 nM and 100 nM gemcitabine respectively. Two-way ANOVA analysis showed that at day 3, there was a significant difference between doses of 100 nM and 3 nM gemcitabine, with a 52% decrease in viability when treated with 100 nM gemcitabine ($p= 0.39$). There was also a 53.6% decrease in viability at a dose of 100 nM gemcitabine compared to 1 nM. At day 2, there were significant differences between untreated CFPAC-1 RAMP-3 KDs and 1 µM, 500 nM and 100 nM gemcitabine doses, all showing a nearly 50% decrease in viability compared to untreated cells.

Furthermore, comparing 100 nM treated CFPAC-1 ADM KDs to scrshRNA KDs at day 3 showed a significant difference ($p= 0.0093$) in viability with a 25.4% decrease in viability in RAMP-3 KDs (Figure

5.2b and d). Previous data from Nouguerède *et al* (2013) showed that in colorectal cancer, treating cells with anti-ADM antibody resulted in 70%% inhibition of proliferation

The LogIC_{50} was determined by non-linear regression for both CFPAC-1 KD cells, scrshRNA and WT cells following 3 days of gemcitabine treatment which showed no significant difference in logIC_{50} (Figure 5.3). The logIC_{50} values determined were -7.774, -7.919, -7.698 and -7.553 in CFPAC-1 ADM KD, CFPAC-1 RAMP-3 KD, CFPAC-1 scrshRNA and CFPAC-1 WT cells respectively. The dose response curve shows that at 1 µM (-6), there is higher viability in scrshRNA at day 3 of 100% compared to between 79%-85% in KDs and WT cells. There was no statistical significance in the difference however, treatment with gemcitabine over a longer time course may show more disparity in means between KDs and scrshRNA. This could be a consideration for future experiments.

Overall, the gemcitabine data shows that proliferation of cells is not significantly altered by knocking down ADM or RAMP-3 in CFPAC-1 cells. The log IC_{50} determined by percentage viability data on day 3 was similar across all cell lines and therefore the null hypothesis was accepted that there is no significant difference between the IC_{50} in KDs and controls (scrshRNA and WT cells) (Figure 5.3). At day 3, the percentage viability is overall highest in CFPAC-1 scrshRNA but there were not significant differences in viability as percentage viability ranged between 92%-105% at all doses of gemcitabine. There are more significant differences between different cells lines and different doses of gemcitabine at day 2 at doses of 1 µM and 100 nM gemcitabine. At a dose of 500 nM there was a significant difference (p= 0.002) between CFPAC-1 ADM KD viability (47.1%) and scrshRNA (60.4%). The lack of significant differences at day 3 between different cell lines may be indicative that the cell lines may have needed longer treatment with gemcitabine. Ouafik *et al* (2002) have shown that treatment of glioma cells with anti-ADM antibody resulted in decreasing viability over 8 days. The viability of cells was decreased by only 16% at day 4 but by day 8 the viability decreased by another 17% to 33%. Although, this experiment was not analysing the effects of gemcitabine on glioma cells, it was measuring the effect of ADM on the viability of cells showing that longer exposure to anti-ADM

resulted in double the decrease in viability. Therefore, longer treatment of cells with gemcitabine and induction of ADM KDs for a longer period of time could be a future consideration for viability assays.

Furthermore, developing KDs in more of the PaCa cell lines characterised in Chapter 3, could provide a bigger insight into the exact role of ADM and RAMP-3 KDs in PaCa cancer. Analysis by Akada *et al* (2005) showed that different PaCa cell lines have different sensitivity to gemcitabine treatment due to mutations and their natural proliferative rate. Furthermore, the exact role of ADM in proliferation has not been fully elucidated as it has been shown to have both inhibitory and stimulatory effects therefore, developing KDs in a larger range of PaCa cell lines may contribute to understanding ADM role in PaCa. Keleg *et al* (2007) have shown ADM to have growth inhibitory effects in 2 out of 5 PaCa cell lines. In prostate cancer, Abasolo *et al* (2004) and Berenguer-Daizé *et al* (2013) show contrasting results in relation to the role of ADM in inducing or inhibiting proliferation. Abasolo *et al* (2004) show that overexpression of ADM results in inhibition of proliferation of prostate cancer cells, whereas Berenguer-Daizé *et al* (2013) show ADM to induces proliferation. However, both studies analysed different prostate cancer cell lines which suggests that other factors may effect proliferation in combination with ADM. Although these results do not directly relate to the effect of gemcitabine on cancer cell lines, it does show that there is variability within cell lines of the same cancer and therefore, the viability results obtained following treatment of CFPAC-1 ADM KDs and RAMP-3 KDs with gemcitabine and 5-FU may differ with the different cell lines characterised in Chapter 3.

5.4.2 Viability assays show that CFPAC-1 KD cells are resistant to 5-FU treatment

CFPAC-1 ADM KDs, CFPAC-1 RAMP-3 KDs and scrshRNA treated with 5-FU showed no significant difference between different doses of 5-FU and the day of treatment (Figure 5.5). WT CFPAC-1 showed a significant difference ($p< 0.0001$) between different doses of 5-FU and the day of treatment (Figure 5.5). Following 3 days of treatment, there was a significant difference ($p=0.03$) between CFPAC-1 WT cells treated with 500 nM and 100 nM 5-FU showing 13.2% less viable cells in the group treated with 500 nM. There was also a significant difference ($p= 0.02$) between CFPAC-1 WT cells treated with 500

nM and 3 nM 5-FU, where there was a 14.5% decrease in viability in 500 nM treated cells compared to 3 nM. However, compared to gemcitabine, the viability of the cells was still high at 500 nM with 88.9% viability. The XY graph analysed by two-way ANOVA showed no significant difference between the different cells lines at each dose of 5-FU doses however, there was a significant difference ($p > 0.0001$) between drug concentrations alone and the different cell types alone ($p= 0.001$) (Figure 5.5). Overall, the percentage viability and therefore proliferation of the KD cells, WT cells and scrshRNA was not significant and suggests that CFPAC-1 cells may be resistant to 5-FU.

Shi *et al* (2002) have shown that PaCa cell lines treated with 5-FU alone are generally resistant to 5-FU which may explain why there is limited response to treatment in both KDs and controls. Chapter 1 also shows that 5-FU is often administered in combination with gemcitabine or if patients are fit enough, it is used in combination with other drugs as part of FOLFIRNOX treatment. Treatment with FOLFIRINOX following pancreatic tumour resection increases survival to 54.3 months compared to gemcitabine alone treatment which increased survival by 35 months (Conroy et al., 2018). These data suggest that combined therapy with 5-FU may be more effective in reducing the viability of CFPAC-1 cells. As discussed above, CFPAC-1 were shown to be sensitive to gemcitabine treatment but this was not mirrored by all PaCa cell lines in the study completed by Akada *et al* (2005) therefore, CFPAC-1 may not be as sensitive to 5-FU as other PaCa cell lines. Therefore, developing KDs in other cell lines characterised in Chapter 3 may provide a useful insight into whether other PaCa cells respond to 5-FU and whether KD of ADM or RAMP-3 changes the response to 5-FU. Furthermore, increasing the dose of 5-FU that CFPAC-1 KDs, scrshRNA and WT cells are treated with may show more changes in the viability of cells.

5.4.3 CFPAC-1 KD cells are sensitive to gemcitabine which induces apoptosis

Analysis of gemcitabine treated CFPAC-1 ADM KDs, showed a significant difference between untreated CFPAC-1 ADM KDs and 1 µM and 500 nM treated ADM KDs ($p= 0.02$). The cells treated with 1 µM gemcitabine showed a 1.03-fold increase in apoptosis compared to untreated cells and at a dose

of 500 nM gemcitabine, there was a 1.3-fold increase in apoptosis compared to untreated cells (p= 0.003) (Figure 5.4).

CFPAC-1 RAMP-3 KDs treated with gemcitabine showed a significant difference in apoptosis between treated and untreated RAMP-3 KDs (p <0.0001). At a dose of 1 µM, there was a 1.1-fold increase (p= 0.009) in apoptosis compared to untreated cells, at 500 nM there was a 1.6-fold increase (p= 0.0002) in apoptosis and at 100 nM there was a 1.7-fold increase (p< 0.0001) in apoptosis compared to untreated cells (Figure 5.4). Overall, the highest fold increase in apoptosis was in CFPAC-1 RAMP-3 KDs compared to untreated cells (1.7-fold increase) at a dose of 100 nM. This was significantly different to CFPAC-1 WT cells that showed a 0.52-fold increase in apoptosis compared to untreated cells (p= 0.0468) (Figure 5.4). This shows that KD of RAMP-3 increases sensitivity to gemcitabine at 100 nM. The viability data in Figure 5.2 also shows that at a concentration of 100 nM gemcitabine, RAMP-3 KDs reduce viability of cells and are therefore more sensitive to gemcitabine treatment. These data suggest that RAMP-3 may play a role in regulating proliferation and apoptosis in PaCa. Furthermore, as previously discussed, Akada *et al* (2005) show that CFPAC-1 cells are sensitive to gemcitabine treatment however, they also show that the increased sensitivity to gemcitabine is related to *BNIP-3. BNIP-3* is part of the Bcl-2 protein family that has been described in Chapter 1 and in this chapter. Bcl-2 is a protein molecule important in regulating apoptosis and has been shown to be regulated by ADM. Akada *et al* (2005) show that in PaCa cell lines sensitive to gemcitabine including CFPAC-1, there is upregulation of BNIP-3, whereas in cell lines with intermediate sensitivity or resistance, BNIP-3 is downregulated. Wu *et al* (2015), have also shown that ADM upregulates Bcl-2 and protects cancer cells from hypoxia induced death promoting cancer cell survival. Based on this evidence and the fact that ADM has been associated with regulation of apoptosis through the Bcl-2 family, the data in Figure 5.4 could indicate that targeting the RAMP-3 receptor by knocking down its expression, could increase the responsiveness of gemcitabine sensitive tumours and induce more apoptosis in PaCa as although CFPAC-1 WT cells were already sensitive to gemcitabine, knocking down RAMP-3 increased this effect by 1.2 fold (p= 0.05). Developing KDs in AsPC-1 which is one of the cell lines characterised in Chapter

3 and that was determined as intermediately- sensitive to gemcitabine by Akada *et al* (2005) would be useful to see whether apoptosis and sensitivity to gemcitabine is altered to the same degree.

Analysis of CFPAC-1 scrshRNA cells treated with different doses of gemcitabine showed a significant difference between untreated cells and cells treated with gemcitabine at a dose of 500 nM ($p= 0.0002$), with a 1.1-fold increase in apoptosis compared to untreated cells (Figure 5.4). There was no significant difference between untreated cells and different doses of gemcitabine for the remainder of concentrations. There was also no significant difference between different doses of gemcitabine and different cell lines. Analysis of CFPAC-1 WT showed a significant difference ($p <0.0001$) in cells treated with different doses of gemcitabine. There was a significant difference between untreated cells and cells treated at 1 µM, 500 nM and 100 nM with a 1.1-fold, 1.4-fold and 1.5-fold increase in apoptosis respectively.

Overall, at lower doses of gemcitabine (1 nM, 3 nM and 10 nM), CFPAC-1 WT cells are the least sensitive to gemcitabine (Figure 5.4). At a dose of 100 nM gemcitabine, CFPAC-1 WT cells and CFPAC-1 scrshRNA both have lower levels of apoptosis compared to the KD cells (Figure 5.4). More specifically, CFPAC-1 RAMP-3 KDs are 3.2-fold more sensitive to gemcitabine than CFPAC-1 WT cells and 2.8-fold more sensitive to gemcitabine than CFPAC-1 scrshRNA. At a dose of 500 nM gemcitabine, all the cell lines have similar levels of apoptosis. Apoptosis decreases slightly at 1 µM however, apoptosis remains similar across all cell lines. There may be a decrease in apoptosis at a higher dose as the cells may have adapted to become more resistant to gemcitabine.

5.4.4 CFPAC-1 KD cells are resistant to 5-FU treatment and do not induce apoptosis

Viability data of KD cells treated with 5-FU showed limited or no change in proliferation in CFPAC-1 KD cells and CFPAC-1 scrshRNA with some response to treatment in CFPAC-1 WT but the results were not significant suggesting the cells may be resistant to 5-FU. Similar results were obtained from apoptosis data, showing limited sensitivity to 5-FU with some response to 5-FU by CFPAC-1 WT cells (Figure 5.7). Analysis of 5-FU treated CFPAC-1 ADM KDs, showed no significant difference between different doses

of 5-FU and untreated cells. The highest increase in apoptosis was at a dose of 10 nM 5-FU (0.1-fold increase) and the lowest percentage of apoptosis was at 500 nM and 100 nM (0.01-fold increase) (Figure 5.7).

Comparing CFPAC-1 ADM KDs to CFPAC-1 WT cells, the largest difference in apoptosis was at a dose of 1μM, ADM KDs showed a 0.08-fold increase in apoptosis compared to a 1.1-fold increase in apoptosis in CFPAC-1 WT cells (Figure 5.7), suggesting that decreasing ADM expression increases resistance to 5-FU and that ADM is important in promoting apoptosis in CFPAC-1 cells. At lower doses of 5-FU, there was no significant difference determined between the different cell lines treated with different concentrations of 5-FU.

CFPAC-1 RAMP-3 KDs treated with different doses of 5-FU showed no significant difference between doses. However, there was a significant difference between CFPAC-1 RAMP-3 KDs and CFPAC-1 WT cells at different doses of 5-FU. The highest amount of apoptosis was at a dose of 1 μM 5-FU (0.3-fold increase compared to untreated) which is significantly lower ($p=0.001$) compared to CFPAC-1 WT cells (1.1-fold increase compared to untreated), this suggests that RAMP-3 KDs also increase resistance to 5-FU (Figure 5.7). There was also a significant difference between CFPAC-1 RAMP-3 KDs and CFPAC-1 scrshRNA at a dose of 1 μM 5-FU, RAMP-3 KDs had 0.3-fold increase inapoptosis compared to a 0.2-fold decrease in CFPAC-1 scrshRNA ($p= 0.003$). 500 nM 5-FU caused a 0.6-fold decrease in apoptosis in RAMP-3 KDs compared to WT cells ($p= 0.01$), again suggesting that reducing levels of RAMP-3 may cause resistance to 5-FU and apoptosis (Figure 5.7). Between concentrations of 1 nM- 100 nM 5-FU, there was a decrease in apoptosis between 0.3-0.4-foldcompared to WT cells showing that there isn't much difference in apoptosis between the different doses of 5-FU and therefore any changes are not dose dependent.

Analysis of scrshRNA treated with different doses of 5-FU showed a significant difference between different doses of 5-FU ($p< 0.0001$). Tukey's multiple comparison test showed that there was a significant difference between untreated scrshRNA and 1 μM 5-FU and untreated scrshRNA and 3 nM

5-FU treated scrshRNA, showing 0.2-fold decrease and 0.18-fold increase in apoptosis respectively (Figure 5.7). The decrease in apoptosis at a dose of 1 µM 5-FU could indicate that the cells begin to develop resistance to 5-FU. Analysis also showed a significant difference between different doses of 5-FU and KD cell lines compared to CFPAC-1 scrshRNA. The biggest difference in apoptosis was at 1 µM when comparing CFPAC-1 scrshRNA to CFPAC-1 WT cells which, showing a 1.3-fold decrease in apoptosis in CFPAC-1 scrshRNA. The highest amount of apoptosis in the scrshRNA group was at a concentration 3 nM 5-FU with a 0.18-fold increase in apoptosis compared to untreated cells. Overall, the data suggests that CFPAC-1 scrshRNA are resistant to 5-FU treatment as at all doses of 5-FU, there is limited response to treatment (Figure 5.7).

CFPAC-1 WT cells treated with 5-FU had a lower percentage of apoptosis than gemcitabine treated cells but the changes were still significantly different ($p < 0.0001$). The largest increase in apoptosis was at 500 nM with 1.1-fold increase in apoptosis compared to untreated ($p = 0.001$). At all other concentrations of 5-FU, CFPAC-1 WT cells had similar percentage increases in apoptosis (Figure 5.7).

Compared to gemcitabine treatment, the 5-FU apoptosis data shows that CFPAC-1 cells are resistant to 5-FU. Shi *et al* (2002) have shown that repeated exposure of PaCa cells to 5-FU increases resistance of the cells and increased IC_{50} values by 2.1-fold and 1.8-fold in Capan-1 and T3M4 cells. They found that Bcl-x_L mRNA expression was significantly upregulated in Capan-1 cells following repeated exposure to 5-FU, making the cells more resistant to 5-FU. They also showed an increase in Bcl-2 mRNA expression in T3M4, Capan-1 and AsPC-1 cells of 2.5-fold, 1.8-fold and 1.5-fold following 5-FU treatment. They concluded that Bcl-2 plays an important role in chemo-resistance. ADM closely regulates Bcl-2 under hypoxic conditions, therefore ADM and RAMP-3 KDs in CFPAC-1 and other PaCa cell lines following exposure to both hypoxia and 5-FU may be a good indicator of whether targeting ADM and RAMP-3 could improve patient response to 5-FU.

Future considerations for 5-FU apoptosis assays may be to expose PaCa cells to hypoxic conditions. Koong *et al* (2000) showed that in 7 patients with PaCa undergoing pancreatic resection, areas of the

pancreas with tumour had median $p0_2$ oxygen levels of 0-5.3 mmHg. In contrast, adjacent normal tissue had median $p0_2$ oxygen levels of 9.3-92.7 mmHg showing that pancreatic tumours are significantly more hypoxic. Furthermore, ADM has been shown to be elevated in hypoxic conditions and inhibit apoptosis by increasing Bcl-2 levels. This has been shown to be mediated by the CLR/RAMP receptor in osteosarcoma and endometrial cancer (Oehler et al., 2001; Wu et al., 2015). Therefore, exposing PaCa cells with ADM and RAMP-3 KDs to hypoxic conditions may provide a more accurate representation of the effects of ADM and RAMP-3 in PaCa and also may affect response to chemotherapy.

5.5 Conclusion

In conclusion, both viability and apoptosis results showed that CFPAC-1 KD, scrshRNA and WT cells were more sensitive to gemcitabine than 5-FU. Gemcitabine viability data shows that following 3 days of gemcitabine treatment at doses of 1 µM, 500 nM and 100 nM, CFPAC-1 ADM KDs and CFPAC-1 RAMP-3 KDs have a significant decrease in viability (Figure 5.2). CFPAC-1 RAMP-3 KDs are slightly more viable compared to ADM KDs. CFPAC-1 ADM KDs were shown to have a significant decrease in viability compared to CFPAC-1 scrshRNA at a dose of 100 nM gemcitabine ($p= 0.009$). CFPAC-1 ADM KDs have similar viability to CFPAC-1 WT cells following treatment with gemcitabine (Figure 5.2). Overall, the data suggest that knocking down ADM and RAMP-3 in CFPAC-1 cells does not significantly change the sensitivity of the cells to gemcitabine. However, this may be as CFPAC-1 are already sensitive to gemcitabine which has been shown in other studies. Therefore, ADM and RAMP-3 may play a more crucial role in cell lines that have intermediate sensitivity or resistance to apoptosis (Akada et al., 2005).

Apoptosis data following gemcitabine treatment showed a significant difference between untreated CFPAC-1 ADM KDs and 1 µM and 500 nM gemcitabine treatment with 1.03-fold and 1.3-fold increase in apoptosis relative to untreatedrespectively. This was also shown in CFPAC-1 RAMP-3 KDs with significant increases in apoptosis also at 100 nM, this showed the highest fold increase in apoptosis increase compared to untreated cells. CFPAC-1 WT cells also showed a significant increase in apoptosis at 1 µM, 500 nM and 100 nM and scrshRNA showed a significant difference between untreated and treated cells at 500 nM (Figure 5.4). Overall, there was not a significant difference between the different cell lines however, the data does show that CFPAC-1 cells are sensitive to gemcitabine treatment.

Following 5-FU treatment, the viability of CFPAC-1 ADM KDs, CFPAC-1 RAMP-3 KDs, CFPAC-1 scrshRNA and CFPAC-1 WT cells was not significantly different at different doses (Figure 5.5). WT cells showed the most response following 5-FU treatment. However, at higher doses including 500 nM 5-FU, the

viability of cells was still high at 88.9%. These data suggest that CFPAC-1 cells may be resistant to 5-FU and knocking down ADM or RAMP-3 does not improve the response of cells to this treatment. Apoptosis data also shows that that CFPAC-1 KD and scrshRNA cells are not sensitive to 5-FU treatment with very small increases in apoptosis (Figure 5.7). At a dose of 1 µM 5-FU, there was a 0.2-fold decrease in apoptosis suggesting that cells may have developed resistance at the higher dose of 5-FU. The most significant effect of 5-FU was in CFPAC-1 WT cells at 1 µM where there was 1.1-fold increase in apoptosis compared to untreated cells (Figure 5.5). There were also significant increases in apoptosis compared to untreated cells at doses of 500 nM and 100 nM 5-FU.

The apoptosis data overall shows that KD and control cells were most responsive to gemcitabine treatment compared to 5-FU. In the gemcitabine treated cells, apoptosis was the highest in RAMP-3 KDs treated with 500 nM gemcitabine. On average, the highest amount of apoptosis was in RAMP-3 KDs with an average 0.7-fold increase in apoptosis and the lowest amount of apoptosis was in scrshRNA at 0.2-fold increase in apoptosis. This comparison suggests that reducing levels of RAMP-3 may improve response to gemcitabine. In 5-FU treated cells, the highest apoptosis was in CFPAC-1 WT cells with an average increase of 0.5-fold apoptosis. This shows that KDs have no effect on improving response to 5-FU.

In future, changing the experimental conditions of both viability and apoptosis assays may show a more significant role of ADM and RAMP-3 in regulating the tumour microenvironment and improving response to chemotherapies. Koong *et al* (2000) have shown that hypoxia is a key feature of the PaCa tumour environment as previously discussed. Furthermore, Wu *et al* (2015) and Oehler *et al* (2001) have shown the relationship between increasing ADM expression following hypoxia and increasing Bcl-2 expression in cancer which prevents apoptosis. Therefore, exposing the cells to hypoxic conditions may show the effects of ADM and RAMP-3 KDs on proliferation and apoptosis of cells more significantly. Treatment of cells for a longer period of time with gemcitabine or 5-FU may also be beneficial as Ouafik *et al* (2002) showed that viability assays showed half the viability at day 8

compared to day 4 measurements in glioma cells. Higher doses of gemcitabine and combinational therapy may also provide further insight into the effect of the chemotherapies and whether ADM and RAMP-3 KDs alter the response. Combinational therapy has been shown to improve overall survival in PaCa patients (Conroy et al., 2011; Neoptolemos et al., 2010). Finally, developing KDs in a larger group of PaCa cell lines could show whether KDs may be more or less beneficial dependent on the cell lines and whether personalised therapy may be more beneficial to PaCa patients. Akada *et al* (2005) have shown that whilst CFPAC-1 cells are sensitive to gemcitabine, AsPC-1 cells have intermediate sensitivity so developing KDs in these cells that have been characterised in Chapter 3 may be useful.

CHAPTER 6: EFFECT OF ADM KD ON THE PaCa MICROENVIRONMENT

6.1 Introduction

The pancreatic tumour microenvironment is composed of a complex network of cells that all play a role in the development and progression of PaCa. One of the key characteristics of PaCa is desmoplasia (dense fibrous scar tissue), caused by an increase in PSCs and excessive deposition of extracellular matrix (ECM) often resulting in chemo-resistance. The ECM is normally tightly regulated by molecules that promote degradation and deposition of the ECM however, this becomes dysregulated as desmoplasia develops.

Immune cells, endothelial cells, neuronal cells and pericytes also play an important role in the development of the stroma around the tumour and contribute to chemo-resistance within the tumour. An important interaction within the stromal environment is the crosstalk between PaCa tumour cells and PSCs, they have a bi-directional relationship which results in increased proliferation and migration of each other. This has a downstream effect on immune cells, endothelial cells, the ECM and neuronal cells that infiltrate the tumour microenvironment (Figure 6.1). ADM has been shown to be associated with many of the cells associated with the pancreatic tumour microenvironment that drive desmoplasia and resistance to chemotherapy (Bhardwaj *et al*., 2016; Dai *et al*., 2020; Ishikawa *et al*., 2003; Keleg *et al*., 2007; Xu *et al*., 2016). This chapter will discuss the complex microenvironment and the role that ADM plays in creating it.

6.1.2 Pancreatic stellate cells (PSCs) role in desmoplasia

In a healthy pancreas, PSCs are generally inactive and play some role in the maintenance and degradation of ECM by producing matrix metalloproteinases (MMPs) and tissue inhibitors of metalloproteinases (TIMPS). When inactive, they have vitamin A containing fat droplets in their cytoplasm. Following injury to the pancreas or inflammation, PSCs lose their vitamin A droplets and change phenotype to a myofibroblast-type cell. This was shown by Apte *et al* (1998) in isolated rat PSCs, after 24 hours of culturing PSCs, the cells were positive for desmin and contained lipid droplets but negative for α-SMA with an angular type structure. However, after 48 hours of culture,

immunocytochemistry showed the cells were positive for both desmin and α-SMA and lost their lipid droplets. Bachem *et al* (1998) also isolated rat PSCs to show how the phenotype and expression of ECM proteins changes over time. They showed that early primary PSCs contained lipid droplets and expressed vimentin in all PSCs and desmin in 20-40% of the cells. The lipid droplets were located in the cytoplasm and peri-nuclear region of cells. However, within 4-8 days of primary culture, the number of lipid droplets began depleting and expression levels of α-SMA changed (30-50%), whilst vimentin and desmin expression remained at 100%. Once the cells were passaged, over 90% of the cells expressed α-SMA, desmin was expressed in 20-50% of cells and vimentin was still expressed in all the cells. The PSCs also changed phenotype to become more flattened with long cytoplasmic extensions. The change in phenotype correlated with increased expression of collagen I, collagen III, fibronectin and laminin which was determined by immunofluorescence. These data suggest that activated PSCs play a key role in the development of the ECM around the tumour. Furthermore, activated PSCs release inflammatory cytokines, chemokines and growth factors for example, TGF-β, VEGF, PDGF and angiotensin. These promote cancer cell proliferation and metastases and proliferation of endothelial cells and alteration in immune response (Hwang et al., 2008; C. Li, Cui, Yang, Wang, & Zhuo, 2020; Masamune et al., 2008). It is important to note that PSCs are a subtype of CAF, when PSCs are activated they become a type of CAF. In studies describing the role of fibroblasts in other cancers as well as PaCa, the term CAF is often used.

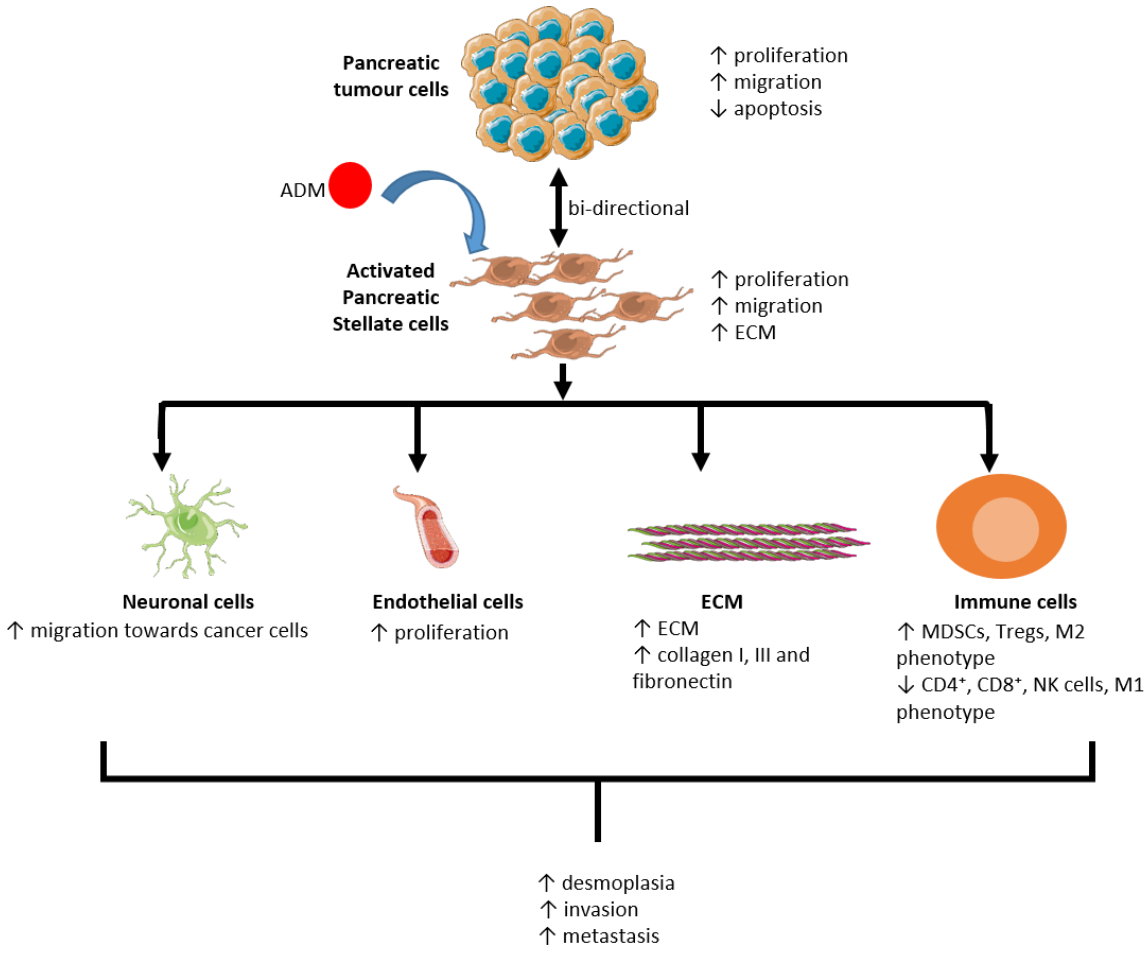

Figure 6.1 The role of activated PSCs in the crosstalk with PaCa tumour cells**.** PaCa cells and pancreatic stellate cells (PSCs) have a bidirectional relationship, tumour cells increase the proliferation, migration and the amount of extracellular matrix (ECM) produced by PSCs. PSCs increase the proliferation and migration of tumour cells and inhibit apoptosis. Adrenomedullin (ADM) receptors have been shown to be present in PSCs, therefore together with the increased proliferation and migration induced by cancer cells, ADM plays a role in activating pro-tumorigenic pathways. PSCs increase neuronal migration towards cancer cells and increase the proliferation of endothelial cells inducing angiogenesis. Furthermore, they increase the production of ECM by increasing production of collagen I, III and fibronectin. PSCs also have a role in immune regulation by increasing numbers of myeloid derived suppressor cells (MDSCs), regulatory T cells (Tregs) and M2 phenotype macrophages which favour a pro-tumorigenic environment. However, they also decrease $CD4^+$ T cells, $CD8^+$ T cells, natural

killer cells (NK cells) and M1 phenotype macrophages which promote anti-tumour activity. Ultimately this results in increased desmoplasia, invasion and metastasis of PaCa.

Masamune *et al* (2008) have shown that following hypoxic induction of PSCs, nuclear expression of HIF-1α (hypoxic marker) and collagen I production and migration of PSCs increased. PSCs have also been shown to excessively secrete matrix proteins which include collagen, laminin and fibronectin in the extracellular matrix (ECM) which induces desmoplasia. They also secrete both MMPs and TIMPs which become uncontrolled and dysregulate ECM production resulting in fibrosis (Armstrong et al., 2004).

Masamune *et al* (2008) also show that PSCs exposed to hypoxic conditions increase the proliferation and migration of endothelial cells and induce angiogenesis. Furthermore, analysis of resected patient PaCa samples showed that in areas of fibrosis, there was increased nuclear expression of HIF-1α in α-SMA positive PSCs, suggesting hypoxia is important in the activation of PSCs. Hwang *et al* (2008) have shown the influence of human PSCs on proliferation, migration and invasion of PaCa cells and how they alter response to PaCa treatments. Treating BxPC-3 and Panc-1 cells with PSC conditioned media increased proliferation, migration, invasion and colony formation of these PaCa cells. These cells were also less responsive to gemcitabine and radiation therapy by inhibition of apoptosis. *In vivo,* co-injection of tumour cells with PSCs resulted in increased incidence of primary tumour establishment, increased size of tumour and metastasis. These data suggest that PSCs are activated in hypoxic conditions causing the activation of pro-tumorigenic pathways including deposition of collagen I, angiogenesis, promoting cancer cell proliferation and migration and as a consequence tumour establishment and metastasis.

The immune system can also be regulated by activated PSCs. Li *et al* (2020) combined PAN02 PaCa cells with PSCs and injected them orthotopically, using PaCa cells alone as a control. Combining PaCa cells with PSCs resulted in an increase in proliferation and metastases which was accompanied by changes to the immune microenvironment. Tumour weight significantly increased in PaCa cells

combined with PSCs which correlated with increased α-SMA expression. The number of myeloid derived suppressor cells (MDSCs) and T regulatory cells (Tregs) were also increased in the bone marrow, spleen and tumour tissue following co-transplantation of PaCa cells with PSCs. However, $CD4^+$, $CD8^+$ and NK cells decreased in tumour tissues and spleen. The M2 macrophage phenotype also increased and the M1 phenotype decreased in tumours with combined PaCa cells and PSCs. These data suggest that activated PSCs reduce the activity of anti-tumour immune cells and increase immune cells that help evade immune detection.

Benyahia *et al* (2017) have shown that ADM and its receptors are highly expressed in CAFs derived from invasive breast carcinoma compared to normal human dermal fibroblasts (NHDF). ADM mRNA expression was shown to be 4-24 fold higher in CAFs compared to NHDF. RAMP-2, RAMP-3 and CLR were also shown to be expressed in CAFs derived from breast carcinoma. *In vitro,* ADM was shown to induce proliferation of CAFs and *in vivo* combination of CAFs with PaCa cells resulted in increased tumour volume. Administration of anti-ADM receptor (αAMR) to matrigel plugs containing CAFs *in vivo* showed a decrease in neovascularisation and a depletion of vessel structures. Histological analysis of matrigel plugs showed a depletion of vascular endothelial cells (CD31), induced apoptosis (cleaved caspase-3) and decreased tumour cell proliferation (Ki67). These results demonstrate that ADM and its receptor have been shown to be expressed in CAFs and that they induce pro-tumorigenic phenotypes that result in the growth of PaCa tumours and potentially metastases.

In PaCa, Dai *et al* (2020) have shown that RAMP-3 KO mice were associated with decreased PDPN or α-SMA positive CAFs in the periphery of tumours in metastatic sites following histological analysis. Therefore, RAMP-3 KO CAFs were developed and co-cultured with PAN02 cells showing decreased migration, proliferation and metastasis of tumour cells. These results were also shown *in vivo* where RAMP-3 KOs in CAFs implanted with PAN02 cells resulted in decreased metastasis. The results suggest that ADM/RAMP-3 expressed in CAFs drives tumour metastasis and play an important role in the development of PaCa. In conclusion, ADM could be a valuable therapeutic target for treatment of

PaCa as PSCs/CAFs have been shown to be involved with multiple pathways leading to the formation of desmoplasia and stromal microenvironment around the pancreatic tumour.

6.1.2 The extracellular matrix (ECM) in PaCa progression

The ECM is composed of a complex network of molecules and acts as a scaffold, playing an important role in maintaining tissue architecture. It is important for structural integrity and provides tensile strength (Armstrong et al., 2004). Disruption to the ECM by alterations induces pro-tumorigenic effects. The ECM is composed of fibronectin, laminin, glycoproteins, proteoglycans and glycosaminoglycans (Walker, Mojares, & Hernández, 2018). Type I and III collagens are the main structural proteins of PaCa tumours, together with fibronectin, these proteins are strongly upregulated by stromal fibroblasts. Figure 6. shows that activation of PSCs is associated with increased ECM resulting in desmoplasia. Increased ECM is associated with poorer patient survival as demonstrated by Whatcott *et al* (2015), excessive ECM deposition in primary and metastatic primary tumours was associated with poorer OS. They found that both primary and metastatic tumours were highly fibrotic and that Kaplan-Meier curves showed a correlation between high collagen I levels and poorer median survival. Patients with low collagen I levels had median overall survival of 14.6 months compared to 6.4 months in patients with high collagen I levels. These data demonstrate the impact ECM can have on PaCa progression and clinical outcome.

Armstrong *et al* (2004) also showed a relationship between collagen I and development of the ECM and desmoplasia. Overall, this study showed that PaCa cells promote proliferation and collagen synthesis by activating PSCs that induce collagen I, MMPs and TIMP synthesis. Collagen I was shown to be a major product of PSCs, providing PaCa cells with a survival advantage by inhibiting apoptosis and increasing proliferation of cells following treatment with 5-FU. Furthermore, histological analysis of normal pancreatic tissue compared to PaCa patient samples showed low levels of α-SMA in normal pancreas and a marked increase in PaCa samples. PaCa α-SMA expression was located in fibrotic bands and around malignant glands showing that α-SMA is associated with malignancy. The same pattern

was seen with collagen I, where normal tissue had low levels of collagen I and PaCa tissues expressed high levels of collagen I in large tracts that surround the malignant epithelium in PDAC.

Furthermore, *in vitro* analysis showed that PaCa cell line (AsPC-1, Panc-1 and MiaPaCa-2) supernatants increased proliferation of PSCs and that AsPC-1 supernatant stimulated PSC collagen synthesis. Additionally, PSCs were shown to be a primary source of MMP-2 which promote the accumulation of ECM (Armstrong et al., 2004). Similar to Armstrong *et al* (2004), Bachem *et al* (2005) also showed that human PaCa patient tissues were associated with a high number of α-SMA and desmin positive cells that correlated with intense collagen and fibronectin staining. PaCa cells (MiaPaCa-2, Panc-1 and SW850) were also shown to stimulate the proliferation of PSCs, inducing ECM synthesis. PSCs co-cultured with PaCa cells showed more intense collagen I, III and fibronectin immunostaining compared to PaCa cells cultured alone. Furthermore, *in vivo* subcutaneous models showed that tumours grew faster when PaCa cells were inoculated together with PSCs, compared to PaCa cells alone. This again correlated with increased expression of α-SMA staining and desmin positive cells in the mixed cell group. Together, these data show the complex network between PaCa tumour cells, PSCs and predominantly collagen I in both promoting ECM development and in promoting cancer cell proliferation. These results clearly demonstrate the bi-directional relationship of cancer cells and PSCs described in Figure 6.1. They also show how the cells work together to develop a more aggressive PaCa phenotype which is resistant to chemotherapy.

The role of ADM in inducing the pro-tumorigenic phenotype associated with increased collagen I and α-SMA expression has been shown by Bhardwaj *et al* (2016). They showed the relationship between MYB (an oncogenic transcription factor), ADM and induction of the desmoplastic reaction by promoting production of ECM proteins. Orthotopic injection of MYB overexpressing PaCa cells into the mouse pancreas, increased desmoplasia significantly compared to MYB-silenced PaCa cells. Immunostaining of the PaCa tumours showed an increase in collagen I, fibronectin and α-SMA. Furthermore, they showed that MYB has binding sites on ADM and Sonic hedgehog (SHH) promoters

by *in silico* analysis. This was confirmed by chromatin-immunoprecipitation and co-culture of PSCs with MYB expressing PaCa cells. Co-cultures of these cells with ADM antagonist resulted in decreased viability and therefore decreased proliferation of PSCs. This suggests that MYB expression in PaCa cells induces effects on PSCs through ADM. MYB and ADM co-operate to induce proliferation of PSCs and have potential to activate downstream effects of PSCs including increased collagen I and fibronectin expression which increases ECM production and formation of stromal tissue around the tumour. Overall, this produces a more aggressive PaCa phenotype.

6.1.3 Immune cells

Evading immune surveillance is one of the original hallmarks of cancer recognised by Hanahan & Weinberg (2000). The immune system is important in healthy tissue, it acts as surveillance system to detect any changes within normal tissue such as viruses or bacteria. In cancer, cells evade the immune system which leads to favourable conditions for the tumour microenvironment and promotion of tumour cell survival (Hanahan & Weinberg, 2011). Clark *et al* (2007) showed that immunosuppressive cells appear during early progression of PaCa and continue to outweigh anti-tumour immune cells throughout the whole development of PaCa. TAMs, MDSC and Treg cells were found to be the particularly dominant population of cells from the very beginning.

The TGF-β inflammatory pathway is a key pathway activated during PaCa and is a potent inducer of desmoplasia. Aoyagi *et al* (2004) have demonstrated this as TGF-β expression is higher in PaCa patient tumours compared to non-neoplastic tissues. Increased TGF-β correlated with increased collagen I and III expression. However, further immunohistochemistry analysis showed that there was only faint TGF-β cytoplasmic staining in PaCa cells. Infiltrating granulocytes which were predominantly identified as neutrophils were shown to secrete TGF-β. Overall, it was shown that instead of directly interacting with tumour cells, TGF-β released from granulocytes stimulated PSCs to produce collagen I and III. This result is another example of how cells of the tumour microenvironment do not stick to their single

niche but interact with multiple cells within the tumour microenvironment to induce a more aggressive phenotype without directly acting on tumour cells themselves.

ADMs role in the regulation of the immune system in both PaCa and other cancers including ovarian cancer, melanoma, lung and breast cancer is described in Chapter 1, Section 1.4.5. In PaCa, Xu *et al* (2016) showed the role of MMCs in the regulation of immune cells. Infiltration of MMCs into the stromal environment was shown to be associated with poorer prognosis in patients. MMC differentiation into macrophages and MDSCs was correlated with high ADM expression in PaCa. ADM was also shown to increase migration and invasion of MMCs and induce M2 macrophage polarisation. Bone marrow derived macrophages (BMDMs) were treated with 100nM ADM for 24 hours which resulted in increased expression of CD206+ and Arg-1 (both markers of M2 macrophage phenotype). Flow cytometry showed a 2-fold increase in F4/80+ CD206+ phenotype in BMDMs. Furthermore, culturing BMDMs in Panc-1 conditioned mediated also showed an increase in F4/80+ CD206+ and Arg-1. These data suggest that ADM induces MMC differentiation to produce M2 phenotype macrophages which promote an immunosuppressive microenvironment and tumour growth.

The role of ADM in polarising macrophages has also been shown in ovarian cancers and melanoma (Chen et al., 2011; Pang et al., 2013). Chen *et al* (2011) suggest that ADM polarises macrophages to an M2 phenotype in an autocrine manner. Culturing macrophages in B16/F10 melanoma conditioned media resulted in increased expression of ADM and its receptor. ADM has also been associated with mast cell degranulation in gastric cancer (Lv et al., 2018). In breast and lung cancer, mast cells have been shown to be ADM producing. A549 lung cancer cells treated with conditioned media from HMC-1 mast cells transduced with either scrshRNA (HMC-1Scr) or ADM shRNA to produce KDs (HMC-1ADM) showed that HMC-1Scr increased proliferation of A549 cells more than ADM KDs. ADM KDs mast cells showed no increase in A549 cell proliferation. Furthermore, ADM was shown to have a pro-angiogenic role in mast cells by increasing expression of VEGF and FGF. This effect was neutralised by treatment with ADM neutralising antibody (Zudaire et al., 2006).

Overall, these studies highlight the significance of immune cells within the PaCa tumour microenvironment and show that dysregulation of the immune system is critical to PaCa progression. ADM has also been shown to be associated with multiple cells of the immune system however, further elucidation of ADM's role in regulating the immune system is needed.

6.1.4 Endothelial cells and angiogenesis

Angiogenesis has been described as an important process involved in supplying oxygen and nutrients to tumours to promote cancer cell survival. There is much debate over the vascularity of PaCa tumours and how much of an influence this has on patient survival. VEGF has been previously associated with a less favourable prognosis in PaCa patients by Ikeda *et al* (1999), they showed that hypervascularity was correlated with poorer prognosis in patients. Niedergethmann *et al* (2002) showed a correlation between VEGF expression, increased microvessel density (MVD) and survival after curative resection, suggesting that higher expression of VEGF and MVD correlate with increased chance of PaCa recurrence. However, Van Der Zee *et al* (2011) compared vascularity in the tumours of the PDAC head and in peri-ampullary tumours. They found that in peri-ampullary tumours there was a higher MVD compared to PDAC in the head of the pancreas. High MVD in PDAC was associated with lymph node involvement although these factors did not correlate with overall survival, recurrence free survival or cancer specific survival. Barău *et al* (2013) showed that PaCa tumours are characterised by high MVD in tumours compared to peri-tumoural areas. Furthermore, they found that MVD correlated with differentiation of tumours, poorly differentiated tumours had the highest MVD compared to moderately and well differentiated tumours. However, the level of MVD did not correlate with distant and lymph node metastases. Instead, Barău *et al* (2013) suggest that the dense stroma that forms around the tumour induces a hypoxic environment which allows only the most aggressive tumour cells to survive regardless of the MVD. These data highlight the conflicting opinion of the influence of vasculature on PaCa tumour survival.

Intense desmoplasia around PaCa tumours has been shown to increase the interstitial fluid pressure (IFP) in tumours. This has been suggested to result in compression of blood vessels in tumours creating a hypovascular and hypoxic microenvironment. The blood vessel compression has been suggested to result in inhibition of effective drug penetration and delivery (Koong et al., 2000; Provenzano et al., 2012). Changes in IFP around PDAC tumours has been clearly demonstrated by Provenzano *et al* (2012). They measured IFP around a healthy pancreas in mice and in PDAC tumours that were developed in genetically engineered mice (GEM). In healthy mice, the IFP was 8-13 mmHg and in PDAC tumours the IFP increased to 75-130 mmHg. This clearly demonstrates that the development of PDAC tumours causes dysregulation of IFP and has potential to effect drug penetration.

PSCs also play an important role in the regulation of vascularity, they have been shown to induce both angiogenesis and the development of ECM around PaCa tumours and therefore, influence both MVD and desmoplasia around the tumours. Under hypoxic conditions, it has been shown that PSCs increase the production of vascular endothelial growth factor (VEGF), collagen I and migration of PSCs. Conditioned media from PSC exposed to hypoxia induced HUVEC proliferation, migration and angiogenesis *in vitro* and *in vivo.* These results show that PSCs are important in the regulation of angiogenesis within the PaCa microenvironment (Masamune et al., 2008).

The role of ADM in inducing angiogenesis in PaCa and other cancers has been widely investigated as demonstrated in chapter 1, section 1.4.3. In PaCa, Ishikawa *et al* (2003) showed that *in vivo* treatment of PaCa tumours with ADM_{22-52} antagonist resulted in decreased tumour growth and smaller blood vessels following analysis by CD31 immunostaining. This indicates that ADM may have a role in inducing angiogenesis in PaCa. Keleg *et al* (2007) also analysed the role of ADM in PaCa under hypoxic conditions. They showed that 3 out of 5 cells lines had increased ADM expression following hypoxia. Addition of recombinant ADM to these cell lines also resulted in increased VEGF expression. Proliferation of HUVECs was increased 2-fold in hypoxic conditions compared to normoxic conditions which also correlated with increasing ADM expression. Therefore, ADM potentially induces angiogenic

effects through induction of VEGF expression in PaCa. Dai *et al* (2020) developed RAMP-2 endothelial cell KO mice and analysed the effects that this had on angiogenesis and tumour metastases. KO of RAMP-2 resulted in decreased angiogenesis however, metastasis increased which was correlated with increased expression of both RAMP-3 and PDPN (markers of CAFs). These data suggest that the ADM/RAMP-3 system can overcome a reduction in angiogenesis in PaCa by inducing pro-tumorigenic effects through the RAMP-3 receptor and by activating CAFs. CAFs have been previously described to increase endothelial cell production (Figure 6.1) so this may be one of the mechanisms through which metastases is induced. Together, these data demonstrate that although ADM may regulate angiogenesis, MVD and angiogenesis do not necessarily indicate the prognosis of patients. The hypoxic environment generated by the development of the stroma which causes compression of blood vessels and increased IFP, may have more of an impact on patient overall survival as therapies become less successful at penetrating tumours.

6.1.5 Neuronal cells

The role of nerves in PaCa still needs further elucidation and understanding of this could be significant not only in the treatment of PaCa but also in the management of pain. Liebl *et al* (2014) showed neural invasion to be present in all 132 PaCa patient samples they analysed following tumour resection. Stopczynski *et al* (2014) have shown that neural invasion was present at all stages of PDAC and not limited to just late stages. Perineural invasion (PNI) is a common feature in PaCa and defined as the presence of neoplastic cells along nerve cells and sometimes within different layers of nerve fibres. PaCa cells have been shown to grow along nerve cells and within the perineural space suggesting cancer cells invade the neuronal cells (Kayahara et al., 2007). Furthermore, Ceyhan *et al* (2008) have shown that PaCa cells change morphology prior to migration towards neuron cells and become more elongated. Once PaCa cells have migrated they form clusters around the neuronal cells.

Pain is a common symptom described by PaCa patients which is often caused by neuronal invasion. Dang *et al* (2006) showed an example of this by analysing nerve growth factor (NGF) expression in

primary PaCa patient samples. They specifically analysed expression of two NGF receptors; TrkA and p75NGFR which are commonly associated with back and abdominal pain. They found that patients with high TrkA expression had more PNI and a higher degree of pain. However, high expression of p75NGFR was associated with longer overall survival in patients.

PSCs also play a role in inducing PNI as shown in Figure 6.1 Li *et al* (2014) show that in tissue sections from PaCa patients, 61.4% had PNI which correlated with strong sonic hedgehog (SHH) expression. Furthermore, they showed that SHH overexpression in tumours activated the SHH pathway in PSCs. Overexpression of SHH in PSCs was associated with increased cancer cell migration and invasion along nerve axons together with increased tumour growth and metastasis *in vitro* and *in vivo.* Increased expression of MMP-2, MMP-9 and NGF was also associated with increased SHH expression in PSC. These data show the important role of the activation of PSCs by SHH paracrine signals from PaCa cells, in inducing PNI. Bhardwaj *et al* (2016) have shown MYB induces activation of PSCs by interacting with ADM and SHH promoters which promotes tumour growth (Chapter 1, Section 1.3.6). There is currently limited research around the association of ADM in PNI and therefore, however investigating the association between ADM, SHH and MYB in PNI could be an important consideration in future research as ADM has been shown to have such a prominent role involving other cells of the tumour microenvironment. ADM/RAMP-3 expression on the surface of PSCs has been shown by Dai *et al* (2020) and PSCs have been described to induce PNI, investigating the relationship of ADM in inducing PSCs and tumour cells to induce PNI could be a future area of research.

6.1.6 Summary

Overall these data describe the complexity of PaCa tumours and show that the communication between all the cells of the PaCa microenvironment and how they contribute to PaCa's aggressive desmoplastic phenotype. Desmoplastic scar tissue has been shown to account for 70-80% of the tumour mass (Kadaba et al., 2013). This is largely responsible for the lack of response to currently available chemotherapies as the scar tissue and dense hypovascular ECM of the tumour create a

barrier to these therapies. This chapter's introduction shows how ADM interacts with most cells of the PaCa microenvironment including PSCs/CAFs, immune cells, endothelial cells and proteins on the ECM. Most recently, Dai *et al* (2020) showed the important interaction between ADM and CAFs *in vivo*, co-transplantation of RAMP-3 KOs CAFs/PAN02 showed a reduction in metastasis in mice. Therefore, ADM could be a key modulator of the desmoplastic reaction and progression of PaCa. The AM_2 (CLR/RAMP-3) receptor which potentially mediates some of ADM's pro-tumoural functions could be a valuable target to improve response to currently available chemotherapies.

6.1.7 Hypothesis

The null hypothesis is that knocking down ADM has no influence on tumour growth and metastases *in vivo*. Therefore, ADM has no effect on cells of the tumour microenvironment that promote tumour growth and metastases including immune cells and proliferating tumour cells.

6.1.8 Aims and objectives

The aim of this chapter was to determine the effect of CFPAC-1 ADM KD on the growth of tumours compared to CFPAC-1 scrshRNA controls and wild-type CFPAC-1 cells (WT) *in vivo*. The other aim was to determine whether there were differences within the tumour microenvironment composition in mice inoculated with either CFPAC-1 ADM KDs, CFPAC-1 scrshRNA or wild-type cells *in vivo*.

To determine the impact ADM has on tumour growth and the microenvironment, two *in vivo* experiments were designed. The first *in vivo* experiment involved orthotopic injection of CFPAC-1 ADM KDs and scrshRNA into the pancreas. This was used to compare whether tumour growth was increased or decreased following ADM KD. Furthermore, different doxycycline induction regimes were compared to assess whether the rate of tumour growth was altered between doxycycline induced and non-induced KDs or scrshRNA controls. Tumour growth was measured using *in vivo* imaging system (IVIS) which measured the bioluminescent signal of tumours and showed any signs of metastasis. The orthotopic *in vivo* model was also used to determine whether the microenvironment was different between CFPAC-1 ADM KDs and CFPAC-1 scrshRNA controls. This was determined by performing

immunohistochemistry on tissue sections to measure Ki67, α-SMA and endomucin. Immune cells in mouse blood samples were also measured to determine if there were any differences between groups.

The second *in vivo* experiment was a subcutaneous model comparing CFPAC-1 ADM KDs, CFPAC-1 scrshRNA and CFPAC-1 WT cells. The main objective was to determine differences in tumour size between doxycycline induced and non-induced ADM KDs and controls. This was determined by measuring tumour volume with Vernier callipers.

6.2 Methods

6.2.1 In vivo orthotopic model

6.2.1.1 Mice

Orthotopic tumour xenograft studies were carried out in 5 to 6 week old female nude BALB/c mice from Charles River. Before beginning the experiment, all procedures were reviewed and approved by the local Research Ethics Committees in the University of Sheffield and complied with UK Animals (Scientific Procedures) Act 1986. Studies were performed under project licence PF61050A3.

6.2.1.2 Cell preparation for orthotopic injection

CFPAC-1 ADM KDs transduced with luciferase (CFPAC-1 ADM KD-LucRFP) and CFPAC-1 scrshRNA cells transduced with luciferase (CFPAC-1 scrshRNA-LucRFP) as described in Chapter 4, Section 4.2.4. They were harvested in T175 flasks and counted as described in Chapter 2, Sections 2.1.1 and 2.1.4. The day before the procedure, Matrigel was thawed on ice in the fridge to prevent the Matrigel from solidifying. Bijou tubes, 1 mL tips and PBS were chilled in the fridge overnight. The cells were prepared at a concentrations of 10 million cells/mL in a mix of Matrigel:PBS (3:2 ratio). The cell preparation was carried out using ice cold PBS and tips that had been kept in the fridge over night to minimise chances of Matrigel solidifying.

6.2.1.4 Orthotopic injection of cells into pancreas

Insulin syringes (27 G, 1 mL) were used for intrapancreatic injections and kept on ice during the procedure to prevent the cell/matrigel mix from solidifying prior to injection. The mice were anaesthetised by isofluorene inhalation and checked for pedal reflex and placed on a heating pad at 37 ^{o}C.

Once it was confirmed that the mice had been anaesthetised, the abdomen was surgically sterilised and a sterile scalpel was used to make an incision into the skin and abdominal wall on the upper left flank near the spleen. The spleen is located by the pancreas and was lifted through incision. The

pancreas was spread on a sterile swab before intrapancreatic injection of the 40 µL CFPAC-1 ADM KD Luc-RFP or CFPAC-1 scrshRNA Luc-RFP (400,000 cells/injection). The needle was left at the site of injection for a minimum of 10 seconds to minimise risk of cells leaking. The spleen and pancreas were placed back into the abdominal cavity and the incision was closed by a two-layer suture. The abdominal wall was stitched together using a continuous 5-0 polydioxanone absorbable suture. The skin was stitched back together using interrupted 6-0 polypropylene suture and cutting needle. Iodine was applied to the sutures to act as an antiseptic and mice were observed for 30 minutes in a temperature controlled incubator with mash. The mice continued to be monitored on a daily basis to ensure no infection developed following surgery.

6.2.1.5 Doxycycline preparation and regime

Three days after surgery, CFPAC-1 ADM KDs and scrshRNA were either induced with water containing 0.5 mg/mL doxycycline or and given normal water. 5 mL of doxycycline was added to 1 litre of water to make a final concentration of 0.5 mg/mL. The water containing doxycycline was changed every 2 days. The mice were split into three groups dependent on their doxycycline water regime which is outlined in Table 6.1 and Figure 6.2.

Table 6.1 Doxycycline water regime. CFPAC-1 ADM KD and scrshRNA were divided into three groups according to their doxycycline treatment.

Doxycycline regime	Day 0	Day 17	Day 34	Day 45
Dox on	Water containing 0.5 mg/mL dox changed every 2 days	Water containing 0.5 mg/mL dox changed every 2 days	Water containing 0.5 mg/mL dox changed every 2 days	Endpoint
Dox on/off/on	Water containing 0.5 mg/mL dox changed every 2 days	Dox treatment stopped. Water without doxycycline given to mice	Dox treatment restarts	Endpoint
No dox	Water without dox	Water without dox	Water without dox	Endpoint

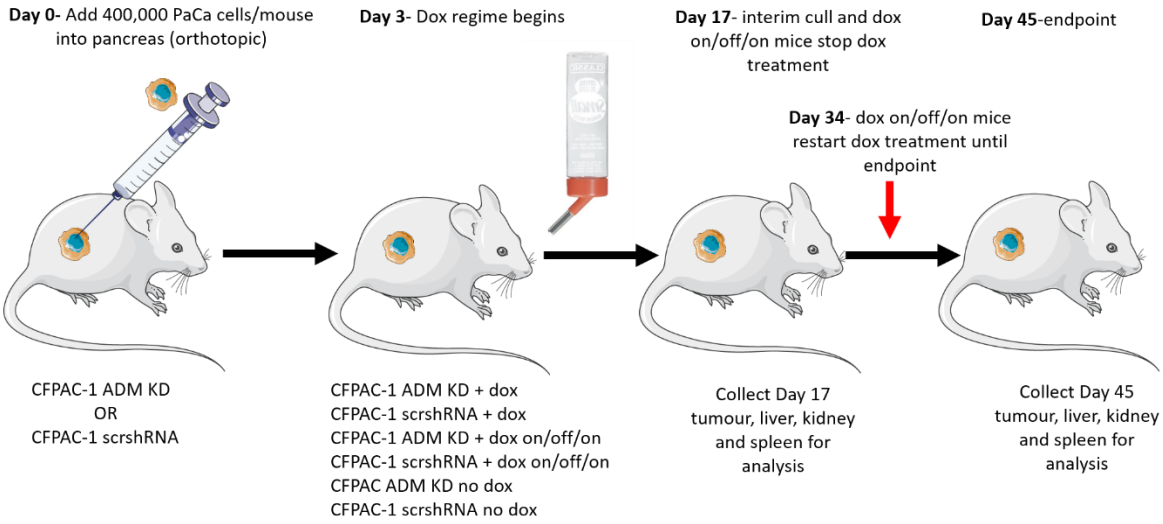

Figure 6.2 Orthotopic *in vivo* schematic. Female BALB/c nude mice were injected with 400,000 CFPAC-1 ADM KDs or CFPAC-1 scrshRNA cells directly into the pancreas. After 3 days, mice were divided into groups dependent on their doxycycline water regime (dox, dox on/off/on or no dox). At day 17 half the mice were culled and tumours, liver, kidney and spleen were collected for analysis. The mice in the dox on/off/on group had their water changed to contain no dox. At day 34, mice in the dox on/off/on group were given doxycycline again to re-induce KDs. Day 45 was the endpoint of the experiment and tumours, livers, kidneys and spleens were collected for analysis.

6.2.1.6 Measuring tumour growth by IVIS

Tumour growth was monitored and imaged by measuring bioluminescence using the PerkinElmer Lumina II in vivo imaging system (IVIS). The first measurement was taken at day 3 before KDs were either induced with doxycycline containing water or left non-induced with normal water. Measurements continued twice weekly to ensure tumour growth was within limits.

To measure bioluminescence, mice were anaesthetised with inhaled isoflurane and injected with 100 µL D-Luciferin (8.6 µg/mL) subcutaneously. Mice continued to be anaesthetised for 10 minutes to allow D-luciferin to circulate before mice were placed in IVIS to image white light and bioluminescence for later analysis. The mice were placed back in their cages and continued to be monitored for 30 minutes after to ensure they had fully recovered. The bioluminescent images were quantified using

the LivingImage software (Figure 6.3) by drawing regions of interest (ROI) around the primary tumour. The total flux (p/sec) was recorded and plotted on GraphPad 9.2.0. Mouse weights were also measured twice weekly to ensure that weight did not drop more than 20% from starting weight.

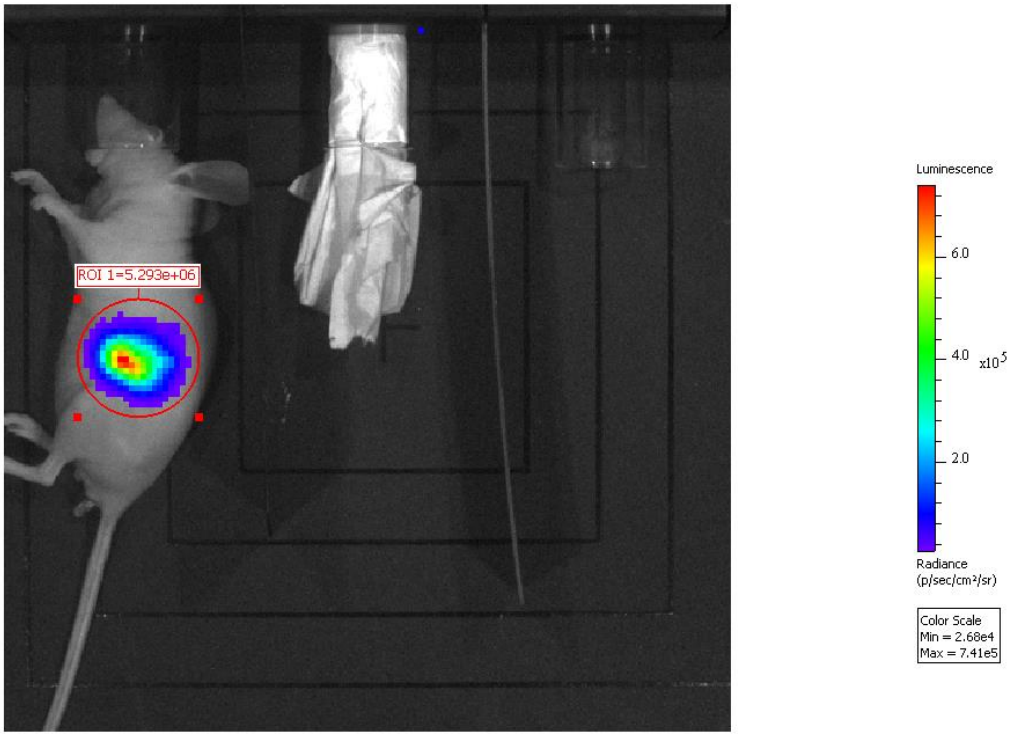

Figure 6.3 Bioluminescent quantification of pancreatic tumours. Region of interests (ROI) were drawn around the tumours to determine total flux (p/sec) which was recorded and plotted on GraphPad 9.2.0.

6.2.1.7 In Vivo Endpoint

The endpoint for each group of mice was either on day 17 (for interim analysis) or on day 45. The mice were anaesthetised with isoflurane and injected subcutaneously with 100 µL of D-luciferin (8.6 µg/mL) for analysis of tumours luminescence. D-luciferin was left to circulate around mice for 10 minutes before blood was withdrawn by cardiac puncture (25 G needle and 1 mL syringe). The needles were removed to prevent haemolysis before the blood was collected in Vacutainer tubes containing EDTA. The culling of mice was confirmed by cervical dislocation as recommended by the Schedule 1 guidelines outlined Animals (Scientific Procedures) Act 1986. The pancreas tumour and organs were

collected and bioluminescence was measured using IVIS to quantify endpoint tumour bioluminescence and detect any metastasis Figure 6.4). Tumour and organs were weighed and fixed in 10% neutral buffered formalin. Fixed samples were sent to the Histology core facility for paraffin embedding and sectioning for immunohistochemistry analysis.

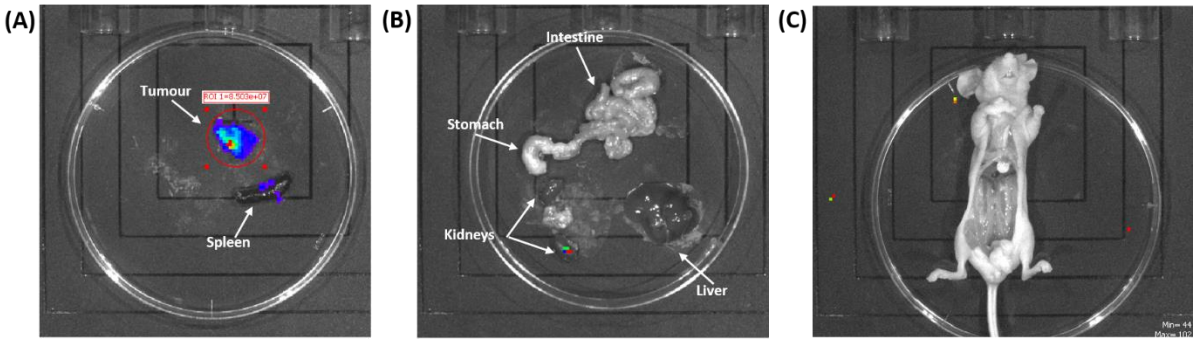

Figure 6.4 Bioluminescence of (A) Primary pancreatic tumour and spleen, (B) organs (C) and empty body measured by IVIS to check for metastasis from primary tumour site.

6.2.1.8 Endpoint analysis of immune cells

Following collection of whole blood by cardiac puncture in Vacutainer tubes containing EDTA, 20 µL aliquots of whole blood were collected in 0.5 mL Eppendorf tubes for analysis of immune cells by the scil Vet abc Plus haematology analyser. 10 µL of whole blood was aspirated by the scil Vet abc Plus to determine the percentage of monocytes, eosinophils and lymphocytes. Data was plotted on GraphPad 9.2.0 and analysed by Two-way ANOVA and Tukey's multiple comparison test.

6.2.1.8 Ki67 staining of orthotopic tumours (immunohistochemistry)

For analysis of the effects of ADM KD on proliferation of CFPAC-1 cells, tumour sections from the orthotopic experiment were prepared by the Histology Core facility and analysed using anti-Ki67 proliferation marker subsequently. The samples analysed were CFPAC-1 ADM KDs and CFPAC-1 scrshRNA from the dox on, dox on/off/on and no dox groups (refer to Table 6.1) from both day 17 cull and day 45 culls.

The slides were first dewaxed for 5 minutes in Coplin jars containing xylene and then rehydrated through an alcohol gradient from 100% to 70% for 2 minutes at each concentration. The slides were then rehydrated for 5 minutes in water and placed in 250 mL Tris-EDTA (TE) buffer (10 mM Tris, 1 mM EDTA, pH 8.0) in a water bath for 25 minutes. The slides were cooled for 20 minutes at room temperature before being rinsed in TE buffer 3 times for 5 minutes. A wax border was drawn around the sample to prevent reagents leaking off the slide.

The sections were next blocked for 1 hour with goat serum in Tris Buffer Saline with 0.05% Tween (TBS-T) (50 mM Tris, 150 mM NaCl, 0.05% Tween 20, pH 7.6). This was followed by incubation in the Ki67 primary antibody (rabbit polyclonal, ab15580) at a concentration of 1:250 in TBS-T blocking buffer for 1 hour at room temperature. The slides were then washed 3 times in TBS (50 mM Tris, 150 mM NaCl, pH 7.6) for 5 minutes, followed by application of the secondary biotinylated goat anti-rabbit (Vector Labs, PK-4001) antibody diluted 1:150 in blocking serum containing TBS-T for 30 minutes at room temperature. The slides were again rinsed 3 times for 5 minutes in TBS and ABC (avidin-biotin complex) was applied for 30 minutes at room temperature.

The slides were again rinsed in TBS 3 times for 5 minutes before ImmPACT DAB (Vector Labs, SK-4105) was applied for 2 minutes. One drop of DAB was diluted in 1 mL DAB reagent. Excess DAB was removed before the slides were rinsed in water for 5 minutes. Slides were counterstained in haematoxylin for 20 seconds and then dehydrated in alcohol, starting at a concentration of 70% and ending in 100% alcohol for 2 minutes at each concentration. The slides were placed in xylene for a final 5 minutes before mounting. Coverslips were mounted onto slides with DPX mounting medium. Coverslips were left to air dry before analysis of slides on QuPath.

6.2.1.9 Analysis of Ki67 positive cells using QuPath

Slides stained for Ki67 were analysed and the percentage of positive Ki67 staining was quantified using QuPath. The first step was to manually annotate the slide to select the region of interest (ROI) which was considered the whole tumour/tissue section for this analysis (Figure 6.5). Following this, the

analyse tab was selected followed by positive cell detection to set the parameters for positive cell detection (Figure 6.6). Optical density summary was detected and a single threshold value was selected to discriminate between truly positive cells (brown DAB staining) and false positive cells (background brown staining). After running positive cell detection on QuPath, cells stained positively with DAB for Ki67 were shown in red and cells that were not detected of Ki67 positive and therefore had no brown DAB staining were shown in blue (Figure 6.7a). Selecting the annotations tab on QuPath showed the percentage of cells stained positively for Ki67 (Figure 6.7b). The percentage of Ki67 positive cells was plotted in GraphPad Prism 9.2.0 and analysed by two-way ANOVA analysis.

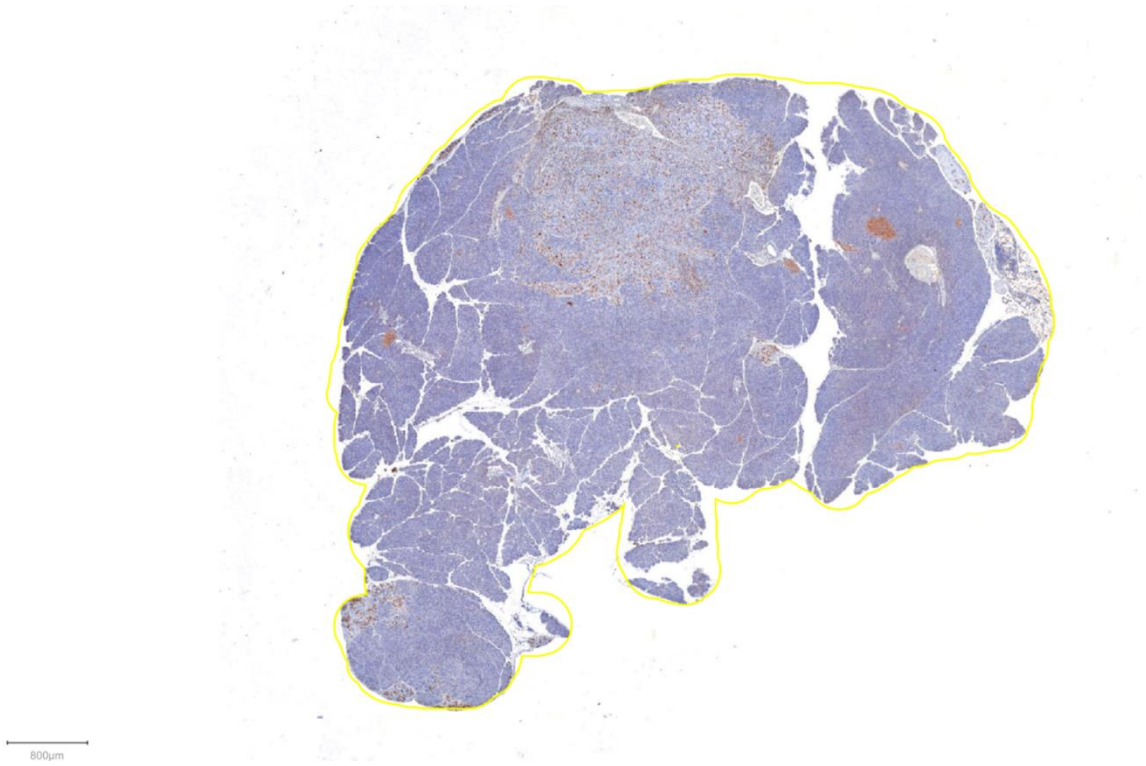

Figure 6.5 Ki67 tumour section annotation on QuPath. Slides were annotated (yellow border) to select region of interest to detect the number of Ki67 positive cells.

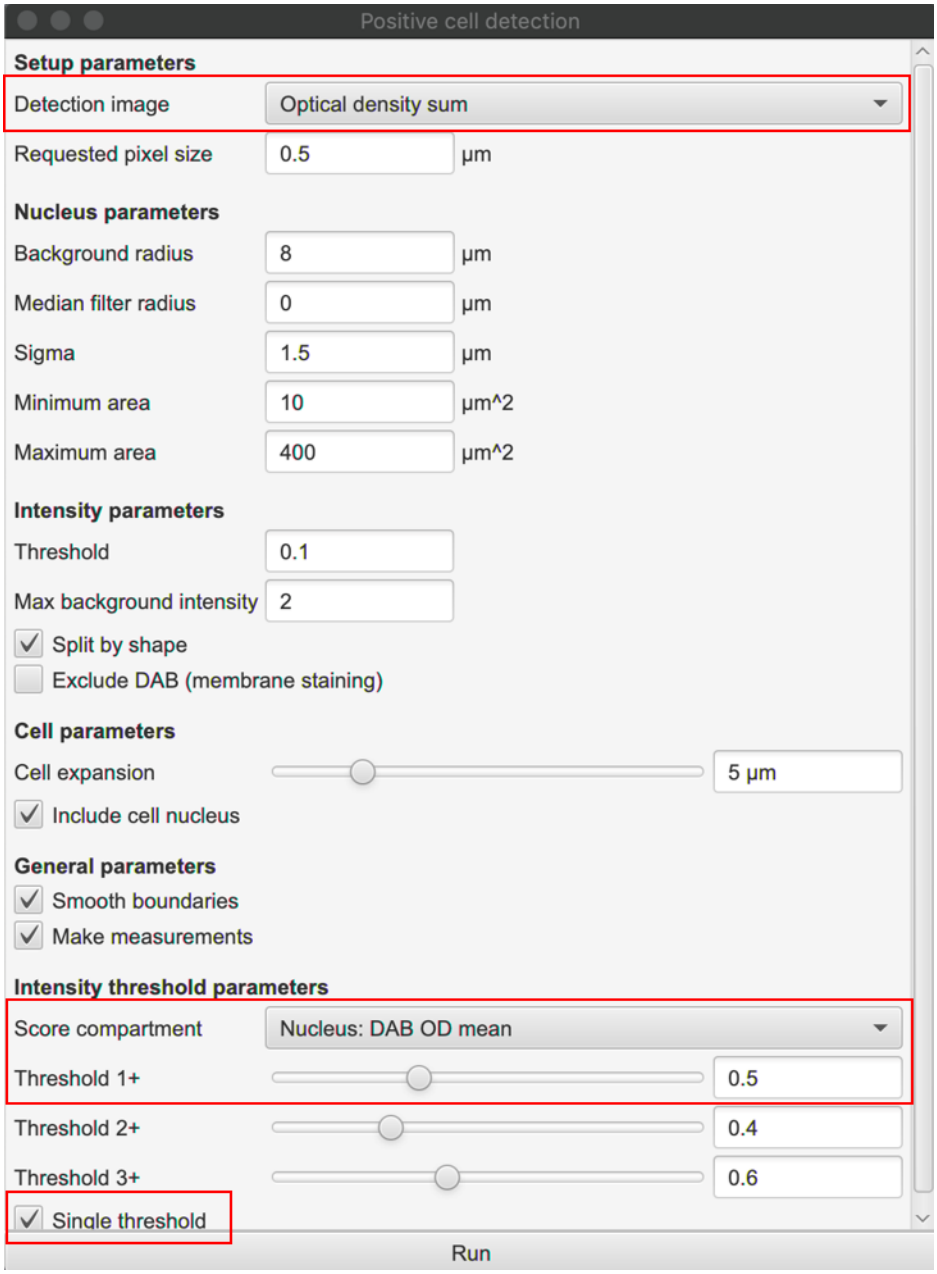

Figure 6.6 QuPath positive cell detection parameters. The detection image is first selected and changed to optical density summary. The score compartment selected was Nucleus: DAB OD mean and the single threshold was selected as 0.5 to discriminate between positively Ki67 cells and unstained cells.

(A)

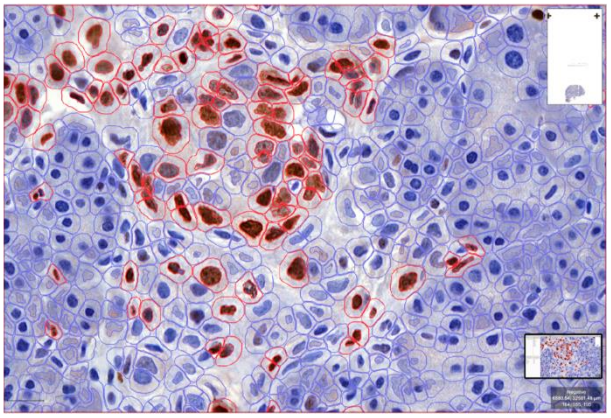

(B)

Key	Value
Image	1M12.mrxs
Name	PathAnnotationObject
Class	
Parent	Image
ROI	Geometry
Centroid X µm	9526.1276
Centroid Y µm	29987.9296
Num Detections	162307
Num Negative	149909
Num Positive	12398
Positive %	7.6386
Num Positive per mm^2	403.5042
Area µm^2	30725827.475
Perimeter µm	26141.9957

Figure 6.7 Analysis of Ki67 positive cells using QuPath. **(A)** Ki67 positive cells shown in red (DAB stained) and negative shown in blue following positive cell detection analysis. **(B)** The final output is shown under the annotation panel which calculates the number of Ki67 positive cells (red box).

6.2.2 In vivo subcutaneous model

6.2.2.1 Mice

Subcutaneous tumour xenograft studies were carried out in 5 to 6 week old female nude BALB/c mice from Charles River. Before beginning the experiment, all procedures were reviewed and approved by the local Research Ethics Committees in the University of Sheffield and complied with UK Animals (Scientific Procedures) Act 1986. Studies were performed under project licence PF61050A3.

6.2.2.2 Cell preparation for subcutaneous injection

CFPAC-1 ADM KD-LucRFP, CFPAC-1 scrshRNA-LucRFP and CFPAC-1-LucRFP were harvested in triple layer T175 flasks and counted as described in Chapter 2, Section 2.1.1 and 2.1.4. The day before the procedure, Matrigel was thawed on ice in the fridge to prevent the Matrigel from solidifying. Bijoux tubes, 1 mL tips and PBS were chilled in the fridge overnight. The cells were prepared at a concentration of 30 million cells/mL in a mix of Matrigel:PBS (3:2 ratio). The cell preparation was carried out using ice cold PBS and tips that had been kept in the fridge over night to minimise chances of Matrigel solidifying.

6.2.2.3 Subcutaneous injection of cells

25 G needles and 1 mL syringes (insulin syringes) were used for subcutaneous injection of CFPAC-1 ADM KD-LucRFP, CFPAC-1 scrshRNA-LucRFP and CFPAC-1-LucRFP into the left dorsal flank of mice. Each mouse was injected with 100 µL of cells (3 million cells/mouse). Mice were split into 6 groups dependent on cell type and doxycycline induction (Table 6.2). CFPAC-1-LucRFP cells were also induced with doxycycline to see if doxycycline effected growth of tumours without inducible shRNA. Doxycycline was prepared as described in Section 6.2.1.5.

Table 6.2 The subcutaneous *in vivo* experiment was split into 6 groups according to cell type and whether KD cells were induced by doxycycline (0.5 mg/mL).

Cells	Doxycycline induced (0.5 mg/mL)
CFPAC-1 ADM KD-LucRFP	Yes
CFPAC-1 ADM KD-LucRFP	No
CFPAC-1 scrshRNA-LucRFP	Yes
CFPAC-1 scrshRNA-LucRFP	No
CFPAC-1-LucRFP	Yes
CFPAC-1-LucRFP	No

6.2.2.4 Measuring subcutaneous tumour growth

Tumour growth was measured using Vernier callipers twice a week. Tumour volume (mm^3) was determined by the formula below:

$$V = \left[\pi \left(\frac{w}{2}\right)^2 \times \ell\right]$$

v represents the tumour volume, *w* is tumour width and ℓ is tumour length. The mice body weights were also recorded 3 times a week to ensure that the body weight did not drop more than 20% from starting weight.

6.2.3.5 In vivo endpoint

Mice were anaesthetised by inhalation of isoflurane and blood was collected by cardiac puncture using a 25 G needle and 1 mL syringe. The needle was removed before the blood was dispensed into

Vacutainer tubes containing EDTA. Cervical dislocation was used to cull the animals before collection of tumour and organs. The tumour, liver, kidney and spleen were collected and weighed before being fixed in 10% neutral buffered saline. Samples were sent to the Histology Core facility for samples to be embedded in paraffin and sectioned for immunohistochemistry.

6.3 Results

In vivo orthotopic models were developed using CFPAC-1 ADM KD cells and CFPAC-1 scrshRNA controls as described in Section 6.2. The KDs and controls were either induced with doxycycline (dox on), were both induced and not induced by doxycycline (dox on/off/on) or not induced at all (no dox). The purpose of this experiment was to determine whether KD of ADM altered tumour growth measured by luminescence of tumours and weight of tumours *ex vivo*. Further analysis included measuring organs weights, determining whether there were alterations to immune cell percentages between groups and analysing the percentage of positive Ki67 proliferating tumour cells. A subcutaneous model was also developed to determine changes in tumour volume and weight between doxycycline induced and un-induced CFPAC-1 ADM KDs and scrshRNA controls. This was determined by regular measurements of tumours using Vernier callipers and measuring tumour weight ex vivo. Weights of mice were also measured 3 times a week to ensure that weight did not drop below 20% of their starting weight.

6.3.1 Comparison of orthotopic tumour weight and luminescence of CFPAC-1 ADM KDs and scrshRNA

Figure 6.8a shows tumour weights following day 17 interim cull. Two-way ANOVA analysis showed a significant difference in CFPAC-1 ADM KDs and CFPAC-1 scrshRNA (p= 0.05) and between different doxycycline conditions (p= 0.03).CFPAC-1 ADM KDs in the no dox group had the highest average tumour weight of 195.7 mg and the lowest was in dox on/off/on group at 147.1 mg. CFPAC-1 scrshRNA followed the same pattern in results with slightly lower tumour weights, the average highest tumour weight was in the no dox group at 167.0 mg and lowest in the dox on/off/on group at 141.6 mg. The dox on group in scrshRNA was only 4.2 mg heavier than dox on/off/on showing only a small difference in tumour weight between groups.

Day 45 two-way ANOVA analysis of tumour weight showed a significant difference between the CFPAC-1 ADM KDs and scrshRNA (p= 0.0010). Tumour weights were higher in the CFPAC-1 ADM KD

group compared to scrshRNA controls. CFPAC-1 ADM KDs induced with doxycycline were 289 mg heavier than CFPAC-1 scrshRNA control average. CFPAC-1 ADM KDs in the dox on/off/on group were 313.4 mg heavier in weight compared to scrshRNA control average. CFPAC-1 ADM KDs in the no dox group had the largest increase in tumour weight of 554.6 mg compared to scrshRNA controls. In both CFPAC-1 ADM KDs and scrshRNA no dox groups, tumour weights were the highest (Figure 6.8b). However, Tukey's multiple comparison tests showed no significant differences between these different conditions.

Two-way ANOVA analysis of ex vivo tumour luminescence at day 17 showed no significant difference between different doxycycline conditions and KDs compared to controls (Figure 6.8c). However, at day 45 there was a significant difference between the different doxycycline conditions ($p< 0.0001$). Tukey's multiple comparison test showed that there was a statistical difference between CFPAC-1 ADM KDs in the dox on/off/on group and no dox group ($p= 0.03$). There was also a significant difference between CFPAC-1 scrshRNA dox on and no dox ($p= 0.01$) and CFPAC-1 scrshRNA in the dox on/off/on and no dox group ($p= 0.008$) (Figure 6.8d).

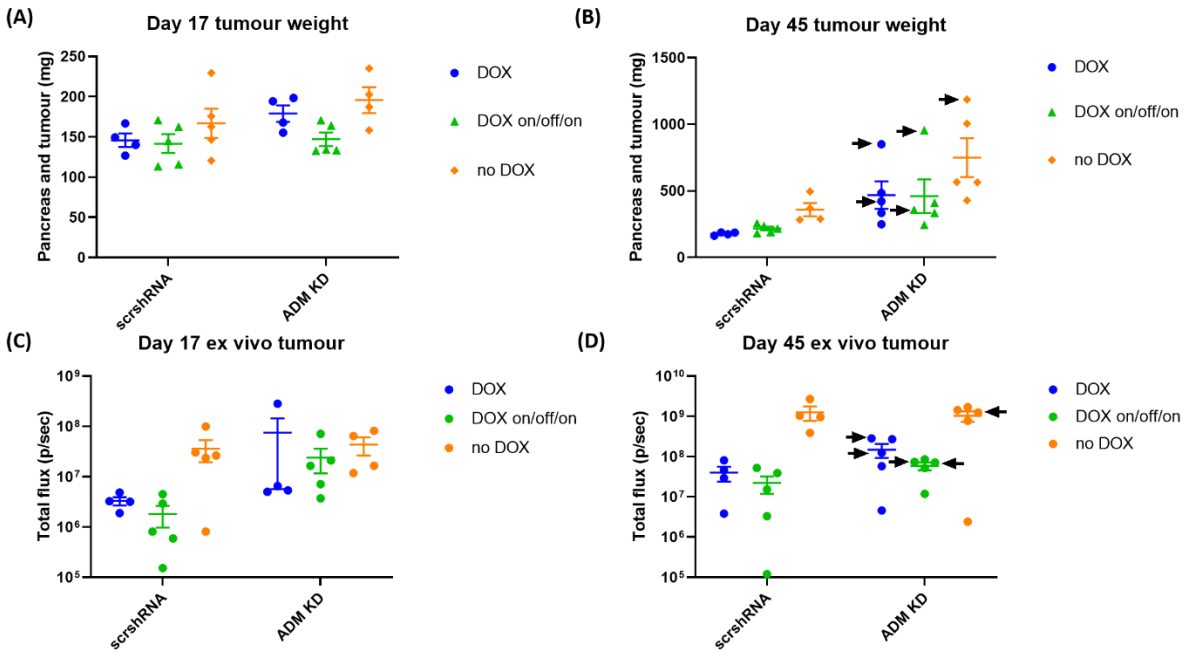

Figure 6.8 Day 17 and Day 45 tumour weights following orthotopic injection of CFPAC-1 ADM KDs or CFPAC-1 scrshRNA into 5-6 week old BALB/C female mice. KDs and scrshRNA control were either induced with dox (dox), induced with dox which was stopped at day 17 and then re-induced on day 34 as described in methods (dox on/off/on) or not induced by dox (no dox) **(A)** Day 17 interim cull tumour weight. The tumour weight of CFPAC-1 ADM KDs and scrshRNA was measured in dox (blue), dox on/off/on (green) and no dox (orange) samples **(B)** Day 45 endpoint cull tumour weight in CFPAC-1 ADM KD and scrshRNA samples following dox, dox on/off/on or no dox treatment **(C)** Day 17 interim cull tumour luminescence. The luminescent signal of CFPAC-1 ADM KD and CFPAC-1 scrshRNA samples was measured in dox (blue), dox on/off/on (red) and no dox (green) samples and plotted as total flux (p/sec) **(D)** Day 45 endpoint cull tumour luminescence following dox, dox on/off/on and no dox treatment. Arrows indicate mice that had to be culled on day 38 due to significant weight loss and tumour size. Two-way ANOVA analysis was used for statistical analysis of samples.

6.3.2 Comparison of CFPAC-1 ADM KD and CFPAC-1 scrshRNA tumour luminescence determined by IVIS

The luminescence of tumours was measured following subcutaneous injection of D-luciferin by IVIS. This method was used to compare luminescent signal between ADM KDs and controls in dox on, dox on/off/on and no dox groups. Measuring the luminescent signal also was used as a method to identify any areas of metastasis. Figure 6.9a shows that the luminescent signals in each group (dox on, dox on/off/on and no dox) were not significantly different between CFPAC-1 ADM KDs and CFPAC-1 scrshRNA controls. ADM KDs and scrshRNA in the no dox group had the highest luminescent signal. CFPAC-1 ADM KD induced with doxycycline had higher luminescent signal than scrshRNA, both groups had more luminescence than dox on/off/on group until day 31. CFPAC-1 ADM KDs in the dox on/off/on group had slightly higher luminescence compared to scrshRNA dox on/off/on. CFPAC-1 scrshRNA induced with doxycycline had the smallest changes in luminescence over 45 days. By the endpoint at day 45, all the cells had a similar luminescent signal except CFPAC-1 ADM KDs and CFPAC-1 scrshRNA controls induced with dox.

Figure 6.9b shows the tumour percentage luminescence relative to the initial day 3 luminescent signals. This was calculated as the CFPAC-1 scrshRNA controls had a slightly lower luminescent signal when measured by IVIS *in vitro* following transduction with Luc-RFP described in Chapter 4, Section 4.2.4. Following normalisation to day 3, the data still shows similarities to the luminescence data shown in Figure 6.9a. Both cell types in the no dox group had the highest percentage luminescence, by day 45 CFPAC-1 scrshRNA had slightly more luminescence. This was followed by CFPAC-1 ADM KDs in the dox on/off/on until day 38 where induced CFPAC-1 ADM KDs (dox on) had the highest percentage luminescence. The increase in luminescence in the CFPAC-1 ADM dox on group at day 38 and then the sudden decline at day 42 (Figure 6.9) relates to the premature endpoint of a mouse due to significant weight loss and tumour size (Figure 6.8). At day 45, both CFPAC-1 ADM KDs and CFPAC-1 scrshRNA in dox on/off/on and dox induced group had similar percentage luminescence. At the

endpoint, CFPAC-1 scrshRNA without doxycycline induction had the highest percentage luminescence and CFPAC-1 ADM dox on/off/on had the lowest percentage luminescence. Overall CFPAC-1 ADM dox on/off/on had the smallest changes in luminescence over 45 days.

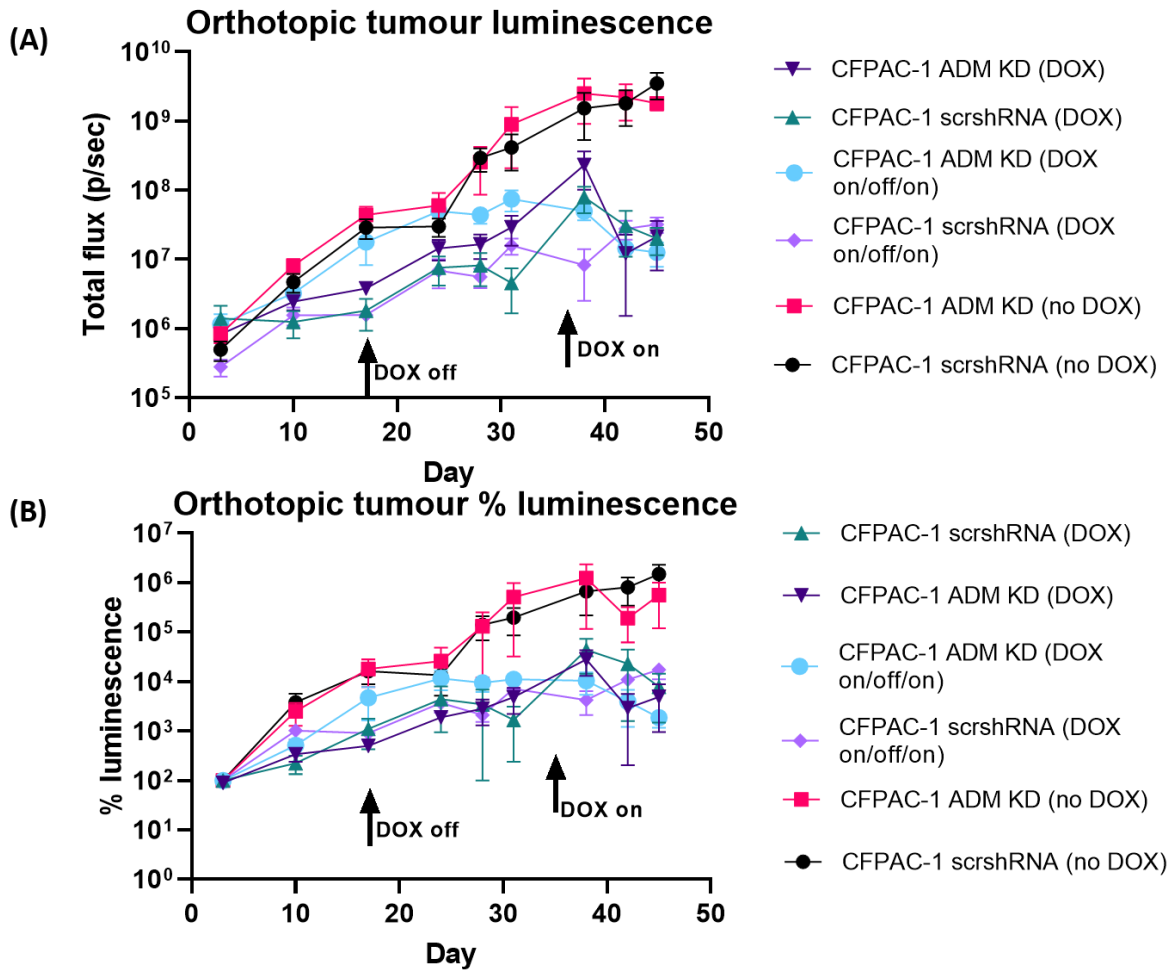

Figure 6.9 CFPAC-1 ADM KD and CFPAC-1 scrshRNA tumour luminescence following orthotopic injection of cells into the pancreas determined by IVIS. Cells were either induced with doxycycline or non-induced and split into 3 groups; dox on, dox on/off/on or no dox. **(A)** Log tumour luminescence measured once a week over 45 days. **(B)** Percentage tumour luminescence relative to the first luminescence read on day 3. Data is presented as mean ± SEM.

6.3.3 Orthotopic model interim and endpoint organ weights

Once mice reached their endpoints, liver, kidney and spleen were collected from CFPAC-1 ADM KDs and CFPAC-1 scrshRNA. The organs were imaged using IVIS to determine if there was any metastasis (Figure 6.12) and organs were weighed to see if there were any differences in organ weight between KDs and controls and also within the different doxycycline conditions. Two-way ANOVA analysis shows no significant differences between weights of CFPAC-1 ADM KDs and CFPAC-1 scrshRNA organs and the different doxycycline treatments on day 17 and day 45 (Figure 6.10).

Although there were no significant differences found on day 17 between CFPAC-1 ADM KDs and scrshRNA control organ weights, IVIS imaging did show some potential stomach metastasis in 5 of the mice at day 45. This was represented by an increase in luminescent signal in the stomach. Two mice from CFPAC-1 scrshRNA dox on group showed potential luminescent signal in the stomach, one mouse from the CFPAC-1 ADM KD dox on group showed a luminescent signal in the stomach and two mice from the CFPAC-1 scrshRNA no dox group had a luminescent signal in the stomach (Figure 6.11). An example of this is shown in Figure 6.12a.

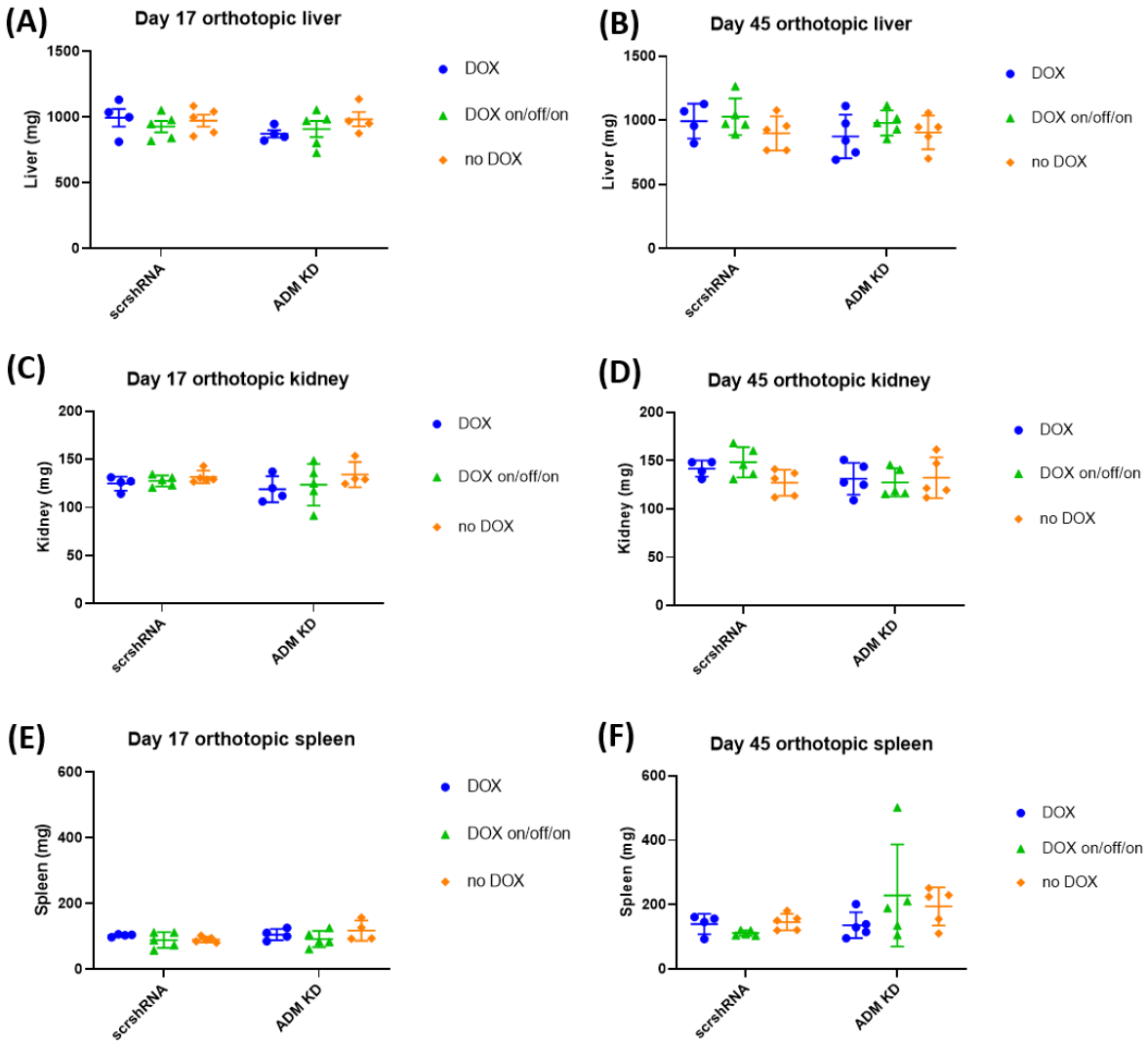

Figure 6.10 CFPAC-1 ADM KDs and CFPAC-1 scrshRNA day 17 and 45 organ weights following orthotopic injection of cells into pancreas. ADM KD and control scrshRNA cells were grouped by whether they were induced by doxycycline or not induced by doxycycline into 3 groups; dox on, dox on/off/on and no dox **(A)** Day 17 liver weight of CFPAC-1 ADM KD and scrshRNA. **(B)** Day 45 liver weight of CFPAC-1 ADM KD and scrshRNA. **(C)** Day 17 kidney weight of CFPAC-1 ADM KD and scrshRNA. **(D)** Day 45 kidney weight of CFPAC-1 ADM KD and scrshRNA. **(E)** Day 17 spleen weight of CFPAC-1 ADM KD and scrshRNA. **(F)** Day 45 kidney weight of CFPAC-1 ADM KD and scrshRNA. Data presented as mean ± SEM.

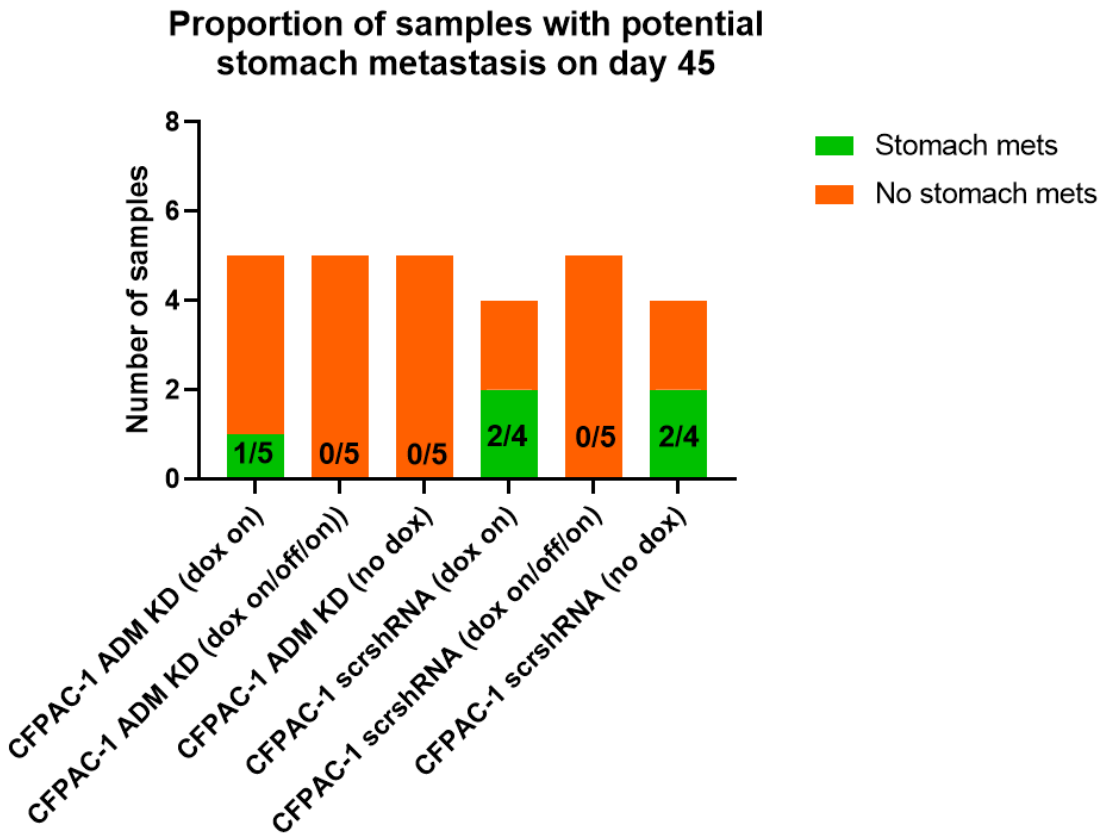

Figure 6.11 A graph to show proportion of mice with potential stomach metastases in CFPAC-1 ADM KD and CFPAC-1 scrshRNA groups (data includes Day 38 and day 45 mice). Mice with potential stomach metastases had luminescent signal in stomach following endpoint cull (day 45). The graph shows 1 out of 5 mice in CFPAC-1 ADM dox on group to have potential metastases. In CFPAC-1 scrshRNA dox on and no dox group, 2 out of 4 mice had potential stomach metastases.

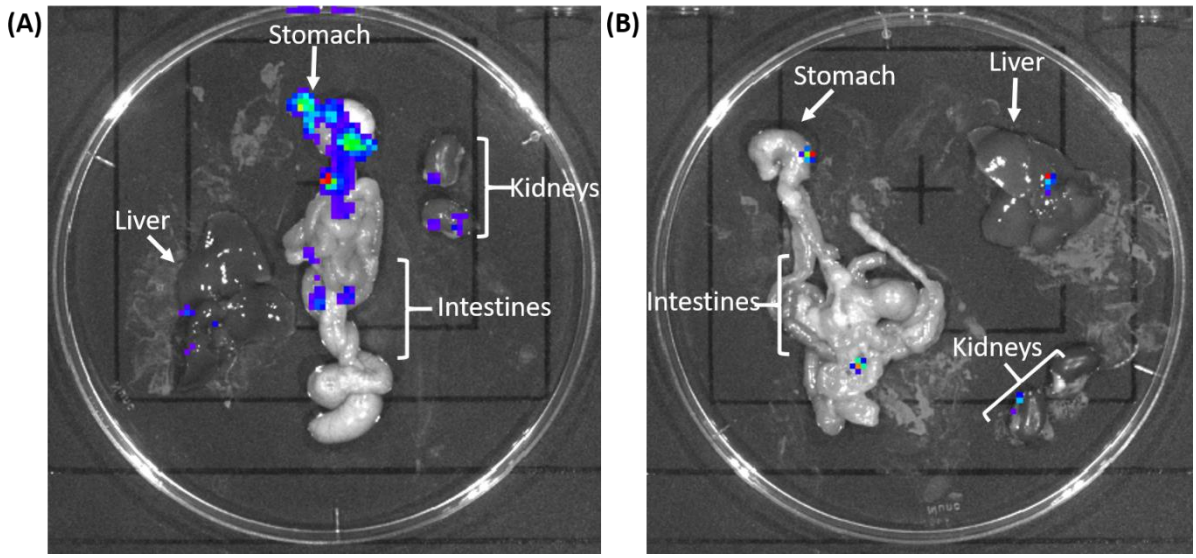

Figure 6.12 CFPAC-1 scrshRNA day 45 no DOX and DOX on/off/on organ IVIS luminescence. Following culling of mice at day 45 endpoint, luminescence of organs was measured to see if any metastasis was apparent. **(A)** CFPAC-1 scrshRNA no DOX IVIS luminescence with potential stomach metastasis. **(B)** CFPAC-1 scrshRNA DOX on/off/on IVIS luminescence with minimal luminescent signal present.

6.3.4 CFPAC-1 ADM KD and CFPAC-1 scrshRNA immune analysis

Whole blood was collected on day 17 and day 45 by cardiac puncture from CFPAC-1 ADM KDs and CFPAC-1 scrshRNA for immune cell analysis. The values obtained for monocytes, eosinophil and lymphocytes were compared to the values provided by Charles River for BALB/C female mice. Figure 6.13a and b show that monocytes were within normal range at day 17 and 45 with one outlier in ADM KDs and scrshRNA in the no dox group. The percentage of eosinophils in both CFPAC-1 ADM KDs and CFPAC-1 scrshRNA were shown to be both within range and outside of the normal range determined by Charles River. The variability in distribution was amongst both ADM KD and scrshRNA and different doxycycline conditions at day 17 and day 45. The lymphocyte percentage in both CFPAC-1 ADM KDs and scrshRNA were within normal range on day 17 and day 45. However, CFPAC-1 ADM KDs without doxycycline treatments had lower levels of lymphocytes on day 17 (Figure 6.13).

Two-way ANOVA analysis of day 17 data showed no significant difference between CFPAC-1 ADM KDs and scrshRNA and the different doxycycline conditions in monocytes and eosinophils. However, there

was a significant difference between different doxcycline conditions (p=0.04), ADM KDs compared to scrshRNA (p= 0.03) and in interactions (p= 0.04) following analysis of lymphocytes (Figure 6.13e and f). Tukey's multiple comparison tests showed specific significant differences between CFPAC-1 ADM KDs and scrshRNA not induced with doxycycline (p= 0.02). The CFPAC-1 ADM no dox group had 26% fewer lymphocytes that the CFPAC-1 scrshRNA group. However, CFPAC-1 ADM group has 3 mice compared to 5 mice in the CFPAC-1 scrshRNA. Also the CFPAC-1 ADM KD group has an outlier showing only 5.9% lymphocytes, compared to 47.2% and 43.8% for the other two repeats. The multiple comparison test also showed a significant difference (p= 0.02) between CFPAC-1 ADM KDs in the dox on/off/on group and no dox group. Lymphocytes without doxycycline induction had overall lower percentage of lymphocytes on day 17.

Two-way ANOVA analysis of day 45 monocyte and lymphocyte percentage in whole blood mouse samples showed significant differences only between the different doxycycline conditions in monocytes (p=0.20) and lymphocytes (p=0.03) (Figure 6.13). However, eosinophils showed no significant differences between different doxycycline conditions. Tukey's multiple comparison tests showed no significant differences for all immune cells.

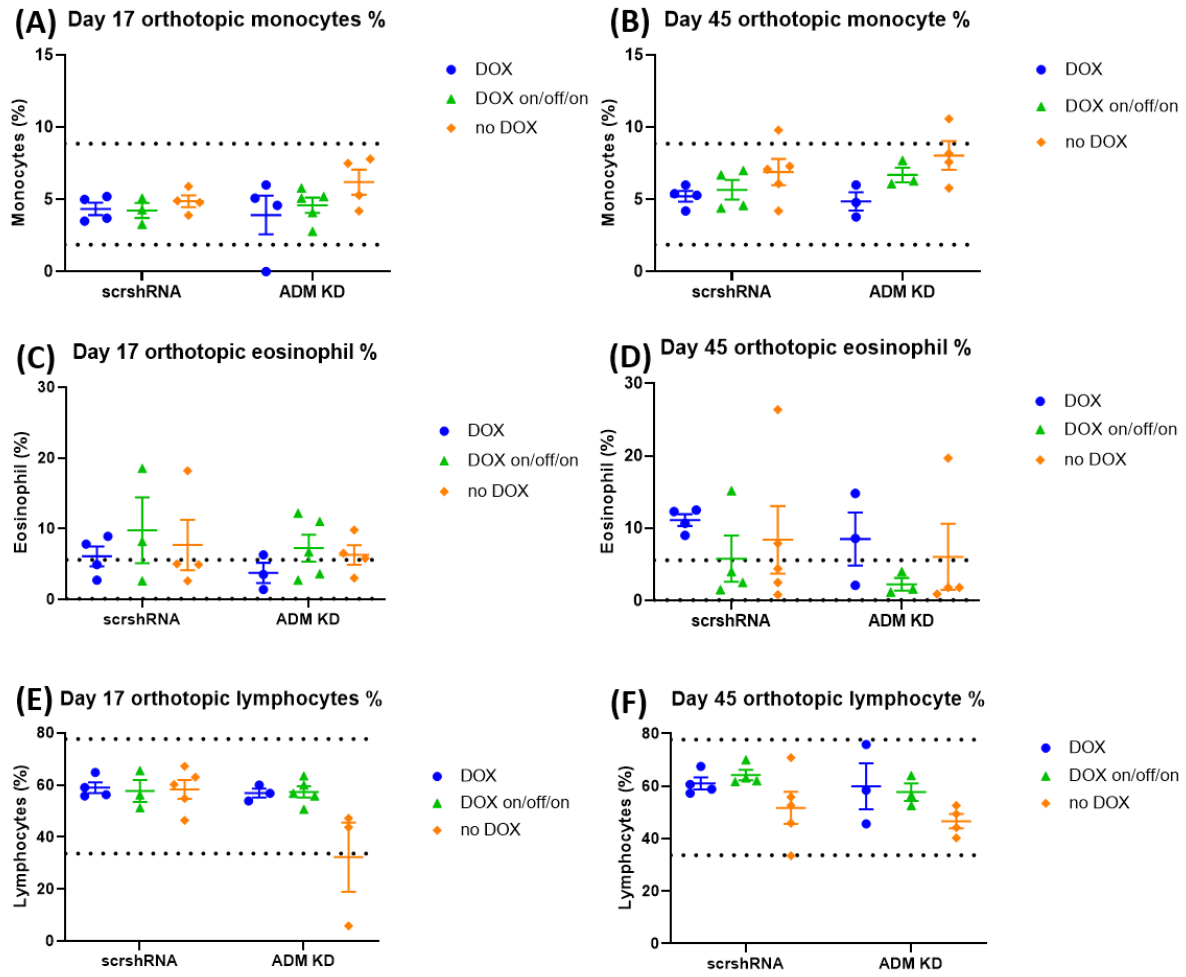

Figure 6.13 Day 17 and day 45 CFPAC-1 ADM KD and CFPAC-1 scrshRNA whole blood immune analysis. On the day of cull, blood was collected by mice by cardiac puncture and whole blood was analysed for immune cells in cells grouped by dox on, dox on/off/on and no dox. Dotted lines indicate normal levels of monocytes, eosinophils and lymphocytes in BALB/C female nude mice determined by supplier, Charles River. **(A)** Monocyte percentage in whole blood collected from CFPAC-1 ADM and CFPAC-1 scrshRNA on day 17 **(B)** Monocyte percentage in whole blood collected from CFPAC-1 ADM KD and CFPAC-1 scrshRNA on day 45. **(C)** Eosinophil percentage in whole blood collected from CFPAC-1 ADM KD and CFPAC-1 scrshRNA on day 17. **(D)** Eosinophil percentage in whole blood collected from CFPAC-1 ADM KD and CFPAC-1 scrshRNA on day 45. **(E)** Lymphocyte percentage in CFPAC-1 ADM KDs and CFPAC-1 scrshRNA on day 17. **(F)** Lymphocyte percentage in CFPAC-1 ADM KDs and CFPAC-1 scrshRNA on day 45. Data presented as mean ±SEM.

6.3.5 Comparison of CFPAC-1 ADM KD and scrshRNA histology and Ki67 proliferating cells

Tumours of CFPAC-1 ADM KD and CFPAC-1 scrshRNA were collected on day 17 and 45, fixed in formalin and sectioned for immunohistochemistry. Sectioned tumours were H&E stained (Figure 6.14, Figure 6.15 and Figure 6.16) and were also analysed for the number of Ki67 positive cells by immunohistochemistry (Figure 6.17).

Figure 6.14 show IVIS images and H&E stains of CFPAC-1 scrshRNA and CFPAC-1 ADM KD mice that were doxycycline-induced for the whole experiment. They show that at day 45, luminescent signal was higher than in day 17 samples. In Figure 6.14a, there is no or very low luminescent signal at day 17 in CFPAC-1 scrshRNA which correlates with the uniform pancreatic structure shown in Figure 6.14b where there is no apparent tumour cells. This also correlated with Ki67 analysis which showed that in the total area, there was only 1.5% Ki67 positive cells (Figure 6.17). Figure 6.14c shows that in CFPAC-1 scrshRNA induced with doxycycline, there is a significant increase in luminescent signal on day 45. This also correlates with the H&E which shows a less uniform pancreatic structure and poor differentiation of cells (Figure 6,14d). This correlates with the increased percentage of Ki67 positive cells (37.4%) in the tumour section analysed (Figure 6.17). Figure 6.14e and Figure 6.14f show CFPAC-1 ADM KDs on day 17. The IVIS signal on day 17 is higher than the CFPAC-1 scrshRNA group on day 17. The majority of the section, shows that the pancreas is well differentiated and maintains normal structure. However, a small portion of the section looks less well differentiated suggesting initiation of tumour establishment. This is represented by the Ki67 staining which showed that 7.5% of cells were positively stained (Figure 6.17). Figure 6.14g and Figure 6.14h represent CFPAC-1 ADM KDs induced with doxycycline on day 45. They show that the luminescent signal of the tumour increased and that the tumour section looks less well differentiated compared to day 17. 36% of cells were shown to be Ki67 positive on day 45 (Figure 6.17).

Figure 6.15 shows IVIS images and H&E stains of CFPAC-1 scrshRNA and CFPAC-1 ADM KDs in the dox on/off/on group. Figure 6.15a shows a luminescent signal at day 17 in CFPAC-1 scrshRNA that is higher than the signal in CFPAC-1 scrshRNA in doxycycline induced group (Figure 6.15a). The H&E stain in Figure 6.15b is representative of day 17 CFPAC-1 scrshRNA dox on/off/on group and shows a well differentiated pancreas without tumour cells. Ki67 analysis of the section showed no KI67 positive cells (Figure 6.17). Figure 6.15c shows CFPAC-1 scrshRNA at day 45 with an increased luminescent signal and the tumour section (Figure 6.15d) looks less well differentiated. The Ki67 positive cells increased by 38.5% (Figure 6.17) compared to day 17. Day 17 CFPAC-1 ADM KDs shown in Figure 6.15e had a higher luminescent signal compared to day 17 CFPAC-1 scrshRNA (Figure6.15a). The percentage of Ki67 positive cells was also higher than in day 17 scrshRNA, showing 4.5% of the cells to be Ki67 positive (Figure 6.17). The tissue section looks well differentiated in Figure 6.15f showing few signs of tumour establishment. Figure 6.15g represents CFPAC-1 ADM KDs on day 45 in dox on/off/on group, the IVIS signal increased on day 45 compared to day 17 CFPAC-1 ADM KDs in the same group. The tumour section shown in Figure 6.15h shows that pancreas is less well differentiated. Furthermore, the number of Ki67 positive cells increased to 64.7% (Figure 6.17).

Figure 6.16 shows CFPAC-1 scrshRNA and CFPAC-1 ADM KDs that were not induced with doxycycline. Figure 6.a showed luminescent tumour signal in day 17 scrshRNA samples, this signal was the highest out of all doxycycline groups (Figure 6.14, Figure 6.15 and Figure 6.16). Figure 6.b shows the H&E stain for day 17 CFPAC-1 scrshRNA where only the right hand side of the section was analysed as other as the remainder of the slide had sections of other organs. Ki67 analysis shown in Figure 6.17 showed only 2.3% Ki67 positive cells. At day 45, the CFPAC-1 scrshRNA in the no dox group showed an increased luminescent signal (Figure 6.16c), this correlated with poorer differentiation of the pancreas (Figure 6.16d) and an increased number of Ki67 positive cells (38.5%) as shown by Ki67 data (Figure 6.17). Day 17 CFPAC-1 ADM KDs that were not induced with doxycycline showed a luminescent signal on day 17 (Figure 6.16e) and a well differentiated pancreatic section (Figure 6.16f). Figure 6.17 showed only 4.5% of cells were Ki67 positive. At day 45, luminescent signal increased in no dox CFPAC-1 ADM

KDs. The H&E section also looks significantly less well differentiated compared to day 17 (Figure 6.16h). This is represented number of Ki67 positive cells detected by immunohistochemistry (50.7%).

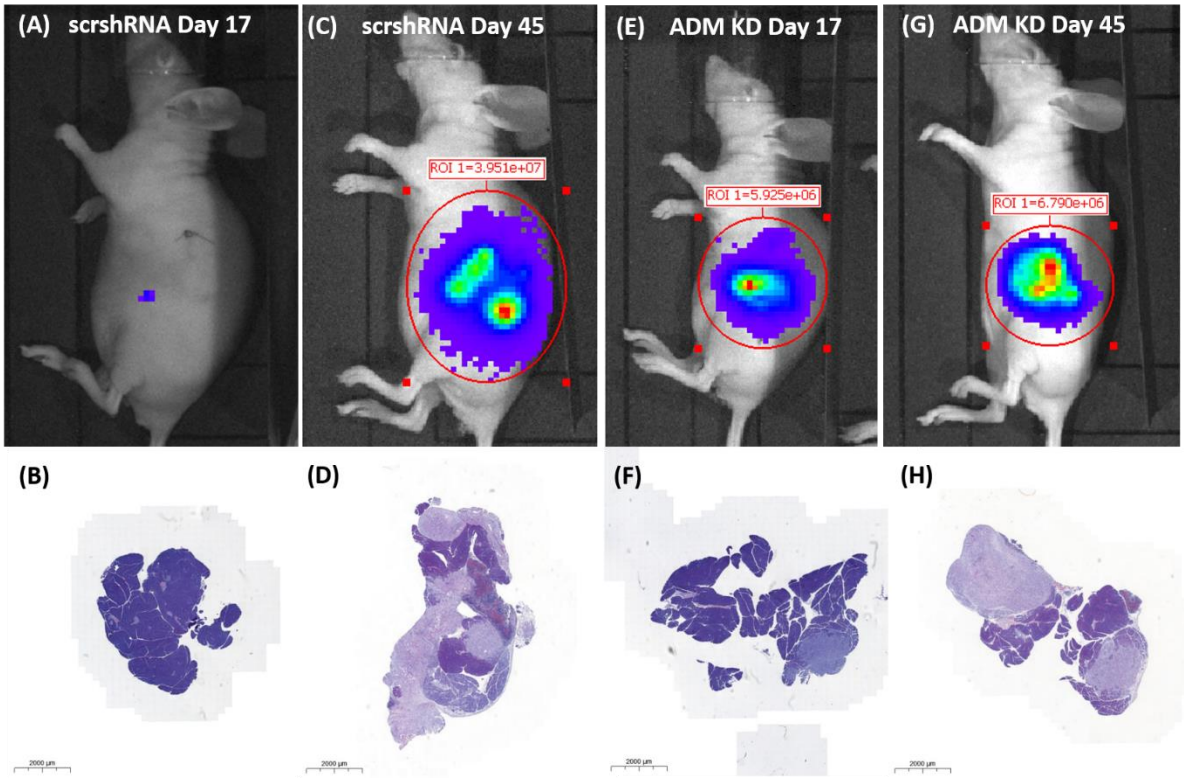

Figure 6.14 Day 17 and Day 45 CFPAC-1 scrshRNA and CFPAC-1 ADM KD doxycycline induced IVIS images and H&E stains. ScrshRNA and ADM KD mice were culled either on day 17 or day 45, the luminescence of tumours was measured using IVIS and tumours were collected for sectioning. Tumours were stained with H&E and Ki67 (not show in image). **(A)** Day 17 CFPAC-1 scrshRNA induced with doxycycline IVIS image. **(B)** Day 17 CFPAC-1 scrshRNA induced with doxycycline H&E (1.5% Ki67 positive staining). **(C)** Day 45 CFPAC-1 scrshRNA induced with doxycycline IVIS image. **(D)** Day 45 CFPAC-1 scrshRNA induced with doxycycline H&E (37.4% Ki67 positive staining). **(E)** Day 17 CFPAC-1 ADM KD induced with doxycycline IVIS image. **(F)** Day 17 CFPAC-1 ADM KD induced with doxycycline H&E stain (7.5% Ki67 positive staining). **(G)** Day 45 CFPAC-1 ADM KD induced with doxycycline IVIS image. **(H)** Day 45 CFPAC-1 ADM KD induced with doxycycline H&E stain (36% Ki67 positive staining).

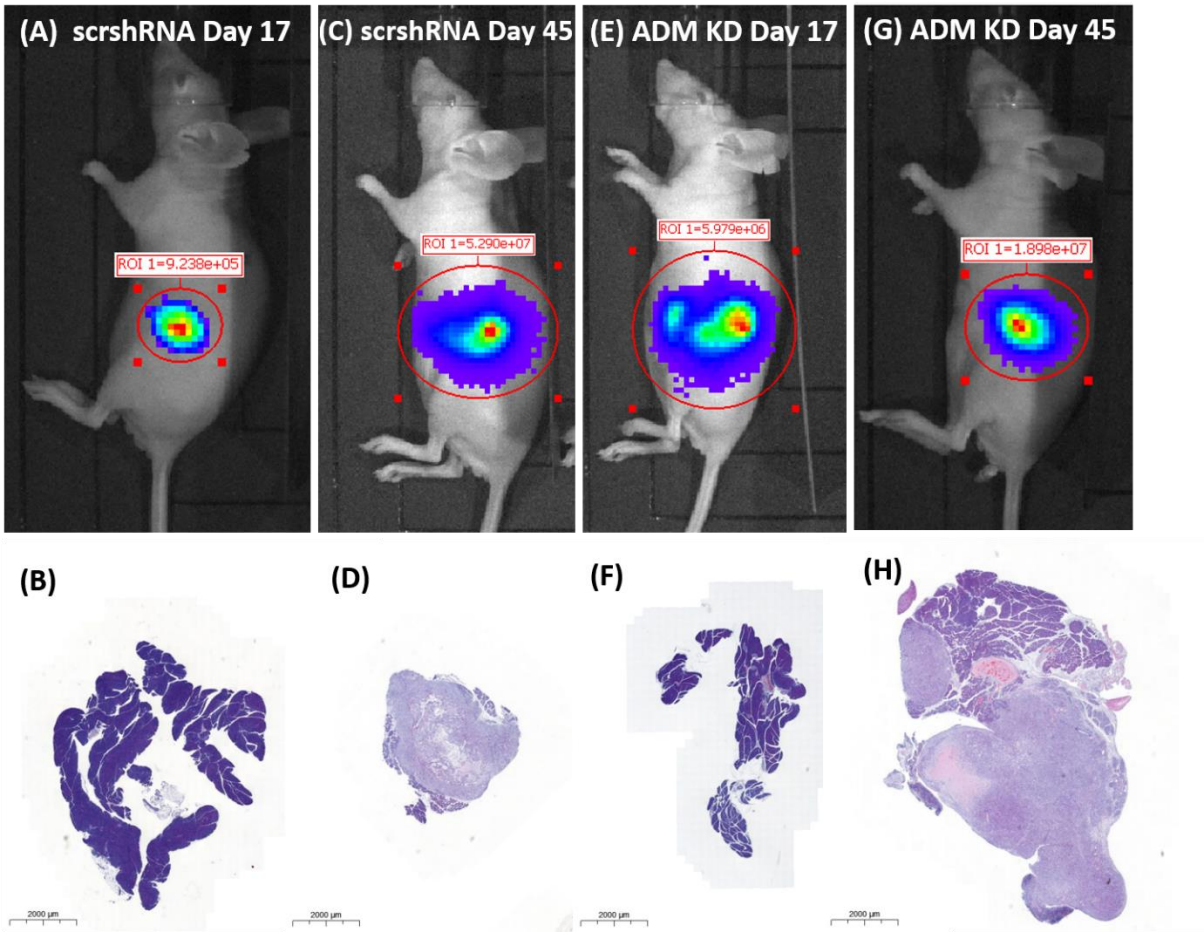

Figure 6.15 Day 17 and day 45 CFPAC-1 scrshRNA and CFPAC-1 ADM KD dox on/off/on IVIS images and H&E stains. ScrshRNA and ADM KD mice were culled either on day 17 or day 45, the luminescence of tumours was measured using IVIS and tumours were collected for sectioning. Tumours were stained with H&E and Ki67 (not show in image). **(A)** Day 17 CFPAC-1 scrshRNA dox on/off/on IVIS image. **(B)** Day 17 CFPAC-1 scrshRNA dox on/off/on H&E (0% Ki67 positive staining). **(C)** Day 45 CFPAC-1 scrshRNA dox on/off/on IVIS image. **(D)** Day 45 CFPAC-1 scrshRNA dox on/off/on H&E (38.5% Ki67 positive staining). **(E)** Day 17 CFPAC-1 ADM KD dox on/off/on IVIS image. **(F)** Day 17 CFPAC-1 ADM KD dox on/off/on H&E (4.5 % Ki67 positive staining). **(G)** Day 45 CFPAC-1 ADM KD dox on/off/on IVIS image. **(H)** Day 45 CFPAC-1 ADM KD induced dox on/off/on H&E (64.7% Ki67 positive staining).

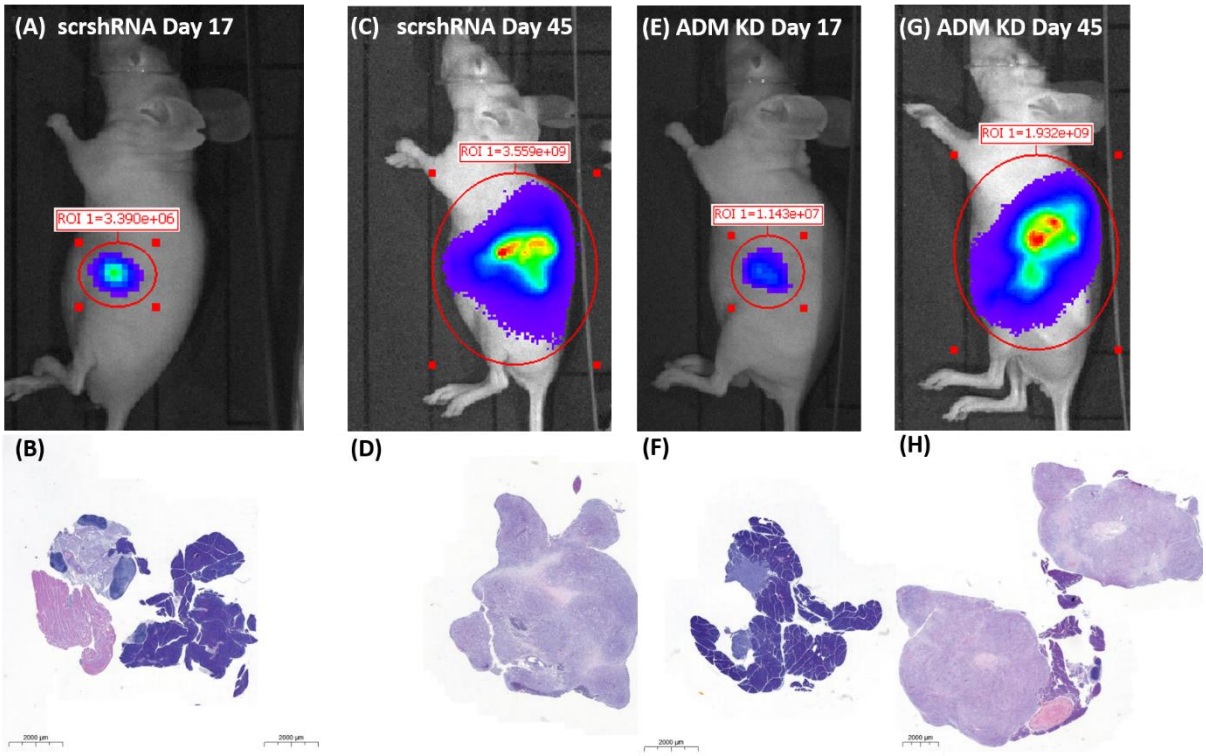

Figure 6.16 Day 17 and day 45 CFPAC-1 scrshRNA and CFPAC-1 ADM KD no dox IVIS images and H&E stains. ScrshRNA and ADM KD mice were culled either on day 17 or day 45, the luminescence of tumours was measured using IVIS and tumours were collected for sectioning. Tumours were stained with H&E and Ki67 (not show in image). **(A)** Day 17 CFPAC-1 scrshRNA no dox IVIS image. **(B)** Day 17 CFPAC-1 scrshRNA no dox H&E (2.3% Ki67 positive staining, only analysed PaCa tissue on the right of the section). **(C)** Day 45 CFPAC-1 scrshRNA no dox IVIS image**. (D)** Day 45 CFPAC-1 scrshRNA no dox H&E (44.1% Ki67 positive staining). **(E)** Day 17 CFPAC-1 ADM KD no dox IVIS image. **(F)** Day 17 CFPAC-1 ADM KD no dox H&E (3.2 % Ki67 positive staining). **(G)** Day 45 CFPAC-1 ADM KD no dox IVIS image. **(H)** Day 45 CFPAC-1 ADM KD induced no dox H&E (50.7% Ki67 positive staining).

Figure 6.14, Figure 6.15 and Figure 6.16 show that the pancreas becomes less differentiated by day 45. At day 17 most sections appear to be a well differentiated pancreas without established tumour cells. Figure 6.17a shows day 17 Ki67 percentages in both CFPAC-1 ADM KDs and CFPAC-1 scrshRNA samples in dox on, dox on/off/on group and no dox groups. Two-way ANOVA analysis shows a significant difference (p= 0.009) between CFPAC-1 ADM KD and CFPAC-1 scrshRNA. Comparison of day

45 CFPAC-1 ADM KDs and CFPAC-1 scrshRNA Ki67 positive cells showed no significant differences between cell types or doxycycline conditions (Figure 6.17b).

Comparison of CFPAC-1 ADM KDs on day 17 and day 45 showed a significant difference ($p < 0.0001$) between the day 17 and day 45 in all doxycycline conditions (Figure 6.17c). Tukey's multiple comparison test showed CFPAC-1 ADM KDs induced with doxycycline had a 31% increase in Ki67 positive cells by day 45 ($p = 0.04$). CFPAC-1 ADM KDs in the doxycycline on/off/on group showed a 38.7% increase in Ki67 positive cells ($p = 0.002$) and in no dox CFPAC-1 ADM KDs, there was a 49.8% increase in Ki67 positive cells by day 45 ($p = 0.001$).

Two-way ANOVA analysis showed a significant difference between different doxycycline conditions ($p = 0.01$) and interactions ($p = 0.0061$). Tukey's multiple comparison test showed a 61.2% increase in Ki67 positive cells in the doxycycline induced group by day 45 ($p < 0.0001$) and a 31.2% increase in percentage of Ki67 positive cells in dox on/off/on group ($p = 0.001$). CFPAC-1 scrshRNA in the no dox group showed a 39.7% increase percentage of Ki67 positive cells ($p < 0.0001$). Furthermore, there was a significant difference at day 45 in CFPAC-1 scrshRNA Ki67 positive cells when comparing doxycycline on and dox on/off/on groups. Cells induced with doxycycline (dox on group) had 31.7% more Ki67 positive cells. An important consideration is in the CFPAC-1 scrshRNA day 45 doxycycline groups, there are fewer samples and therefore, more repeats would provide a more accurate representation in the differences between groups.

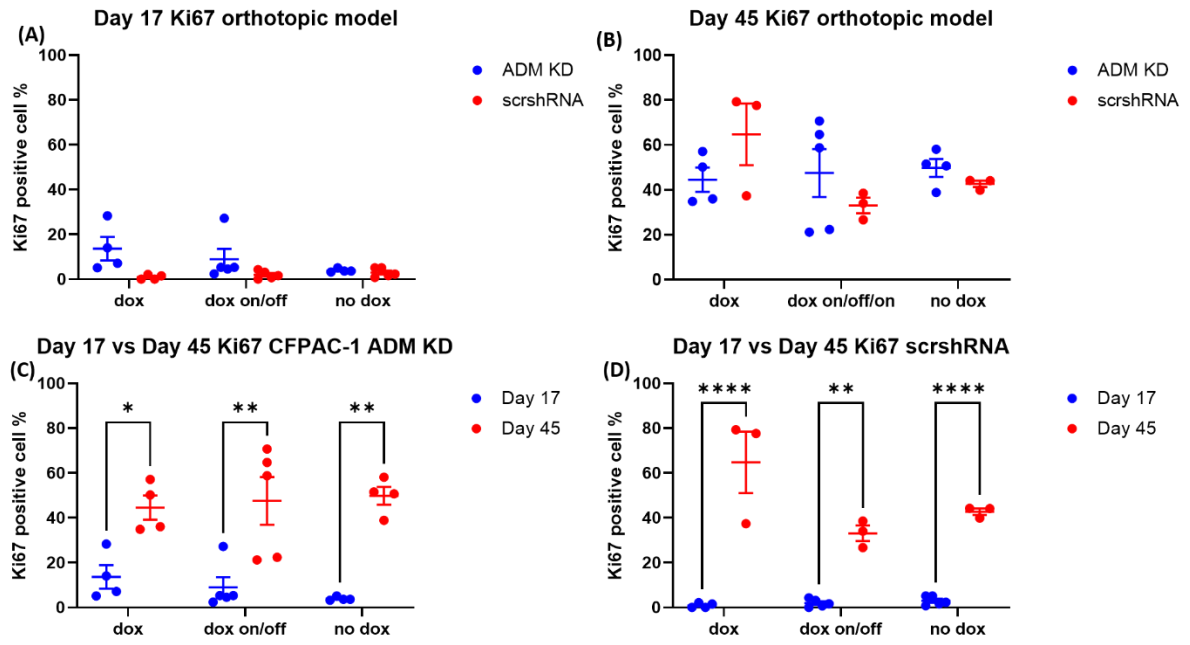

Figure 6.17 Ki67 positive percentage cells in CFPAC-1 ADM KDs and CFPAC-1 scrshRNA. Tissue sections collected from orthotopic experiment were analysed by immunohistochemistry for the percentage of Ki67 positive cells. **(A)** Comparison of day 17 Ki67 % positive cells in CFPAC-1 ADM KD and CFPAC-1 scrshRNA samples **(B)** Comparison of day 45 Ki67 % positive in CFPAC-1 ADM KDs and CFPAC-1 scrshRNA. **(C)** Comparison of day 17 and day 45 CFPAC-1 ADM KD Ki67 % positive cells following different doxycycline regimes described in methods. **(D)** Comparison of day 17 and day 45 CFPAC-1 scrshRNA % positive cells following different dox regimes described in methods. Data presented as mean ± SEM.

6.3.6 *In vivo* differences in tumour volume and weight following between CFPAC-1 ADM KDs, CFPAC-1 scrshRNA and CFPAC-1 WT cells (subcutaneous)

A subcutaneous *in vivo* experiment was designed to compare tumour volume and weight between CFPAC-1 ADM KDs, scrshRNA and WT cells that were either induced with dox or not induced. Comparison of tumour volumes (Figure 6.18a) shows that WT cells both induced with dox and untreated showed the largest tumour volume with similar tumour volumes between both dox conditions. CFPAC-1 ADM KDs induced with doxycycline and untreated had the next largest tumour

volumes, followed by CFPAC-1 scrshRNA in both dox groups. The CFPAC-1 scrshRNA tumour volume did not significantly increase over the period of the experiment, particularly in the dox induced group.

Analysis of subcutaneous tumour weight (Figure 6.18) by two-way ANOVA shows a significant difference between CFPAC-1 ADM KD, scrshRNA and WT cells ($p < 0.0001$) and between induced and non-induced groups ($p = 0.004$). There is a significant difference between CFPAC-1 ADM KD and scrshRNA induced with dox ($p=0.005$), ADM KDs tumour weight was 333.7 mg more than scrshRNA. There was also a significant difference between tumour weight of CFPAC-1 scrshRNA and CFPAC-1 WT cells induced with dox ($p < 0.0001$). WT cells tumour weight was 558.6 mg more than scrshRNA. Untreated CFPAC-1 scrshRNA and CFPAC-1 WT also show a significant difference in tumour weight ($p = 0.0006$) as WT cells weighed 400 mg more than scrshRNA cells.

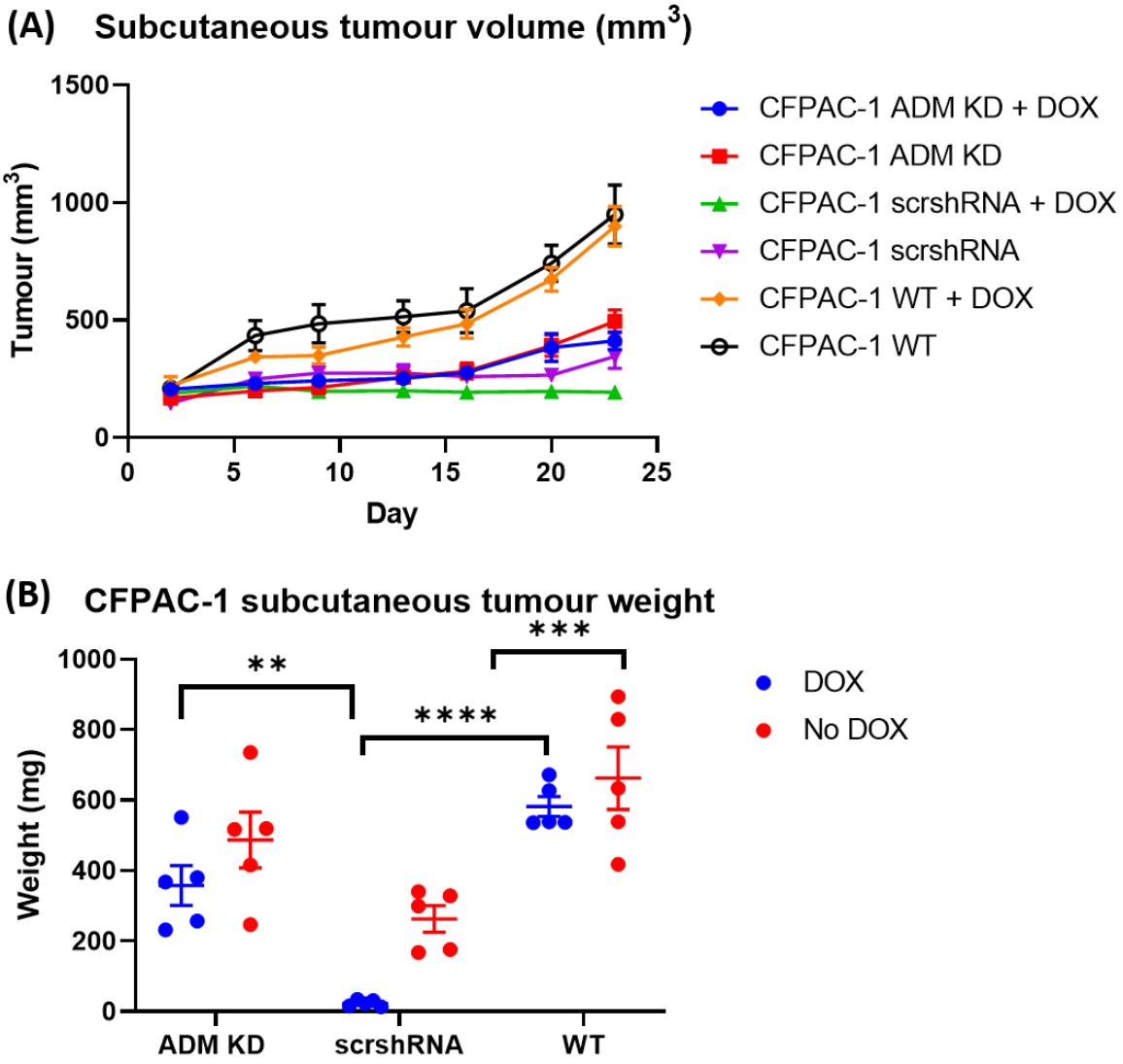

Figure 6.18 Subcutaneous tumour volume (mm^3) and weight (mg) of CFPAC-1 ADM KDs, CFPAC-1 scrshRNA and CFPAC-1 WT cells either induced with doxycycline (dox) or untreated (no dox). **(A)** Comparison of tumour volume (mm^3) between subcutaneous dox induced and non-induced CFPAC-1 ADM KD, CFPAC-1 scrshRNA and CFPAC-1 WT cells. **(B)** Comparison of tumour weight (mg) between subcutaneous dox induced and non-induced CFPAC-1 ADM KD, CFPAC-1 scrshRNA and CFPAC-1 WT cells. Both data are presented as mean ±SEM.

6.3.7 *In vivo* analysis of organ weights of CFPAC-1 ADM KD compared to CFPAC-1 scrshRNA and CFPAC-1 WT cells

Once the subcutaneous experiment reached its endpoint, liver, kidney and spleen were collected to determine any differences between groups. This includes changes in organ weight which may be caused by metastasis of tumour cells to other organs. Organs were also collected for sectioning and H&E staining which would show potential signs of metastasis following analysis. Two-way ANOVA analysis comparing liver weight (Figure 6.19a) showed significant difference between different doxcycline conditions (p= 0.005) and between CFPAC-1 ADM KD, scrshRNA and WT cells (p= 0.01) and in interactions. Tukey's multiple comparison test showed a significant difference between CFPAC-1 scrshRNA induced with doxycycline and non-induced scrshRNA (p= 0.01). The liver weight of the non-induced scrshRNA was 204 mg more than the induced scrshRNA. There was also a significant different between non-induced CFPAC-1 ADM KD and CFPAC-1 scrshRNA where scrshRNA weighed 223 mg more than ADM KDs.

Two-way ANOVA analysis of kidney weight showed no significant differences following two-way ANOVA analysis (Figure 6.19b). Analysis of spleen weights showed a significant difference (p= 0.004) between doxycycline induced and non-induced groups (Figure 6.19c). Tukey's multiple comparisons test more specifically showed a significant difference (p= 0.03) between CFPAC-1 scrshRNA induced and non-induced where in the non-induced group, the spleen weight was increased by 35.9 mg.

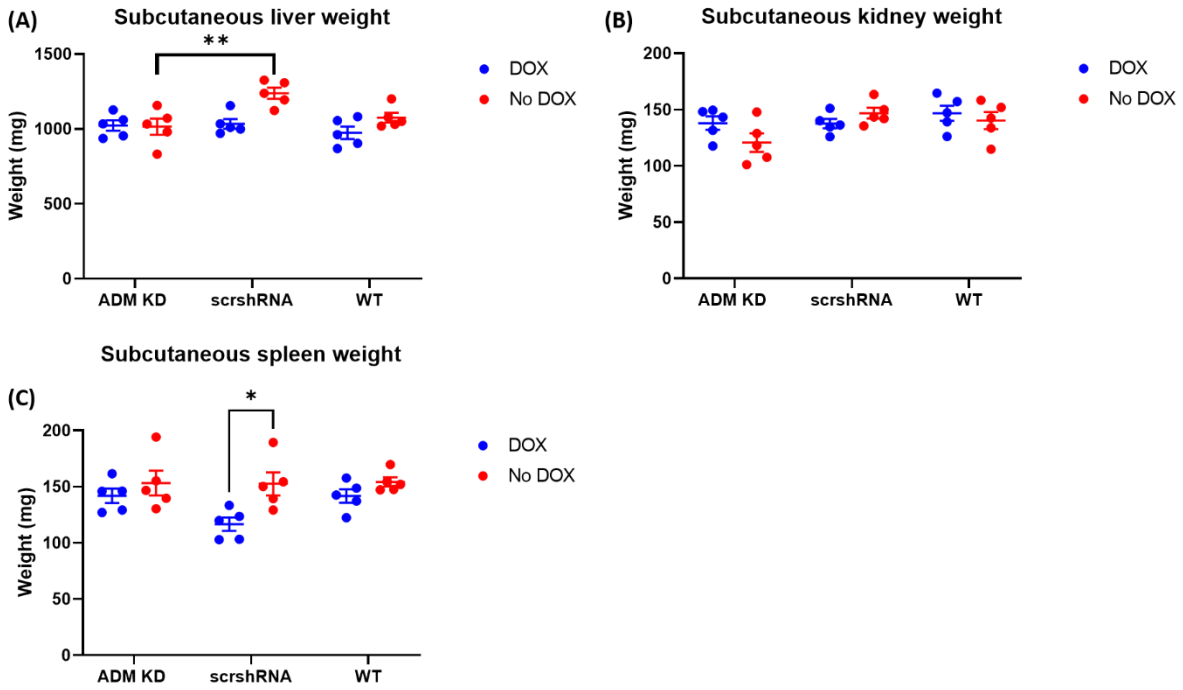

Figure 6.19 Subcutaneous organ weights in CFPAC-1 ADM KDs, scrshRNA and WT cells following induction of KD with doxycycline (dox) or no doxycycline treatment (no dox). **(A)** Liver weight following subcutaneous injection of CFPAC-1 ADM KD, scrshRNA and WT cells. **(B)** Kidney weight following subcutaneous injection of CFPAC-1 ADM KD, scrshRNA and WT cells. **(C)** Spleen weight following subcutaneous injection of CFPAC-1 ADM KD, scrshRNA and WT cells. Data presented as mean ±SEM and was statistically analysed by two-way ANOVA.

6.4 Discussion

The aim of this chapter was to determine the effects of knocking down ADM in CFPAC-1 cells on tumour growth and interactions with cells of the tumour microenvironment. To do this, *in vivo* orthotopic and subcutaneous experiments with CFPAC-1 ADM KDs, CFPAC-1 scrshRNA and CFPAC-1 WT cells were prepared. The data collected from the orthotopic experiment showed the effects of ADM KDs on tumour growth by imaging tumours twice weekly using IVIS to detect tumour luminescence and by weighing tumours *ex vivo* on day 17 at the interim cull or on day 45 following the endpoint cull. The same data was collected for CFPAC-1 scrshRNA controls. Organs were also imaged using IVIS to identify any areas of potential metastasis on both day 17 and day 45 and weighed. Whole blood was collected to analyse whether there were any differences between immune cells in ADM KDs and scrshRNA control. Tumours collected at day 17 and 45 were also collected for sectioning, H&E staining and immunohistochemistry analysis of Ki67, α-SMA and endomucin. Due to time constraints following the COVID-19 pandemic, full analysis of α-SMA and endomucin was not completed. Another aim of this experiment was to determine whether different doxycycline regimes (dox on, dox on/off/on or no dox) effected tumour growth.

The aim of the subcutaneous experiment was to see whether tumour volume changed between CFPAC-1 ADM KDs, CFPAC-1 scrshRNA and CFPAC-1 WT. The experiment also informed whether doxycycline induction of KDs compared to no doxycycline induction effected tumour volume within each group.

6.4.1 CFPAC-1 ADM KDs, scrshRNA and WT cell effect on tumour growth and proliferation

Tumour growth was monitored by IVIS (orthotopic), measuring tumour weight (orthotopic and subcutaneous) and by measuring tumour volume (subcutaneous). After the tumours were weighed, they were fixed in formalin before sectioning for analysis of Ki67 positive cells by immunohistochemistry. Ki67 determines the number of proliferating cells and is used as a predictive

for aggressiveness of cancers in clinic. Myoteri *et al* (2017) analysed 53 PDAC sections, 54.7% had a high percentage (>16% immunostained nuclei) of Ki67 positive cells, 43.4% had a low percentage (<15% immunostained nuclei) of Ki67 positive cells and 1.9% had no Ki67 positive cells. The amount of Ki67 positive cells correlated with the stage of cancer; the majority of cases with high Ki67 expression were diagnosed with stage III or IV PDAC, low Ki67 expression correlated with stage I and II PDAC and the sample with no Ki67 was stage I PDAC. This shows the value in Ki67 in predicting how developed PDAC is.

Overall, the results obtained from the orthotopic model showed that KD of ADM resulted in higher tumour weight in mice at day 45 compared to CFPAC-1 scrshRNA controls. There was a significant difference (p= 0.03) between CFPAC-1 ADM KD and scrshRNA tumour weights with ADM KD tumour weight being larger on average (Figure 6.8). This correlated with the luminescence and Ki67 data showing that both ADM KDs and scrshRNA not induced with doxycycline had the highest luminescent signal (Figure 6.9) and percentage of Ki67 positive cells respectively (Figure 6.17). This shows a correlation between more developed tumours and increasing number of Ki67 positive cells. Higher Ki67 percentage was associated with more poorly differentiated tumours (Figure 6.14 to Figure 6.16). As the group with no doxycycline induction had higher tumour weights, the data suggests that doxycycline induction of ADM KD or scrshRNA slightly inhibits tumour growth. However, there were no significant differences between different doxycycline conditions in both CFPAC-1 ADM KDs and scrshRNA.

Within all 3 CFPAC-1 ADM KD group, 5 mice had to be culled prematurely on day 38 due to significant weight loss and palpation. These mice were in different doxycycline groups, two mice were in the doxycycline induced group, two mice were in the dox on/off/on group and one mouse from the group without dox induction. These data demonstrate that the different doxycycline conditions did not alter the rate of tumour growth. Furthermore, the prematurely culled mice also did not have significantly more Ki67 positive cells. All Ki67 slides were stained by the same operator over two days, the large

difference in Ki67 positive cells may be attributed to the analysis of slides on QuPath. The whole tissue was analysed, in future, analysing the tumour section alone would be a valuable addition to the data. This may reduce large differences in the number of Ki67 positive cells between day 17 and day 45.

Ex vivo, the tumours collected were imaged using IVIS to detect luminescent tumour signal (Figure 6.8c and d). At day 17 luminescent signal in CFPAC-1 ADM KDs was similar between different doxycycline groups however, there was a larger variation in luminescent signal. This may be as tumours were not fully established by day 17. CFPAC-1 scrshRNA results correlated with the tumour weights determined, showing that in doxycycline induced and dox on/off/on mice, the luminescent signal was lower than in the mice that hadn't been induced with doxycycline. Overall, CFPAC-1 ADM KDs had higher luminescent signal at day 17 compared to scrshRNA. However, *in vitro* measurement of luminescent signal showed that ADM KDs transduced with Luc-RFP had a higher luminescent signal which may be partially responsible for the higher luminescent signal.

At day 45, ex vivo CFPAC-1 ADM KDs and scrshRNA in the no dox group had the highest luminescent signal. This correlates with the tumour weights and Ki67 percentage positive cells shown in Figure 6.8, Figure 6.9 and Figure 6.17. ADM KDs and scrshRNA induced with dox or in the dox group had lower luminescent signal and tumour weights. However, there was no significant difference between the two groups.

The subcutaneous model data compared CFPAC-1 ADM KDs, CFPAC-1 scrshRNA and CFPAC-1 WT cell tumour volumes, showing WT cells to have the largest tumour volume and weight, followed by ADM KDs and scrshRNA respectively (Figure 6.18). The higher tumour volume in ADM KDs compared to scrshRNA correlates with the observations in the orthotopic model. ADM KDs induced with doxycycline had a significantly higher tumour volume than scrshRNA in the doxycycline induced group. The results also showed a statistical difference in tumour weight between induced and non-induced scrshRNA and WT cells. WT cells were significantly higher in tumour volume compared to scrshRNA. An important consideration is that scrshRNA tumours induced with doxycycline did not appear to

establish and therefore the data should be interpreted with precaution until tumours have been H&E stained to determine if there are any signs of malignancy. However, comparison of ADM KDs to scrshRNA does mimic the data established in the orthotopic model. Although, there is no significant difference between ADM KDs and WT cell tumour volume, ADM KDs did have lower tumour volume overall suggesting that ADM KD may play some role in the regulation of tumour growth. However, further histological analysis and potentially comparison of ADM mRNA in tumours collected to determine if ADM and scrshRNA had similar levels of ADM throughout the experiment.

Overall, tumour size, luminescence and volume of ADM KDs was higher compared to scrshRNA control. Furthermore, although Ki67 did correlate with tumour progression in terms of less well differentiated tumours at day 45, ADM KD did not appear to significantly influence the percentage of Ki67 positive cells compared to scrshRNA. Keleg *et al* (2007) have shown that ADM has both stimulatory and inhibitory effects on different PaCa cell lines following addition of recombinant ADM to the cells. Two out of the five cell lines were inhibited by addition of recombinant ADM and in the remainder of cell lines, ADM did not have a significant effect on growth. The effects on proliferation were determined *in vitro* however, these results do demonstrate that PaCa cells may not all be responsive to exogenous ADM in normoxic conditions. It also shows that different cell lines within the same type of cancer respond differently to ADM therefore, developing ADM KDs in other cell lines may be valuable.

However, *in vivo,* Ishikawa *et al* (2003) show that intra-tumoural injection of ADM antagonist to PCI-43 PaCa cells resulted in inhibition of tumour growth. This study is not directly comparable to the orthotopic and subcutaneous models from this study as KDs were not developed in PCI-43 cells however, it does demonstrate inhibition of ADM was shown to reduce tumour growth which is opposing to the results shown in Figure 6.8. Figure 6.18 also shows that ADM KD resulted in some inhibition of tumour growth compared to WT cells however, scrshRNA controls had lower or similar tumour weight compared to ADM KDs.

Wang *et al* (2014) injected SW480 cells with ADM KDs subcutaneously into mice which resulted in significant reduction in tumour growth. In 70% of mice transduced with ADM KD, there was no detectable tumour at the endpoint. This was associated with inhibition of angiogenesis and activation of apoptosis. Interestingly, they did show that there was no significant difference between Ki67 positive cells in ADM KD cells and control cells. This suggests that ADM may not have a direct effect on proliferation. This is further supported by the Keleg *et al* (2007) showing ADM to have either no effect on cell proliferation or an inhibitory effect. This may explain the lack of significant differences in Ki67 positive cells between CFPAC-1 ADM KDs and CFPAC-1 scrshRNA shown in Figure 6.17. Yao *et al* (2019) also developed ADM KDs but in osteosarcoma showing a decrease in tumour volume compared to scrshRNA and blank controls. Both these data suggest that ADM has a pro-tumorigenic role as suppression of its expression results in decreased tumour volume. This data is in contrast to the results shown in Figure 6.8 and Figure 6.18.

Karpinich *et al* (2013) compared the number of Ki67 positive foci in ADM KD and ADM overexpressing murine Lewis lung carcinoma cells injected subcutaneously into C57BL/6 mice. They found that ADM KD had low numbers of Ki67 positive cells compared to scrshRNA and empty vector controls tumours. ADM overexpressing lung cells had increased Ki67 positive cells compared to controls. Yao *et al* (2019) also developed ADM KDs in osteosarcoma cells showing a decrease in tumour volume compared to scrshRNA and blank controls. Both these data suggest that ADM has a pro-tumorigenic role as suppression of its expression results in decreased tumour volume and number of Ki67 cells, whilst overexpression in lung cancer cells resulted in an increased number in Ki67 proliferating cells. This data is in contrast to the results shown in Figure 6.8 and Figure 6.17.

Abasolo *et al* (2003) and Abasolo *et al* (2004) overexpressed ADM in prostate cancer cell lines and injected them subcutaneously into mice. They found that in PC-3 prostate cancer cell overexpressing ADM, tumour growth was inhibited. *In vitro,* overexpression of ADM in PC-3 and LNCaP cells was associated with decreased proliferation however, this was not replicated in DU145 cell overexpressing

ADM. These data, similar to Keleg (2007) suggest that different cancer cell lines of the same cancer type respond differently to ADM. Although this data relates to overexpression of ADM, it suggests that KD of ADM may increase PC-3 tumour growth as shown in CFPAC-1 ADM KDs in Figure 6.8 when compared to scrshRNA.

Other studies investigating the role of ADM in cancer, have not developed ADM KDs or overexpressed ADM in tumour cells. However, they have injected αAM intra-tumourally or intra-peritoneally to assess the effects of ADM on tumour growth or volume *in vivo*. Nouguerède *et al* (2013) show that treating HT-29 colorectal tumour xenografts with αAM reduced tumour growth. This was also shown Berenguer-Daizé *et al* (2013) in Du145 and LNCaP prostate cancer cells. Treatment with αAM decreased the overall tumour volume compared to controls. Tumour growth of LNCaP cells was shown to increase following intra-peritoneal and intra-tumoural injection of ADM. This suggests that ADM induces pro-tumorigenic effects such as increasing proliferation of cancer cells in a variety of cancers.

Oehler *et al* (2002) overexpressed ADM in two endometrial cell lines, Ishikawa cells and RL95.2, and implanted the cells subcutaneously. RL95.2 overexpressing ADM showed an increase in tumour growth. However, Ishikawa cells overexpressing ADM and implanted together with MDA-435S carrier cells as the cells alone are weakly tumorigenic, showed ADM overexpression to have a small impact on tumour growth. Martinez *et al* (2002) overexpressed ADM in T47D breast cancer cells and implanted them subcutaneously *in vivo*. The empty plasmid control group in this study showed no tumour development in a group of 10 mice and in ADM overexpressing cells, 3 out of 10 mice developed tumours. These show the variability even between mice, not only cell line. These data also suggest that different cell lines may respond differently to ADM overexpression or silencing and therefore, it is important to develop KDs in multiple cell lines to provide a bigger picture on the impact of ADM on *in vivo* tumour growth and proliferation.

Overall, these data show that different cancers have different responses to changes in ADM expression or treatment with ADM or αAM. There are even different responses between different cell

lines of the same cancer, this has been demonstrated in PaCa. This highlights the value of developing ADM KDs or KOs in multiple cell lines of the same type of cancer to get a wider perspective on the effects and ADM which may infer why certain cell lines respond differently.

An important technical consideration is the administration of doxycycline, the successful induction of KDs relies on mice drinking the water containing doxycycline. The downfall with addition of doxycycline to water is that it can make the water taste bitter and therefore, mice may not want to drink water as frequently. To overcome this, it has been suggested that adding sucrose to the water may encourage mice to drink water more. However, this has been found to induce severe dehydration in mice resulting in weight loss, skin thinning and loss of elasticity to skin. This was shown by Cawthorne, Swindell, Stratford, Dive, & Welman (2007) who showed this effect was induced regardless of presence or tumour cells. Therefore, mice may have consumed less water than required to induce KDs which may have contributed to the results obtained. Chapter 4 discusses the effect of basal leakiness of promoters in successful induction of KDs. Meyer-ficca *et al* (2004) have shown that basal leakiness of promoters within shRNA which meant that mRNA expression in induced and non-induced KDs is similar. This may explain why differences in tumour weight and volume generally were not significantly different between different doxycycline conditions.

6.4.2 CFPAC-1 ADM KD and CFPAC-1 scrshRNA effects on organs

Organs from the *in vivo* orthotopic model were collected and imaged using IVIS on either day 17 or day 45 to identify luminescence in organs other than the pancreas (liver, kidney, spleen and GI tract) that could be representative of metastasis. Organs (liver, kidney and spleen) were also collected in both orthotopic and subcutaneous experiments to record differences in organ weight and for H&E analysis. In the orthotopic experiment, luminescent signal was identified in 4 CFPAC-1 scrshRNA mice stomachs and one from CFPAC-1 ADM KD at day 45 (Figure 6.12). The signal in stomachs was identified in CFPAC-1 scrshRNA induced with dox (x2), CFPAC-1 scrshRNA no dox (x2) and in CFPAC-1 ADM KD that was induced with dox (x1) (Figure 6.11). The stomachs were also noticeably harder, H&E sections

of the stomach showed no signs of tumour development. Furthermore, stomach metastasis is not a common occurrence in PaCa patience, literature on stomach metastasis is reported by individual cases as opposed to an overview due to the limited occurrence. Therefore, stomach hardening may be due to inefficient gastric emptying. Barkin *et al* (1986) and Leung & Silverman (2009) have described delayed gastric emptying (also known as gastroparesis) in patients with unresectable PaCa. Delayed gastric emptying is often accompanied with symptoms of nausea, vomiting and early satiety.

There were no significant differences found between weights of liver, kidney, spleen in CFPAC-1 ADM KDs and scrshRNA and different doxycycline conditions on day 17 and day 45. Figure 6.10 shows that on day 45 one of the spleens in the CFPAC-1 ADM KD dox on/off/on group was noticeably higher, the tumour weight was also noticeably higher in this mouse (Figure 6.8). This spleen was from the group of mice whose endpoint ended prematurely due to significant weight loss, palpation and high luminescent signal in tumour. There was no luminescent signal detected in the spleen therefore metastasis is unlikely to be the cause of the enlargement. There is limited literature relating pancreatic cancer to an enlarged spleen, therefore, histological analysis of the enlarged spleen may provide further insight into the cause of it. One explanation may be due to the significant size of the tumour putting pressure on the spleen and the veins supplying the spleen, causing it to enlarge.

Comparison of subcutaneous organs showed a significant difference between CFPAC-1 ADM KDs and CFPAC-1 scrshRNA livers following induction with doxycycline. CFPAC-1 scrshRNA induced with doxycycline had the largest liver weight compared to CFPAC-1 ADM KD suggesting that KD of ADM may decrease liver size. There were no significant differences between kidney weight in CFPAC-1 ADM KD, scrshRNA and WT cells. Comparing spleen weight, there was a significant difference between CFPAC-1 scrshRNA that was induced and not induced. The no dox CFPAC-1 scrshRNA group overall had heavier spleens, this suggests that doxycycline may decrease liver volume.

Overall, these data show that organs were not significantly affected by KD of ADM. There were no signs of luminescent signal in most organs except 5 stomachs (Figure 6.11 and Figure 6.12) however,

did not show signs of metastasis when comparing H&E sections from normal stomachs and stomach that had luminescent signal (Figure 8.1). The stomachs were however, noticeably harder which may be attributed to delayed gastric emptying (Barkin et al., 1986; Leung & Silverman, 2009).

6.4.3 CFPAC-1 ADM KDs and CFPAC-1 scrshRNA effects on immune cells

Immune cells within the PaCa microenvironment adapt to produce a pro-tumorigenic environment. PaCa is associated with increased infiltration of TAMs, MDSCs and Tregs which are all associated with immune suppressive effects helping the tumour evade detection and promoting cancer cell survival. An important consideration when interpreting the current data, BALB/c nude mice are athymic therefore, they have no T cells. A further important consideration is that CFPAC-1 cells are derived from a male patient however, the host species were female BALB/C nude mice and analysis of immune cells was based on data provided by Charles River on female mice. A future consideration would be to use both male and female cell lines in both male and female mouse strains.

At day 17, in both CFPAC-1 ADM KDs and scrshRNA, monocyte percentages were within the normal range for BALB/c nude female mice specified by Charles River. At day 45, the monocyte percentage was mainly within normal range with one outlier in both CFPAC-1 ADM and scrshRNA with no doxycycline induction. There was a significant difference between CFPAC-1 ADM KDs and scrshRNA in doxycycline induced and non-induced groups at day 45 (Figure 6.13). These data suggest that KD of ADM decreases the number of blood monocytes present. Sanford *et al* (2013) have shown that low monocyte levels in patient blood samples is associated with increased patient survival. Compared to healthy controls, inflammatory monocytes were shown to be increased in blood and decreased in bone marrow in PaCa patient samples. This was correlated with decreased patient survival following tumour resection. Therefore, the lower levels of monocytes detected in ADM KDs could indicate that ADM regulates monocyte levels. However, these results were also determined in scrshRNA samples suggesting that doxycycline administration may be effecting monocyte levels. Monocyte levels in the

no doxycycline group were still within normal monocyte range but more at the upper end of the scale. Therefore, ADM may not have a significant role in the regulation of monocytes.

However, ADM has been associated with increased expression of CD11b+ which is a marker for myelomonocytic cells (MMC). MMCs can differentiate into blood monocytes, macrophages or dendritic cells. Xu *et al* (2016) have shown that patients express CD11b+ in pancreatic tissues and that, CD11b+ expression is associated with increased ADM expression. MMCs have also been shown to express the receptors for ADM (CLR and RAMPs). ADM was shown to induce migration and invasion and MMC cells and inducing macrophages and MDSCs to express pro-tumour phenotypes. *In vivo,* MMC cell depletion was associated with supressed tumour growth. These data show the potential value in investigating the relationship between ADM expression and expression of myelomonocytes. Using mice with a fully functional immune system and analysing potential infiltrating cells into the tumour microenvironment when comparing CFPAC-1 ADM KDs to CFPAC-1 scrshRNA controls may provide a valuable insight into the role of ADM in regulating immune cells in PaCa.

The percentage of eosinophils ay day 17 in both CFPAC-1 ADM KDs and scrshRNA were both inside and outside normal eosinophil range. In the dox on/off/on and no dox CFPAC-1 scrshRNA group, the majority of mice had eosinophil percentages higher than the normal range (Figure 6.13). However, at day 45 only the doxycycline induced group showed the majority of blood samples to be outside the normal eosinophil percentage range (Figure 6.13). CFPAC-1 ADM KDs induced with doxycycline on day 17, the majority of blood samples were within the normal eosinophil percentage range. The dox on/off/on and no dox group blood samples were mainly outside of normal eosinophil percentage range. On day 45, CFPAC-1 ADM KD induced with doxycycline group, predominantly had eosinophil percentages outside the normal range. However, dox on/off/on and no dox ADM KDs were more within range by day 45. Manohar, Verma, Venkateshaiah, & Mishra (2017) have shown eosinophils have some role in development of pancreatic malignancy following pancreatitis. Both eosinophils and degranulated eosinophils were identified in both malignant and non-malignant pancreatic tissue

sections. It was suggested that eosinophils have a role in the development of fibrosis and therefore pancreatic malignancy. However, there are no studies linking the regulation of eosinophil numbers to ADM expression and progression of PaCa.

At day 45, both CFPAC-1 scrshRNA and ADM KDs induced with doxycycline blood samples increased the percentage of eosinophils to outside the normal range. This suggests that doxycycline potentially has an effect on eosinophil percentage as there were no significant differences between scrshRNA and ADM KDs. To determine whether there was a specific association between ADM KD and eosinophils in the progression of PaCa, staining pre-malignant and malignant patient tissues at different stages of PaCa may be the first step.

There was a significant difference in lymphocytes between CFPAC-1 ADM KD and scrshRNA however, the mice used for this experiment were athymic and therefore, the results are only representative of the B lymphocyte and natural killer cell (NK cell) population, not T lymphocytes. At day 17, there was a significant difference between CFPAC-1 ADM KDs and scrshRNA not induced with doxycycline, with ADM KDs having a lower percentage of lymphocytes. However, at day 45 there were no significant differences between CFPAC-1 ADM KDs and scrshRNA in the no dox group however, the average percentage of lymphocytes in ADM KDs still remained lower. The lower percentage of lymphocytes in ADM KDs may be associated with the immune system adapting to avoid immune detection and therefore allowing the tumour to proliferate further, shown by the increased tumour weight in ADM KDs. At day 17 and day 45, the percentage of lymphocytes in the doxycycline induced and doxycycline on/off/on group were similar. Although, the differences in percentage of lymphocytes are small between induced KDs and non-induced KDs, the data could indicate reducing expression of ADM has a positive impact on lymphocytes, increasing their infiltration into tumours and therefore reducing tumour growth. However, understanding why CFPAC-1 scrshRNA has similar responses needs further elucidation. Furthermore, the majority of data was within normal lymphocyte percentage range so effects of ADM may not be significant on B lymphocytes and NK cells.

NK cells have been described to have a positive effect within the innate immune system with the ability to detect cancer cells. However, in PDAC, patients have been described to have significantly lower NK cell blood counts compared to healthy individuals ($p< 0.001$). Patients with lower NK cell counts had poorer clinical outcomes and poorer response to chemotherapy. This study was only completed in a small number of patients all located in South Korea however, it does suggest that depletion of NK cells in PaCa has a negative impact. There are currently no studies on the association between ADM and NK cells in cancer. B lymphocytes have more pro-tumorigenic activity and have been suggested to induce M2 macrophage phenotype polarisation which increases cancer cell growth and aid in avoiding immune surveillance (Biswas & Mantovani, 2010). In PDAC, Spear *et al* (2019) show that B cells have both a immunosuppressive and immuno-stimulatory effect. In secondary lymphoid organs, B cells have an immunosuppressive effect however, when recruited within the tumour microenvironment, B cells have an immuno-stimulatory effect. Suggesting they have an anti-tumoural effect however, there have been no studies associating ADM with B cell regulation in cancer.

Overall, further research is required to find associations between ADM and immune cells within the PaCa microenvironment. Using the current data collected, further analysis on immune cells could be completed on tissue sections by staining for activated B lymphocytes with CD19, CD25 or CD30 markers. To gain further understanding of the effect of ADM KDs on macrophage polarisation, using conditioned media from ADM KDs, CFPAC-1 scrshRNA or CFPAC-1 WT cells on macrophages could inform whether there are differences in the numbers of polarised macrophages by analysis with flow cytometry.

Furthermore, Li *et al* (2020) have shown that when PaCa cells were combined with PSCs, tumour weight increased and CD4+, CD8+ and NK cells cells decreased promoting a pro-tumorigenic microenvironment. Therefore, developing an *in vivo* model with C57BL/6 mice and injecting ADM KD and scrshRNA orthotopically may add value to understanding the involvement of T cells within the immune system. T cell infiltration could be analysed by immunohistochemistry but also collecting the

spleen, tumour and bone marrow cells from the tibia and fibia to analyse any changes to the of CD4+, CD8+ and NK by flow cytometry as described by Li *et al* (2020). This would show whether there is a relationship between ADM and regulation of T lymphocytes.

6.4.4 Conclusion

In conclusion, these data provide preliminary information on the potential role of ADM within the tumour microenvironment. The introduction demonstrates the interplay between ADM with many cells and the tumour microenvironment including tumour cells, PSCs, endothelial cells, immune cells, the ECM and neuronal cells. Dai *et al* (2020) most recent publication shows the important role of PaCa cells and CAFs in inducing metastasis in PaCa, mediated through ADM and RAMP-3 receptor expression. This highlights the value of investigating the role of ADM in PaCa and also shows that developing successful RAMP-3 KDs could provide important information regarding the tumorigenesis of PaCa.

Currently, the data shows that CFPAC-1 ADM KDs increased tumour growth compared to scrshRNA controls. In both ADM KD and scrshRNA, at day 45 the tumour weight is highest in the no doxycycline groups (Figure 6.8) which also correlated with the higher luminescent signals shown in Figure 6.9. Therefore, doxycycline induction may have some effect on decreasing tumour growth however, this is not exclusive to ADM KDs as the same result was shown in scrshRNA controls. Analysis of subcutaneous tumour volume showed that ADM KDs and scrshRNA mice had lower tumour volumes in both doxycycline induced and non-induced groups compared to WT CFPAC-1 cells (Figure 6.18).

Organ weights were not significantly affected by knockdown of ADM and scrshRNA with some anomalies in organ weight (Figure 6.19). The spleen was shown to be significantly enlarged in one of the mice culled prematurely in the CFPAC-1 ADM KD group at day 38. Furthermore, five stomachs imaged using IVIS were shown to have luminescent signal at day 45 however, based on current analysis this is not associated with stomach metastasis. Analysis of organs from the subcutaneous experiment showed there was a significant difference between liver weight when comparing CFPAC-1 ADM KD and CFPAC-1 scrshRNA induced without doxycycline induction. The liver volume was larger in the scrshRNA group (Figure 6.19).

H&E analysis and Ki67 analysis of tumour sections showed that at day 45, tumours appeared more poorly differentiated that day 17 pancreas sections (Figure 6.14, Figure 6.15 and Figure 6.16). This was associated with increasing numbers of Ki67 positive cells (Figure 6.17). Overall, there was no significant differences between Ki67 positive cells when comparing CFPAC-1 ADM KDs and scrshRNA on day 45. There were also no significant different between Ki67 positive cells and the different doxycycline regimes.

Immune cell analysis showed that monocyte percentage was within the normal range specified by Charles River for BALB/c nude mice. Eosinophils showed more varied data with the percentage of eosinophils being within and outside the number range in both CFPAC-1 ADM KDs and scrshRNA on day 17 and day 45. Lymphocytes were shown to be mainly within normal percentage range in both ADM KDs and scrshRNA (Figure 6.13).

Staining of tumour sections for α-SMA and endomucin was also completed by immunohistochemistry to analyse potential differences in PSC expression and endothelial cell density when comparing ADM KDs to scrshRNA. However, analysis has not been completed prior to submission therefore this is an area of future work. Developing ADM KDs in multiple cell lines may be beneficial as it has been demonstrated widely in PaCa, prostate and renal cancer that different cell lines respond differently to ADM. Some cell lines were completely unresponsive to ADM, some showed increased proliferation, whilst other decreased proliferation in response to ADM. Furthermore, validation of RAMP-3 KDs by QPCR for use in *in vivo* applications may provide useful information into the specific role of RAMP-3 in inducing pathological roles in PaCa.

CHAPTER 7: GENERAL DISCUSSION

7.1 General discussion

The overall aim of this study was to elucidate the role of ADM in PaCa, more specifically its role in the cross-talk between PaCa tumour cells and cells of the tumour microenvironment (PSCs, endothelial cells, immune cells and neuronal cells). ADM and its receptor components have been previously shown to be expressed in multiple cancers (Table 3.1) and to have a role in regulating proliferation, apoptosis, angiogenesis, migration and invasion, and immune regulation. Desmoplasia is also a prominent feature in PaCa that results in deposition of scar tissue around the tumour. Within the desmoplastic environment, there is an increase in fibroblasts (often PSCs) which results in excessive deposition of ECM. The scar tissue around the tumour creates a barrier, which makes it difficult for current chemotherapies to penetrate. Having a full understanding of the role of ADM in the development of desmoplasia, and its interactions with cells that promote a pro-tumorigenic environment could provide a novel approach to targeting PaCa in combination with currently used chemotherapies. Recent evidence has shown CAFs to have an important role in PaCa, by promoting metastases in PaCa through the RAMP-3/CLR receptor (Dai et al., 2020).

Due to the COVID-19 pandemic full elucidation of the role of ADM and RAMP-3 in the development of the stromal environment was not completed. There was no access to the laboratories for 5 months and therefore all planned experiments were unable to be completed. The closure of laboratories had a large impact on the *in vivo* studies. Analysis of the effect of ADM KD on the stromal microenvironment was limited as a consequence of this closure. Analysis of α-SMA and endomucin immunostaining was unable to be completed as a consequence. Analysis of tumour ADM and RAMP-3 expression was also unable to be completed. Furthermore, investigation of the role of RAMP-3 in the stromal environment may have been explored.

The focus of this study was to characterise a panel of seven PaCa cell lines to show that ADM and its receptor components (CLR, RAMP-1, RAMP-2 and RAMP-3) are expressed in PaCa at both mRNA and protein level. The functional role of ADM and its receptor components was determined by cAMP

assays by stimulating cells with different ligands (ADM, CGRP and intermedin) (Jailani., 2019). Therefore, once expression of ADM was confirmed in all cell lines, ADM and RAMP-3 KDs were developed for both *in vitro* and *in vivo* studies in CFPAC-1 cells. *In vitro,* the effect of ADM and RAMP-3 KDs on the viability and apoptosis of cells following gemcitabine and 5-FU treatment was determined. *In vivo,* CFPAC-1 ADM KDs were used to determine the role of ADM in tumour growth, metastasis and regulation of the immune system.

The null hypotheses were:

1) PaCa cell lines do not express ADM and its receptor components therefore, ADM has no functional role in PaCa.
2) ADM and RAMP-3 have no involvement in the regulation of proliferation and apoptosis therefore knockdowns will not affect these processes.
3) Knockdown of ADM has no influence on tumour growth and metastases. Therefore, the cells of the tumour microenvironment (including immune cells and proliferating tumour cells) will also not effected by ADM KD.

7.1.1 Characterisation

Characterisation of seven PaCa cell lines was completed using endpoint PCR, QPCR and western blotting to determine mRNA and protein expression. ADM, CLR, RAMP-1, RAMP-2 and RAMP-3 were expressed at mRNA level in all seven cell lines as shown by endpoint PCR. This was confirmed by sequencing the PCR samples (Figure 3.3 to 3.12). QPCR confirmed expression of ADM in all cell lines which is shown in Table 3.5. Western blotting confirmed expression of RAMP-1, RAMP-2 and RAMP-3 at protein level in all cell lines (Figure 3.13 to Figure 3.15). Confirming the expression of ADM and RAMP-3 was essential before developing knockdowns in CFPAC-1 cell lines.

Ishikawa *et al* (2003) have previously characterised 5 PaCa cell lines including BxPC-3. They showed all cell lines express ADM and that ADM mRNA expression increased following exposure of cells to hypoxic conditions. CLR was only expressed in 2 out of 5 cell lines including BxPC-3 and RAMP-2 was expressed in 4 out of 5 cell lines however, the cell lines were not characterised for RAMP-3 mRNA expression. Keleg *et al* (2007) characterised 5 different PaCa cell lines for mRNA expression showing that ADM, CLR, RAMP-1 and RAMP-2 were expressed in all cell lines. RAMP-3 expression was only confirmed in one of the cell lines, T3M4. Ramachandran *et al* (2007) characterised 8 PaCa cell lines including BxPC-3, CFPAC-1 and HPAF-II in which CLR was not detected at mRNA level. RAMP-1 and RAMP-2 were expressed in all cell lines however, RAMP-3 expression was not determined in any of the cell lines.

These data demonstrate the variability in ADM and its receptor expression between different PaCa cell lines but also, within the same cell lines. Ramachandran *et al* (2007) and Keleg *et al* (2007) both characterised Panc-1 PaCa cells, Keleg *et al* (2007) showed that Panc-1 cells expressed CLR whilst Ramachandran *et al* (2007) showed no CLR expression. Furthermore, BxPC-3 cells were shown to express CLR by Ishikawa *et al* (2003) however, Ramachandran *et al* (2007) showed that BxPC-3 cells did not express CLR. Differences in primer design could affect whether ADM and its receptor components are detected by PCR. Optimisation of primers is essential for successful detection of

mRNA. During primer design, careful selection of primers with a high GC content (40-60%) is essential for the stability of primers. Furthermore, designing primers with similar melting temperatures so that annealing temperatures are similar (52^{o}C to 58^{o}C). Annealing temperatures above 65^{o}C cause secondary annealing (Abd-Elsalam, 2003; A. Apte & Daniel, 2009). Other factors within the PCR reaction including $MgCl_2$ content may also effect success of PCR product detection. $MgCl_2$ acts as a co-factor to Taq Polymerase and also aids in primer binding to specific target. Furthermore, the method used to detect mRNA could potentially influence whether mRNA expression is detected, Ishikawa *et al* (2003) used northern blotting which is less sensitive that PCR. However, this does not mean that cell lines that show no mRNA expression are wrong, other external factors may affect whether ADM and its receptor components are detected, Keleg *et al* (2007) showed how hypoxia increased the expression of ADM in cell lines suggesting that the hypoxic microenvironment which has been described in PaCa tumours may also influence whether ADM and its receptor components are expressed in some cases. There is currently limited literature confirming the expression of ADM and all its receptor components at mRNA level in PaCa cell lines therefore, this is one of the first studies to show it in a panel of seven PaCa cell lines. This was the first data collected that suggested ADM its receptor components may potentially play a role in PaCa tumorigenesis and therefore, further investigation into the role of ADM was explored by developing ADM and RAMP-3 KDs in CFPAC-1 cells.

Western blotting was used to detect protein in PaCa cell lines which showed all cells expressed RAMP-1, RAMP-2 and RAMP-3 (Figure 3.13 to 3.15). CLR antibody optimisation was attempted however, the inconsistency in results did not provide confidence in the quality of the antibody. The inconsistency in results may be related to the quality of the antibody, polyclonal antibodies have affinity for the same antigen as monoclonal antibodies but different epitopes. Multiple non-specific bands were identified that were not at 55 kDa suggesting the antibody lacks specificity potentially due to lack of rigorous testing on multiple samples by the supplier. The same samples were used for CLR optimisation as the RAMP antibodies therefore, the samples used were not an issue.

Optimisation using different protein concentrations, blocking buffers, primary and secondary antibody concentrations were tested to try and gain consistency between blots however, the results remained inconsistent. Therefore, characterisation of CLR in the 7 PaCa cell lines was not completed. Chapter 3 discussed the limited protein characterisation of ADM and its receptor components in PaCa cell lines. Expression of ADM, RAMPs and CLR at protein level have only been shown by Berenguer-daize *et al* (2013) in DU145 prostate cancer cells. However, as discussed by Hay & Pioszak (2016), there is a lack of available antibodies that have been rigorously tested and therefore bands detected are often artefacts. This demonstrates the need for more thorough research into antibodies that have been extensively tested and can confidently be used within research. This would also help in further validating CFPAC-1 ADM KDs at protein level in this study.

7.1.2 Knockdown development and validation

ADM and RAMP-3 KDs were developed using inducible lentiviral shRNA in CFPAC-1 cells after ADM and RAMP-3 expression was confirmed by endpoint PCR and sequencing. ADM expression was confirmed by both endpoint PCR and QPCR. CFPAC-1 cells were also selected as they have previously been shown to increase cAMP production with high potency and efficacy following ADM ligand stimulation showing that the receptor is functional (Figure 3.16).

Successful KD of ADM in CFPAC-1 cells was confirmed by QPCR showing a 71% decrease in ADM expression after 7 days of doxycycline induction compared to CFPAC-1 scrshRNA (Figure 4.12). CFPAC-1 ADM KDs that were not induced with doxycycline had an 89% decrease in ADM expression compared to scrshRNA. Meyer-ficca *et al* (2004) have demonstrated that inducible KDs are prone to promoter leakiness and that FBS may contain traces of doxycycline which may have contributed to the significant decrease in ADM expression in non-induced CFPAC-1 ADM KDs. Induction of KDs in both CFPAC-1 ADM KDs and CFPAC-1 RAMP-3 KDs was further confirmed by inducing the cells with doxycycline over 7 days and showing that GFP expression increased from day 1 to day 7, particularly following 500 ng/mL doxycycline induction (Figure 4.6 to 4.11).

Following confirmation of a significant reduction in ADM expression by QPCR (Figure 4.12), CFPAC-1 ADM KDs and CFPAC-1 scrshRNA were transduced with firefly luciferase to develop cells suitable for *in vivo* imaging. Successful transduction of firefly luciferase was confirmed by measuring luminescence of cells (Figure 4.14 and Figure 4.15). All cells were treated with D-luciferin, Figure 4.14 showed that luminescence only increased in the cells transduced with firefly luciferase which confirmed successful transduction. Successful transduction was also confirmed by measuring luminescence using IVIS which showed luminescent signal only in cells transduced with luciferase (Figure 4.15).

The role of ADM in the development of PaCa and other cancers has been extensively shown. ADM has been shown to be associated with inducing proliferation, inhibiting apoptosis, inducing angiogenesis and regulating the immune system (Dai et al., 2020; Ishikawa et al., 2003; Keleg et al., 2007; Ramachandran et al., 2007; Xu et al., 2016). Furthermore, there is accumulating evidence that ADM and its receptors are expressed in PSCs. PSCs have been shown to be involved in the development of desmoplasia around PaCa tumours by producing excessive collagen I and other cells of the ECM (Dai et al., 2020; Masamune et al., 2008; Ramachandran et al., 2007). There is currently more literature relating ADM expression in other cancers including breast, colorectal and prostate cancers. These provide the foundations to understanding the potential role of ADM in PaCa but also demonstrate how differently different cancers may respond to ADM showing that it is important to understand the role of ADM in each cancer individually. Dai *et al* (2020), Wang *et al* (2014) and Yao *et al* (2019) have all shown the value of developing ADM/RAMP-3 KDs in PaCa, colorectal cancer and osteosarcoma respectively for both *in vitro* and *in vivo* use. These combined factors validate why ADM and RAMP-3 KDs were developed in CFPAC-1 cells.

7.1.3 Viability and apoptosis

The effect of CFPAC-1 ADM and RAMP-3 KDs on viability and apoptosis was compared to CFPAC-1 scrshRNA controls and WT cells. This was to determine whether KDs improved response to currently

available chemotherapies used to treat PaCa, gemcitabine and 5-FU. Comparison of viability in ADM KDs, RAMP-3 KDs, scrshRNA and WT cells was determined to see whether KDs alone effected proliferation (Figure 4.13). These data show that KD of ADM and RAMP-3 reduced the viability of CFPAC-1 cells compared to WT cells. However, scrshRNA were the least viable cells. Keleg *et al* (2007) have previously shown that addition of recombinant ADM to 5 PaCa cell lines had both stimulatory and inhibitory effects, suggesting that the role ADM in PaCa proliferation may be dependent on the cell line. In other cancers including prostate, breast, renal and colorectal cancer, addition of exogenous ADM or overexpression of ADM has been associated with increased proliferation of cells (Berenguer-Daize et al., 2013; Berenguer et al., 2008; Deville et al., 2009; Martinez et al., 2002; Nouguerède et al., 2013). However, Abasolo *et al* (2004) have shown ADM overexpression inhibits proliferation of two prostate cancer cell lines.

The specific role of RAMP-3 in regulating proliferation has been demonstrated by both Dai *et al* (2020) and Nouguerède *et al* (2013) in both PaCa and colorectal cancer respectively. RAMP-3 KOs developed in CAF/PAN02 cells resulted in smaller tumour size and a decreased number of Ki67 positive cells suggesting that proliferation is reduced by KOs (Dai et al., 2020). In colorectal cancer, treating cells with an anti-RAMP-3 receptor antibody resulted in 70% inhibition of proliferation (Nouguerède et al., 2013). These data combined with literature shows that ADM predominantly has a stimulatory effect on proliferation. It also shows that RAMP-3 has a role in inducing cancer cell proliferation suggesting that ADM may induced its proliferative effects through the RAMP-3 receptor. However, some exceptions in ADM inducing proliferation have been demonstrated in both PaCa and prostate cancer (Abasolo et al., 2004; Keleg ., et al., 2007). This study shows that KD of ADM and RAMP-3 reduces the proliferation of CFPAC-1 PaCa cells however, this was not significant.

CFPAC-1 ADM KDs treated with 1 µM, 500 nM and 100 nM gemcitabine showed between 63.6% to 68.2% decrease in viability compared to untreated cells (Figure 5.2). RAMP-3 KDs showed no significant differences between different doses of gemcitabine and untreated cells however, RAMP-3

KDs were shown to be significantly less viable at 100 nM compared to scrshRNA. Both CFPAC-1 ADM KDs and RAMP-3 KDs had an increase in apoptosis at higher doses of gemcitabine compared to untreated cells and WT cells (Figure 5.4). CFPAC-1 scrshRNA had no significant increases in apoptosis except at 500 nM where apoptosis increased by 1.1-fold compared to untreated cells. CFPAC-1 WT cells had significant differences between treated and untreated cells at doses of 1 μM, 500 nM and 100 nM.

Combining the viability and apoptosis data, the results suggest that at a dose of 100 nM gemcitabine CFPAC-1 ADM KD viability is decreased and apoptosis is increased significantly compared to CFPAC-1 scrshRNA and CFPAC-1 WT cells respectively. CFPAC-1 scrshRNA treated at this dose of gemcitabine showed 61.8% viability compared to ADM KDs that had 36.4% viability. Apoptosis data comparing RAMP-3 KDs to WT cells at a dose of 100 nM gemcitabine, showed 110% more apoptosis in RAMP-3 KDs. Akada *et al* (2005) have previously shown that CFPAC-1 cells are sensitive to gemcitabine treatment showing that after 72 hours of treatment, viability was less than 20%. CFPAC-1 cells also had the lowest IC_{50} out of the 3 cell lines that were sensitive. High sensitivity to gemcitabine correlated with higher expression of *BNIP3* which is a pro-apoptotic molecule that is part of the Bcl-2 family. ADM has been previously shown to regulate Bcl-2 expression to promote anti-apoptotic effects in both osteosarcoma and ovarian cancer cells (Oehler., 2001; Wu et al., 2015). Therefore, reducing expression of ADM and RAMP-3 in CFPAC-1 cells could have potentially altered the ratio of pro-apoptotic (BNIP3) and anti-apoptotic Bcl-2 family molecules to promote more apoptosis and improved response to gemcitabine. To confirm this, analysis of Bcl-2 family gene expression would need to be confirmed, particularly as at higher doses of gemcitabine (500 nM and 1 μM), apoptosis decreased slightly. However, apoptosis remained higher in RAMP-3 KDs compared to WT CFPAC-1 and scrshRNA.

Viability and apoptosis data show that both KD cells and controls are unresponsive to 5-FU treatment. CFPAC-1 ADM KDs, RAMP-3 KDs and scrshRNA showed no significant differences

between treated and untreated cells (Figure 5.5). CFPAC-1 WT cells were also less responsive compared to treatment with gemcitabine, the largest decrease in viability was 14.5% at a 500 nM dose of 5-FU compared to 3 nM. Apoptosis data showed no significant differences between different doses of 5-FU and CFPAC-1 ADM KD and RAMP-3 KD (Figure 5.7). CFPAC-1 scrshRNA showed that at the highest dose of 5-FU (1 µM), the amount of apoptosis decreased by 0.2-fold compared to untreated cells. The largest increase in apoptosis was at 3 nM when apoptosis increased by 0.2-fold compared to untreated. CFPAC-1 WT cells were also less responsive to 5-FU than gemcitabine however, at a dose of 1 µM, they showed a 1.1-fold increase in apoptosis compared to untreated cells. Shi *et al* (2002) show that after 72 hours of 5-FU and gemcitabine PaCa treatment, PaCa cell viability decreased, gemcitabine treated cells were more sensitive with nM IC_{50} values compared to µM IC_{50} values following 5-FU treatment. However, repeated exposure to 5-FU, PaCa cells were resistant to 5-FU. Data from this study also suggests that CFPAC-1 cells are resistant to 5-FU and that KD of RAMP-3 or ADM does not improve response. Regine *et al* (2008) compared patient response to gemcitabine and 5-FU monotherapy. This showed that patients were more sensitive to gemcitabine with a median free survival of 20.5 months compared to 16.9 months in 5-FU treated patients. 3-year survival was also higher in gemcitabine treated patients at 31% compared to 22% in 5-FU treated patients. Although, this data is related to patients and is not an *in vitro* model, it does highlight that patients are also less responsive to 5-FU. It also shows that regardless of the treatment patients receive, median free survival and 3-year survival is still low. Using higher doses of 5-FU may be a future consideration for *in vitro* experiments. However, these data do show that alternative treatments are needed to improve PaCa patient outcome.

7.1.4 In vivo

Orthotopic and subcutaneous models were developed using CFPAC-1 ADM KDs, scrshRNA and WT cells to compare effects of ADM KD on tumour growth, metastases, immune cells and proliferation. CFPAC-1 ADM KD-LucRFP and CFPAC-1 scrshRNA-LucRFP cells were injected orthotopically into the pancreas and mice were split into three groups dependent on whether the KD was induced with

doxycycline or not (Table 6.1 and Figure 6.2). The luminescence of tumours and weight of mice was measured twice weekly to monitor tumour growth and ensure mice have no significant weight loss. At the endpoint of the experiment (day 17 or day 45), luminescence of tumours and organs was measured by IVIS. Furthermore, the weight of tumours, liver, kidney and spleen were recorded. Tumours and organs were sent to histology for sectioning and H&E staining, the remaining sections for stained for Ki67 by immunohistochemistry. The subcutaneous model was used to compare differences in tumour volume between CFPAC-1 ADM KDs, scrshRNA and WT cells.

Overall, tumour weight was shown to be highest in CFPAC-1 ADM KDs compared to CFPAC-1 scrshRNA in the orthotopic model. Tumours that were not induced with doxycycline had the highest tumour weight, suggesting that doxycycline does induce KDs and therefore effect tumour size. Tumours in the dox on/off/on group had a larger tumour weight than dox on suggesting that temporarily inhibiting the induction of ADM KDs, drove a temporary increase in tumour growth (Figure 6.8). Ex vivo analysis of tumour luminescence showed no significant differences between CFPAC-1 ADM KD and scrshRNA tumour luminescence however, there were significant differences between the different doxycycline conditions. Luminescent signal was higher in CFPAC-1 ADM KDs in the no dox group compared to dox on/off/on. CFPAC-1 scrshRNA had a significant difference in luminescent signal between no dox and dox on/off/on and between no dox and dox on. Luminescence was highest in the no dox group suggesting that in scrshRNA control, induction of scrshRNA results in slower tumour growth. (Figure 6.9).

Comparison of tumour volume and weight from the subcutaneous *in vivo* model showed that CFPAC-1 WT cells had the largest tumour volume and weight. CFPAC-1 ADM KD tumour volume and weight was smaller than WT cells but larger than CFPAC-1 scrshRNA. The difference in tumour weight was significantly different between doxycycline induced CFPAC-1 ADM KDs and scrshRNA. These data are consistent with the orthotopic model showing that ADM KDs had larger tumour weights. Although the no doxycycline groups had lower tumour volumes and weights, there was no significant

difference between doxycycline induced and non-induced cells (Fig 6.18). CFPAC-1 WT cells that were induced with doxycycline and non-induced were significantly larger than CFPAC-1 scrshRNA (Figure 6.18).

Analysis of IVIS luminescence, H&E tumour sections and Ki67 positive cells in CFPAC-1 ADM KDs and scrshRNA showed that at day 45, luminescence increased (Figure 6.14 to 6.16), the pancreas was more poorly differentiated showing a more malignant phenotype (Figure 6.14 to 6.16) and that the number of Ki67 positive cells increased (Figure 6.17) compared to day 17. Analysis of Ki67 positive cells showed that at day 17 there was a significant difference between ADM KD and scrshRNA. ADM KDs had overall more Ki67 positive cells in both dox on and dox on/off/on groups. At day 45, there was no significant difference in the number of Ki67 positive cells between ADM KDs and scrshRNA, there were also no significant differences between the different doxycycline conditions. CFPAC-1 ADM KDs overall had the largest percentage increase in Ki67 (49.8%) in the no dox group and the lowest percentage increase in the dox on group (31%) at day 45. This suggests that inducing ADM KDs with doxycycline, slows down the rate of tumour growth which is supported by the data showing lower tumour weight in doxycycline induced ADM KDs (Figure 6.8 and 6.18). CFPAC-1 scrshRNA showed that cells in the dox on group showed the largest increase in Ki67 positive cells (61.2%). ScrshRNA cells in the dox on/off/on had the smallest increase in Ki67 positive cells of 31.2% (Figure 6.15). These data combined suggest that ADM KDs in CFPAC-1 permanently induced by doxycycline have reduced numbers of Ki67 positive cells compared to scrshRNA permanently induced with doxycycline. However, overall ADM KDs do not slow down the rate of tumour growth compared to scrshRNA in CFPAC-1 cells.

In PaCa, specific ADM KD studies have not been completed however, intra-tumoural injection of ADM antagonist into PaCa cells resulted in inhibition of tumour growth. By the experimental endpoint, 70% of the mice had a barely detectable tumour (Ishikawa et al., 2003). This suggests that ADM may have a role in promoting PaCa tumour growth in cancer. In other cancers including

colorectal, osteoscarcoma, hepatocellular cancer and bladder cancer, KD of ADM was associated with decreasing tumour growth (Dai et al., 2013; Li et al., 2014; Liu et al., 2013; Wang et al., 2014; Yao et al., 2019). These data indicate that ADM does have pro-tumorigenic effects. Overexpression of ADM in various cancer cell lines has shown more variable data. Abasolo *et al* (2003) and Abasolo *et al* (2004) showed that ADM overexpression in PC-3 prostate cancer cells resulted in reduced tumour growth. Furthermore, Oehler *et al* (2002) showed overexpression of ADM in endometrial cell lines resulted in increased tumour growth in RL95.2 however, overexpression of ADM in Ishikawa cells had a low impact tumour growth. (Martinez et al., (2002) showed that overexpression of ADM in T47D breast cancer cells resulted in establishment of tumours in 3 out of 10 mice, whilst empty plasmid showed no tumour development. Studies analysing the effect of αAM on tumour growth in colorectal cancer, prostate cancer and glioblastoma all showed that tumour volume decreased (Berenguer-Daize et al., 2013; Nouguerède et al., 2013; L. H. Ouafik et al., 2002). Together these data demonstrate the varied responses between different cancer cell lines to ADM stimulation or inhibition. ADM KD data predominantly shows evidence for decreasing tumour volume which is in contrast to the data obtained from this study. Furthermore, treatment of tumours with antagonists or α-AM induced a decrease in tumour volume. In contrast, overexpression of ADM shows more varied results, this could be due to inconsistency in the amount of overexpression between different studies or due to the cancer type. Factors such as how well tumours initially establish regardless of KD or overexpression of a gene could be that the results provide more varied data. The overexpression data highlights the value in replicating experiments in multiple cell lines as different cell lines may show contrasting results. Although, the data predominantly shows that ADM may have a pro-tumorigenic effect, based on data from this study and studies showing the effect of ADM expression, the role of ADM in tumour growth requires further elucidation which could be determined by repeating experiments in multiple cell lines.

Furthermore, Dai *et al* (2020) demonstrated that RAMP-3 KOs themselves did not cause a decrease in tumour growth as tumour growth between RAMP-3 KO and wild-type PAN02 cells was the same.

RAMP-2 KO in endothelial cells was responsible for a decrease in tumour growth but was shown increase metastases together with increased RAMP-3 expression. Therefore, whether tumours increase or decrease in growth in response to ADM may be influenced by which RAMP is expressed more dominantly (RAMP-2 or RAMP-3) and therefore which receptor is activated (AM_1 or AM_2). Karpinich *et al* (2013) developed ADM KD and cells overexpressing ADM in Lewis lung cell carcinoma cells. They found that tumour volume did not differ between ADM overexpressing cells, ADM KD cells and scrshRNA controls. However, there were more significantly more Ki67 positive cells in ADM overexpressing cells compared to scrshRNA which correlated with increased lymphatic vessel size and lymph node lymphangiogenesis. Therefore, this study suggested this may correlate with ADM overexpression inducing distant metastases. Together with Dai *et al* (2020) data, this suggests that ADM in Lewis lung cell carcinoma may predominantly induce its pro-tumorigenic effects through RAMP-3 in this model. However, comparison of expression of RAMP-2 and RAMP-3 in the tumours would need to be determined to confirm this. These two studies may explain why CFPAC-1 ADM KDs showed no difference in tumour volume compared to scrshRNA controls. Analysis of RAMP-3 expression between CFPAC-1 scrshRNA and ADM KD and staining for lymphangiogenesis using markers including LYVE-1 may also provide further insight into why there is no difference in tumour volume. This could also be applied to the subcutaneous model where although WT cells had a higher tumour volume, it was not significantly different. Comparing RAMP-3 expression and expression of molecules that are known to promote distant metastases may inform why tumour volumes were not significantly different.

There are also some technical considerations that may have effected tumour volume. CFPAC-1 ADM KDs developed used inducible lentiviral knockdowns which require induction with doxycycline. This relies on the mice consuming enough water to induce KDs however, Cawthorne *et al* (2007) suggested that the bitter taste of doxycycline could affect consumption of water. Although, there were no obvious signs of dehydration throughout the course of the *in vivo* experiments. Adding sucrose to water to reduce the bitter taste of doxycycline and increase water consumption have

been suggested however, this lead to severe dehydration. Potentially giving mice food containing doxycycline may be a better alternative as doxycycline has been shown to remain stable in food. Furthermore, consumption of food containing doxycycline was not reduced in mice compared to mice provided with their usual feed (Cawthorne et al., 2007).

Organs were collected from both orthotopic and subcutaneous experiments to analyse whether any metastases developed and also to determine any differences in organ weight between groups. Analysis of organs by IVIS showed 5 of the stomach collected to have luminescent signal however, based on current analysis by H&E, there is no obvious metastases. Further analysis such as comparison of Ki67 positive cells between a stomach without a luminescent signal and a stomach without a luminescent signal could be compared. Comparison of liver, kidney and spleen weights between day 17 and day 45 in both CFPAC-1 ADM KDs and CFPAC-1 scrshRNA showed no significant differences (Figure 6.10). Analysis of organs from subcutaneous experiments showed a significant difference between the weight of liver in CFPAC-1 ADM KDs compared to scrshRNA not induced with doxycycline with scrshRNA livers weighing more (Fig 6.19). Liver metastases has previously been shown to correlate with RAMP-3 expression in PaCa (Dai et al., 2020) however, analysis of liver of liver sections by H&E would need to be completed before confirming any metastases.

Immune cell analysis of whole blood collected from mice following orthotopic injection of CFPAC-1 ADM KDs and CFPAC-1 scrshRNA into the pancreas showed, the percentage of monocytes was within the normal range for BALB/c nude mice on day 17 and day 45. At day 45, monocyte percentage was raised in both CFPAC-1 ADM KDs and scrshRNA cells that were not induced with doxycycline (Figure 6.13). Eosinophil percentage was varied in both CFPAC-1 ADM KDs and scrshRNA on day 17 and day 45 with lymphocyte percentage both inside and outside the normal range for BALB/c nude mice (Figure 6.13). Lymphocyte percentage was predominantly normal in both CFPAC-1 ADM KDs and scrshRNA. CFPAC-1 ADM KD cells not induced with doxycycline had lower levels of lymphocytes on both day 17 and day 45. Comparison of ADM KDs to scrshRNA on day 17 without

doxycycline induction, showed that ADM KDs had significantly less lymphocytes (26% less). On day 45 monocytes and eosinophils showed that there were significant differences between different doxycycline conditions.

There is limited literature associating ADM with monocytes, eosinophils and lymphocytes. Sanford *et al* (2013) have shown that low monocyte levels in patient samples correlated with increased patient survival. Therefore, the increase in monocytes in both CFPAC-1 ADM KD and scrshRNA not induced with doxycycline at day 45 in this study may correlate with tumour progression. However, this may not specifically be linked to ADM expression as scrshRNA groups had similar results. Xu *et al* (2016), have shown a correlation between increased ADM expression and increased myelomonocytic differentiation into M2 phenotype macrophages and myeloid derived suppressor cells that exhibit a pro-tumorigenic phenotype. Analysing tumour sections for specific monocytic cells including M2 phenotype macrophages may provide a more specific insight into the role of ADM in regulating monocytic cells. Eosinophils have been suggested to have a role in the development of fibrosis and pancreatic malignancy however, no specific associations have been made with ADM (Manohar et al., 2017). This study shows large variability between percentage of eosinophils however, on day 45 there are more eosinophils outside the 'normal' range for BALB/c nude mice suggesting that tumour progression may increase eosinophil percentage. However, there were no significant differences between ADM KD and scrshRNA suggesting that this is change is not necessarily driven by ADM. When interpreting the lymphocyte results, an important consideration is that the mice are athymic and therefore, interpretation of results only relates to NK cells and B lymphocytes. Higher percentages of NK cells have been associated with better prognosis in PaCa patients however, this has not been shown to be regulated by ADM in literature. It has also been suggested that B cells have an immuno-stimulatory effects in PaCa tumour microenvironments however, this is also not specifically associated with ADM expression. Together with data from this study, ADM appears to not regulate B lymphocytes and NK cells in this CFPAC-1 xenograft model.

7.1.5 Future work

Current data shows that ADM and its receptor components are expressed in all cell lines however, the role of ADM in PaCa has not been fully elucidated. The data also shows that that reducing levels of ADM does not significantly affect tumour growth. There were also no significant differences between Ki67 positive staining between CFPAC-1 ADM KDs and scrshRNA controls. However, endomucin and α-SMA staining analysis needs to be completed to see if ADM has an effect on angiogenesis or the percentage of α-SMA positive PSCs. These would inform whether ADM has an effect on cells within the tumour microenvironment, as opposed to tumour cells themselves. Ishikawa *et al* (2003) showed that treating PaCa cells with AM_{22-52} resulted in smaller blood vessels. Furthermore, Keleg *et al* (2007) showed that hypoxic conditions increased both ADM expression and VEGF expression. Proliferation of HUVEC cells increased with increasing ADM expression. Dai *et al* (2020) also show that RAMP-2 KO in endothelial cells is associated with decreased angiogenesis. Together these data show that ADM has been shown to have an important role in the regulation of angiogenesis. Therefore, comparison of CFPAC-1 ADM KDs to CFPAC-1 scrshRNA endomucin may inform whether vasculature within the tumour was effected by reducing ADM in CFPAC-1 cells. Dai *et al* (2020) have also shown that increased RAMP-3 expression correlated with increased α-SMA expression and a more aggressive phenotype as it is associated with activated PSCs. The pro-tumorigenic effects of PSCs are discussed in Chapter 6 and shown in Figure 6.1. Therefore, although tumour growth may not have decreased as a result of ADM KDs, the number of α-SMA positive PSCs may have reduced. This would inform whether KD of ADM results in a less aggressive PaCa tumour phenotype. To confirm this, analysis of α-SMA positive staining by QuPath needs to be completed.

Analysing mRNA expression of ADM, RAMP-2 and RAMP-3 in tumours collected from CFPAC-1 ADM KDs, scrshRNA and WT cells by QPCR would be completed in future. This would show if RAMP-2 or RAMP-3 expression is more dominant and may provide a further explanation as to why tumour growth was not significantly different between groups. Dai *et al* (2020) showed that activation of RAMP-2 by exogenous ADM in RAMP-3 KO mice reduced tumour growth and metastases. However,

that tumour size was no different between RAMP-3 KO PAN02 cells and RAMP-3 +/+ PAN02 cells. RAMP-2 KOs in endothelial cells showed decreased tumour growth but increased metastases which was correlated with increased RAMP-3 expression. These data demonstrate the contrasting roles that RAMP-2 and RAMP-3 have in PaCa, finding out whether RAMP-2 or RAMP-3 expression is more dominant in CFPAC-1 ADM KDs may explain the lack of significant differences between tumour size when comparing to scrshRNA. This could be determined by extracting RNA from tumours collected from both orthotopic and subcutaneous experiments and measuring expression of ADM, RAMP-2 and RAMP-3 in tumours. Staining tumours for RAMP-2 and RAMP-3 by immunohistochemistry could also be used to identify if expression is localised to a particular area of the tumour.

Developing ADM or RAMP-3 KDs in other PaCa cell lines that have been shown to have functional ADM receptors for example, AsPC-1 and HPAF-II (Figure 3.16) could provide a wider perspective of the different responses PaCa cell lines have to ADM/RAMP-3 KDs. It would show if the results obtained from this study would be replicated or whether there are differences between cell lines. Keleg *et al* (2007) have shown that different PaCa cell lines responded differently to recombinant ADM, two of the cell lines had increased proliferation whilst the remainder were unresponsive. Furthermore, Akada *et al* (2005) have shown that different cell lines responded differently to gemcitabine. CFPAC-1 cells were shown to be sensitive, ASPC-1 cells were intermediately sensitive. Together, these data show that all PaCa cells do not all have the same responses therefore, comparing the effect of ADM or RAMP-3 KDs in other cell lines may provide different insights into the role of ADM in PaCa progression both *in vitro* and *in vivo.*

In future, using CFPAC-1 RAMP-3 KDs *in vivo* after further validation of successful KD may help clarify how much of a role the CLR/RAMP-3 receptor has in inducing pro-tumorigenic effects. To date, the important physiological role of the CLR/RAMP-2 system in regulating blood pressure and in embryological development has been determined. However, until recently, the pathological role of RAMP-3 has been more speculation based, as opposed to evidence based with more focus on ADM

itself. Recently, Dai *et al* (2020) showed how KD of RAMP-3 in PaCa supressed tumour metastases suggesting that RAMP-3 plays an important role in the spread of PaCa. Following KD of RAMP-2 in endothelial cells which supressed tumour growth, they showed that the number of CAFs on the periphery of metastatic tumours was significantly higher together with increased expression of RAMP-3. Therefore, they developed RAMP-3 KOs in CAFs which showed tumour weight and metastases decreased. Furthermore, *in vitro* cultures showed decreased proliferation and migration of PAN02 cells co-cultured with RAMP-3 KO CAFs. These data demonstrate the important role of RAMP-3 in metastasis and tumour growth. Developing RAMP-3 KDs in both human PaCa cells and CAFs and exploring the effect this has on other cells that have been previously shown to be regulated by PSCs in Figure 6.1 could add to the picture of the exact role RAMP-3 and PSCs have in PaCa progression and development.

In vitro, conditioned media from RAMP-3 KD PSCs/CFPAC-1 cells could be used to treat macrophages. The percentage of M2 phenotype macrophages in the KD group compared to WT or scrshRNA control PSCs/CFPAC-1 could be compared by flow cytometry to see if they have a role in the altering macrophages to the M2 phenotype. The migration and proliferation of macrophages could also be compared. These experiments could also be conducted using HUVEC cells to see if migration and proliferation is altered when co-cultured with RAMP-3 KD PSCs/CFPAC-1 cells. *In vivo,* co-injection of these cells into mice with a more functional immune system could be used to see if tumour growth is altered but also whether the population of immune cells is different between KDs and controls. This could be completed by staining for CD206 M2 phenotype macrophage marker on tumour sections. Furthermore, analysis of endothelial cells by endomucin expression and differences in ECM by measuring collagen I expression which has shown to be tightly regulated by PSCs could be completed (Armstrong et al., 2004; Max G. Bachem et al., 2005; Masamune et al., 2008). These data could potentially provide a bigger picture for the cross-talk of ADM, RAMP-3, PaCa tumour cells and PSCs. Demonstrating that ADM induces its pro-tumorigenic effects predominantly through RAMP-3 could provide a novel target for the treatment of PaCa. Particularly if the role of RAMP-3 in the

development of PaCa is associated with the development of ECM and therefore, desmoplasia around the tumour tissue. Finding a method to break down the ECM barrier around the tumour, could improve response to currently used chemotherapies.

7.1.6 Conclusion

In conclusion, the data show that ADM and its receptor components are expressed in a panel of 7 PaCa cell lines. Previously collected data also showed that in 5 out of 7 of cell lines ADM has a functional role by increasing cAMP production. Therefore, the null hypothesis that ADM and its receptor components are not expressed and have no functional role in PaCa is disproved. Furthermore, KD of ADM and RAMP-3 in CFPAC-1 was shown to decrease proliferation of CFPAC-1 cells compared to CFPAC-1 WT cells however, this was not shown to be significant. Treatment of CFPAC-1 ADM KDs and RAMP-3 KDs with gemcitabine and 5-FU showed that cells were responsive to gemcitabine but not 5-FU. The viability of KD cells was not significantly different from the CFPAC-1 WT cells and scrshRNA controls. However, at a dose of 100 nM gemcitabine, the amount of apoptosis significantly increased in RAMP-3 KDs and ADM KDs suggesting they may improve response to chemotherapy compared to WT cells. Therefore, the current data partially disproves the null hypothesis that ADM and RAMP-3 have no involvement in the regulation of proliferation and apoptosis as proliferation was decreased in CFPAC-1 ADM KDs and RAMP-3 KDs (not significantly) and apoptosis increased at some doses of gemcitabine (significantly).

Current data suggests that ADM knockdown in CFPAC-1 cells has no effect on tumour growth and metastases which proves the null hypothesis. There is currently limited data related to the KD or overexpression of ADM in PaCa. Ishikawa *et al* (2003) showed that treatment of PCI-43 PaCa tumours with ADM antagonist resulted in decreased tumour size compared to controls. Other studies have demonstrated different PaCa cell lines respond differently to ADM in terms of proliferation and response to gemcitabine or 5-FU (Akada et al., 2005; Keleg et al., 2007). Therefore, a definitive role of ADM in regulating tumour size and weight would need further elucidation by

developing the same KDs in other PaCa cell lines. Furthermore, the receptor that ADM binds to may also effect whether tumour size and metastases are altered (Dai et al., 2020). Therefore, developing KDs specific to RAMP-3 in multiple PaCa cell lines may provide a more useful insight into the crosstalk of ADM and RAMP-3 in the development of PaCa tumours.

The data obtained from this study, together with previous studies around PaCa have demonstrated the potential significance of ADM and RAMP-3 in PaCa, particularly the association between RAMP-3 expression in CAFs and tumorigenesis. However, further research is needed showing the connection between ADM, RAMP-3, CAFs (PSCs) and PaCa development. Understanding the exact role ADM and RAMP-3 have in activating PSCs and the downstream effects of this on the ECM and desmoplasia still needs determining. The role ADM has in inducing other cells within the PaCa tumour microenvironment is also essential however, for an ADM/RAMP-3 antagonist to be able to target cells within the tumour microenvironment, it must first be able to target the desmoplastic scar tissue around the tumour. This would enable penetration of an ADM antagonist in combination with current chemotherapies to the target site (tumour cells). Therefore, future research should shift to the role of ADM and RAMP-3 in the development of the desmoplastic environment with focus on the role of PSC in inducing this.

APPENDIX

Table 8.1 Reagents, manufacturers and product codes

Reagent	Company/ Product code
Cell culture	
Dulbecco's Modified Eagle Medium, GlutaMAX	Thermo Fisher, 31966
RPMI 1640, GlutaMAX	Thermo Fisher, 61870
McCoy's 5A (Modified) Medium, GlutaMAX	Thermo Fisher, 36600
Fetal Bovine Serum (FBS)	Gibco, 10270
Sodium Pyruvate (NaPyr)	Thermo Fisher, 11360
Penicillin-Streptomycin (P/S)	Thermo Fisher, 15140
TrypLE Express Enzyme	Thermo Fisher, 14040
Dulbecco's Phosphate-Buffered Saline (PBS)	Thermo Fisher, 12605
Trypan Blue Solution, 0.4%	Thermo Fisher, 15250
PBS	Thermo Fisher, 10010
Polymerase chain reaction (PCR), endpoint and QPCR	
ReliaPrep™ RNA Cell Miniprep Precision	Promega, Z6012
High-Capacity RNA-to-cDNA™ Kit	Thermo Fisher, 4387406
GoTaq® G2 Flexi DNA Polymerase	Promega, M7801
HighRanger Plus 100 bp DNA Ladder	Norgen Biotek, 12000
nanoScript2 Reverse Transcription Kit	Primerdesign
RT-NanoScript2 Double-dye (Hydrolysis) probe geNorm 6 gene kit	Primerdesign, ge-DD-6
RNaseZap® RNase Decontamination Solution	Thermo Fisher, AM9780
Gel electrophoresis	
Agarose	Fisher Scientific BP1356
Tris Acetate EDTA (TAE)	National Diagnostics, EC861
Ethidium Bromide	Sigma Aldrich, E1385
FullRanger 100bp DNA Ladder	GeneFlow, L3-0014
Protein extraction, BCA assay and Western Blotting	
Halt™ Protease and Phosphatase Inhibitor cocktail (100 X)	Thermo Fisher, 78446
DC protein assay	Biorad, 5000111
4 X Laemmli Sample buffer	Biorad, 1610747
Precision Plus Protein™ Dual Colour Standards Ladder	Biorad, 1610374
4-20% Mini-PROTEON® TGX™ Precast Protein Gels	Biorad, 4561096
10 X Tris/Glycine/SDS	Biorad, 1610732
SuperSignal West Dura Extended Duration Substrate	Thermo Fisher, 34075
cAMP assay	
LANCE cAMP 384 Kit	PerkinElmer, AD0264
384-well Optiplates	PerkinElmer, 6007299
Hank's Buffered Saline Solution (HBSS)	Thermo Scientific, 24020
Hank's Buffered Saline Solution (no Ca2+, no Mg2+)	Thermo Scientific, 14170
Stabilizer, 7.5% (DTPA-purified BSA)	PerkinElmer, CR84
3-isobutyl-1-methylxanthine	Sigma-Aldrich, I5879
HEPES	Fisher Scientific, BP310-1
Forskolin	Sigma-Aldrich, F3917
Human adrenomedullin	Anaspec, AS-60447
Human calcitonin gene-related peptide	Sigma-Aldrich, SCP0060
Human intermedin	Bachem, H-6064
Viability assay	
RealTime-Glo™ MT Cell Viability Assay	Promega, G9712
Corning™ Costar™ 96-Well White Clear-Bottom Plates	Corning, 3610

Apoptosis assay	
Caspase-Glo™ 3/7 Apoptosis Assay	Promega, G8093
Compound preparation for viability and apoptosis assay	
Gemcitabine HCl	HY-B0003, CS-0735
5-Fluorouracil (5-FU)	Sigma-Aldrich, F6627
Dimethyl Sulfoxide (DMSO)	Sigma-Aldrich, D8418
In vivo (cell preparation, IVIS and endpoint)	
Corning® Matrigel® Basement Matrix	Corning, 354234
Dulbecco's PBS	Thermo Fisher, 14040
Isoflurane (IsoFlo)	Zoetis, 50019100
XenoLight D-Luciferin	PerkinElmer, 122799
Doxycycline 100 mg/mL oral solution	Karidox, 100675

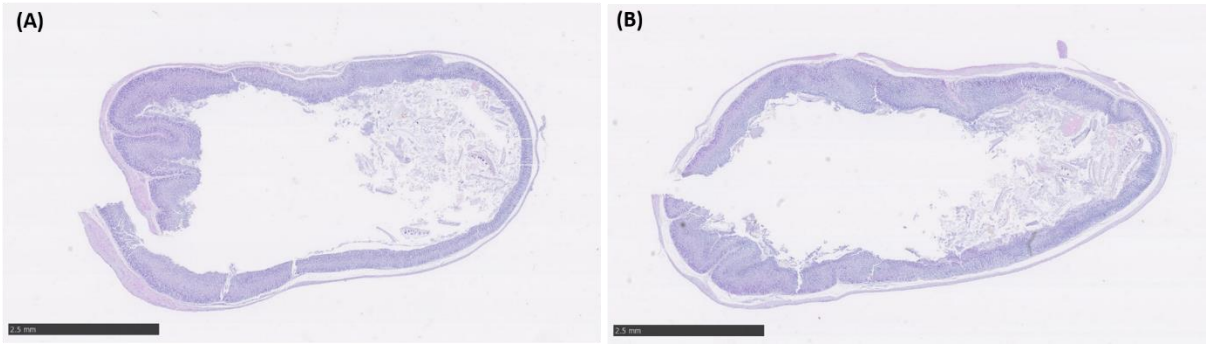

Figure 8.1 Example H&E stomach histology collected at day 45 from CFPAC-1 scrshRNA no dox group. **(A)** CFPAC-1 scrshRNA no dox stomach section from mouse with luminescent signal in stomach following IVIS analysis. **(B)** CFPAC-1 scrshRNA no dox stomach section from mouse with no luminescent signal in stomach following IVIS analysis.

References

Abasolo, I., Montuenga, L. M., & Calvo, A. (2006). Adrenomedullin prevents apoptosis in prostate cancer cells. *Regulatory Peptides*, *133*, 115–122. https://doi.org/10.1016/j.regpep.2005.09.026

Abasolo, I., Wang, Z., Montuenga, L. M., & Calvo, A. (2004). Adrenomedullin inhibits prostate cancer cell proliferation through a cAMP-independent autocrine mechanism. *Biochemical and Biophysical Research Communications*, *322*, 878–886. https://doi.org/10.1016/j.bbrc.2004.08.006

Abasolo, I., Yang, L., Haleem, R., Xiao, W., Pio, R., Cuttitta, F., … Wang, Z. (2003). Overexpression of adrenomedullin gene markedly inhibits proliferation of PC3 prostate cancer cells in vitro and in vivo. *Molecular and Cellular Endocrinology*, *199*, 179–187.

Abd-Elsalam, K. A. (2003). Bioinformatic tools and guideline for PCR primer design. *Journal of Biotechnology*, *2*(5), 91–95.

Abedi, S. H., Ahmadzadeh, A., & Mohammad Alizadeh, A. H. (2017). Pancreatic Squamous Cell Carcinoma. *Case Reports in Gastroenterology*, *11*(1), 219–224. https://doi.org/10.1159/000448069

Adsay, N. V., Merati, K., Basturk, O., Iacobuzio-Donahue, C., Levi, E., Cheng, J. D., … Klimstra, D. S. (2004). Pathologically and biologically distinct types of epithelium in intraductal papillary mucinous neoplasms: Delineation of an “intestinal” pathway of carcinogenesis in the pancreas. *American Journal of Surgical Pathology*, *28*(7), 839–848. https://doi.org/10.1097/00000478-200407000-00001

Aggarwal, G., Ramachandran, V., Javeed, N., Arumugam, T., Dutta, S., Klee, G. G., … Chari, S. T. (2012). Adrenomedullin is up-regulated in patients with pancreatic cancer and causes insulin resistance in β cells and mice. *Gastroenterology*, *143*(6), 1510-1517.e1. https://doi.org/10.1053/j.gastro.2012.08.044

Ajish, C., Yang, S., Kumar, S. D., & Yub, S. (2020). Proadrenomedullin N-terminal 20 peptide (PAMP) and its C-terminal 12-residue peptide , PAMP (9 e 20): Cell selectivity and antimicrobial mechanism. *Biochemical and Biophysical Research Communications*, *527*(3), 744–750. https://doi.org/10.1016/j.bbrc.2020.04.063

Akada, M., Crnogorac-Jurcevic, T., Lattimore, S., Mahon, P., Lopes, R., Sunamura, M., … Lemoine, N. R. (2005). Intrinsic chemoresistance to gemcitabine is associated with decreased expression of BNIP3 in pancreatic cancer. *Clinical Cancer Research*, *11*(8), 3094–3101. https://doi.org/10.1158/1078-0432.CCR-04-1785

Akerstrom, G., & Hellman, P. (2007). Surgery on neuroendocrine tumours. *Best Practice and Research: Clinical Endocrinology and Metabolism*, *21*(1), 87–109. https://doi.org/10.1016/j.beem.2006.12.004

Al-Shehri, A., Silverman, S., & King, K. . (2008). Squamous cell carcinoma of the pancreas. *Current Oncology*, *15*(6), 293–297.

Amin, M. B., Edge, S., Greene, F., Byrd, D. R., Brookland, R. K., Washington, M. K., … Meyer, L. R. (2017). *AJCC Cancer Staging Manual. 8th Edition*.

Andea, A., Sarkar, F., & Adsay, V. N. (2003). Clinicopathological Correlates of Pancreatic Intraepithelial Neoplasia: A Comparative Analysis of 82 Cases With and 152 Cases Without Pancreatic Ductal Adenocarcinoma. *Modern Pathology*, *16*(10), 996–1006. https://doi.org/10.1097/01.MP.0000087422.24733.62

Aoyagi, Y., Oda, T., Kinoshita, T., Nakahashi, C., Hasebe, T., Ohkohchi, N., & Ochiai, A. (2004). Overexpression of TGF-beta by infiltrated granulocytes correlates with the expression of collagen mRNA in pancreatic cancer. *British Journal of Cancer*, *91*, 1316–1326. https://doi.org/10.1038/sj.bjc.6602141

Apte, A., & Daniel, S. (2009). PCR Primer Design. *Cold Spring Harbor Protocol*, *4*(3), 1–11.

https://doi.org/10.1101/pdb.ip65

Apte, M. V., Haber, P. S., Applegate, T. L., Norton, I. D., McCaughan, G. W., Korsten, M. A., … Wilson, J. S. (1998). Periacinar stellate shaped cells in rat pancreas: Identification, isolation, and culture. *Gut*, *43*(1), 128–133. https://doi.org/10.1136/gut.43.1.128

Arango, D., Wilson, A. J., Shi, Q., Corner, G. A., Arañes, M. J., Nicholas, C., … Augenlicht, L. H. (2004). Molecular mechanisms of action and prediction of response to oxaliplatin in colorectal cancer cells. *British Journal of Cancer*, *91*(11), 1931–1946. https://doi.org/10.1038/sj.bjc.6602215

Armstrong, T., Packham, G., Murphy, L. B., Bateman, A. C., Conti, J. A., Fine, D. R., … Iredale, J. P. (2004). Type I Collagen Promotes the Malignant Phenotype of Pancreatic Ductal Adenocarcinoma. *Clinical Cancer Research*, *10*, 7427–7437. https://doi.org/10.1016/j.canlet.2014.10.020

Artinyan, A. V. O., Soriano, P. A., Prendergast, C., Low, T., Ellenhorn, J. D. I., & Kim, J. (2008). The anatomic location of pancreatic cancer is a prognostic factor for survival. *HPB*, *10*, 371–376. https://doi.org/10.1080/13651820802291233

Asada, Y., Seiichiro, H., Murutsuka, K., Kitamura, K., Tsuji, T., Sakata, J., … Sumiyoshi, A. (1999). Novel distribution of adrenomedullin-immunoreactive cells in human tissues. *Histochemical Cell Biology*, *112*, 185–191.

Bachem, M. G., Schneider, E., Gross, H., Weidenbach, H., Schmid, R. M., Menke, A., … Crawford, J. M. (1998). Identification, culture, and characterization of pancreatic stellate cells in rats and humans. *Gastroenterology*, *115*(2), 421–432. https://doi.org/10.1016/S0016-5085(98)70209-4

Bachem, Max G., Schünemann, M., Ramadani, M., Siech, M., Beger, H., Buck, A., … Adler, G. (2005). Pancreatic carcinoma cells induce fibrosis by stimulating proliferation and matrix synthesis of stellate cells. *Gastroenterology*, *128*(4), 907–921. https://doi.org/10.1053/j.gastro.2004.12.036

Barău, A., Ruiz-Sauri, A., Valencia, G., Gómez-mateo, M. C., Sabater, L., Ferrandez, A., & Llombart-

bosch, A. (2013). High microvessel density in pancreatic ductal adenocarcinoma is associated with high grade. *European Journal of Pathology*, *462*, 541–546. https://doi.org/10.1007/s00428-013-1409-1

Bardeesy, N., & DePinho, R. A. (2002). Pancreatic cancer biology and genetics. *Nature Reviews Cancer*, *2*(12), 897–909. https://doi.org/10.1038/nrc949

Barkin, J. S., Goldberg, R. I., Sfakianakis, G. N., & Levi, J. (1986). Pancreatic Carcinoma is Associated with Delayed Gastric Emptying. *Digestive Diseases and Sciences*, *31*(3), 265–267.

Ben, Q., Xu, M., Ning, X., Liu, J., Hong, S., Huang, W., … Li, Z. (2011). Diabetes mellitus and risk of pancreatic cancer: A meta-analysis of cohort studies. https://doi.org/10.1016/j.ejca.2011.03.003

Benyahia, Z., Dussault, N., Cayol, M., Sigaud, R., Berenguer-Daizé, C., Delfino, C., … Ouafik, L. (2017). Stromal fibroblasts present in breast carcinomas promote tumor growth and angiogenesis through adrenomedullin secretion. *Oncotarget*, *8*(9), 15744–15762. https://doi.org/10.18632/oncotarget.14999

Berenguer-Daize, C., Boudouresque, F., Bastide, C., Tounsi, A., Benyahia, Z., Acunzo, J., … Ouafik, L. (2013). Adrenomedullin Blockade Suppresses Growth of Human Hormone – Independent Prostate Tumor Xenograft in Mice. *Clinical Cancer Research*, *19*(22), 6138–6150. https://doi.org/10.1158/1078-0432.CCR-13-0691

Berenguer, C., Boudouresque, F., Dussert, C., Daniel, L., Muracciole, X., Grino, M., … Ouafik, L. H. (2008). Adrenomedullin , an autocrine / paracrine factor induced by androgen withdrawal , stimulates ‘ neuroendocrine phenotype ’ in LNCaP prostate tumor cells. *Oncogene*, 506–518. https://doi.org/10.1038/sj.onc.1210656

Bhardwaj, A., Srivastava, S. K., Singh, S., Tyagi, N., Arora, S., Carter, J. E., … Singh, A. P. (2016). MYB promotes desmoplasia in pancreatic cancer through direct transcriptional up-regulation and

cooperative action of sonic hedgehog and adrenomedullin. *Journal of Biological Chemistry*, *291*(31), 16263–16270. https://doi.org/10.1074/jbc.M116.732651

Bilimoria, K. Y., Bentrem, D. J., Ko, C. Y., Ritchey, J., Stewart, A. K., Winchester, D. P., & Talamonti, M. S. (2007). Validation of the 6th Edition AJCC Pancreatic Cancer Staging System Report From the National Cancer Database. *American Cancer Society*, *110*, 738–744. https://doi.org/10.1002/cncr.22852

Biswas, S. K., & Mantovani, A. (2010). Macrophage plasticity and interaction with lymphocyte subsets : cancer as a paradigm. *Nature Immunology*, *11*(10), 889–896. https://doi.org/10.1038/ni.1937

Blom, J., Giove, T. J., Pong, W. W., Blute, T. A., & Eldred, W. D. (2012). Evidence for a functional adrenomedullin signaling pathway in the mouse retina. *Molecular Vision*, *18*, 1339–1353.

Blom, J. W., Osanto, S., & Rosendaal, F. R. (2005). High risk of venous thrombosis in patients with pancreatic cancer : A cohort study of 202 patients. *European Journal of Cancer*, *42*, 410–414. https://doi.org/10.1016/j.ejca.2005.09.013

Bold, R. J., Chandra, J., & Mcconkey, D. J. (1999). Gemcitabine-Induced Programmed Cell Death (Apoptosis) of Human Pancreatic Carcinoma Is Determined by Bcl-2 Content. *Annals of Surgical Oncology*, *6*(3), 279–285.

Bouschet, T., Martin, S., & Henley, J. M. (2012). Receptor-activity-modifying proteins are required for forward trafficking of the calcium-sensing receptor to the plasma membrane. *Journal of Cell Science*, *118*(20), 4709–4720. https://doi.org/10.1242/jcs.02598.Receptor-activity-modifying

Boyd, C. A., Benarroch-Gampel, J., Sheffield, K. M., Cooksley, C. D., & Raill, T. S. (2012). 415 Patients with Adenosquamous Carcinoma of the Pancreas: A Population-Based Analysis of Prognosis and Survival. *Journal of Surgical Research*, *173*(1), 12–19. https://doi.org/10.1016/j.jss.2011.06.015.

Brekhman, V., Lugassie, J., Zaffryar-Eilot, S., Sabo, E., Kessler, O., Smith, V., … Neufeld, G. (2011). Receptor activity modifying protein-3 mediates the protumorigenic activity of lysyl oxidase-like protein-2. *The FASEB Journal*, *25*(1), 55–65. https://doi.org/10.1096/fj.10-162677

Burns, M. J., Nixon, G. J., Foy, C. A., & Harris, N. (2005). Standardisation of data from real-time quantitative PCR methods - Evaluation of outliers and comparison of calibration curves. *BMC Biotechnology*, *5*, 1–13. https://doi.org/10.1186/1472-6750-5-31

Burns, M., & Valdivia, H. (2008). Modelling the limit of detection in real-time quantitative PCR. *European Food Research and Technology*, *226*(6), 1513–1524. https://doi.org/10.1007/s00217-007-0683-z

Bustin, S. A., Benes, V., Garson, J. A., Hellemans, J., Huggett, J., Kubista, M., … Wittwer, C. T. (2009). The MIQE guidelines: Minimum information for publication of quantitative real-time PCR experiments. *Clinical Chemistry*, *55*(4), 611–622. https://doi.org/10.1373/clinchem.2008.112797

Cai, B., An, Y., Lv, N., Chen, J., Tu, M., Sun, J., … Miao, Y. (2013). miRNA-181b increases the sensitivity of pancreatic ductal adenocarcinoma cells to gemcitabine in vitro and in nude mice by targeting BCL-2. *Oncology Reports*, *29*(5), 1769–1776. https://doi.org/10.3892/or.2013.2297

Campello, E., Ilich, A., Simioni, P., & Key, N. S. (2019). The relationship between pancreatic cancer and hypercoagulability: a comprehensive review on epidemiological and biological issues. *British Journal of Cancer*, *121*(5), 359–371. https://doi.org/10.1038/s41416-019-0510-x

Cawthorne, C., Swindell, R., Stratford, I. J., Dive, C., & Welman, A. (2007). Comparison of doxycycline delivery methods for Tet-Inducible gene expression in a subcutaneous xenograft model. *Journal of Biomolecular Techniques*, *18*(2), 120–123.

Ceyhan, G. O., Ekin, I., Altintas, B., Rauch, U., Thiel, G., Müller, M. W., … Schäfer, K. (2008). Neural invasion in pancreatic cancer : A mutual tropism between neurons and cancer cells.

Biochemical and Biophysical Research Communications, *374*, 442–447. https://doi.org/10.1016/j.bbrc.2008.07.035

Chakraborty, S., & Singh, S. (2013). Surgical resection improves survival in pancreatic cancer patients without vascular invasion- a population based study. *Annals of Gastroenterology*, (March), 346–352.

Chanjuan, S., & Hruban, R. H. (2012). Intraductal Papillary Mucinous Neoplasm. *Human Pathology*, *43*, 1–16. https://doi.org/10.1016/j.humpath.2011.04.003

Chauhan, M., Yallampalli, U., Banadakappa, M., & Yallampalli, C. (2015). Involvement of receptor activity-modifying protein 3 (RAMP3) in the vascular actions of adrenomedullin in rat mesenteric artery smooth muscle cells. *Biology of Reproduction*, *93*(5), 1–8. https://doi.org/10.1095/biolreprod.115.134585

Chen, Pan, Pang, X., Zhang, Y., & He, Y. (2012). Effect of inhibition of the adrenomedullin gene on the growth and chemosensitivity of ovarian cancer cells. *Oncology Reports*, *27*, 1461–1466. https://doi.org/10.3892/or.2012.1655

Chen, Peiwen, Huang, Y., Bong, R., Ding, Y., Song, N., & Wang, X. (2011). Tumor-Associated Macrophages Promote Angiogenesis and Melanoma Growth via Adrenomedullin in a Paracrine and Autocrine Manner. *Clinical Cancer Research*, *17*(11), 7230–7240. https://doi.org/10.1158/1078-0432.CCR-11-1354

Chen, Peiwen, Huang, Y., Bong, R., Ding, Y., Song, N., Wang, X., … Luo, Y. (2011). Tumor-associated macrophages promote angiogenesis and melanoma growth via adrenomedullin in a paracrine and autocrine manner. *Clinical Cancer Research*, *17*(23), 7230–7239. https://doi.org/10.1158/1078-0432.CCR-11-1354

Chen, Q., Chen, P., Pang, Þ. X., & Hu, Y. (2015). Adrenomedullin Up-regulates the Expression of Vascular Endothelial Growth Factor in Epithelial Ovarian Carcinoma Cells via JNK / AP-1

Pathway. *International Journal of Gynaecology*, *25*(6), 953–960. https://doi.org/10.1097/IGC.0000000000000465

Chen, W. H., Horoszewicz, J. S., Leong, S. S., Shimano, T., Penetrante, R., Sanders, W. H., … Chu, T. M. (1982). Human pancreatic adenocarcinoma: In vitro and in vivo morphology of a new tumor line established from ascites. *In Vitro*, *18*(1), 24–34. https://doi.org/10.1007/BF02796382

Chen, Y. W., Hsiao, P. J., Weng, C. C., Kuo, K. K., Kuo, T. L., Wu, D. C., … Cheng, K. H. (2014). SMAD4 Loss triggers the phenotypic changes of pancreatic ductal adenocarcinoma cells. *BMC Cancer*, *14*(1), 1–14. https://doi.org/10.1186/1471-2407-14-181

Christopoulos, A., Christopoulos, G., Morfis, M., Udawela, M., Laburthe, M., Couvineau, A., … Sexton, P. M. (2003). Novel Receptor Partners and Function of Receptor Activity-modifying Proteins *, *278*(5), 3293–3297. https://doi.org/10.1074/jbc.C200629200

Christopoulos, G., Perry, K. J., Morfis, M., Tilakaratne, N., Gao, Y., Fraser, N. J., … Sexton, P. M. (1999). Multiple Amylin Receptors Arise from Receptor Activity- Modifying Protein Interaction with the Calcitonin Receptor Gene Product, *242*, 235–242.

Clark, C. E., Hingorani, S. R., Mick, R., Combs, C., Tuveson, D. A., & Vonderheide, R. H. (2007). Dynamics of the immune reaction to pancreatic cancer from inception to invasion. *Cancer Research*, *67*(19), 9518–9527. https://doi.org/10.1158/0008-5472.CAN-07-0175

Cloyd, J. M., & Poultsides, G. A. (2015). Non-functional neuroendocrine tumors of the pancreas : Advances in diagnosis and management. *World Journal of Gastroenterology*, *21*(32), 9512–9525. https://doi.org/10.3748/wjg.v21.i32.9512

Cockcroft, J. R., Noon, J. P., Gardner-Medwin, J., & Bennett, T. (1997). Haemodynamic effects of adrenomedullin in human resistance and capacitance vessels. *British Journal of Clinical Pharmacology*, *44*(1), 57–60. https://doi.org/10.1046/j.1365-2125.1997.00622.x

Conroy, T., Hammel, P., Hebbar, M., Ben Abdelghani, M., Wei, A. C., Raoul, J. L., … Bachet, J. B.

(2018). FOLFIRINOX or gemcitabine as adjuvant therapy for pancreatic cancer. *New England Journal of Medicine*, *379*(25), 2395–2406. https://doi.org/10.1056/NEJMoa1809775

Conroy, Thierry, Desseigne, F., Ychou, M., Bouché, O., Guimbaud, R., Becouarn, Y., … Ducreux, M. (2011). FOLFIRINOX versus Gemcitabine for Metastatic Pancreatic Cancer. *The New England Journal of Medicine*, *364*(19), 1817–1825.

Costanzo, F. Di, Carlini, P., Doni, L., Massidda, B., Mattioli, R., Iop, A., … Maria, O. G. Di. (2005). Gemcitabine with or without continuous infusion 5-FU in advanced pancreatic cancer : a randomised phase II trial of the Italian oncology group for clinical research (GOIRC). *British Journal of Cancer*, *93*, 185–189. https://doi.org/10.1038/sj.bjc.6602640

Couch, F. J., Johnson, M. R., Rabe, K. G., Brune, K., De Andrade, M., Goggins, M., … Hruban, R. H. (2007). The prevalence of BRCA2 mutations in familial pancreatic cancer. *Cancer Epidemiology Biomarkers and Prevention*, *16*(2), 342–346. https://doi.org/10.1158/1055-9965.EPI-06-0783

Crippa, S., Salvia, R., Warshaw, A. L., Domínguez, I., Bassi, C., Falconi, M., … Castillo, C. F. (2008). Mucinous Cystic Neoplasm of the Pancreas is Not an Aggressive Entity. *Annals of Surgery*, *247*(4), 571–579. https://doi.org/10.1097/sla.0b013e31811f4449

Cunningham, D., Chau, I., Stocken, D., Davies, C., Dunn, J., Valle, J., … Neoptolemos, J. (2005). Phase III randomised comparison of gemcitabine (GEM) versus gemcitabine plus capecitabine (GEM-CAP) in patients with advanced pancreatic cancer. *European Journal of Cancer Supplements*, *3*(4), 2005.

Dackor, R., Fritz-six, K., Smithies, O., & Caron, K. (2007). Receptor Activity-modifying Proteins 2 and 3 Have Distinct Physiological Functions from Embryogenesis to Old Age *. *The Journal of Biological Chemistry*, *282*(25), 18094–18099. https://doi.org/10.1074/jbc.M703544200

Dai, K., Tanaka, M., Kamiyoshi, A., Sakurai, T., Ichikawa-Shindo, Y., Kawate, H., … Shindo, T. (2020). Deficiency of the adrenomedullin-RAMP3 system suppresses metastasis through the

modification of cancer-associated fibroblasts. *Oncogene*, *39*(9), 1914–1930. https://doi.org/10.1038/s41388-019-1112-z

Dai, X., Ma, W., He, X., & Kumar, R. (2013). Elevated expression of adrenomedullin is correlated with prognosis and disease severity in osteosarcoma. *Med Oncology*, *30*. https://doi.org/10.1007/s12032-012-0347-0

Dang, C., Zhang, Y., Ma, Q., & Shimahara, Y. (2006). Expression of nerve growth factor receptors is correlated with progression and prognosis of human pancreatic cancer. *Gastroenterology*, *21*, 850–858. https://doi.org/10.1111/j.1440-1746.2006.04074.x

Dawson, D. W., Hertzer, K., Moro, A., Donald, G., Chang, H.-H., Go, V. L., … Eibl, G. (2013). High Fat, High Calorie Diet Promotes Early Pancreatic Neoplasia in the Conditional KrasG12D Mouse Model. *Cancer Prevention Research*, *6*(10), 1–19. https://doi.org/10.1158/1940-6207.CAPR-13-0065

De La Cruz, M. S. D., Young, A. P., & Ruffin, M. T. (2014). Diagnosis and management of pancreatic cancer. *American Family Physician*, *89*(8), 626–632.

Deng, B., Zhang, S., Miao, Y., Han, Z., Zhang, X., Wen, F., & Zhang, Y. (2012). Adrenomedullin expression in epithelial ovarian cancers and promotes HO8910 cell migration associated with upregulating integrin a 5 b 1 and phosphorylating FAK and paxillin. *Journal of Experimental & Clinical Cancer Research*, *31*(19), 1–9.

Deville, J. L., Bartoli, C., Berenguer, C., Fernandez-Sauze, S., Kaafarani, I., Delfino, C., … Daniel, L. (2009). Expression and role of adrenomedullin in renal tumors and value of its mRNA levels as prognostic factor in clear-cell renal carcinoma. *International Journal of Cancer*, *125*(10), 2307–2315. https://doi.org/10.1002/ijc.24568

Distler, M., Aust, D., Weitz, J., Pilarsky, C., & Grützmann, R. (2014). Precursor lesions for sporadic pancreatic cancer: PanIN, IPMN, and MCN. *BioMed Research International*, *2014*(Figure 2).

https://doi.org/10.1155/2014/474905

Distler, Marius, Kersting, S., Niedergethmann, M., Aust, D. E., Franz, M., & Felix, R. (2013). Pathohistological Subtype Predicts Survival in Patients With Intraductal Papillary Mucinous Neoplasm (IPMN) of. *Annals of Surgery*, *258*, 324–330. https://doi.org/10.1097/SLA.0b013e318287ab73

Dreyer, S. B., Jamieson, N. B., Bailey, P. J., Mckay, C. J., Cancer, P., Initiative, G., … Chang, D. K. (2018). Defining the molecular pathology of pancreatic body and tail adenocarcinoma, 183–191. https://doi.org/10.1002/bjs.10772

Edge, S. B., Byrd, D. R., Compton, C. C., Fritz, A. G., Greene, F. L., & Trotti, A. (2015). *AJCC Cancer Staging Manual. 7th edition*.

El Kamar, F. G., Grossbard, M. L., & Kozuch, P. S. (2003). Metastatic Pancreatic Cancer: Emerging Strategies in Chemotherapy and Palliative Care. *The Oncologist*, *8*(1), 18–34. https://doi.org/10.1634/theoncologist.8-1-18

Faivrea, S., Chan, D., Salinas, R., Woynarowska, B., & Woynarowski, J. M. (2003). DNA strand breaks and apoptosis induced by oxaliplatin in cancer cells. *Biochemical Pharmacology*, *66*(2), 225–237. https://doi.org/https://doi.org/10.1016/S0006-2952(03)00260-0

Fang, Y., Su, Z., Xie, J., Xue, R., Ma, Q., Li, Y., … Shen, B. (2017). Genomic signatures of pancreatic adenosquamous carcinoma (PASC). *Journal of Pathology*, *243*, 155–159. https://doi.org/10.1002/path.4943

Fatima, J. (2010). Pancreatoduodenectomy for Ductal Adenocarcinoma. *Archives of Surgery*, *145*(2), 167. https://doi.org/10.1001/archsurg.2009.282

Ferlay, J., Colombet, M., Soerjomataram, I., Dyba, T., Randi, G., Bettio, M., … Bray, F. (2018). Cancer incidence and mortality patterns in Europe: Estimates for 40 countries and 25 major cancers in 2018. *European Journal of Cancer*, *103*, 356–387. https://doi.org/10.1016/j.ejca.2018.07.005

Fernandez-Sauze, S., Delfino, C., Mabrouk, K., Dussert, C., Chinot, O., Martin, P. M., … Boudouresque, F. (2004). Effects of adrenomedullin on endothelial cells in the multistep process of angiogenesis: Involvement of CRLR/RAMP2 and CRLR/RAMP3 receptors. *International Journal of Cancer*, *108*(6), 797–804. https://doi.org/10.1002/ijc.11663

Flahaut, M., Rossier, B. C., & Firsov, D. (2002). Respective roles of calcitonin receptor-like receptor (CRLR) and receptor activity-modifying proteins (RAMP) in cell surface expression of CRLR/RAMP heterodimeric receptors. *Journal of Biological Chemistry*, *277*(17), 14731–14737. https://doi.org/10.1074/jbc.M112084200

Foord, S. M., Wise, A., Brown, J., Main, M. J., & Fraser, N. J. (1999). The N-terminus of RAMPs is a critical determinant of the glycosylation state and ligand binding of calcitonin receptor-like receptor. *Biochemical Society Transactions*, *27*(4), 535–539.

Francesco, D. A., Claudio, L., Laura, A., Mara, L. R., Paolo, A., & Giovanni, R. (2016). Adrenomedullin in pancreatic carcinoma : A case-control study of 22 patients. *Integrative Cancer Science and Therapeutics*, *3*(2), 390–392. https://doi.org/10.15761/ICST.1000175

Friedlander, S. Y. G., Chu, G. C., Snyder, E. L., Girnius, N., Dibelius, G., Crowley, D., … Jacks, T. (2009). Context-Dependent Transformation of Adult Pancreatic Cells by Oncogenic K-Ras. *Cancer Cell*, *16*(5), 1–21. https://doi.org/10.1016/j.ccr.2009.09.027.Context-Dependent

Fritz-Six, K. L., Dunworth, W. P., Li, M., & Caron, K. M. (2008). Adrenomedullin signaling is necessary for murine lymphatic vascular development. *Journal of Clinical Investigation*, *118*(1), 40–50. https://doi.org/10.1172/JCI33302

Fujita, Y., Mimata, H., Nasu, N., Nomura, T., Nomura, Y., & Nakagawa, M. (2002). Involvement of adrenomedullin induced by hypoxia in angiogenesis in human renal cell carcinoma. *International Journal of Urology*, *9*(6), 285–295. https://doi.org/10.1046/j.1442-2042.2002.00469.x

Fukuda, K., Tsukada, H., Oya, M., Onomura, M., Kodama, M., Nakamura, H., … Seino, Y. (1999). Adrenomedullin promotes epithelial restitution of rat and human gastric mucosa in vitro. *Peptides*, *20*(1), 127–132. https://doi.org/10.1016/S0196-9781(98)00146-6

Garayoa, M., Martínez, A., Lee, S., Pio, R., An, W. G., Neckers, L., … Cuttitta, F. (2000). Hypoxia-inducible factor-1 (HIF-1) up-regulates adrenomedullin expression in human tumor cell lines during oxygen deprivation: a possible promotion mechanism of carcinogenesis. *Molecular Endocrinology*, *14*(6), 848–862. https://doi.org/10.1210/mend.14.6.0473

Giacalone, P., Vuaroqueaux, V., Daure, J., Houafic, L., & Martin, P. (2003). Expression of adrenomedullin in human ovaries , ovarian cysts and cancers Correlation with estrogens receptor status. *European Journal of Obstetrics and Gynecology and Reproducitve Biology*, *110*, 224–229. https://doi.org/10.1016/S0301-2115(03)00186-6

Gonzalez, A. B. De, Sweetland, S., & Spencer, E. (2003). A meta-analysis of obesity and the risk of pancreatic cancer. *British Journal of Cancer*, *89*, 519–523. https://doi.org/10.1038/sj.bjc.6601140

Greillier, L., & Tounsi, A. (2015). Functional Analysis of the Adrenomedullin Pathway in Malignant Pleural Mesothelioma. *Journal of Thoracic Oncology*, *11*(1), 94–107. https://doi.org/10.1016/j.jtho.2015.09.004

Gumusel, B., Chang, J.-K., Hyman, A., & Lippton, H. (1995). Adrenotensin: An ADM gene producit with the opposite effects of ADM. *Pharmacology Letter*, *57*(8), 90–93.

Hackeng, W. M., Hruban, R. H., Offerhaus, G. J. A., & Brosens, L. A. A. (2016). Surgical and molecular pathology of pancreatic neoplasms. *Diagnostic Pathology*, 1–17. https://doi.org/10.1186/s13000-016-0497-z

Hague, S., Zhang, L., Oehler, M. K., Manek, S., Mackenzie, I. Z., Bicknell, R., & Rees, M. C. P. (2000). Expression of the Hypoxically Regulated Angiogenic Factor Adrenomedullin Correlates with

Uterine Leiomyoma Vascular Density 1. *Clinical Cancer Research*, *6*, 2808–2814.

Haigh, P. I., Bilimoria, K. Y., & DiFronzo, A. (2011). Early Postoperative Outcomes After Pancreaticoduodenectomy in the Elderly. *Archives of Surgery*, *146*(6), 715–723.

Hanahan, D., & Weinberg, R. A. (2000). The Hallmarks of Cancer. *Cell*, *100*, 57–70.

Hanahan, D., & Weinberg, R. A. (2011). Hallmarks of cancer: The next generation. *Cell*, *144*(5), 646–674. https://doi.org/10.1016/j.cell.2011.02.013

Hasegawa, K., Suetsugu, A., Nakamura, M., Matsumoto, T., Aoki, H., Kunisada, T., … Hoffman, R. M. (2017). Imaging the role of multinucleate pancreatic cancer cells and cancer-associated fibroblasts in peritoneal metastasis in mouse models. *Anticancer Research*, *37*(7), 3435–3440. https://doi.org/10.21873/anticanreS.11711

Hay, D. L., & Pioszak, A. A. (2016). RAMPs (Receptor-Activity Modyfying Proteins): New Insights and Roles. *Annual Review of Pharmacology and Toxicology*, *56*, 469–487. https://doi.org/10.1016/j.cogdev.2010.08.003.Personal

Hay, D. L., Poyner, D. R., & Sexton, P. M. (2006). GPCR modulation by RAMPs. *Pharmacology and Therapeutics*, *109*, 173–197. https://doi.org/10.1016/j.pharmthera.2005.06.015

Hermann, P. C., Sancho, P., Cañamero, M., Martinelli, P., Madriles, F., Michl, P., … Heeschen, C. (2014). Nicotine Promotes Initiation and Progression of KRAS-Induced Pancreatic Cancer via Gata6-Dependent Dedifferentiation of Acinar Cells in Mice. *Gastroenterology*, *147*(5), 1119-1133.e4. https://doi.org/10.1053/j.gastro.2014.08.002

Hino, M., Nagase, M., Kaname, S., Shibata, S., Nagase, T., Oba, S., … Fujita, T. (2005). Expression and regulation of adrenomedullin in renal glomerular podocytes. *Biochemical and Biophysical Research Communications*, *330*(1), 178–185. https://doi.org/10.1016/j.bbrc.2005.02.142

Hirsch, A. B., McCuen, R. W., Arimura, A., & Schubert, M. L. (2003). Adrenomedullin stimulates

somatostatin and thus inhibits histamine and acid secretion in the fundus of the stomach. *Regulatory Peptides*, *110*(3), 189–195. https://doi.org/10.1016/S0167-0115(02)00208-2

Howes, N., Lerch, M. M., Greenhalf, W., Stocken, D. D., Ellis, I. A. N., Simon, P., … Whitcomb, D. C. (2004). Clinical and Genetic Characteristics of Hereditary Pancreatitis in Europe. *Clinical Gastroenterology and Hepatology*, *3565*(04), 252–261.

Hruban, R. H., Adsay, N. V., Albores-Saavedra, J., Compton, C., Garrett, E. S., Goodman, S. N., … Offerhaus, G. J. A. (2001). Pancreatic intraepithelial neoplasia: A new nomenclature and classification system for pancreatic duct lesions. *American Journal of Surgical Pathology*, *25*(5), 579–586. https://doi.org/10.1097/00000478-200105000-00003

Hsiang, Y. H., & Liu, L. F. (1988). Identification of mammalian dna topoisomerase i as an intracellular target of the anticancer drug camptothecin. *Cancer Research*, *48*(7), 1722–1726.

Hsu, C. P., Hsu, J. Te, Liao, C. H., Kang, S. C., Lin, B. C., Hsu, Y. P., … Hwang, T. L. (2018). Three-year and five-year outcomes of surgical resection for pancreatic ductal adenocarcinoma: Long-term experiences in one medical center. *Asian Journal of Surgery*, *41*(2), 115–123. https://doi.org/10.1016/j.asjsur.2016.11.009

Huggett, M. T., & Pereira, S. P. (2011). Diagnosing and managing pancreatic cancer. *Practitioner*, *255*(1742), 21–23.

Hwang, R. F., Moore, T., Arumugam, T., Ramachandran, V., Amos, K. D., Rivera, A., … Logsdon, C. D. (2008). Cancer-associated stromal fibroblasts promote pancreatic tumor progression. *Cancer Research*, *68*(3), 918–926. https://doi.org/10.1158/0008-5472.CAN-07-5714

Ichikawa-Shindo, Y., Sakurai, T., Kamiyoshi, A., Kawate, H., Iinuma, N., Yoshizawa, T., … Shindo, T. (2008). The GPCR modulator protein RAMP2 is essential for angiogenesis and vascular integrity. *The Journal of Clinical Investigation*, *118*(1), 29–39. https://doi.org/10.1172/JCI33022.in

Iimuro, S., Shindo, T., Moriyama, N., Amaki, T., Niu, P., Takeda, N., … Nagai, R. (2004a). Angiogenic

effects of adrenomedullin in ischemia and tumor growth. *Circulation Research*, *95*(4), 415–423. https://doi.org/10.1161/01.RES.0000138018.61065.d1

Iimuro, S., Shindo, T., Moriyama, N., Amaki, T., Niu, P., Takeda, N., … Nagai, R. (2004b). Angiogenic effects of adrenomedullin in ischemia and tumor growth. *Circulation Research*, *95*(4), 415–423. https://doi.org/10.1161/01.RES.0000138018.61065.d1

Ikeda, N., Adachi, M., Taki, T., Huang, C., Hashida, H., Takabayashi, A., … Kanehiro, H. (1999). Prognostic significance of angiogenesis in human pancreatic cancer. *British Journal of Cancer*, *79*(9/10), 1553–1563.

Iodice, S., Gandini, S., Maisonneuve, P., & Lowenfels, A. B. (2008). Tobacco and the risk of pancreatic cancer : a review and meta-analysis. *Langenbecks Arch Surg*, *393*, 535–545. https://doi.org/10.1007/s00423-007-0266-2

Ishikawa, T., Chen, J., Wang, J., Okada, F., Sugiyama, T., Kobayashi, T., … Kobayashi, M. (2003). Adrenomedullin antagonist suppresses in vivo growth of human pancreatic cancer cells in SCID mice by suppressing angiogenesis. *Oncogene*, *22*(8), 1238–1242. https://doi.org/10.1038/sj.onc.1206207

Ishimitsu, T., Kojima, M., Kangawa, K., Hino, J., Matsuoka, H., Kitamura, K., … Matsuo, H. (1994). Genomic structure of human adrenomedullin gene. *Biochemical and Biophysical Research Communications*, *203*(1), 631–639.

Ishimitsu, T., Nishikimi, T., Saito, Y., Kitamura, K., Eto, T., & Kangawa, K. (1994). Plasma Levels of Adrenomedullin , a Newly Identified Hypotensive Peptide ,. *Journal of Clinical Investigation*, *94*, 2158–2161.

Ishiyama, Y., Kitamura, K., Ichiki, Y., Nakamura, S., Kida, O., Kangawa, K., & Eto, T. (1993). Hemodynamic effects of a novel hypotensive peptide, human adrenomedullin, in rats. *European Journal of Pharmacology*, *241*, 271–273.

Isumi, Y., Kubo, A., Katafuchi, T., Kangawa, K., & Minamino, N. (1999). Adrenomedullin suppresses interleukin-1 L -induced tumor necrosis factor- K production in Swiss 3T3 cells, *463*, 110–114.

Jacobs, E. J., Chanock, S. J., Fuchs, C. S., LaCroix, A., McWillaims, R. R., Steplowski, E., … Zwlwniuch-Jacquotte, A. (2010). Family history of cancer and risk of pancreatic cancer : a pooled analysis from the Pancreatic Cancer Cohort Consortium (PanScan). *International Journal of Cancer*, *127*, 1421–1428. https://doi.org/10.1002/ijc.25148

Jensen, R. T., Mitry, E., Ramage, J. K., Perren, A., & Connor, J. M. O. (2007). Gastrinoma (Duodenal and Pancreatic), *20892*, 173–182. https://doi.org/10.1159/000098009

Jougasaki, M., Chi-Ming, W., Aarhus, L. L., Heublein, D. M., Sandberg, S. M., & Burnett, J. C. (1995). Renal localization and actions a natriuretic peptide of adrenomedullin : *American Journal of Physiology, Renal Physiology*.

Jung, J. G., Lee, K. T., Woo, Y. S., Lee, J. K., Lee, K. H., & Rhee, J. C. (2015). Behavior of Small, Asymptomatic, Nonfunctioning Pancreatic Neuroendocrine Tumors (NF-PNETs). *Medicine*, *94*(26), 1–7. https://doi.org/10.1097/MD.0000000000000983

Kaafarani, I., Fernandez-Sauze, S., Berenguer, C., Chinot, O., Delfino, C., Dussert, C., … Ouafik, L. (2009). Targeting adrenomedullin receptors with systemic delivery of neutralizing antibodies inhibits tumor angiogenesis and suppresses growth of human tumor xenografts in mice. *FASEB Journal*, *23*(10), 3424–3435. https://doi.org/10.1096/fj.08-127852

Kadaba, R., Birke, H., Wang, J., Hooper, S., Andl, C. D., Maggio, D., … Hemant, M. (2013). Imbalance of desmoplastic stromal cell numbers drives aggressive cancer processes. *The Journal of Pathology*, *230*(1), 107–117. https://doi.org/10.1002/path.4172.Imbalance

Kalluri, R. (2016). The biology and function of fibroblasts in cancer. *Nature Reviews Cancer*, *16*, 582–598. https://doi.org/10.1038/nrc.2016.73

Karpinich, N. O., Kechele, D. O., Espenschied, S. T., Willcockson, H. H., Fedoriw, Y., & Caron, K. M.

(2013). Adrenomedullin gene dosage correlates with tumor and lymph node lymphangiogenesis. *FASEB*, *27*(2), 590–600. https://doi.org/10.1096/fj.12-214080

Kayahara, M., Nakagawara, H., & Kitagawa, H. (2007). The Nature of Neural Invasion by Pancreatic Cancer. *Pancreas*, *35*(3), 218–223.

Keleg, S., Kayed, H., Jiang, X., Penzel, R., Giese, T., Büchler, M. W., … Kleeff, J. (2007). Adrenomedullin is induced by hypoxia and enhances pancreatic cancer cell invasion. *International Journal of Cancer*, *121*(1), 21–32. https://doi.org/10.1002/ijc.22596

Kim, W., Moon, S., Sung, M. J., Kim, S. H., Lee, S., So, J., & Park, S. K. (2003). Angiogenic role of adrenomedullin through activation of Akt, mitogen-activated protein kinase, and focal adhesion kinase in endothelial cells. *The FASEB Journal*, *13*(1), 1937–1939.

Kitamura, K., Kangawa, K., Kawamoto, M., Ichiki, Y., Nakamura, S., Matsuo, H., & Eto, T. (1993). Adrenomedullin: A Novel Hypotensive Peptide Isolated from Human Pheochromocytoma. *Biochemical and Biophysical Research Communications*. https://doi.org/10.1006/bbrc.1993.1451

Kitamura, Kazuo, Kato, J., Kawamoto, M., Tanaka, M., Chino, N., Kangawa, K., & Eto, T. (1998). The intermediate form of glycine-extended adrenomedullin is the major circulating molecular form in human plasma. *Biochemical and Biophysical Research Communications*, *244*(2), 551–555. https://doi.org/10.1006/bbrc.1998.8310

Kitamura, Kazuo, Sakata, J., Kangawa, K., Kojima, M., Matsuo, H., & Eto, T. (1993). Cloning and characterisation of cDNA encoding a precursor for human adrenomedullin. *Biochemical and Biophysical Research Communications*, *194*(2), 720–725.

Kitani, M., Asada, Y., Sakata, J., Kitamura, K., Sumiyoshi, A., & Eto, T. (1999). Cell density of adrenomedullin-immunoreactive cells in the gastric endocrine cells decreases in antral atrophic gastritis. *Histopathology*, *34*(2), 134–139. https://doi.org/10.1046/j.1365-2559.1999.00573.x

Kleeff, J., & Korc, M. (1998). Up-regulation of transforming growth factor (TGF)-β receptors by TGF-β1 in COLO-357 cells. *Journal of Biological Chemistry*, *273*(13), 7495–7500. https://doi.org/10.1074/jbc.273.13.7495

Kocemba, K. A., Andel, H. Van, Mahtouk, K., Versteeg, R., Kersten, M. J., Spaargaren, M., & Pals, S. T. (2013). The hypoxia target adrenomedullin is aberrantly expressed in multiple myeloma and promotes angiogenesis. *Leukemia*, *27*(8), 1729–1737. https://doi.org/10.1038/leu.2013.76

Kommalapati, A., Tella, S. H., Goyal, G., Ma, W. W., & Mahipal, A. (2018). Contemporary management of localized resectable pancreatic cancer. *Cancers*, *10*(1), 1–15. https://doi.org/10.3390/cancers10010024

Koong, A. C., Mehta, V. K., Le, Q. T., Fisher, G. A., Terris, D. J., Brown, J. M., … Vierra, M. (2000). Pancreatic tumors show high levels of hypoxia. *International Journal of Radiation Oncology Biology Physics*, *48*(4), 919–922. https://doi.org/10.1016/S0360-3016(00)00803-8

Kopantzev, E. P., Kopantseva, M. R., Grankina, E. V., Mikaelyan, A., Egorov, V. I., & Sverdlov, E. D. (2019). Activation of IGF/IGF-IR signaling pathway fails to induce epithelial-mesenchymal transition in pancreatic cancer cells. *Pancreatology*, *19*(2), 390–396. https://doi.org/10.1016/j.pan.2019.01.010

Kozlova, A. A., Verkhovskii, R. A., Ermakov, A. V, & Bratashov, D. N. (2020). Changes in Autofluorescence Level of Live and Dead Cells for Mouse Cell Lines. *Journal of Fluorescence*, *30*, 1483–1489.

Kubo, A., Minamino, N., Isumi, Y., Katafuchi, T., Kangawa, K., Dohi, K., & Matsuo, H. (1998). Production of adrenomedullin in macrophage cell line and peritoneal macrophage. *Journal of Biological Chemistry*, *273*(27), 16730–16738. https://doi.org/10.1074/jbc.273.27.16730

Larsson, S. C., Orsini, N., & Wolk, A. (2007). Body mass index and pancreatic cancer risk : A meta-analysis of prospective studies. *International Journal of Cancer*, *120*, 1993–1998.

https://doi.org/10.1002/ijc.22535

Lenhart, P. M., Broselid, S., Barrick, C. J., Leeb-Lundberg, F., & Caron, K. M. (2013). G-potein Coupled Receptor 30 Interacts with Receptor Activity Modifying protein 3 and Confers Sex-Dependent Cardioprotection. *Journal of Molecular Endocrinology*, *51*(1), 191–202. https://doi.org/10.1530/JME-13-0021.G-protein

Leung, J., & Silverman, W. (2009). Diagnostic and Therapeutic Approach to Pancreatic Cancer-Associated Gastroparesis. *Digestive Diseases and Sciences*, *54*, 401–405. https://doi.org/10.1007/s10620-008-0354-3

Li, C., Cui, L., Yang, L., Wang, B., & Zhuo, Y. (2020). Pancreatic Stellate Cells Promote Tumor Progression by Promoting an Immunosuppressive Microenvironment in Murine Models of Pancreatic Cancer. *Pancreas*, *49*(1), 120–127. https://doi.org/10.1097/MPA.0000000000001464

Li, D., Morris, J. S., Liu, J., Hassan, M. M., Day, R. S., Bondy, M. L., & Abbruzzese, J. L. (2009). Body Mass Index and Risk, Age of Onset, and Survival in Patients With Pancreatic Cancer. *Journal of American Medical Association*, *301*(24), 2553–2562. https://doi.org/10.1001/jama.2009.886.Body

Li, F., Yang, R., Zhang, X., Liu, A., Zhao, Y., & Guo, Y. (2014). Silencing of hypoxia-inducible adrenomedullin using RNA interference attenuates hepatocellular carcinoma cell growth in vivo. *Molecular Medicine Reports*, *10*(3), 1295–1302. https://doi.org/10.3892/mmr.2014.2320

Li, M., Yee, D., Magnuson, T. R., Smithies, O., & Caron, K. M. (2006). Reduced maternal expression of adrenomedullin disrupts fertility , placentation , and fetal growth in mice. *The Journal of Clinical Investigation*, *116*(10). https://doi.org/10.1172/JCI28462.into

Li, X., Wang, Z., Ma, Q., Xu, Q., Liu, H., Duan, W., … Ma, J. (2014). Sonic Hedgehog Paracrine Signaling Activates Stromal Cells to Promote Perineural Invasion in Pancreatic Cancer. *Clinical Cancer*

Research, *20*(16). https://doi.org/10.1158/1078-0432.CCR-13-3426

Li, Z., Takeuchi, S., Ohara, N., & Maruo, T. (2003). Paradoxically abundant expression of Bcl-2 and adrenomedullin in invasive cervical squamous carcinoma. *International Journal of Clinical Oncology*, *8*(2), 83–89. https://doi.org/10.1007/s101470300015

Liebl, F., Demir, I. E., Mayer, K., Schuster, T., D'Haese, J. G., Becker, K., … Ceyhan, G. O. (2014). The Impact of Neural Invasion Severity in Gastrointestinal Malignancies. *Annals of Surgery*, *260*(5), 900–908. https://doi.org/10.1097/SLA.0000000000000968

Lim, S. Y., Ahn, S., Park, H., Lee, J., Choi, K., Choi, C., … Choi, Y. (2014). Transcriptional regulation of adrenomedullin by oncostatin M in human astroglioma cells : Implications for tumor invasion and migration, 1–7. https://doi.org/10.1038/srep06444

Liu, A., Zhang, X., Li, F., Zhao, Y.-L., Guo, Y., & Yang, R. (2013). RNA interference targeting adrenomedullin induces apoptosis and reduces the growth of human bladder urothelial cell carcinoma. *Medical Oncology*, *30*(616), 1–9. https://doi.org/10.1007/s12032-013-0616-6

Lv, Y., Peng, L., Wang, Q., Chen, N., Teng, Y., Wang, T., … Zhuang, Y. (2018). Degranulation of mast cells induced by gastric cancer-derived adrenomedullin prompts gastric cancer progression, 1–12. https://doi.org/10.1038/s41419-018-1100-1

Lynch, S. M., Vrieling, A., Lubin, J. H., Kraft, P., Mendelsohn, J. B., Hartge, P., … Stolzenberg-solomon, R. Z. (2009). Meta- and Pooled Analyses Cigarette Smoking and Pancreatic Cancer : A Pooled Analysis From the Pancreatic Cancer Cohort Consortium. *American Journal of Epidemiology*, *170*(4), 403–413. https://doi.org/10.1093/aje/kwp134

Mahata, M., Mahata, S. K., Parmer, R. J., & Connor, D. T. O. (1998). Proadrenomedullin N-Terminal 20 Peptide. Minimal Active Region to Regulate Nicotinic Receptors. *Hypertension*.

Man, D., Wu, J., Shen, Z., & Zhu, X. (2018). Prognosis of patients with neuroendocrine tumor : a SEER database analysis. *Cancer Managment and Research*, *10*, 5629–5638.

Manfredi, J. J., & Horwitz, S. B. (1984). TAXOL: AN ANTIMITOTIC AGENT WITH A NEW MECHANISM OF ACTION. *Pharmacology and Therapeutics*, *25*, 83–125. https://doi.org/10.1016/j.nucmedbio.2011.06.001

Manohar, M., Verma, A. K., Venkateshaiah, S. U., & Mishra, A. (2017). Significance of Eosinophils in Promoting Pancreatic malignancy. *Jounral of Gastroenterology, Pancreatology and Liver Disorders*, *5*(1).

Martínez-Herrero, S., & Martínez, A. (2016). Adrenomedullin regulates intestinal physiology and pathophysiology. *Domestic Animal Endocrinology*, *56*, S66–S83. https://doi.org/10.1016/j.domaniend.2016.02.004

Martínez-Herrero, Sonia, & Martínez, A. (2013). Cancer Protection Elicited by a Single Nucleotide Polymorphism Close to the Adrenomedullin Gene. *The Journal of Clinical Endocrinology and Metabolism*, *98*(4), 807–810. https://doi.org/10.1210/jc.2012-4193

Martinez, A., Kapas, S., Miller, M.-J., Ward, Y., & Cuttitta, F. (2000). Coexpression of Receptors for Adrenomedullin, Calcitonin Gene-Related Peptide, and Amylin in Pancreatic beta-Cells. *Endocrinology*, *141*(1), 406–411.

Martinez, A., Lopez, J., Bhathena, S. J., Elsasser, T. H., Miller, M.-J., Moody, T. W., … Cuttitta, F. (1996). Regulation of Insulin Secretion and Blood Glucose Metabolism by Adrenomedullin. *Endocrinology*, *137*(6), 2626–2632. Retrieved from https://academic.oup.com/endo/article-abstract/137/6/2626/3037563

Martinez, A., Vos, M., Guedez, L., Kaur, G., Chen, Z., Garayoa, M., … Cuttitta, F. (2002). The Effects of Adrenomedullin Overexpression in Breast Tumor Cells. *Journal of the National Cancer Institute*, *94*(16), 1226–1237. https://doi.org/10.1093/jnci/94.16.1226

Martínez, A., Vos, M., Guédez, L., Kaur, G., Chen, Z., Garayoa, M., … Cuttitta, F. (n.d.). *The Effects of Adrenomedullin Overexpression in Breast Tumor Cells*. Retrieved from

https://academic.oup.com/jnci/article-abstract/94/16/1226/2912269

Masamune, A., Kikuta, K., Watanabe, T., Satoh, K., Hirota, M., & Shimosegawa, T. (2008). Hypoxia stimulates pancreatic stellate cells to induce fibrosis and angiogenesis in pancreatic cancer. *American Journal of Physiology - Gastrointestinal and Liver Physiology*, *295*(4), 709–717. https://doi.org/10.1152/ajpgi.90356.2008

McLatchie, L. M., Fraser, N. J., Main, M. J., Wise, A., Brown, J., Thompson, N., … Foord, S. M. (1998). RAMPS regulate the transport and ligand specificity of the calcitonin- receptor-like receptor. *Nature*. https://doi.org/10.1038/30666

Meeran, K., O'Shea, D., Upton, P. D., Small, C. J., Ghatei, M. A., Byfield, P. H., & Bloom, S. R. (1997). Circulating adrenomedullin does not regulate systemic blood pressure but increases plasma prolactin after intravenous infusion in humans: A pharmacokinetic study. *Journal of Clinical Endocrinology and Metabolism*, *82*(1), 95–100. https://doi.org/10.1210/jc.82.1.95

Melis, M., Marcon, F., Masi, A., Pinna, A., Sarpel, U., Miller, G., … Newman, E. (2012). The safety of a pancreaticoduodenectomy in patients older than 80 years : risk vs . benefits. *HPB*, *14*, 583–588. https://doi.org/10.1111/j.1477-2574.2012.00484.x

Meyer-ficca, M. L., Meyer, R. G., Kaiser, H., Brack, A. R., Kandolf, R., & Küpper, J. (2004). Comparative analysis of inducible expression systems in transient transfection studies. *Analytical Biochemistry*, *334*, 9–19. https://doi.org/10.1016/j.ab.2004.07.011

Meyrath, M., Palmer, C. B., Reynders, N., Vanderplasschen, A., Ollert, M., Bouvier, M., … Chevigné, A. (2021). Proadrenomedullin N - Terminal 20 Peptides (PAMPs) Are Agonists of the Chemokine Scavenger Receptor ACKR3/CXCR7. *ACS Pharmacology and Translational Science*, *4*, 813–823. https://doi.org/10.1021/acsptsci.1c00006

Michelsen, J., Thiesson, H., Walter, S., Ottosen, P. D., Skøtt, O., & Jensen, B. L. (2006). Tissue expression and plasma levels of adrenomedullin in renal cancer patients. *Clinical Science*, *70*,

61–70. https://doi.org/10.1042/CS20060030

Mimura, T., Masuda, A., Matsumoto, I., Shiomi, H., Yoshida, S., Sugimoto, M., … Azuma, T. (2010). Predictors of Malignant Intraductal Papillary Mucinous Neoplasm of the Pancreas. *Journal of Clinical Gastroenterology*, *44*(9), 224–229.

Minami, F., Sasaki, N., Shichi, Y., Gomi, F., Michishita, M., Ohkusu-Tsukada, K., … Ishiwata, T. (2021). Morphofunctional analysis of human pancreatic cancer cell lines in 2- and 3-dimensional cultures. *Nature Scientific Reports*, *11*(1), 1–10. https://doi.org/10.1038/s41598-021-86028-1

Minegishi, T., Nakamura, M., Abe, K., Tano, M., Andoh, A., Yoshida, M., … Kangawa, K. (1999). Adrenomedullin and atrial natriuretic peptide concentrations in normal pregnancy and pre-eclampsia. *Molecular Human Reproduction*, *5*(8), 767–770. https://doi.org/10.1093/molehr/5.8.767

Miwa, M., Ura, M., Nishida, M., Sawada, N., Ishikawa, T., Mori, K., … Ishitsuka, H. (1998). Design of a novel oral fluoropyrimidine carbamate, capecitabine, which generates 5 fluorouracil selectively in tumours by enzymes concentrated in human liver and cancer tissue. *European Journal of Cancer*, *34*(8), 1274–1281. https://doi.org/10.1016/S0959-8049(98)00058-6

Moran, R. G., & Keyomars, K. (1987). Biochemical Rationale for the Synergism of 5-fluorouracil and Folinic Acid. *NCI Monographs*, *5*, 159–163.

Morton, J. P., Timpson, P., Karim, S. A., Ridgway, R. A., Athineos, D., Doyle, B., … Sansom, O. J. (2010). Mutant p53 drives metastasis and overcomes growth arrest/senescence in pancreatic cancer. *Proceedings of the National Academy of Sciences of the United States of America*, *107*(1), 246–251. https://doi.org/10.1073/pnas.0908428107

Muniraj, T., Uk, M., Vignesh, S., Shetty, S., Thiruvengadam, S., & Aslanian, H. R. (2013). Pancreatic neuroendocrine tumors. *Disease-a-Month*, *59*(1), 5–19. https://doi.org/10.1016/j.disamonth.2012.10.002

Myoteri, D., Dellaportas, D., Lykoudis, P. M., Apostolopoulos, A., Marinis, A., & Zizi-sermpetzoglou, A. (2017). Prognostic Evaluation of Vimentin Expression in Correlation with Ki67 and CD44 in Surgically Resected Pancreatic Ductal Adenocarcinoma. *Gastroenterology Research and Practice*. https://doi.org/10.1155/2017/9207616

Nash, K. L., & Lever, A. M. L. (2004). Green fluorescent protein : green cells do not always indicate gene expression. *Gene Therapy*, *11*, 882–883. https://doi.org/10.1038/sj.gt.3302246

Neoptolemos, J. P., Stocken, D. D., Bassi, C., Ghaneh, P., Cunningham, D., Goldstein, D., … Büchler, M. W. (2010). Adjuvant Chemotherapy With Fluorouracil Plus Folinic Acid vs Gemcitabine Following Pancreatic Cancer Resection. *Journal of the American Medical Association*, *304*(10), 1073–1081.

Niedergethmann, M., Hildenbrand, R., Wostbrock, B., Hartel, M., Sturm, J. W., Richter, A., & Post, S. (2002). High Expression of Vascular Endothelial Growth Factor Predicts Early Recurrence and Poor Prognosis after Curative Resection for Ductal Adenocarcinoma of the Pancreas. *Pancreas*, *25*(2), 122–129. https://doi.org/10.1097/01.MPA.0000015372.82709.EE

Nishikimi, T. (2007). Adrenomedullin in the Kidney-Renal Physiological and Pathophysiological Roles. *Current Medicinal Chemistry*, *14*(15), 1689–1699. https://doi.org/10.2174/092986707780830943

Nishimatsu, H., Suzuki, E., Nagata, D., Moriyama, N., Satonaka, H., Walsh, K., … Goto, A. (2001). Vasorelaxation via the Phosphatidylinositol 3-Kinase / Akt – Dependent Pathway in Rat Aorta. *Circulation Research*, 63–70.

Nouguerède, E., Berenguer, C., Garcia, S., Bennani, B., Delfino, C., Nanni, I., … Ouafik, L. (2013). Expression of adrenomedullin in human colorectal tumors and its role in cell growth and invasion in vitro and in xenograft growth in vivo. *Cancer Medicine*, *2*(2), 196–207. https://doi.org/10.1002/cam4.51

Oehler, M. K., Fischer, D. C., Orlowska-Volk, M., Herrle, F., Kieback, D. G., Rees, M., & Bicknell, R. (2003). Tissue and plasma expression of the angiogenic peptide adrenomedullin in breast cancer. *British Journal of Cancer*, *89*(10), 1927–1933. https://doi.org/10.1038/sj.bjc.6601397

Oehler, M. K., Norbury, C., Hague, S., Rees, M. C. P., & Bicknell, R. (2001). Adrenomedullin inhibits hypoxic cell death by upregulation of Bcl-2 in endometrial cancer cells: A possible promotion mechanism for tumour growth. *Oncogene*, *20*(23), 2937–2945. https://doi.org/10.1038/sj.onc.1204422

Oehler, Martin K., Hague, S., Rees, M. C. P., & Bicknell, R. (2002). Adrenomedullin promotes formation of xenografted endometrial tumors by stimulation of autocrine growth and angiogenesis. *Oncogene*, *21*(18), 2815–2821. https://doi.org/10.1038/sj/onc/1205374

Okumura, H., Nagaya, N., Itoh, T., Okano, I., Hino, J., Mori, K., … Kangawa, K. (2004). Adrenomedullin Infusion Attenuates Myocardial Ischemia/Reperfusion Injury Through the Phosphatidylinositol 3-Kinase/Akt-Dependent Pathway. *Circulation*, *109*(2), 242–248. https://doi.org/10.1161/01.CIR.0000109214.30211.7C

Okusaka, T., Okada, S., Ueno, H., Ikeda, M., Shimada, K., Yamamoto, J., … Sakamoto, M. (2001). Abdominal Pain in Patients with Resectable Pancreatic Cancer with Reference to Clinicopathologic Findings. *Pancreas*, *22*(3), 279–284.

Olsson, M., & Zhivotovsky, B. (2011). Caspases and cancer. *Cell Death and Differentiation*, *18*, 1441–1449. https://doi.org/10.1038/cdd.2011.30

Orth, M., Metzger, P., Gerum, S., Mayerle, J., Schneider, G., Belka, C., … Lauber, K. (2019). Pancreatic ductal adenocarcinoma: Biological hallmarks, current status, and future perspectives of combined modality treatment approaches. *Radiation Oncology*, *14*(1), 1–20. https://doi.org/10.1186/s13014-019-1345-6

Ouafik, L., Berenguer-daize, C., & Berthois, Y. (2009). Adrenomedullin promotes cell cycle transit and

up-regulates cyclin D1 protein level in human glioblastoma cells through the activation of c-Jun / JNK / AP-1 signal transduction pathway. *Cellular Signalling*, *21*, 597–608. https://doi.org/10.1016/j.cellsig.2009.01.001

Ouafik, L. H., Sauze, S., Delfino, C., Vuaroqueaux, V., Dussert, C., Palmari, J., & Dufour, H. (2002). Neutralization of Adrenomedullin Inhibits the Growth of Human Glioblastoma Cell Lines in Vitro and Suppresses Tumor Xenograft Growth in Vivo. *American Journal of Pathology*, *160*(4), 1279–1292.

Oulidi, A., Bokhobza, A., Gkika, D., Vanden Abeele, F., Lehen'kyi, V., Ouafik, L., … Prevarskaya, N. (2013). TRPV2 Mediates Adrenomedullin Stimulation of Prostate and Urothelial Cancer Cell Adhesion, Migration and Invasion. *PLoS ONE*, *8*(5), 1–7. https://doi.org/10.1371/journal.pone.0064885

Pan, F. C., & Wright, C. (2011). Pancreas organogenesis: From bud to plexus to gland. *Developmental Dynamics*, *240*(3), 530–565. https://doi.org/10.1002/dvdy.22584

Pang, X., Shang, H., Deng, B., Wen, F., & Zhang, Y. (2013). The interaction of adrenomedullin and macrophages induces ovarian cancer cell migration via activation of RhoA signaling pathway. *International Journal of Molecular Sciences*, *14*(2), 2774–2787. https://doi.org/10.3390/ijms14022774

Park, C.-S., Yoon, J., Lee, J., Jong, S., Jung, S., Kim, W., … Lee, H. (2008). Hypoxia-inducible adrenomedullin accelerates hepatocellular carcinoma cell growth. *Cancer Letters*, *271*(2), 314–322. https://doi.org/10.1016/j.canlet.2008.06.019

Passaglia, P., Gonzaga, N. A., Tirapelli, D. P. C., Tirapelli, L. F., & Tirapelli, C. R. (2014). Pharmacological characterisation of the mechanisms underlying the relaxant effect of adrenomedullin in the rat carotid artery. *The Journal of Pharmacy and Pharmacology*, *66*(12), 1734–1746. https://doi.org/10.1111/jphp.12299

Pereira, S. P., Health, D., Oldfield, L., Medicine, C. C., Ney, A., Health, D., … Angeles, L. (2020). Early detection of pancreatic cancer. *Lancet Gastroenterol Hepatol*, *5*(7), 698–710. https://doi.org/10.1016/S2468-1253(19)30416-9.Early

Perysinakis, I., Margaris, I., & Kouraklis, G. (2014). Ampullary cancer – a separate clinical entity ? *Histopathology*, *64*, 759–768. https://doi.org/10.1111/his.12324

Pío, R., Martínez, A., & Cuttitta, F. (2001). Cancer and diabetes: Two pathological conditions in which adrenomedullin may be involved. *Peptides*, *22*(11), 1719–1729. https://doi.org/10.1016/S0196-9781(01)00530-7

Pío, R., Martínez, A., Unsworth, E. J., Kowalak, J. A., Bengoechea, J. A., Zipfel, P. F., … Cuttitta, F. (2001). Complement Factor H Is a Serum-binding Protein for Adrenomedullin, and the Resulting Complex Modulates the Bioactivities of Both Partners. *Journal of Biological Chemistry*, *276*(15), 12292–12300. https://doi.org/10.1074/jbc.M007822200

Plunkett, W., Huang, P., Xu, Y. Z., Heinemann, V., Grunewald, R., & Gandhi, V. (1995). Gemcitabine: Metabolism, Mechanisms of Action, and Self-Potentiation. *Seminars in Oncology*, *22*(11), 3–10. Retrieved from https://pubmed.ncbi.nlm.nih.gov/7481842/

Porta, M., Fabregat, X., Malats, N., Guarner, L., Carrato, A., Miguel, A. De, … Real, F. X. (2005). Exocrine pancreatic cancer : symptoms at presentation and their relation to tumour site and stage. *Clinical and Translational Oncology*, *7*(November 2004), 189–197.

Procacci, P., Moscheni, C., Sartori, P., Sommariva, M., & Gagliano, N. (2018). Tumor–stroma cross-talk in human pancreatic ductal adenocarcinoma: A focus on the effect of the extracellular matrix on tumor cell phenotype and invasive potential. *Cells*, *7*(10), 1. – 12 of 12. https://doi.org/10.3390/cells7100158

Promega. (2016). *RealTime-Glo ™ MT Cell Viability Assay*.

Promega. (2019). *Caspase-Glo ® 3/7 Assay*.

Provenzano, P. P., Cuevas, C., Chang, A. E., Goel, V. K., Von Hoff, D. D., & R, H. S. (2012). Enzymatic targetting of the stroma ablates physical barriers to treatment of pancreatic ductal adenocarcinoma. *Cancer Cell*, *21*(3), 418–429. https://doi.org/10.1016/j.ccr.2012.01.007.Enzymatic

Qiao, F., Fang, J., Xu, J., Zhao, W., Ni, Y., & Andreas, B. (2017). The role of adrenomedullin in the pathogenesis of gastric cancer. *Oncotarget*, *8*(51), 88464–88474. https://doi.org/10.18632/oncotarget.18881

Rahib, L., Smith, B. D., Aizenberg, R., Rosenzweig, A. B., Fleshman, J. M., & Matrisian, L. M. (2014). Projecting cancer incidence and deaths to 2030: The unexpected burden of thyroid, liver, and pancreas cancers in the united states. *Cancer Research*, *74*(11), 2913–2921. https://doi.org/10.1158/0008-5472.CAN-14-0155

Ramachandran, V., Arumugam, T., Hwang, R. F., Greenson, J. K., Simeone, D. M., & Logsdon, C. D. (2007). Adrenomedullin is expressed in pancreatic cancer and stimulates cell proliferation and invasion in an autocrine manner via the adrenomedullin receptor, ADMR. *Cancer Research*, *67*(6), 2666–2675. https://doi.org/10.1158/0008-5472.CAN-06-3362

Ramachandran, V., Arumugam, T., Langley, R., Hwang, R. F., Sood, A. K., Lopez-berestein, G., & Logsdon, C. D. (2009). The ADMR Receptor Mediates the Effects of Adrenomedullin on Pancreatic Cancer Cells and on Cells of the Tumor Microenvironment, *4*(10). https://doi.org/10.1371/journal.pone.0007502

Rawla, P., Sunkara, T., & Gaduputi, V. (2019). Epidemiology of Pancreatic Cancer: Global Trends, Etiology and Risk Factors. *World Journal of Oncology*, *10*(1), 10–27. https://doi.org/10.14740/wjon1166

Regine, W. F., Winter, K. A., Abrams, R. A., Safran, H., Hoffman, J. P., Konski, A., … Rich, T. A. (2008). Fluorouracil vs gemcitabine chemotherapy before and after fluorouracil-based chemoradiation

following resection of pancreatic adenocarcinoma: A randomized controlled trial. *Journal of the American Medical Association*, *299*(9), 1019–1026. https://doi.org/10.1001/jama.299.9.1019

Riveiro, M. E., Berenguer-daize, C., Kane, A. O., & Oua, L. H. (2021). Targeting Adrenomedullin in Oncology : A Feasible Strategy With Potential as Much More Than an Alternative Anti-Angiogenic Therapy. *Frontiers in Oncology*, *10*(January), 1–23. https://doi.org/10.3389/fonc.2020.589218

Rocchi, P., Zamora, A. J., Muracciole, X., Lechevallier, E., Martin, P., & Ouafik, L. H. (2001). Expression of Adrenomedullin and Peptide Amidation Activity in Human Prostate Cancer and in Human Prostate Cancer Cell Lines. *Cancer Research*, *61*, 1196–1206.

Rossowski, W. J., Jiang, N. Y., & Coy, D. H. (1997). Adrenomedullin, amylin, calcitonin gene-related peptide and their fragments are potent inhibitors of gastric acid secretion in rats. *European Journal of Pharmacology*, *336*(1), 51–63. https://doi.org/10.1016/S0014-2999(97)01252-1

Roy, P. K., Venzon, D. J., Shojamanesh, H., Abou-Saif, A., Peghini, P., Doppman, J. L., … Jensen, R. T. (2000). Zollinger-Ellison Syndrome- Clinical Presentation in 261 patients. *Medicine*, *79*, 379–411.

Ryu, T. Y., Park, J., & Scherer, P. E. (2014). Hyperglycemia as a Risk Factor for Cancer Progression, 330–336.

Sakata, J., Asada, Y., Shimokubo, T., Kitani, M., Inatsu, H., Kitamura, K., … Eto, T. (1998). Adrenomedullin in the gastrointestinal tract. Distribution and gene expression in rat and augmented gastric adrenomedullin after fasting. *Journal of Gastroenterology*, *33*(6), 828–834. https://doi.org/10.1007/s005350050183

Salomone, S., Caruso, A., Cutuli, V. M., Mangano, N. G., Prato, A., Amico-Roxas, M., … Clementi, G. (2003). Effects of adrenomedullin on the contraction of gastric arteries during reserpine-induced gastric ulcer. *Peptides*, *24*(1), 117–122. https://doi.org/10.1016/S0196-9781(02)00283-

Sanabria Mateos, R., & Conlon, K. C. (2016). Pancreatic cancer. *Surgery*, *34*(6), 282–291. https://doi.org/10.1016/j.mpsur.2016.03.011

Sanford, D. E., Belt, B. A., Panni, R. Z., Mayer, A., Deshpande, A. D., Carpenter, D., … Linehan, D. C. (2013). Inflammatory Monocyte Mobilization Decreases Patient Survival in Pancreatic Cancer : A Role for Targeting the CCL2 / CCR2 Axis. *Human Cancer Biology*, *19*(7), 3404–3416. https://doi.org/10.1158/1078-0432.CCR-13-0525

Santi, D. V., McHenry, C. S., & Sommer, H. (1974). Mechanism of Interaction of Thymidylate Synthetase with 5-Fluorodeoxyuridylate. *Biochemistry*, *13*(3), 471–481. https://doi.org/10.1021/bi00700a012

Sassone-Corsi, P. (2012). The Cyclic AMP pathway. *Cold Spring Harbor Perspectives in Biology*, *4*(12), 3–5. https://doi.org/10.1101/cshperspect.a011148

Scheithauer, W., Schüll, B., Schmid, K., Raderer, M., Haider, K., Kwasny, W., … Kornek, G. V. (2003). Original article Biweekly high-dose gemcitabine alone or in combination with capecitabine in patients with metastatic pancreatic adenocarcinoma : a randomized phase II trial. *Annals of Oncology*, *14*(1), 97–104. https://doi.org/10.1093/annonc/mdg029

Schniewind, B., Christgen, M., Kurdow, R., Haye, S., Kremer, B., & Kalthoff, H. (2004). RESISTANCE OF PANCREATIC CANCER TO GEMCITABINE TREATMENT IS DEPENDENT ON MITOCHONDRIA-MEDIATED APOPTOSIS. *International Journal of Cancer*, *109*, 182–188. https://doi.org/10.1002/ijc.11679

Schönauer, R., Els-Heindl, S., & Beck-Sickinger, A. G. (2017). Adrenomedullin – new perspectives of a potent peptide hormone. *Journal of Peptide Science*, *23*(7–8), 472–485. https://doi.org/10.1002/psc.2953

Schoumacher, R. A., Ram, J., Iannuzzi, M. C., Bradbury, N. A., Wallace, R. W., Hon, C. T., … Frizzell, R.

A. (1990). A cystic fibrosis pancreatic adenocarcinoma cell line. *Proceedings of the National Academy of Sciences of the United States of America*, *87*(10), 4012–4016. https://doi.org/10.1073/pnas.87.10.4012

Serafin, D. S., Harris, N. R., Nielsen, N. R., Mackie, D. I., & Caron, K. M. (2020). Dawn of a New RAMPage. *Trends in Pharmacological Sciences*, *41*(4), 249–265. https://doi.org/10.1016/j.tips.2020.01.009

Shi, X., Liu, S., Kleeff, J., Friess, H., & Büchler, M. W. (2002). Acquired Resistance of Pancreatic Cancer Cells towards 5-Fluorouracil and Gemcitabine Is Associated with Altered Expression of Apoptosis-Regulating Genes. *Oncology*, *62*, 354–362.

Shi, Y., He, Z., Jia, Z., & Xu, C. (2016). Inhibitory effect of metformin combined with gemcitabine on pancreatic cancer cells in vitro and in vivo. *Molecular Medicine Reports*, *14*(4), 2921–2928. https://doi.org/10.3892/mmr.2016.5592

Shimekake, Y., Nagata, K., Shigeki, O., Kambayashi, Y., Teraoka, H., Kitamura, K., … Matsuo, H. (1995). Adrenomedullin Stimulates Two Signal Transduction Pathways, cAMP Accumulation and Ca2+ Mobilisation, in Boving Aortic Endothelial Cells. *The Journal of Biological Chemistry*, *9*(3), 4412–4417.

Shindo, T., Kurihara, Y., Nishimatsu, H., Moriyama, N., Kakoki, M., Wang, Y., … Kurihara, H. (2001). Vascular Abnormalities and Elevated Blood Pressure in Mice Lacking Adrenomedullin Gene. *Circulation*, *104*, 1964–1971.

Siclari, V. A., Mohammad, K. S., Tompkins, D. R., Davis, H., Mckenna, C. R., Peng, X., … Chirgwin, J. M. (2014). Tumor-expressed adrenomedullin accelerates breast cancer bone metastasis, 1–14. https://doi.org/10.1186/s13058-014-0458-y

Siegel, R. L., Miller, K. D., & Jemal, A. (2018). Cancer statistics, 2018. *CA: A Cancer Journal for Clinicians*, *68*(1), 7–30. https://doi.org/10.3322/caac.21442

Simone, C. G., Toro, T. Z., Chan, E., Feely, M. M., Trevino, J. G., & George, T. J. (2013). Characteristics and Outcomes of Adenosquamous Carcinoma of the Pancreas. *Gastrointestinal Cancer Research*, (June), 75–79.

Smeenk, H. G., Incrocci, L., Kazemier, G., van Dekken, H., Tran, K. T. C., Jeekel, J., & van Eijck, C. H. J. (2005). Adjuvant 5-FU-Based Chemoradiotherapy for Patients Undergoing R-1/R-2 Resections for Pancreatic Cancer. *Digestive Surgery*, *22*(5), 321–328. https://doi.org/10.1159/000089250

Sobin, L., Gospodarowicz, M., & Wittekind, C. (2009). *TNM Classification of Malignant Tumours*. *UICC* (7th ed.). Wiley-Blackwell.

Sommerville, C. A. M., Limongelli, P., Pai, M., Ahmad, R., Stamp, G., Habib, N. A., … Jiao, L. R. (2009). Survival Analysis After Pancreatic Resection for Ampullary and Pancreatic Head Carcinoma : An Analysis of Clinicopathological Factors. *Journal of Surgical Oncology*, *100*, 651–656. https://doi.org/10.1002/jso.21390

Spear, S., Candido, J. B., Mcdermott, J. R., Ghirelli, C., Maniati, E., Beers, S. A., … Capasso, M. (2019). Discrepancies in the Tumor Microenvironment of Spontaneous and Orthotopic Murine Models of Pancreatic Cancer Uncover a New Immunostimulatory Phenotype for B Cells. *Frontiers in Immunology*, *10*, 1–18. https://doi.org/10.3389/fimmu.2019.00542

Steiner, S., Muff, R., Gujer, R., Fischer, J. A., & Born, W. (2002). The Transmembrane Domain of Receptor-Activity-Modifying Protein 1 Is Essential for the Functional Expression of a Calcitonin Gene-Related Peptide Receptor †, 11398–11404. https://doi.org/10.1021/bi020279r

Stopczynski, R. E., Normolle, D. P., Hartman, D. J., Ying, H., DeBerry, J. J., Bielefeldt, K., … Davis, B. M. (2014). Neuroplastic changes occur early in the development of pancreatic ductal adenocarcinoma. *Cancer Research*, *74*(6), 1718–1727. https://doi.org/10.1158/0008-5472.CAN-13-2050.Neuroplastic

Sugo, S., Minamino, N., Kangawa, K., Miyamoto, K., Kitamura, K., Sakata, J., … Matsuo, H. (1994).

Endothelial cells actively synthesis and secrete adrenomedullin. *Biochem Biophys Res Commun*, *201*(3), 1160–1166.

Sugo, S., Minamino, N., Shoji, H., Kangawa, K., Kitamura, K., Eto, T., & Matsuo, H. (1994). Production and secretion of adrenomedullin from vascular smooth muscle cells: augmented production by Tumor Necrosis Factor-α. *Biochem Biophys Res Commun*.

Tajima, A., Osamura, R. Y., Takekoshi, S., Itoh, Y., Sanno, N., Mine, T., & Fujita, T. (1999). Distribution of adrenomedullin (AM), proadrenomedullin N-terminal 20 peptide, and AM mRNA in the rat gastric mucosa by immunocytochemistry and in situ hybridization. *Histochemistry and Cell Biology*, *112*(2), 139–146. https://doi.org/10.1007/s004180050400

Takahashi, C., Shridhar, R., Huston, J., & Kenneth, M. (2018). Correlation of tumor size and survival in pancreatic cancer. *Journal of Gastrointestinal Oncology*, *9*(7), 910–921. https://doi.org/10.21037/jgo.2018.08.06

Tan, M. H., Nowak, N. J., Loor, R., Ochi, H., Sandberg, A. A., Lopez, C., … Chu, T. M. (1986). Characterization of a new primary human pancreatic tumor line. *Cancer Investigation*, *4*(1), 15–23. https://doi.org/10.3109/07357908609039823

Tomasello, G., Ghidini, M., Costanzo, A., Ghidini, A., Russo, A., Barni, S., … Petrelli, F. (2019). Outcome of head compared to body and tail pancreatic cancer: A systematic review and meta-analysis of 93 studies. *Journal of Gastrointestinal Oncology*, *10*(2), 259–269. https://doi.org/10.21037/jgo.2018.12.08

Tsuchida, T., Ohnishi, H., Tanaka, Y., Mine, T., & Fujita, T. (1999). Inhibition of stimulated amylase secretion by adrenomedullin in rat pancreatic acini. *Endocrinology*, *140*(2), 865–870. https://doi.org/10.1210/endo.140.2.6478

Tsuchiya, K., Hida, K., Hida, Y., Muraki, C., Nakagawa, K., Shindoh, M., & Harabayashi, T. (2010). Adrenomedullin antagonist suppresses tumor formation in renal cell carcinoma through

inhibitory effects on tumor endothelial cells and endothelial progenitor mobilization. *International Journal of Oncology*, *36*, 1379–1386. https://doi.org/10.3892/ijo

Tummers, W. S., Groen, J. V., Sibinga Mulder, B. G., Farina-Sarasqueta, A., Morreau, J., Putter, H., … Swijnenburg, R. J. (2019). Impact of resection margin status on recurrence and survival in pancreatic cancer surgery. *British Journal of Surgery*, *106*(8), 1055–1065. https://doi.org/10.1002/bjs.11115

Uemura, M., Yamamoto, H., Takemasa, I., Mimori, K., Mizushima, T., Ikeda, M., … Mori, M. (2011). Hypoxia-inducible adrenomedullin in colorectal cancer. *Anticancer Research*, *31*(2), 507–514.

Ueno, H., Kosuge, T., Matsuyama, Y., Yamamoto, J., Nakao, A., Egawa, S., … Kanemitsu, K. (2009). A randomised phase III trial comparing gemcitabine with surgery-only in patients with resected pancreatic cancer : Japanese Study Group of Adjuvant Therapy for Pancreatic Cancer. *British Journal of Cancer*, *101*(6), 908–915. https://doi.org/10.1038/sj.bjc.6605256

Valsangkar, N. P., Morales-oyarvide, V., Thayer, S. P., Ferrone, C. R., Wargo, J. A., Warshaw, A. L., & Fernandez-del Castillo, C. (2012). 851 resected cystic tumors of the pancreas: A 33-year experience at the Massachusetts General Hospital. *Surgery*, *152*(3 0 1), 1–15. https://doi.org/10.1016/j.surg.2012.05.033

Van Der Zee, J. A., Van Eijck, C. H. J., Hop, W. C. J., Van Dekken, H., Dicheva, B. M., Seynhaeve, A. L. B., … Ten Hagen, T. L. M. (2011). Angiogenesis: A prognostic determinant in pancreatic cancer? *European Journal of Cancer*, *47*(17), 2576–2584. https://doi.org/10.1016/j.ejca.2011.08.016

Van Tienhoven, G., Versteijne, E., Suker, M., Groothuis, K. B. C., Busch, O. R., Bonsing, B. A., … van Eijck, C. H. J. (2018). Preoperative chemoradiotherapy versus immediate surgery for resectable and borderline resectable pancreatic cancer (PREOPANC-1): A randomized, controlled, multicenter phase III trial. *Journal of Clinical Oncology*, *36*(18_suppl), LBA4002–LBA4002. https://doi.org/10.1200/jco.2018.36.18_suppl.lba4002

Venkatanarayan, A., Raulji, P., Norton, W., Chakravarti, D., Coarfa, C., Su, X., … Flores, E. R. (2015). IAPP driven metabolic reprogramming induces regression of p53 - deficient tumours in vivo. *Nature*, *517*(7536), 626–630. https://doi.org/10.1038/nature13910.IAPP

Von Hoff, D. D., Ervin, T. J., Arena, F. P., Chiorean, Gabriela E Infante, J. R., Moore, M. J., Seay, T. E., … Renschler, M. F. (2017). Randomized phase III study of weekly nab-paclitaxel plus gemcitabine versus gemcitabine alone in patients with metastatic adenocarcinoma of the pancreas (MPACT). *Journal of Clinical Oncology*, *13*(4). https://doi.org/10.1200/jco.2013.31.4_suppl.lba148

Walker, C., Mojares, E., & Hernández, A. del R. (2018). Role of Extracellular Matrix in Development and Cancer Progression. *International Journal of Molecular Sciences*, *19*(3028), 1–31. https://doi.org/10.3390/ijms19103028

Wang, L., Gala, M., Yamamoto, M., Pino, M. S., Kikuchi, H., Shue, D. S., … Chung, D. C. (2014). Adrenomedullin is a therapeutic target in colorectal caner. *International Journal of Cancer*, *134*(9), 2041–2050. https://doi.org/10.1038/jid.2014.371

Weber, J., Sachse, J., Bergmann, S., Sparwaßer, A., Struck, J., & Bergmann, A. (2017). Sandwich Immunoassay for Bioactive Plasma Adrenomedullin. *The Journal of Applied Laboratory Medicine*, (September), 222–233. https://doi.org/10.1373/jalm.2017.023655

Werner, J., Combs, S. E., Springfeld, C., Hartwig, W., Hackert, T., & Büchler, M. W. (2013). Advanced-stage pancreatic cancer: Therapy options. *Nature Reviews Clinical Oncology*, *10*(6), 323–333. https://doi.org/10.1038/nrclinonc.2013.66

Whatcott, C. J., Diep, C. H., Jiang, P., Watanabe, A., Lobello, J., Sima, C., … Han, H. (2015). Desmoplasia in primary tumors and metastatic lesions of pancreatic cancer. *Clinical Cancer Research*, *21*(15). https://doi.org/10.1158/1078-0432.CCR-14-1051

Williamson, J. M. L., Thorn, C. C., Spalding, D., & Williamson, R. C. N. (2011). Pancreatic and

peripancreatic somatostatinomas. *Annals of the Royal College of Surgery*, *93*, 356–360. https://doi.org/10.1308/003588411X582681

Winer, L. K., Dhar, V. K., Wima, K., Morris, M. C., Lee, T. C., Shah, S. A., … Patel, S. H. (2019). The Impact of Tumor Location on Resection and Survival for Pancreatic Ductal Adenocarcinoma. *Journal of Surgical Research*, *239*(Ml 0558), 60–66. https://doi.org/10.1016/j.jss.2019.01.061

Wu, X., Hao, C., Ling, M., Guo, C., & Ma, W. E. I. (2015). Hypoxia-induced apoptosis is blocked by adrenomedullin via upregulation of Bcl-2 in human osteosarcoma cells. *Oncology Reports*, *3*(13), 787–794. https://doi.org/10.3892/or.2015.4011

Xu, Meng-dan, Liu, S., Feng, Y., Liu, Q., & Shen, M. (2017). Genomic characteristics of pancreatic squamous cell carcinoma , an investigation by using high throughput sequencing after in-solution hybrid capture, *8*(9), 14620–14635.

Xu, Min, Qi, F., Zhang, S., Ma, X., Wang, S., Wang, C., … Luo, Y. (2016). Adrenomedullin promotes the growth of pancreatic ductal adenocarcinoma through recruitment of myelomonocytic cells. *Oncotarget*, *7*(34). Retrieved from www.impactjournals.com/oncotarget

Yamao, K., Yanagisawa, A., Takahashi, K., Kimura, W., Doi, R., Fukushima, N., … Tanaka, M. (2011). Clinicopathological features and prognosis of mucinous cystic neoplasm with ovarian-type stroma: A multi-institutional study of the Japan pancreas society. *Pancreas*, *40*(1), 67–71. https://doi.org/10.1097/MPA.0b013e3181f749d3

Yao, L., Wang, Y., Ma, W., Han, X., He, X., & Dai, X. (2019). Downregulation of Adrenomedullin Leads to the Inhibition of the Tumorigenesis via VEGF Pathway in Human and Nude Mice Osteosarcoma Models. *Archives of Medical Research*, *50*(1), 47–57. https://doi.org/10.1016/j.arcmed.2019.03.002

Yardley, D. A. (2013). Nab-Paclitaxel mechanisms of action and delivery. *Journal of Controlled Release*, *170*(3), 365–372. https://doi.org/10.1016/j.jconrel.2013.05.041

Yoshihara, F., Nishikimi, T., Okano, I., Horio, T., Yutani, C., Matsuo, H., … Kangawa, K. (2001). Alterations of intrarenal adrenomedullin and its receptor system in heart failure rats. *Hypertension*, *37*(2 I), 216–222. https://doi.org/10.1161/01.HYP.37.2.216

Yu, D.-Y., Yu, Y.-D., Kim, W.-B., Han, H.-J., Choi, S.-B., Kim, D.-S., … Kim, B.-H. (2018). Clinical significance of pancreatic intraepithelial neoplasia in resectable pancreatic cancer on survivals. *Annals of Surgical Treatment and Research*, *94*(5), 247–253. https://doi.org/10.4174/astr.2018.94.5.247

Yuan, C., Morales-oyarvide, V., Babic, A., Clish, C. B., Kraft, P., Bao, Y., … Wolpin, B. M. (2017). Cigarette Smoking and Pancreatic Cancer Survival. *Journal of Clinical Oncology*, *35*(16).

Yuan, C., Rubinson, D. A., Qian, Z. R., Wu, C., Kraft, P., Bao, Y., … Wolpin, B. M. (2015). Survival among patients with pancreatic cancer and longstanding or recent-onset diabetes mellitus. *Journal of Clinical Oncology*, *33*(1), 29–35. https://doi.org/10.1200/JCO.2014.57.5688

Zamboni, G., Hirabayashi, K., Castelli, P., & Lennon, A. M. (2013). Precancerous lesions of the pancreas. *Best Practice and Research: Clinical Gastroenterology*. https://doi.org/10.1016/j.bpg.2013.04.001

Zhang, G., Cheng, Z. Z., Xu, G. H., Jiang, X., Wang, X. X., & Wang, Q. F. (2018). Primary squamous cell carcinoma of the pancreas with effective comprehensive treatment: A case report and literature review. *Medicine (United States)*, *97*(41), 1–5. https://doi.org/10.1097/MD.0000000000012253

Zhang, Yaojun, Huang, J., Chen, M., & Jiao, L. R. (2012). Pancreatology Preoperative vascular evaluation with computed tomography and magnetic resonance imaging for pancreatic cancer : A meta-analysis. *PAN*, *12*(3), 227–233. https://doi.org/10.1016/j.pan.2012.03.057

Zhang, Yi, Xu, Y., Ma, J., Pang, X., & Dong, M. (2017). Adrenomedullin promotes angiogenesis in epithelial ovarian cancer through upregulating hypoxia-inducible factor-1 α and vascular

endothelial growth factor. *Nature Publishing Group*, (401), 1–9. https://doi.org/10.1038/srep40524

Zhou, C., Zheng, Y., Li, L., Zhai, W., Li, R., Liang, Z., & Zhao, L. (2015). Adrenomedullin promotes intrahepatic cholangiocellular carcinoma metastasis and invasion by inducing epithelial-mesenchymal transition. *Oncology Reports*, *34*(2), 610–616. https://doi.org/10.3892/or.2015.4034

Zudaire, E., Martinez, A., Garayoa, M., Pío, R., Kaur, G., Woolhiser, M. R., … Cuttitta, F. (2006). Adrenomedullin is a cross-talk molecule that regulates tumor and mast cell function during human carcinogenesis. *American Journal of Pathology*, *168*(1), 280–291. https://doi.org/10.2353/ajpath.2006.050291